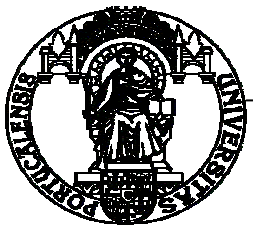

Universidade do Porto
FEUP Faculdade de Engenharia

SILICON-SUBSTITUTED HYDROXYAPATITE FOR BIOMEDICAL APPLICATIONS

Cláudia Manuela da Cunha Ferreira Botelho

Tese submetida à Faculdade de Engenharia da Universidade do Porto para candidatura à obtenção de grau de Doutor em Ciência de Engenharia

Faculdade de Engenharia
Universidade do Porto
2005

This thesis was supervised by:

Professor José Domingos da Silva Santos
Faculdade de Engenharia, Universidade do Porto

Professora Maria Ascensão Lopes
Faculdade de Engenharia, Universidade do Porto

The host institutions of this thesis were:

INEB – Instituto de Engenharia Biomédica, Laboratório de Biomateriais
Universidade do Porto, Portugal

Department of Materials Science and Metallurgy
University of Cambridge, United Kingdom

NAIST – Nara Institute of Science and Technology
Nara, Japan

The research described in this thesis was financially supported by:
FCT - Fundação para a Ciência e Tecnologia, ref. SFRH/BD/6173.

...to Mamã, Papá, Pati e Zé-Tó

"*Effects of silicic acid are destined to play*
a great and major role in therapy",
Louis Pasteur, 1878.

".... Deus quer, o homem sonha, a obra nasce...."
Fernando Pessoa – "O Infante".

Acknowledgement

I would like to demonstrate my deepest appreciation to all my friends and colleagues, who help me throughout my Ph.D., without them this thesis would never exist.

First of all I would like to thank my supervisors Professor José Domingos Santos and Professor Maria Ascensão Lopes, both of whom taught me what research is all about and gave me the opportunity to work in research centres around the world.

I would like to acknowledge everyone at the Instituto de Engenharia Biomédica (INEB), for the help and support through my Ph.D, especially to Professor Mário Barbosa, Professor Fernando Jorge Monteiro, Ana Paula Filipe, Ana Queiroz, Meriem Lamghari, Isabel Amaral, Judite Barbosa, Cristina Barrias, Cristina Martins, Cristina Ribeiro, Carlos Fonseca, Pedro Granja, Manuela Brás and Vanessa Morais. And also to everyone at FEUP most especially D. Fátima, D. Nina and Sr. Ramiro.

I would like to thank Professor William Bonfield and Dr. Serena Best for all the support and guidance throughout my Ph.D. and for the honour to work in their group at the University of Cambridge.

I would like to thank all members of the Cambridge Centre for Medical Materials (CCMM) group for their support.

My thanks to Professor Neil Rushton for his support and scientific input, during my stay at Orthopaedic Research Unit in the Addenbrookes Hospital.

I am most grateful to Dr. Roger Brooks, whom taught everything I know about cell culture, for his support and guidance throughout my stay in Cambridge.

I would like to thank all members of the Orthopaedic Research Unit, Mrs Christine Wilson, Dr. Gavin Spence, Dr. Charlotte Beeton, Dr.Bingkui Ma, Dr. Liliya Bakiyeva, Miss Mariam Habib and Miss Meera Arumugam. And also to Dr. Deborah Ireland from School of Clinical Medicine and Mrs Valerie from the Reumathology department at Addenbrookes Hospital.

My thanks to Dr. Debbie Stokes form Cavendish Laboratory for her assistance with the Environmental Scanning Electron Microscopy and to Dr. Nadia Stelmashenko from the Materials Device group for her assistance on the Atomic Force Microscopy.

My thanks to Dr. Ian Gibson and Dr. Nelesh Patel for all their assistance in the preparation of Silicon-Substituted Hydroxyapatite.

I would like to thank Professor Tanihara for the opportunity to work at NAIST, Japan. Thanks also to Professor Ohtsuki, Professor Ogata and Professor Kamitakahara for all the support and guidance during my stay at NAIST.

Thanks to Dr. Julian Jones for his help with the Inductively Couple Plasma Spectroscopy analysis.

On a personal level, I would like to thank all the CCMM group members, most specially to Val, Meera, Mariam, (my dearest friends), Fiona, Jie, Eng San, Muni, Mark, Judith, Georgina, Alex, Andy, Raeid, Jim, Susan, Anousha, Wayne and last but definitely not the least to Nelesh, all of you made my stay in Cambridge outstanding.

Thanks, also to all my friends at NAIST, Mutsumi Usui, Akira Takase, Yasushi Morihara, Tomohiro Uchino, Akio Takahashi, Hideaki Kumakura, Kazuhiro Takekita, Masato Namekata, most especially to Takahiro Kawai, Akari Takeuchi, Yuko Kozaka, Takao Asai, and Noriko Okuda.

I would like to show my deepest appreciation to the Okuda family, for their outstanding support and friendship during my stay in Nara, Japan

To my “Portuguese” friends, Anabela, Cláudia, Lucília, Nuninho, Nuno, Salomé and Sofia, for their constant support and friendship.

I would like to acknowledge the FCT-Fundação para a Ciência e Tecnologia for their financial support.

Finally I would like to thank my family for their patience and continuous support. Most especially my Mum, my Dad (the Best Parents in the World), my Sister (my best friend!!). A especial thanks to my Boyfriend (the Best in the World, of course!!!) for his constant support and love for the past eleven years. I love you all.

Publications

Botelho CM, Lopes MA, Gibson IR, Best SM, Santos JD. Structural analysis of Si-substituted hydroxyapatite: zeta potential and X-ray photoelectron spectroscopy (XPS). Journal of Materials Science: Materials in Medicine 2002, 13:1123-1127.

Botelho CM, Stokes DJ, Brooks RA, Best SM, Lopes MA, Santos JD, Rushton N, Bonfield W. Effect of human serum proteins on the surface of pure hydroxyapatite and silicon-substituted hydroxyapatite: AFM and ESEM studies. Materials Science Forum, 2003, 455-456:378-382.

Porter AE, Botelho CM, Lopes MA, Santos JD, Best SM, Bonfield W. Ultrastructural comparison of dissolution and apatite precipitation on hydroxyapatite and silicon-substituted hydroxyapatite *in vitro* and *in vivo.* Journal of Biomedical Materials Research 2004, 69A:670-679.

Botelho CM, Brooks RA, Lopes MA, Best SM, Santos JD, Rushton N, Bonfield W. Biological and physical-chemical characterisation of phase pure HA and Si-substituted hydroxyapatite by different microscopy techniques. Key Engineering Materials, 2004, 254-256: 845-848.

Botelho CM, Brooks RA, Best SM, Kawai T, Ogata S, Ohtsuki C, Lopes MA, Best SM, Santos JD, Rushton N, Bonfield W. *In vitro* analysis of protein adhesion to phase pure hydroxyapatite and silicon substituted hydroxyapatite. Key Engineering Materials 2005, 284-286:461-464.

Botelho CM, Brooks RA, Best SM, Lopes MA, Santos JD, Rushton N, Bonfield W. Human osteoblast response to silicon-substituted hydroxyapatite. Journal of Biomedical Materials Research, submitted.

Botelho CM, Brooks RA, Spence G, McFarlane I, Lopes MA, Best SM, Santos JD, Rushton N, Bonfield W. Differentiation of mononuclear precursors into osteoclasts on the surface of Si-substituted hydroxyapatite. Journal of Biomedical Materials Research, submitted.

Abstract

For several decades a great number of researchers worldwide are trying to mimic the mineral phase of bone in order to enhance bone regeneration and formation. It has been shown that the mineral phase of bone is composed by calcium phosphate crystals and several ions such as, fluoride, carbonate, magnesium, sodium and silicon. In 1970´s Carlisle and Schwarz demonstrated the positive effect of silicon on bone mineralization. Therefore, to combine the positive effect of silicon and the bioactive properties of hydroxyapatite (HA), a calcium phosphate with a similar chemical and structural composition to the inorganic phase of bone, a new biomaterial was developed, silicon-substituted hydroxyapatite (Si-HA). It has been shown that this material enhances bone apposition/ingrowth *in vivo* when compared to HA. However, the complexity of the *in vivo* model does not allow the full understanding of the mechanism behind this enhanced bioactivity. Therefore, the *in vitro* testing has been chosen as a model and the most important steps have been studied.

This thesis was designed to address the following aspects; the effect of the incorporation of silicon into the HA lattice, (i) on a physical-chemical point of view; (ii) interaction of Si-HA material with different solutions: tris-hydroxymethyl amino-methane buffer, simulated body fluid (SBF), SBF with human serum proteins; (iii) adhesion of different proteins: albumin and imunoglobulin that are important components of the adsorption layer at the surface of an implanted material, and also collagen type I that can be defined as "a structural protein of the extracellular matrix" and finally, (iv) to study the effect of silicon incorporation on the adhesion, proliferation and differentiation of two types of human cells, osteoblasts and osteoclasts.

On a chemical and structural point of view the incorporation of silicon into the HA structure resulted in a decrease on the surface charge of the material towards more negative values and also a slight increase on the hydrophilicity of the material was observed. XPS and FTIR results clearly support the substitution mechanism proposed by Gibson *et al* for Si-HA. Vibrational wavelength of 888 cm^{-1} and 504 cm^{-1} indicate the presence of SiO_4^{4-} and the binding energy of silicon at 101 eV corresponds to (Si-O) bonding. The XPS and EDX results showed that silicon is preferential released from the Si-HA material. The FTIR spectra also demonstrated a decrease on the intensity of the OH^- band, being a direct result of the substitution of the phosphate groups by the silicate groups and the loss of hydroxyl groups

due to a charge balance. After incubation in SBF an apatite layer was formed on the surface of Si-HA earlier than on unmodified HA. The more electronegative Si-HA surface provides a preferential site for the nucleation of an amorphous calcium phosphate apatite layer than the HA surface. This phenomenon may occur via the adsorption of calcium (Ca^{2+}) ions onto the electronegative surface, resulting on an increase in surface charge and the attraction of phosphate groups (PO_4^{3-}), also combined with a faster supersaturation of SBF due the higher dissolution rate of Si-HA. The presence of human serum proteins delayed the formation of this layer. The proteinaceous layer acted as a barrier to the dissolution and diffusion of ions from the surface to the surrounding medium.

The 0.8 wt % Si-HA material showed to have a higher binding affinity to human serum proteins, when compared to HA and 1.5 wt % Si-HA. In the case of a single protein solution a relation between collagen adhesion and silicon content was observed. The 1.5 wt % Si-HA substrate showed to have higher binding affinity per area to this protein.

The human osteoblast seeded on the Si-HA material proliferated and expressed different osteoblastic markers. The cells responded differently to the two compositions of Si-HA. The cells seeded on 0.8 wt % Si-HA surface had a higher rate of proliferation and increased production of proteins. While in the case of 1.5 wt % Si-HA a higher ALP production at early time points was observed, indicating that the cells were more differentiated. After 21 days calcium phosphate deposits were observed on the surface of HA and Si-HA.

The Si-HA material allowed the differentiation of osteoclast precursors (peripheral mononuclear cells and monocytes CD 14 positive) to mature osteoclasts. These cells expressed the typical osteoclast markers: actin rings, several nuclei, expressed TRAP and presented vitronectin receptors. On the samples seeded with osteoclasts significant differences on the concentration of calcium and phosphorous in the medium were observed, indicating that the osteoclasts were active and resorbing, especially on 1.5 wt % Si-HA.

The results obtained during these studies showed that the enhanced bioactivity of the Si-HA is a combination of acellular and cellular mechanisms. The more negative surface and higher dissolution rate decreases the time required for the formation of an apatite layer, which is considered to be an important factor for osteointegration. And also the enhanced proliferation and differentiation of bone cells (human osteoblast and osteoclast) induced by the presence of Si-HA can lead to faster bone regeneration.

Resumo

Inúmeros investigadores, desde há várias décadas, têm tentado desenvolver materiais semelhantes à fase inorgânica do osso, de forma a aumentar a regeneração óssea. A fase mineral do osso é composta por fosfatos de cálcio e diversos iões tais como: flúor, magnésio, carbonato, sódio e silício. Na década de 70 Carlisle e Schwarz demonstraram o efeito positivo do silício na mineralização óssea. Combinando o efeito positivo do silício e as propriedades bioactivas da hidroxiapatite (HA) um novo material foi desenvolvido, a hidroxiapatite modificada com silício (Si-HA). Os estudos *in vivo* demonstraram que este biomaterial aumenta a regeneração óssea. A complexidade do modelo *in vivo* não permite a determinação do mecanismo subjacente à sua bioactividade, daí a necessidade de estudar as diversas componentes deste sistema num sistema *in vitro*.

Esta tese foi estruturada com o objectivo de se estudar os aspectos relevantes na osteointegração *in vivo* da Si-HA, através de diversos ensaios *in vitro*, nomeadamente: (i) o efeito da incorporação de silício na malha da HA de um ponto de vista físico-químico; (ii) a interacção da Si-HA com diferentes soluções: tris-hidroximetil amino-metano, solução fisiológica simulada (SFS), SFS com proteínas do soro humano; (iii) adsorção de diferentes proteínas: albumina e imunoglobulina que são importantes componentes da camada de proteínas que adere ao material assim que este é implantado e colagénio tipo I que é definido com uma proteína estrutural da matriz extracelular. Por último, (iv) estudar o efeito da incorporação do silício na adesão, proliferação e diferenciação de dois tipos de células humanas, os osteoblastos e os osteoclastos.

Do ponto de vista físico-químico, a incorporação de silício na estrutura de HA resulta na diminuição da carga superficial do material (valores mais negativos) e num pequeno aumento da sua hidrofilicidade. Os resultados de espectroscopia de fotoelectrões de raios -X e espectroscopia de infravermelho suportam claramente o mecanismo de substituição proposto por Gibson *et al*. Os comprimentos de onda a 888 cm^{-1} e 504 cm^{-1} indicam a presença de SiO_4^{4-} e a energia de ligação a 101 eV correspondente à ligação (Si-O). As análises de espectroscopia de fotoelectrões de raio-X e energia dispersiva de raio-X demonstraram que o silício é preferencialmente dissolvido do material para o meio. As análises de infravermelho também demonstraram uma diminuição na intensidade da banda correspondente ao grupo hidroxilo, sendo este resultado uma consequência directa do mecanismo de substituição dos

grupos fosfatos pelos grupos silicatos e da perda de alguns grupos hidroxilo devido ao balanço de carga.

Nos ensaios de imersão em SFS, o tempo necessário para a formação de uma camada de apatite na superfície da Si-HA é menor em comparação com HA. A superfície mais negativa da Si-HA fornece um local preferencial para a nucleação de uma camada amorfa de fosfatos de cálcio, através da adsorção de iões cálcio (Ca^{2+}), resultando num aumento da carga superficial e consequente atracção de grupos fosfato (PO_4^{3-}). Adicionalmente, a sua cinética de dissolução resulta numa mais rápida supersaturação da solução de SFS, conduzindo à precipitação de fosfatos de cálcio. A presença de proteínas do soro humano atrasa a formação da camada de apatite, uma vez que protege a sua superfície, actuando como uma barreira à dissolução e difusão dos iões da superfície do material para o meio.

A incorporação de 0,8 % (p/p) de silício na malha da HA aumenta a adsorção de proteínas do soro humano por unidade de área, quando comparada com HA e 1,5 % (p/p) Si-HA. O colagénio tipo I tem maior afinidade para 1,5 % (p/p) Si-HA.

Os osteoblastos humanos aderiram, proliferaram e diferenciaram-se na superfície do Si-HA, contudo, as células responderam de forma diferente às duas composições. As células cultivadas na superfície de 0,8 % (p/p) Si-HA proliferaram mais rapidamente e produziram níveis mais elevados de proteínas enquanto que, no caso de 1,5 % (p/p) Si-HA as células apresentam maior actividade de fosfatase alcalina, indicando um estádio de maior diferenciação. Após 21 dias, observou-se a formação de fosfatos de cálcio na superfície de HA e nas duas composições de Si-HA.

A Si-HA permitiu a diferenciação de percursores de osteoclastos (células mononucleares do sangue e monócitos CD 14 positivos). As células apresentaram as características típicas de osteoclastos: anéis de actina, vários núcleos, receptores para vitronectina e expressaram TRAP. Nos materiais cultivados com osteoclastos, a concentração de cálcio e fósforo libertado da superfície de Si-HA para meio foi significativamente maior em comparação com HA, sendo este efeito mais evidente na Si-HA com 1,5 % (p/p) de Si, indicando que os osteoclastos estavam mais activos.

Os resultados obtidos indicam que a elevada bioactividade da Si-HA material se deve à combinação de mecanismos celulares e acelulares. A superfície mais electronegativa diminui o tempo necessário para formação da camada de apatite, sendo este factor considerado importante na osteointegração do material *in vivo*. A incorporação de silício na HA teve um efeito positivo na produção de proteínas e diferenciação de osteoblastos, assim como na diferenciação e actividade de osteoclastos.

Resumée

Depuis plusieurs dizaines d'années, les rechercheurs essaient de développer des matériaux qui puissent se ressembler à la phase inorganique de l'os, pour augmenter la régénération osseuse. Il a déjà été démontré que la phase minérale de l'os est composée de phosphates de calcium, et aussi de plusieurs ions comme le fluorure, le magnésium, le carbonate, le sodium et le silicium. Dans les années 70 Carlisle et Schwarz ont démontré l'éfect positif du silicium dans le procès de minéralisation osseuse. De cette façon, en combinant l'éfect positif du silicium et les propriétés bioactives de l'hidroxiapatite (HA), un nouveau matériel a été developé, l´hidroxiapatite modifiée au silicium (Si-HA). Des études en des conditions *in vivo* ont prouvé que ce matériel augmente la régénération de l'os. La complexité du modèle *in vivo* ne permet pas de déterminer le mécanisme derrière sa bioactivité. Donc le système in vivo a´-t- été divisé dans plusieurs étapes *in vitro*.

Cette thèse a-t-été structurée avec l'objectif d'étudier les aspects les plus relevants agissant sur l'osteointégration *in vivo*, en utilisant des essais *in vitro*, en particulier : (i) l'éffet de l'íntégration de silicium dans le réseau de l'hidroxiapatite d'un point de vue physico-chimique ; (ii) l'interaction de Si–HA avec plusieurs solutions : tris-hidroximetil amino-metane, solution physiologique simulée (SPS), SPS avec des protéines du sérum humain; (iii) adhérence de plusieurs protéines: albumine, immunoglobuline, qui sont des composants importants de la couche proteíque adhérant aux matériaux lorsqu'ils sont implantés, le collagèn du type I, lequel est définit comme une proteíne structurelle de la matrice extracellulaire. Finalement, (iv) l'étude de l'effet de l'intégration de silicium dans l'adhésion, la prolifération et la différentiation de deux types de cellules humaines, les ostéoblastes et les ostéoclastes.

Du point de vue physico-chimique l'intégration du silicium dans le réseaux de l'HA résulte dans la diminution de la charge de surface du matériel (des valeurs plus négatifs), et dans l'augmentation de l'hidrofilicité de ce matériel. Les résultats de spectroscopie de photoélectrons de rayons X et de spectroscopie d'infrarouge renforcent clairement l'idée du mécanisme de substitution proposé par Gibson *et al*. Pour les longueurs d'onde de 888 cm^{-1} et de 504 cm^{-1} on obtien la présence de SiO_4^{4-} et l'énergie de liaison à 101 eV correspond à la liaison (Si-O). Les résultats de l'XPS et de dispersion d'énergie de rayons X ont prouvé que le silicium est préférablement dissolu. Les analyses d'infrarouge ont aussi démontré qu'il y a une diminution de l'intensité de la bande correspondant au groupe hidroxil, ce que résulte

directement du mécanisme de substitution des groupes de phosphate par des groupes silicate et de la perte de quelques groupes hidroxil a cause du bilan de charges. Après l'incubation en SPS une couche d'apatite a-t-été formée plus rapidement sur la surface de la Si-HA que sur celle de la HA. D'après le mécanisme proposé, la surface plus négative fournit un endroit préférentiel pour la nucléation d'une couche amorphe de phosphate, par adsorption d'ions Ca^{2+} à la surface plus électronégative, provocant l'augmentation de la charge de surface et par conséquence l'attraction de groupes de phosphate. La présence des protéines du sérum humain retarde la formation de la couche d'apatite, puisque qu'elle va fonctionner comme une barrière a la dissolution et a la diffusion des ions de la surface pour le milieu.

L'intégration de 0,8 % (p/p) de silicium dans la HA accroît l'adhérence des protéines du sérum humain par unité de surface, si comparée avec la HA et avec 1,5 % (p/p) Si-HA. Le collagène du type I a une plus grande affinité avec 1,5 % (p/p) Si-HA.

Les ostéoblastes humains ont adhéré, proliféré et différentié sur la surface de Si-HA. Toutefois, les cellules ont répondu de façon diverse aux différentes compositions de Si-HA. Les cellules cultivés à la surface de 0,8 % (p/p) Si-HA ont proliféré plus rapidement et ont produit une concentration plus élevée des protéines, tandis que dans le cas de 1,5 % (p/p) Si-HA les cellules ont produit une concentration plus élevée de phosphatase alcaline, ce que indique que les cellules étaient plus différentiées. Après 21 jours les cellules ont commencé à produire des phosphates de calcium à la surface de HA de même façon de ce qui est arrivé pour les deux compositions de Si-HA.

Le Si-HA a permit la différentiation des précurseurs d'ostéoclastes (des cellules perfériales mononucléaires du sang et des monocytes CD 14 positifs). Les cellules avaient des caractères typiques d'ostéoclastes : des anneaux d' actine, multinucléaires et positives par rapport a la vitronectine et au TRAP. En présence des ostéoclastes les concentrations de calcium et de phosphore libérées pour le milieu par la Si-HA ont été considérablement supérieures par rapport a l'HA, en étant plus noté cet effet pour 1,5 % (p/p) Si-HA, ce qui indique que les ostéoclastes sont actifs.

Les résultats obtenus indiquent que l'élevée bioactivité de la Si-HA est due a l'association de mécanismes cellulaires et acellulaires. La surface plus électronégative provoque une diminution du temps nécessaire pour la formation de la couche d'apatite, ce que est considère un facteur très important dans l'osteointegration du matériel en des conditions *in vivo*. L'intégration du silicium dans l'HA a eu un effet positif dans la production de proteínes et dans la différentiation des ostéoblastes, aussi bien que dans la différentiation et activité des ostéoclastes.

Contents

Chapter 1

Introduction

General Introduction

Nowadays, the life expectancy is two times higher than in the begin of the 20th century (e.g. in the EUA in 1900 the life expectancy was approximately 48 years and nowadays is around 75-80 years). Therefore, the human body is subjected to higher cumulative stress that results in degradation of the tissues and so new therapies are required to overcome these problems [1, 2].

The bone grafts field has been developed to increase the quality of life of a patient who suffers from a bone disease, (e.g. osteoporosis, osteomalacia, osteogenesis imperfecta) or bone defect (e.g. bone fracture).

A biomaterial can be defined as ”*a nonviable material used in a medical device, intended to interact with biological systems”* [3]. Different materials can be used as biomaterials, namely, polymers, ceramics, glasses and metal alloys. The most important characteristic of a biomaterial is its biocompatibility that can be defined as *“the ability to perform with an appropriate host response in a specific application”* [3].

A bone graft should have particular characteristics depending on its application, for example if high strength is required, a single crystal material should be used, if a quick bond to bone is required, then a bioactive material should be used [1]. Hench defined a bioactive material *as “a non-toxic, biologically active and that forms an interfacial bond with the host”* [1].

The use of bone graft is required to restore skeletal integrity and enhance bone healing in several orthopaedic and maxillofacial procedures. There are several types of bone grafts: autograft, allografts, and xenografts, these grafts have advantages and disadvantages. Autografts are the ideal graft due to the lack of immunological response and the ability to provide osteoinductive growth factors, osteogenic cells and structural scaffolds [4]. The use of autograft, whilst often effective has several disadvantages, such as additional incision site, increased blood loss, limited supply and causes extra morbidity to the patient [5, 6]. As an alternative, allografts can be used. Allografting procedures are less successful then autografts. The processing of allograft tissue does not eliminate the risk of transferring viral contaminants such as HIV, hepatitis B and hepatitis C and the promotion of immunological reactions. When bone from one species is implanted into a member of different species is designated by xenografts. Due to adverse antigenic responses, xenografts are not considered suitable for bone grafting.

Therefore, the limitation in autografts and allografts has led to great advances in the development of synthetic alternatives. Hydroxyapatite (HA), $Ca_{10}(PO_4)_6(OH)_2$ is the most commonly used bone graft material, due to its chemical composition, which is similar to the mineral phase of bone.

HA has the ability to bond and integrate with the host tissue when implanted. Although, the rate by which bone forms directly on its surface is quite slow when compared to others calcium phosphate biomaterials [7, 8]. The natural apatite can be described as a multi-substituted calcium phosphate apatite [9, 10]. Hence, one way to improve HA bioactivity is by the incorporation of different ions into the HA lattice in order to obtain a closer chemical composition to the mineral phase of bone. The most common substitution is by carbonate ions [11, 12], there are also reports regarding the incorporation of other ions present in the mineral phase of bone such as magnesium [13], fluoride [14] and sodium [15]. Santos *et al* showed that the bioactivity of HA can also be enhanced by the incorporation of glass based on the P_2O_5-CaO-Na_2O system, a material recently patented as Bonelike® [16-18]. This system allows the incorporation of different ions such as magnesium, sodium and fluoride, resulting in a material with a chemical composition similar to the mineral phase of bone [19, 20].

Several studies have highlighted the beneficial role of silicon. In 1970s Carlisle *et al* and Schwarz *et al* demonstrated that mineralization requires a minimum of soluble silicon [21-23]. So, combining the properties of HA and the positive effect of silicon, a new biomaterial was developed, silicon-substituted hydroxyapatite, resulting in an worldwide patent, *"Silicon-Substituted Apatite and Process for the Preparation* " [24]

It has been shown that the incorporation of silicon into the HA lattice increases the bone ingrowth/apposition [25]. However, the complexity of the *in vivo* system does not allow the full understanding of the mechanism behind the enhanced bioactivity of Si-HA. So, the *in vitro* testing has been chosen as a model and the most important steps have been studied. This thesis was designed to address the following aspects:

- Effect of the incorporation of silicon into the HA lattice, on a physical-chemical point of view.
- Interaction of Si-HA material with different solutions: tris-hydroxymethyl amino-methane buffer, simulated body fluid (SBF) and SBF with human serum proteins.
- Adhesion of different proteins: albumin and imunoglobulin that are important components of the adsorption layer at the surface of an implanted material.

Also, collagen type I that can be defined as "a structural protein of the extracellular matrix".

- Adhesion, proliferation and differentiation of two types of human cells, osteoblasts and osteoclasts onto the Si-HA surface.

The aim of this thesis is to contribute to the understanding of the biological mechanism behind the enhanced bioactivity of silicon-substituted hydroxyapatite (Si-HA).

The silicon incorporation has a beneficial effect on the bioactivity of hydroxyapatite; and on the activity of human osteoblasts and osteoclasts, as presented in the following chapters.

Bone Physiology

Bone

Bone is a highly specialized form of connective tissue that has different functions: protection for vital organs and bone marrow; mechanical as a support and site for muscle attachment for locomotion; and metabolic, due to its ability to store several ions, especially calcium and phosphate, being therefore the major organ responsible for the maintenance of serum homeostasis and the major site of haematopoiesis (generation of new blood cells) in the human adult.

Structure

Anatomically, long bones can be divided into the following zones: epiphysis, diaphysis (or midshaft) and metaphysis (development zone) (Figure 1). The epiphyses (wider extremities of the long bones) and methaphysis are formed by two independent ossification centres, and are separated by a layer of cartilage designed by epiphyseal cartilage (or growth plate). This layer is composed by proliferative cells and expanding cartilage; it is responsible for the longitudinal growth in long bones. The methaphysis are the regions just below the growth plate, and it is in this area that immature bone growths. The last one, the diaphyses are the middle regions between the methaphysis and they provide mechanical stability. It is in this area that the hematopoietic marrow is located. Bone has two surfaces: the periosteal surface (external surface) and the endosteal surface (internal surface). These surfaces are covered by the periosteum and endosteum, respectively.

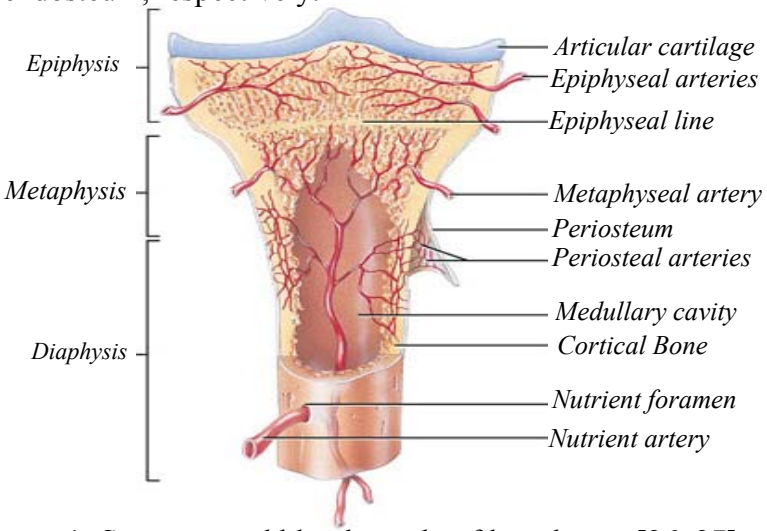

Figure 1- Structure and blood supply of long bones [26, 27].

From the morphological point of view, there are two types of bone: cancellous and cortical bone (Figure 2). These two kinds of bone differ in structure and function.

Figure 2 - Gross specimen of a longitudinally sliced long bone. Inside are the marrow cavity and the bony trabeculae [26].

The cancellous bone is formed by a network of thin calcified trabeculae. The trabeculae are made up of irregular osteon fragments, receiving their nutrients from blood vessels located in the marrow around them. Generally this type of bone is not penetrated by large blood vessels. The voids are filled with hematopoietic marrow in continuity with the medullar cavity of the diaphysis.

The cortical bone is denser (80-90%) than the cancellous bone (15-25%); hence its function is mainly mechanical and protective. It is composed by densely packed collagen fibres that form concentric lamellae. The structural units of the cortical bone are designated by Haversian systems; they are mainly located at the diaphyses. The network of trabeculae in cancellous bone is approximately 20% of the total human bone mass; the remainder is cortical bone (Figure 3).

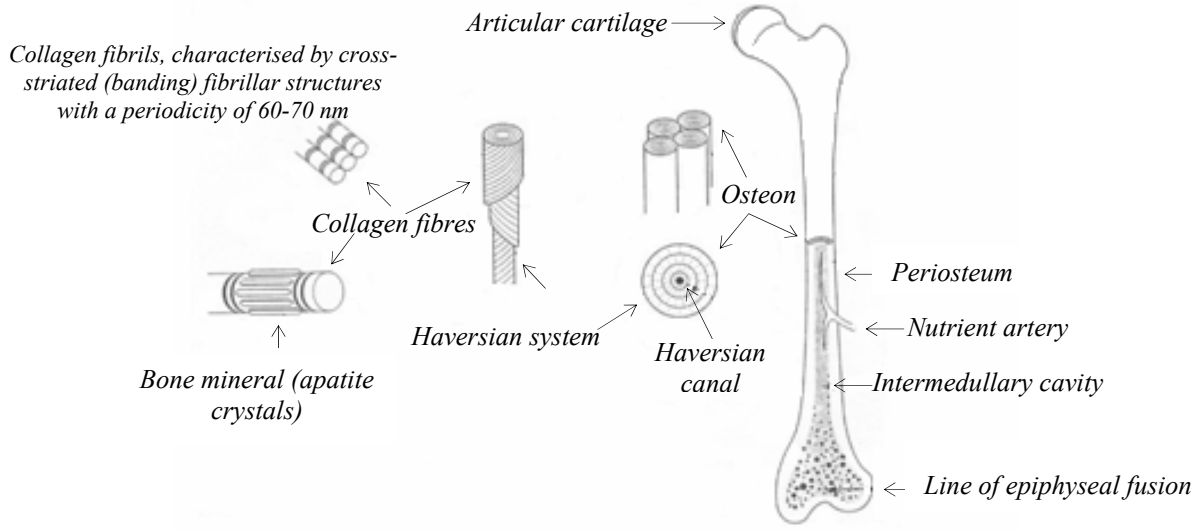

Figure 3- Morphological structure of bone [28].

The Haversian system has a central canal with a blood vessel and is surrounded by concentrically arranged lamellae of bone tissue that run parallel to the canal. Among the lamellae, several lacunae connect with each other and to the central canal by canaliculi.

In the lacunae there are several osteocytes arranged circumferentially around the Haversian canal. Each Haversian system (or osteon) is separated from its neighbour and forms interstitial lamellae by a cement line, but frequently these systems are intercommunicated (Figure 4).

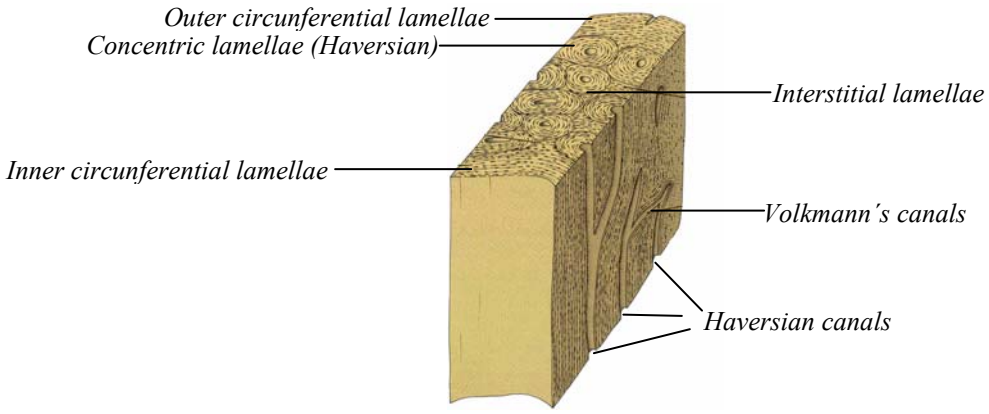

Figure 4 - Three-dimensional diagram of a dried sample of compact bone [26].

Oxygen and nutrients reach the lacunae of bone cells through the canaliculi of the Haversian systems, and the waste products are removed from the osteocyte by the same pathway. The canaliculi deposit their contents into the Haversian systems, which connected to Volkmann's canals, in turn theses canals connect to blood vessels in the periosteum [29].

Periosteum and Blood supply

The periosteum is a layer of dense, fibrous connective tissue that covers the external surface of most bones. It is highly adherent to the epiphysis and less adherent in the diaphyseal region [30]. The principal function of this layer is blood supply to bones. The periosteum is composed by a network of capillaries and capillary-like vessels. The blood vessels in this layer communicate with the cortical bone through the Volkmann's canal.

The blood supply to long bones is made via three main set of arteries: the nutrient artery, the metaphyseal-epiphyseal arteries and the periosteal arteries. The nutrient artery enters the diaphysis diagonally through a distinct foramen and branches into ascending or

descending medullar arteries. Upon reaching the marrow, the arteries divide into arterioles that penetrate the endosteal surface, to supply blood to the diaphyseal cortex. The metaphyseal-epiphyseal arteries originated from the peri-articular arteries, are connected to the bone by a foramina that are localized at specific positions in the thin cortex of the metaphysis. Their function is to supply blood to the spongy medulla and the metaphyseal bone [31].

Bone composition

Bone has two distinct phases: an organic matrix, composed by 80 - 90 % of collagen and the remaining is composed by proteoglycans and several non-collagenous proteins, namely osteocalcin, osteopontin, bone sialoprotein, osteonectin/SPARC (secreted protein acidic and rich in cysteine), decorin and biglycan. The mineral phase strengthens the organic phase with calcium salts.

Bone matrix (Organic Phase)

The bone matrix is composed by collagenous (80-90 %) and non-collagenous proteins. The mineralized tissue has type I and type V collagen, but the most abundant is collagen type I (> 95% of total collagen). The collagen fibres are held together by an amorphous continuous phase called ground substance [32]. Besides collagen the bone matrix is composed by proteoglycans and numerous proteins.

Non-collagenous proteins

Osteocalcin, osteopontin, bone sialoprotein, osteonectin/SPARC (secreted protein acidic and rich in cysteine) are some of the proteins that belong to this group. These proteins have different characteristics, for example osteopontin and bone sialoprotein have the RGD sequence that can be recognized by $\alpha_v\beta_3$ integrin receptor mediating cell attachment and activate cell signalling pathway and they are also involved in the hydroxyapatite binding, but while bone sialoprotein can nucleate the formation of hydroxyapatite crystals *in vitro* [33], osteopontin inhibits the mineral growth [34]. The exact role of osteocalcin in bone formation is not clear but it may be involved in mineral maturation. Biglycan (CS-PGI) is the

proteoglycan with higher representation in bone matrix, its precise involvement in bone formation is unknown, although it can bind to TGF-β and extracellular matrix macromolecules.

Collagen type I

Collagen type I is the most abundant extracellular protein in bone, it belongs to the family of glycoproteins. In 1967 Ramachandran *et al* established the triple-helix model for the collagen fibrils [35]. The triple helix motif has three polypeptide chains. These chains are composed by several repetitions of the amino acid sequence $(Gly\text{-}X\text{-}Y)_n$, where Gly stands for glycine, in most cases X is proline and Y is hydroxyproline, this amino acid stabilizes the triple helix and confers unique characteristics to the protein. Collagen type I is also a fibrillar protein, therefore its triple helix self-assembles into organized fibrils. These fibrils have a very high tensile strength and have a major role in providing a structural framework for body structures such as skeleton, skin, blood vessels, intestines, or fibrous capsules of the organism [36].

The triple helix of most of collagen type I molecules are composed by two α1 chains and one α2 chain coiled around each other. Both chains have a N-terminal peptide, followed by a C-terminal peptide [37-40]. On mature molecules this terminals are cleaved by proteases.

In bone, molecules of collagen type I and type V are organised into collagen fibrils, these molecules are assemble in parallel arrays. Between these molecules there are gaps (37.5 nm) that seem to be filled with "hydroxyapatite" minerals [41]. The fibrils are stabilized by inter and intra-molecular crosslinks, the number and distribution of this crosslinks will determine whether the tissue will mineralise [42].

Bone Mineral

The exact chemical composition and crystal structure of bone mineral has been the subject of intensive study for the last decades. DeJong, in 1926 demonstrated the similarities between the mineral phase of bone and synthetic hydroxyapatite using X-ray diffraction. Hydroxyapatite can be described by the chemical formula $Ca_{10}(PO_4)_6(OH)_2$ and a calcium phosphate ratio of 5:3 (1.67) [43]. Although, several differences have been demonstrated

between hydroxyapatite and the biological apatite that is present in bone tissue, namely, composition, crystallinity , stoichiometry, physical and mechanical properties. Bone mineral is characterized by calcium and hydroxyl deficiency, with a range of Ca:P ratios of 1.37-1.87 and also by several ionic substitutions within the apatite lattice and an internal crystal disorder. In 1969, Posner demonstrated that bone mineral is 10 % deficient in calcium [44] and in 1983 Driessens proposed the following composition for bone mineral: 15 % of magnesium whitlockite ($Ca_9Mg(HPO_4)(PO_4)_6$), 25% sodium and carbonate substituted apatite ($Ca_{8.5}Na_{1.5}[(PO4)_{4.5}(CO_3)_{1.5}](CO_3)$) and 60% of carbonated octacalcium phosphate ($Ca_8(PO_4)_4(OH)_2CO_3$ [45]. Therefore, it is more correct to refer to bone mineral as a substituted apatite and not as hydroxyapatite.

A biological apatite has always carbonate substitutions (CO_3^{2-}) [9-11]. As mentioned before, not only CO_3^{2-} is present in biological apatite, but also sodium (Na^+), magnesium (Mg^{2+}), potassium (K^+), fluoride (F^-), chloride (Cl^-) and also some trace elements such as strontium (Sr^{2+}), lead (Pb^{2+}), barium (Ba^{2+}). The role of many of these ionic species in bone is not fully understood, mainly due to the difficulties in monitoring and quantifying the ionic content in bone mineral. The concentration of these ions is also dependent on diet and pathologies [46], but it is accepted that all these ions are very important in bone biochemistry. Neuman and Neuman, in 1958 described the presence of a layer of fluid, designated by hydration layer [47]. It is believed that this layer binds to the bone crystals surface and the ions are diffused through this layer to and from the crystal surfaces, being this layer responsible for the ionic substitution into apatite lattice. Posner, in 1969 proposed that the ions that cannot be substituted into the lattice are probably adsorbed onto the surface [44].

The divalent ions (cations) such as Mg^{2+}, Sr^{2+} and Ba^{2+} can be incorporated into the lattice on the calcium sites. The mono-valent cations such as Na^+ and K^+ can also replace the calcium, but in this case a balance charge is required, therefore this balance will result in the protonation of an adjacent hydroxyl group. The anions (F^- and Cl^-) will substitute the hydroxyl groups. These substitutions induce complex structures changes at the unit-cell level and play a role on the dissolution rate of the apatite, which may favour osseointegration [48] and also induce crystalline imperfections due to the ionic substitutions combine to make bone mineral metabolically active [49].

The use of X-ray diffraction allowed the detection of an amorphous phase in mature bone [44, 50, 51]. Glimcher *et al* [52, 53] proposed that the initial mineralization occurs by the formation of a poorly crystalline non-stoichiometric apatite that increases in crystallinity and approaches stoichiometry with time although it never reaches.

Bone cells and their origin

The three main type cells related to bone formation, maintenance and resorption are: osteoblasts, osteocytes and osteoclasts, respectively (Figure 5).

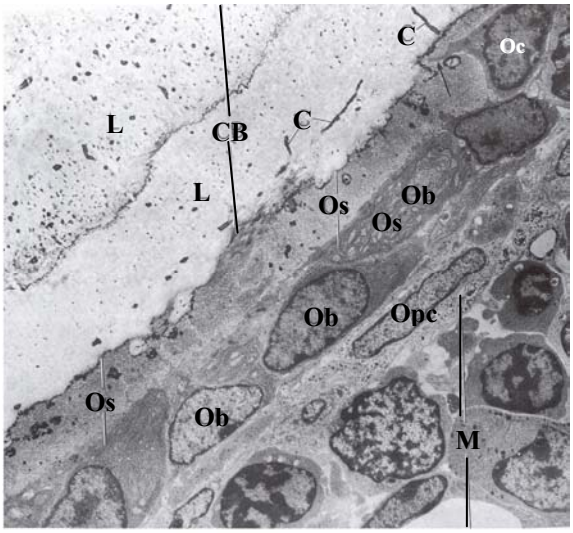

Figure 5 – Transmission electron micrograph of bone. M – marrow cavity; Opc – osteoprogenitor cells; Ob – Osteoblasts; Os – osteoid; Oc – osteocyte; CB – calcified bone matrix; C – canaliculi; and L – boundary between two adjacent lamellae [26].

The source of these cells has been a topic of a great deal of publications and it has been reviewed by different researchers [54-57]. According to Rasmussen and Bordier osteoblasts and osteoclasts derive from a common osteoprogenitor cell that has the ability to differentiate into an osteoblast or an osteoclast, depending on the environmental conditions [58]. Later on, Owen demonstrated that in the embryo the osteoblast is derived from a stromal mesenchyme cell system in marrow and the osteoclast from a haemapoietic cells system in marrow [59].

A mature osteoblast has its origin in a mesenchymal stem cell (bone marrow stromal stem cell or connective tissue mesenchymal stem cell), that is stimulated by local growth factors like fibroblast growth factors, bone morphogenetic proteins and WNt proteins and has transcription factors Runx2 and Osterix. The mesenchymal stem cell will undergo proliferation, differentiation to preosteoblasts until mature osteoblasts [60]. During the pathway to differentiation there are several histochemical markers that allow the identification

of the stage in which the cells are. CBFA-1 is mainly expressed during lineage commitment; histone, collagen, TGFβ1 and osteopontin are especially expressed during proliferation; alkaline phosphatase, bone sialoprotein and also collagen are characteristic during matrix maturation.

The osteocyte is a mature osteoblast that became trapped into the calcified matrix. This cell type is connected to the adjacent lacunae through canaliculi.

The osteoclast cell derives from the fusion of mononuclear cells that are derived from the hematopoetic tissue [61, 62] (Figure 6). These cells are related to the monocyte-macrophage lineage, but they belong to the leukocyte family. The osteoclasts are motile cells and they only form in the close vicinity of mineralized bone [63]. Their differentiation requires transcription factors such as PU-1 and MiTf at the initial stages. When stimulated by M-CSF they differentiate into the monocyte lineage, proliferate and express the RANK receptor. Additionally, these cells need RANKL that is produced by stromal cells, TRAF6, NFkB and c-*Fos*. The differentiation of these cells into osteoclast occurs at promonocyte stage, but monocytes and macrophages can differentiated into osteoclasts when under the right stimuli [60].

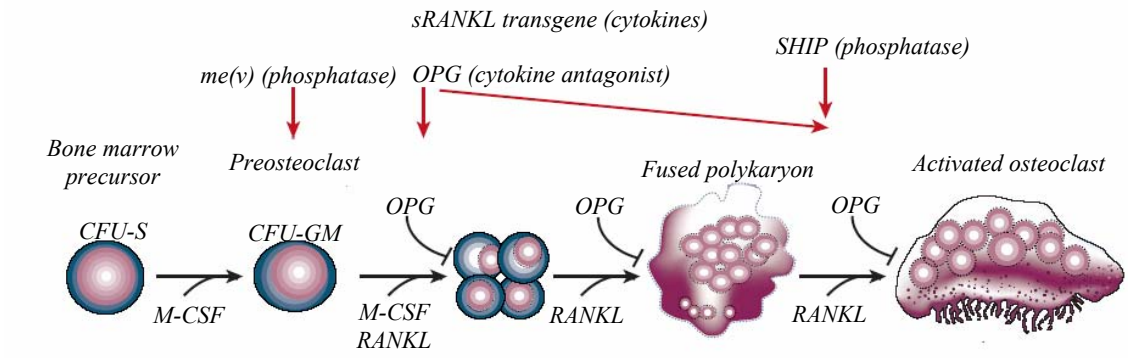

Figure 6 - A sketch of osteoclastogenesis. The maturation occurs from peripheral blood mononuclear cells from the macrophage lineage [64].

Osteoblasts

Osteoblasts are the bone cells responsible for producing bone matrix. These cells have distinct morphology, a round nucleus at the base of the cell facing the opposite bone surface, a basophilic cytoplasm and a prominent Golgi complex located between the nucleus and the apex of the cell (Figure 7), which demonstrates it biosynthetic and secretory ability. When

analyzed at an ultrastructural level this osteoblastic cell as an extremely well developed rough endoplasmatic reticulum with dilated cisternae and a dense granular content, and it is also characterized by a large circular Golgi complex comprising multiple Golgi stacks [60]. The plasmatic membrane is rich in alkaline phosphatase and has receptors for parathyroid hormone and prostaglandins, but not for calcitonin (typical of osteoclasts). The expression of the bone/liver/kidney isoform of alkaline phosphatase in a population of bone cells increases if there is a corresponding shift to a more differentiated state [65]. Additionally, at the membrane some other cytokines are expressed, the colony-stimulating factor I and RANKL, that can be cleaved to activate osteoclastogenesis. These cells can inhibit osteoclasts formation by secreting osteoprotegerin, a decoy RANK receptor capable of inhibiting osteoclast formation. They are also capable of producing several adhesion molecules (integrins), estrogens and vitamin D3. Its cytoplasmatic processes extend deep into the osteoid matrix to be in contact with the osteocyte process through the canaliculi.

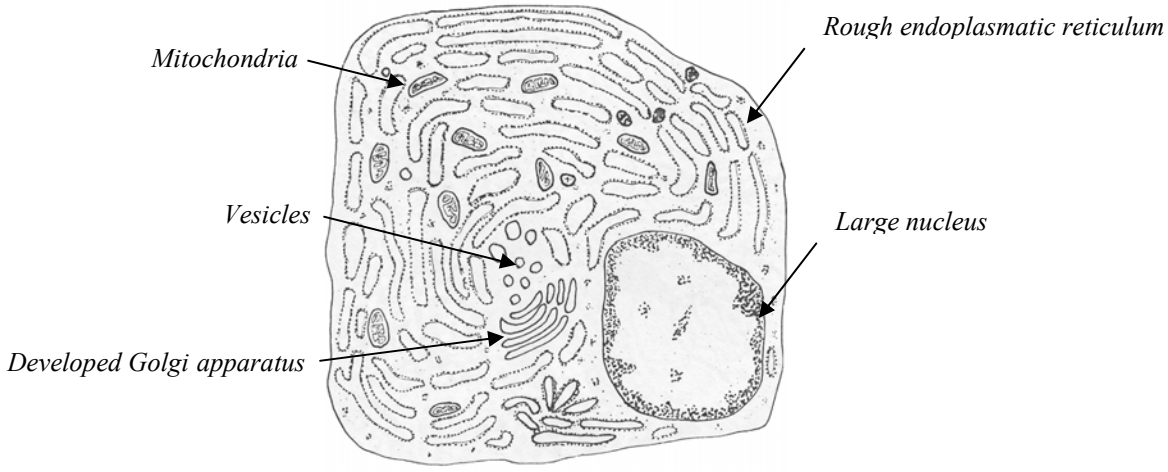

Figure 7 - A sketch of an osteoblast [26].

Osteocytes

During remodelling, some osteoblasts become buried in the osteoid (non-calcified tissue) and differentiate into osteocytes (Figure 8). These cells are surrounded by mineralised bone matrix, with the exception of a 1-2 μm wide space which forms the osteocyte lacunae [26]. Morphological evidence suggests that these cells are spidery in appearance. The lacunae have collagen fibrils and are involved in cytoplasmic processes, via canaliculi that will divide into smaller branches, providing a means of intercellular connection [66]. The marrow space

between the matrix and the cytoplasmic processes contains interstitial fluid where metabolites are transported between cells. The morphology of the osteocyte is dependent on their age and functional activity. At the ultrastructural level a young osteocyte has similar characteristics to a mature osteoblast, although there is a decrease in its volume and importance of the organelles responsible for proteins synthesis (rough endoplasmatic reticulum and Golgi apparatus). With time the osteocyte is located deeper in the calcified bone and accumulates glycogen in the cytoplasm. During osteoclastic bone resorption these cells are phagocytized and digested at the same time as other matrix components. It is believed that these cells may have a role as a mechanosensors and in the local activation of bone turnover. Regeneration of osteocytes is only achieved by resorption and remodelling processes, as osteocytes are non-mitotic cells [66].

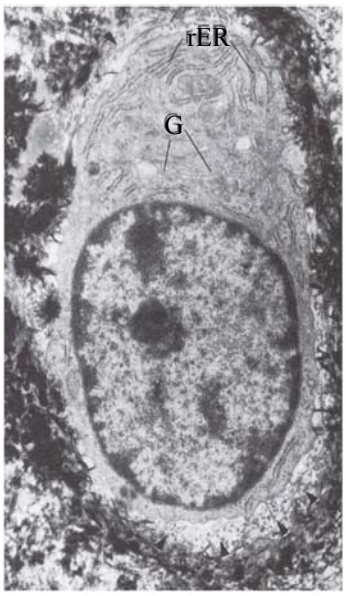

Figure 8 – Electron micrograph of an osteocyte, showing a large rough endoplasmatic reticulum (rER) and a Golgi profile [26]

Osteoclasts

They are bone resorbing cells derived from mononuclear haematopoietic precursor cells [61, 62]. They are fundamental to normal physiological processes of bone turnover and endochondral ossification. These cells are multinucleated and completely differentiated.

Morphologically, an osteoclast is a giant multinucleated cell containing 4-20 nuclei. These cells are usually in contact with calcified bone surface and with a Howship`s lacunae,

resulting from its own resorptive activity. The nuclei appearance varies within the same cell. They can be rounded and euchromatic or irregular in contour and heterochromatic, which possibly reflects the asynchronous fusion of its mononuclear precursors [60].

Osteoclasts attach to the bone surface forming a tight sealing zone enclosing the resorption lacunae. This feature was previously described by Scott and Pease [67]. This "ruffled border" or "brush border" is an area of the plasma membrane composed of a collection of folds and finger-like projections. After the attachment the cell produces an extracellular environment between itself and the bone surface (Figure 9). The ruffled border promotes a sealing zone, where the resorption takes place. This structure is rich in actin filaments, almost devoid of organelles and is organized in the shape of a ring [68]. The ruffled border is formed by protrusions of the plasma membrane known has posodomes [57]. The dissolution of the inorganic phase of bone precedes the matrix degradation [69]. This process involves the acidification of the microenvironment mediated by a vacuolar H^+ - adenosine triphosphate and the secretion of lytic enzymes tartrate-resistant acid phosphatase (TRAP) and pro-cathepsin K in the cell's ruffled membrane [64]. The pH of approximately 4.5 results from the release of hydrochloric acid (HCL) into the microenvironment [70]. This acidic environment will dissolve the bone mineral and subsequently, the demineralised organic component of bone will be degraded by a lysosomal protease cathepsin K (CATK) [71, 72]. The products from bone resorption are endocytosed by the osteoclast and then transported and released to the cell antiresorptive surface.

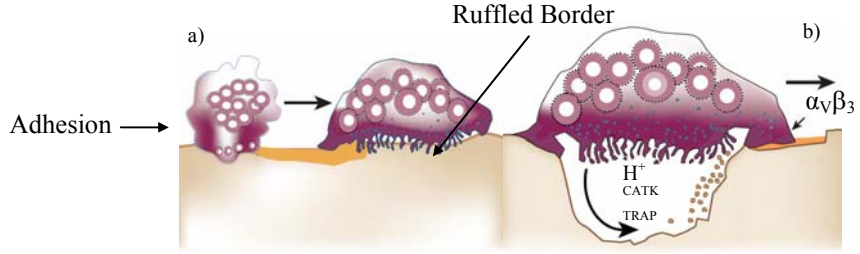

Figure 9 – A sketch of an osteoclast resorbing bone, a – adhesion and cytodiferentiation; b – secretion and resorption [64].

Bone growth

Bone growth or ossification can occur by two distinct methods, intramembraneous (within the membrane) or endochondral (within cartilage) ossification. There is no structural

difference between the bone tissue formed by these methods, this classification is only related to mechanism by which bone was initially formed.

Intramembraneous ossification

Flat bones of the skull and face, mandible and clavicle are formed through the intramembraneous ossification. The first evidence of the intramembraneous bone occurs at early stages of embryonic development. At this stage elongated mesenchymal cells within the mesenchyme migrate and aggregate in specific areas, where bone is to be formed. At the same time some mesenchymal cells proliferate and differentiate into osteoprogenitor cells. Some of these cells come into apposition with the initially formed spicules and differentiate into mature osteoblast laying down more matrix. During the appositional growth the size of the spicules increase and joint in a trabecular network. Due to the mitotic property, osteoprogenitor cells provide a constant source of osteoblast. These new cells lay down bone matrix in successive layers leading to the formation of the woven bone. The immature bone or woven bone is characterized by interconnecting spaces occupied by connective tissue and blood vessels.

Endochondral ossification

The majority of bones in the human skeleton grow through endochrondral ossification (bones of the extremities and those parts of the axial skeleton that bear weight). The growth of this type of bone is preceded by precursors known as cartilage models.

The first step on the formation of endochondral bone is similar to the intramembraneous ossification. The mesenchymal cells proliferate and migrate to the site of future bone. In this case the mesenchymal cells differentiate into chondroblasts (cartilage cells) that produces cartilage matrix. This cartilage (Hyaline Cartilage) acquires the shape of the bone that will be formed (the cartilage model). Ossification occurs within this model, as it is penetrated by blood vessels. The increase in width is due to matrix production by the new chondrocytes that differentiate from the chondrogenic layer of the perichondrium surrounding the cartilage mass. The osteoblasts under the perichondrium in the foetal bone deposit bone around the outside of the cartilage shaft. Once this process occurs, the perichondrium is known as the periosteum, which in turn deposits more layers of bone. It is possible to describe

an osteogenic layer within the periosteum because the cells in this layer are differentiating into osteoblasts. The developing long bones also need to grow in length. The metaphysis in long bones is described as the primary source of ossification and the epiphysis as the secondary source of ossification. Between the metaphysis and epiphysis there is a cartilaginous centre (growth plate or epiphyseal plate). The bone growth ends when the cells stop proliferating at the growth plate and the epiphysis fuses with the metaphysis of the shaft.

Bone remodelling

Bone is a dynamic connective tissue, after the formation of the skeleton, bone keeps changing its internal structure by remodelling. In this process old bone is removed and new bone is formed to replace it. Bone remodelling enables bones to adapt to the mechanical stress and it has a very important role in the mineral metabolism.

Bone remodelling occurs in specific locations and involves a several groups of cells. The mechanism by which bone is remodelled is dependent on the type of bone, cortical or cancellous.

The cortical bone is remodelled by the removal and refilling of osteons or Haversian systems (cutting cone). The activated osteoclast resorbs the old bone from the surface and it stays in a Howship lacunae. As soon as the resorption reaches a certain depth a new phase in the remodelling process starts, the reversal phase, in this step the osteoclast progresses and resorb the whole osteon. On the next step the osteoblast begins to lay down new bone. During the formation of the osteoid the osteoblasts are entrapped and differentiated into osteocytes, leading to a remodelled Haversian system.

Due to the different characteristic of the cancellous bone (large surface area of trabeculae and lack of osteons), the remodelling process will be different. Five different stages can be identified: 1) quiescence – resting state of the bone surface; 2) activation – recruitment of osteoclast to the bone surface; 3) resorption – removal of bone by osteoclast; 4) reversal - the process by which osteoclast stop resorbing bone and osteoblast start producing matrix and 5) formation – deposition of bone by osteoblast.

Wound healing

The healing events following the implantation of a bone graft are quite similar to the healing steps after a bone fracture. A bone fracture is characterized by the loss of bone

continuity [73]. The introduction of an implant will also result in the loss of continuity of bone tissue. An important factor is the presence of blood caused by the disruption of the blood vessels.

The most important difference between bone remodelling and healing is the presence of extravasated blood. In the remodelling process, the osteogenic population is derived from perivascular cells that migrate through the primitive perivascular connective tissue. In the healing process of a fracture and bone grafts implantation the osteogenic population comes from marrow. Osteogenic population migrates through the temporary scaffold provided by the extravasated and clotted blood [74].

When assessing the biological behaviour of a bone graft it is important to have special attention to three different phenomena: 1) the first biological molecules to interact with material are proteins and other macromolecules, therefore cells will subsequently interact with the protein layer; 2) the release of cytokines and growth factors from the degranulation of platelets in the blood clot has a stimulating effect on bone regeneration and finally 3) the properties of the implanted material may have an immense effect on early blood cell reactions.

The blood clot or haematoma caused by the haemorrhage from the damage blood vessels is composed mainly by red blood cells (erythrocytes) and platelets. Besides the clot formation two other mechanisms influence the haemostasis: a transient vasoconstriction at the ends of the damage local blood vessels limits the amount of blood entering the injured site and clot retraction that condenses the haemostatic plug, reducing the wound site. The lack of circulation results in poor oxygenation, which consequently causes local ischemia and necrosis. The leukocytes are involved in clot and necrotic tissue demolition through extracellular and intracellular phagocytic digestion mechanism.

The next step is the formation of granulation tissue. This tissue is characterized by large amount of blood vessels (60% wt) and several types of cells such as: macrophages, pluripotent pericytes, fibroblastic cells, and endothelial cells lining capillaries. All this cells are surrounded by a matrix composed mainly by fibronectin, proteoglycans, hyaluronic acid and collagen type III, that will develop to type I with time [75]. The large number of blood vessels gives the granular appearance. The angiogenesis is initiated mainly from the postcapillary venules. At this site the endothelial cells degrade the subendothelial basement membrane, migrate and proliferate to form hollow capillary buds [74]. The initial haematoma is removed and replaced by a fibrous vascular tissue that undergoes neovascularization [76].

During osteoconduction a migratory osteogenic population of cells spread on the surface of bone or implant. The cells stop migrating as soon as they start producing bone matrix. These cells that migrated are not mature osteoblasts, but they have osteogenic potential. Therefore, the osteoconduction phenomena precede the *de novo* bone formation by these cells [74].

Bone formation requires the migration of osteogenic cells, but also the differentiation to mature secretory cells. The osteoblast that reach the solid surface will produce matrix, although some cells differentiate before reaching the wound or implant site, at this point they stop migrating and start producing matrix, leading to the formation of bony spicule that advances towards the implant or fracture site.

Bone Grafts

Bone grafts are used in several orthopaedic surgical procedures to restore skeletal integrity that was compromised by disease, trauma or ageing and also to promote bone healing.

A bone graft has mechanical and biological functions; it should offer support or fill voids and enhanced the bone regeneration at the implantation site. A perfect bone graft should have several characteristics: a) capacity to form bone, to carry living bone cells (osteoblasts, osteoclasts or their precursors); b) its surface should stimulate osteoprogenitor cells to differentiate into bone forming cells in a osseous or non-osseous site; c) provide a bioactive surface, where the osseous tissue can regenerate [4]. Meaning, the material should be osteogenic, osteoinductive and osteoconductive, respectively.

Bone grafts can be classified according to its origin, autografts if the tissue is obtained from the patient itself; allograft if the tissue is obtained from a different donor, but the same specie, xenograft if the tissue is obtained from a different donor and different specie [77] or synthetic bone grafts (alloplastic).

Autografts

The surgical procedures involving autografts require two surgeries, the first one to harvest the bone from one site within the patient and the second one to implant the tissue into the damage site. The major advantage of the use of autografts is its osteogenic, osteoinductive

and osteoconductive properties [4]. This bone graft contains cartilage matrix, minerals, proteins and osteogenic marrow cells [78]. It has been described that in 1821 von Walther obtained healing of bone plates in a human skull through trephining and a few years later, 1889, another successful surgery involving bone grafting was reported by Seydel, he removed tissue from the tibiae from the patient and implanted in the skull of the same patient [79].

The problems associated with this type of bone grafts are mainly related with its limited supply and the need to subject the patient to a second surgery, which results in more pain and morbidity at the donor site. According to several researchers these symptoms persist even after wound healing [5, 6]. The main source for autografts is the iliac crest. It has been reported that harvesting bone tissue from the iliac crest can lead to several problems, namely arterial injury, hernia, chronic pain, and infection [80].

Allografts

The use of allograft eliminates the need of a second surgery, because tissue from a human donor is harvested and implanted in a different patient. The main source of allografts is cadavers. The use of allografts it has been described since the XIX century. It has been reported that the first successful human allografts was performed in 1881 by Macewen [79]. He removed tissue from the tibiae of a boy and implanted in the humerus of another boy. Around 1916 more than 350 allograft procedures were already performed successfully [79].

Allografting procedures are less successful then autograft. The use of allografts eliminates the need of a second surgery, being this fact one of the great advantages of allografting. Although, the processing of allograft tissue does not eliminate the risk of transferring viral contaminants such as HIV, hepatitis B and hepatitis C or also the transmission of potential unknown diseases and the promotion of immunological reactions. The use of sterilization by gamma radiation (or ethylene oxide) and removal of blood and cellular constituents diminish the risks of infection. The method used on the preparation of the tissue affects its properties, if the tissue is freeze-dried or sterilized by gamma radiation, its structure will be affected, loosing its osteoinductive ability and osteogenic properties, because most of the cells are damaged during the preparation process. Therefore, most allografts do not have cells, resulting in a loss of the osteogenic properties [4, 81].

The use of fresh allograft may be very low due to the risks mentioned previously and severe immunological reactions they may cause. So, a new process for the preparation of

fresh allograft was developed, in this case the bone marrow is removed, following the removal of fat from the bone and finally the minerals are removed by hydrochloric acid. After this process the collagen matrix is not damaged. The biological characteristic of the demineralised allograft is dependent of the demineralisation process. In 1965, Urist implanted decalcified allografts intramuscularly in rabbits, mice, rats and guinea-pigs and he found that new bone was formed [82]. He also found that the decrease in the osteogenic properties of the demineralised allograft was related to the amount of hydrochloric acid used in the process. Urist found that its osteogenic property was due to the presence of glycoproteins, known as transforming growth factor family [79].

Even with the development of new techniques allografting still has the risk of transmitting infections, toxins or contaminants and the preparation methods induce a significant lost of biological and mechanical properties. The limitations of autografts and allografts previously described led to a great advance in the development of synthetic alternatives.

Synthetic Bonegrafts

A wide range of materials have been proposed for bone replacement, such as metals, polymers, ceramics and composites. The principal materials used are titanium, aluminium, stainless steel, cobalt-chromium alloys and titanium alloys [1]. Due to the lack of biological properties their integration with the host tissue is very poor and its use can lead to the resorption of the surrounding bone due to the mismatch on the mechanical properties. This bone grafts do not have osteoconductive, osteoinductive or osteogenic properties. Therefore, their osseointegration is very poor. The mechanical properties of the metallic implants are different form the mechanical properties of bone, which can cause shielding, leading to the eventual resorption of the surrounding bone [83].

For the last forty decades there was an increase interest in ceramics for bone regeneration. Bioceramics may be used to fill spaces, as coatings or as a second phase in a composite [1]. The *in vivo* response to bioceramics will depend on several factors, such as: tissue type, health and age, implant composition and phase, blood circulation in tissue and interface, surface morphology and porosity motion at the interface, chemical reactions, closeness of fit and mechanical load [1].

Bioceramics can be also classified according to biological reaction they elicit *in vivo* (Table 1). Some materials can elicit a toxic response that will damage and/or kill cells or release chemical substances that can go into the blood stream and cause systemic damage to the patient [84], therefore they are not used in clinic.

Table 1 – *Reaction induced by biomaterials after implantation* [1].

Implant	Consequence	Materials
Biologically nearly inert	This material induces a very small response from the host tissue, leading to the formation of a non-adherent fibrous capsule around the implant.	Zirconia, Alumina
Bioactive	This material elicits a specific biological response at the interface of the material resulting in the formation of a bond between the tissue and the material.	Bioactive glasses, Bioactive glass-ceramics, HA, Bonelike®
Resorbable	Implant dissolves and /or is degraded by cells and replaced by tissue.	Tricalcium Phosphate, Bioactive glasses

The physical-chemical properties of the material influence the intensity and time duration of the inflammatory and wound-healing processes [85] caused by the implantation of the bone graft. The haemorrhage caused by the surgical procedure leads to the formation of a blood clot or haematoma containing mainly erythrocytes and platelets [74].

When a nearly inert biomaterial is implanted a sequence of events will follow until the formation of a fibrous capsule. During the inflammation phase, plasma proteins and leukocytes (mainly neutrophils) migrate to the implantation site [86-88]. After the migration of the leukocytes to the implant site, phagocytosis and the release of enzymes start followed by the activation of neutrophils and macrophages. The inflammatory cells such as polymorphonuclear granulocytes, monocytes and macrophages remove the debris and the foreign body. When the cellular mechanism does not have the ability to phagocytate the implant, enzymes of the macrophages will induce the fibroblasts to produce the collagen leading to the formation of the fibrous capsule around the implant. For as long as phagocytic activity continues the capsule becomes thicker. If the surface of particles are too large the macrophages will fuse together to form a giant cell [1] and this capsule will isolate the implant from the rest of the tissue [89]. The biological response to these materials is

dependent on the chemistry of the material, but most important is related to movement. If the implant is not properly fitted the movement will cause a thickness of the capsule until equilibrium is reached. On the other hand if the implant is properly fitted the phagocytic response is transient, the capsule will be very thin and inactive soon after the implantation. In the presence of alumina or zirconia a very thin layer will form, but if the material is more chemical reactive the layer will be thicker [90]. The formation of a capsule membrane around nearly inert materials is a protection mechanism from the host-tissue in order to isolate the implant. Most materials induce this response, like most metals and most polymers [1].

The bioactive materials form an interfacial bond, due to a controlled rate of chemical reactivity leading to the formation of dynamic equilibrium at the interface. The formation of a bioactive interface between the host-tissue and the implant occurs when the tissue apposes directly the implant surface, leading to a biological fixation, which prevents motion of the implant [1]. A common characteristic of the bioactive implants is the formation of a hydroxyl-carbonate apatite layer; this layer has a similar composition and structure to the mineral phase of bone [1].

Synthetic hydroxyapatite (HA) is used as a bone graft substitute, due to its similarity in composition to the mineral phase of bone and to its bioactivity. Several reports showed that HA has the ability to form an interface with bone, without the presence of a fibrous capsule [91-93]. The interfacial strength between bone and HA is significantly higher when compared to the "bond" between bioinert surfaces and host tissue [94].

A resorbable material can be degraded by the body fluids or digested by macrophages. Most important the degradation products cannot be toxic to the cells and should be easily disposed by the cellular mechanisms [1]. The main goal of this type of materials is to degrade slowly and be replaced by the natural tissue, leading to the regeneration of the tissue [1]. The high degree of solubility can pose problems regarding the mechanical performance while the regeneration is taking place. Another problem related to this type of material is the difficulty in matching the dissolution rate of the material with the repair rate of the tissue. The tricalcium phosphate ceramic can be degraded to calcium and phosphate salts in the body and be used as bone filler.

Several bioceramics are nowadays used in clinical, such as: bioactive glasses, HA, tricalcium phosphate [1]. The characteristics of the material should be optimized, depending on the function that the material should play in the body (Figure 10), for example a single crystal such as sapphire can be used as a dental implant due to its high strength, A/W glass-ceramic can be used to replace vertebrae due to its high strength and its ability to bonds to

bone. Bioactive glass has low strength, although they bond very rapidly to bone, therefore they should be use in repair of bone defects.

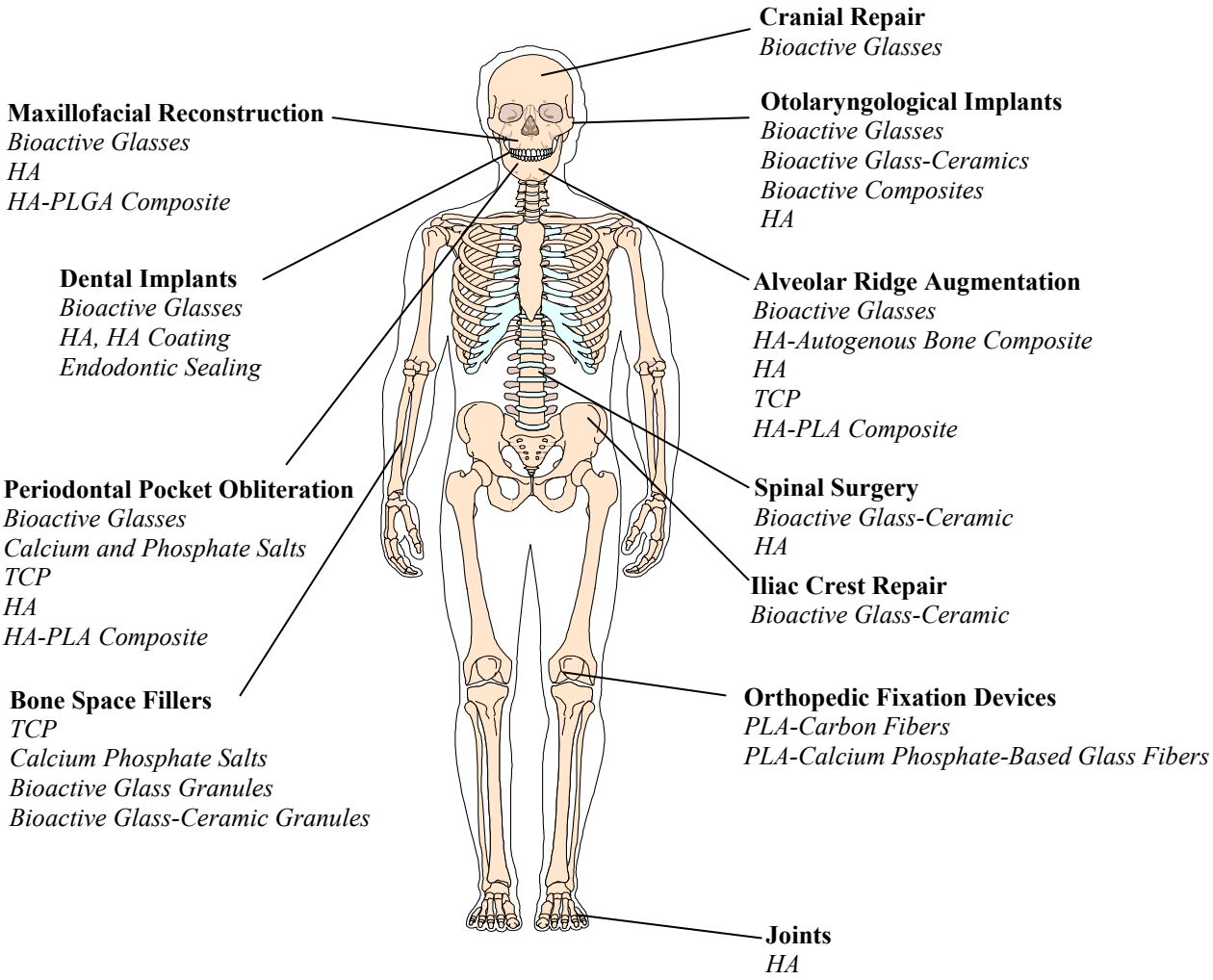

Figure 10 – Clinical uses of bioceramics [1, 27].

Hydroxyapatite and Substituted Apatite

In 1920 Albee reported the first successful bone repair with a calcium phosphate material [95]. Later on, two groups described a method to prepare a ceramic apatite from a mineral fluorapatite [96, 97]. A few years later several groups developed synthetic hydroxyapatite [98-101] to be used as a biomaterial for bone repair. Calcium phosphates are suitable bone grafts substitutes due to their osteoconductivity and its resorbability *in vivo* [92, 102-107].

The word apatite is used to describe a crystalline mineral with the composition $M_{10}(ZO_4)_6X_2$ [108, 109]. The M, Z and X site can be occupied by different ions. Calcium (Ca^{2+}), strontium (Sr^{2+}), barium (Ba^{2+}), lead (Pb^{2+}), can occupy the M site, in the case of the Z site it can be fulfilled by phosphorous (P^{5+}), silicon (Si^{4+}) and the X site by fluoride (F^-), chloride (Cl^-), hydroxyl group (OH^-), or it can be vacant.

Depending on the ions present and the calcium phosphate molar (Ca/P) ratio of the materials, their physicochemical and mechanical characteristics will be distinct [110].

Hydroxyapatite is an inorganic calcium phosphate that can be described by the following chemical formula: $Ca_{10}(PO_4)_6(OH)_2$. This material is characterized by a calcium phosphate ratio (Ca/P) of 1.67. It has a defined crystallographic structure that was initially proposed by Beevers and McIntyre [111] and refined by Posner *et al* [112] using X-ray diffraction. Kay *et al* [113] using neutron diffraction studies showed that HA consists of the hexagonal arrangement of calcium (Ca^{2+}) and phosphate (PO_4^{3-}) ions around columns of monovalent hydroxyl (OH^-) ions. Calcium hydroxide has a hexagonal system, with a space group $P6_3/m$, being characterized by a six-fold c-axis perpendicular to three equivalent a-axes at angles 120º to each other. The unit cell contains a complete representation of the apatite crystal with Ca^{2+}, PO_4^{-3} and OH^- groups closely packed. The cell dimensions are a=b=0.943 nm and c = 0.688 nm (Figure 11)

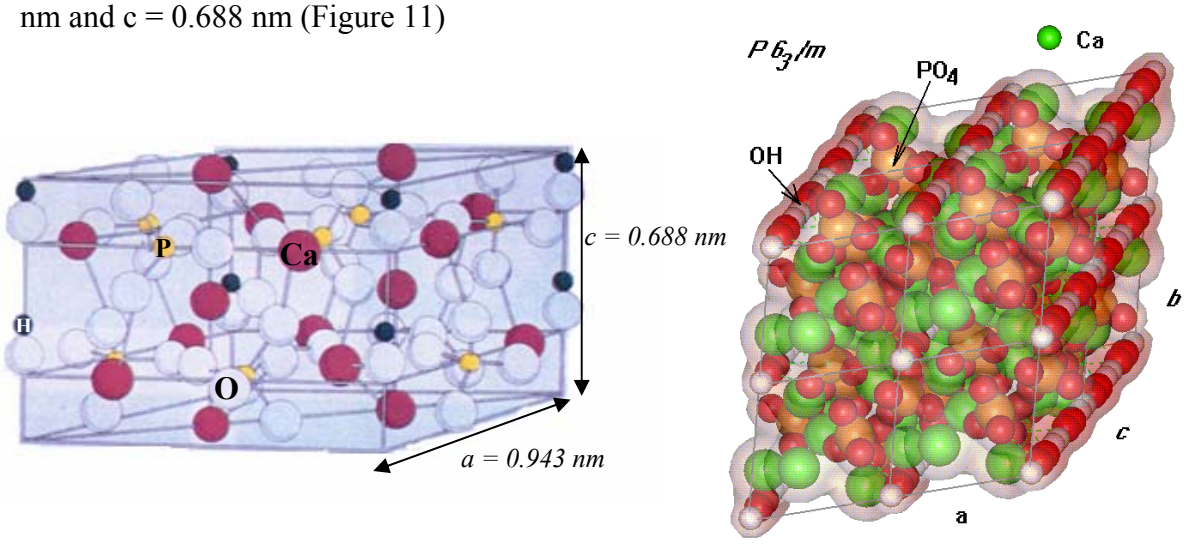

Figure 11 - The structure of hydroxyapatite (adapted from Aoki, 1991 – top image [108]; Bystrov et al , 2003 – bottom image [114]).

Four calcium atoms occupy the Ca(I) position: two at levels z = 0 and two at z = 0.5, the other six calcium ions occupy the Ca(II) positions. A group of three calcium atoms forms

a triangle at z = 0.25 and the remaining three describe a triangle at z = 0.75, surrounding the OH^- groups at the corners of the unit cell. The six phosphate tetrahedra are positioned in a helical arrangement from level z = 0.25 to z = 0.75. The basic skeletal framework of phosphate (PO_4^{3-}) groups provides stability to the apatite structure [10].

The Ca/P ratio will influence the characteristic of the material. In Table 2 are listed different calcium phosphates with various Ca/P ratios. It is believed that the Ca/P ratio will influence the rate of hydrolysis and solubility of the bioceramic. It has been reported that HA is the least soluble calcium phosphate *in vivo* [115]. The bioresorption of the calcium phosphate ceramic it is also dependent on the structure of the material [92]. A microporous ceramic has a larger surface area than a dense ceramic, therefore it will dissolve faster.

Table 2 Calcium to phosphorus ratios of typical calcium phosphate ceramics [108].

Name	*Abbreviation*	*Empirical formula*	*Molar Ca/P ratio*
Tetracalcium phosphate	TeCP	$Ca_4O(PO_4)_2$	2.00
Hydroxyapatite	HA	$Ca_{10}(PO_4)_6(OH)_2$	1.67
Fluorapatite	FA	$Ca_{10}(PO_4)_6F_2$	1.67
Chlorapatite	CA	$Ca_{10}(PO_4)_6Cl_2$	1.67
Tricalcium phosphate	TCP	$Ca_3(PO_4)_2$ (α,β,γ)	1.50
Octacalcium phosphate	OCP	$Ca_8H_2(PO_4)_6.5H_2O$	1.33
Dicalcium phosphate dehydrate (Brushite)	DCPD	$CaHPO_4.2H_2O$	1.00
Dicalcium phosphate (Monetite)	DCP	$CaHPO_4$	1.00
Calcium pyrophosphate (α,β,γ)	CPP	$Ca_2P_2O_7$	1.00
Calcium pyrophosphate dihydrate	CPPD	$Ca_2P_2O_7.\ 2H_2O$	1.00
Heptacalcium phosphate	HCP	$Ca_7(P_5O_{16})_2$	0.70
Tetracalcium dihydrogen phosphate	TDHP	$Ca_4H_2P_6O_{20}$	0.67
Calcium metaphosphate (α,β,γ)	CMP	$Ca(PO_3)_2$	0.50
Monocalcium phosphate monohydrate	MCPM	$Ca(H_2PO_4)_2.2H_2O$	0.50

As discussed in previous sections, HA has a similar chemical composition to bone mineral [43] and it presents osteoconductive properties.

The clinical use of calcium phosphate is limited due to its poor mechanical properties. Several groups developed new approaches in order to enhance the mechanical properties of HA. Bonfield *et al* developed a polyethylene-HA composite [116], Ioku *et al* added a second,

high-strength ceramic phase, such as yttria-doped zirconia [117], and Santos *et al*, introduce a glass reinforced phase, a $CaO\text{-}P_2O_5$ glass [118].

In previous sections it was mentioned that it is not correct to refer to the mineral phase of bone as hydroxyapatite, but that it should be a referred to as a "substituted apatite". Therefore, an approach to increase the bioactivity of HA is to incorporate different ions into the lattice and as mentioned previously the HA lattice is susceptible to ionic substitutions, such as carbonate ions (CO_3^{2-}) [11], magnesium (Mg^{2+}) [13], fluoride (F^-) [14], sodium (Na^+) [15], and silicon (Si^{4+}) [24, 119]. These substitutions cause changes in the lattice parameters, crystal morphology, solubility, crystallinity and thermal stability of HA. The characteristics of the substituted apatite will be dependent on the ion incorporated and the site of substitution. The ions can substitute for calcium, phosphorous or the hydroxyl group. These substitutions can happen independently, just one ion or simultaneously more than one ion [120]. If these substitutions occur simultaneous they may have a synergistic or antagonistic effect on the properties of the apatite. A coupled substitution of Mg^{2+} and CO_3^{2-} has synergistic effect on the solubility of HA and crystallinity , while the substitutions of $Mg^{2+}$and F^- or CO_3^{2-} and F^- have antagonistic effects, the F^- effect will predominate [121-123].

Cationic Substitutions

The cationic substitutions, such as magnesium (Mg^{2+}), barium (Ba^{2+}), lead (Pb^{2+}), potassium (K^+), sodium (Na^+), strontium (Sr^{2+}) take places at the calcium (Ca^{2+}) site. All of these ions introduce specific changes into the apatite substitutions.

The incorporation of Mg^{2+} into the apatite structure changes the lattice parameters and its properties. The *a* axis and the crystallinity decrease and the dissolution rate increases [123]. The substitution of Sr^{2+} for Ca^{2+} results in an increase in the unit cell parameters, both axis *a* and *c* increase. The incorporation of this ion also increases the dissolution of the apatite when compared to Sr-free apatite [124]. The divalent cations such as Ba^{2+} and Pb^{2+} can substitute for Ca^{2+} and due to its size, larger than Ca^{2+}, the lattice parameters increase. The incorporation of other ions like aluminium (Al^{3+}), manganese (Mn^{2+}) and zinc (Zn^{2+}) decrease the crystallinity of the apatites [120]. The incorporation of some of these ions can cause imbalances in the charges causing disorder within the crystal structure of HA. For example, in the case of the substitution of Na^+ into the apatite structure, due to the similarities between the ionic radii of Na^+ and Ca^{2+} no change into the lattice are expected [120], although the

difference in valency caused by this substitution requires a reduction in anionic charge to maintain charge balance. This is achieved through the formation of vacancies on the anion sites [15]. Studies have reported that the substitution of Ca^{2+} by Sr^{2+} ion increases the solubility of the apatite [122, 125], while the presence of Mg^{2+}, Fe^{2+}, Mn^{2+} and Al^{3+} ions restrict the growth of HA and promote the formation of β-tricalcium phosphate (β-TCP).

Anionic Substitutions

The anionic substitutions may occur at the phosphate site or hydroxyl (OH^-) site. Fluoride (F^-) and chloride (Cl^-) will replace some OH^- groups into the HA structure. The presence of F^- has several positive biologic effects, it promotes bone formation *in vivo* [126], enhances mineralization and calcification *in vitro* [122, 127]. On the structural level the incorporation of F^- increases the structural stability of the apatite [128], decreases the *a* axis, but does not influences the *c* axis and induces a higher crystallinity. On the other hand, the incorporation of Cl^- results in an expansion of the *a* axis and a decrease in the *c* axis. The apatites containing Cl^- are stable when exposed to heat resulting in a higher formation of secondary phases, such as β-TCP.

The substitution of carbonate (CO_3^{2-}) can occur in two different atomic sites into the HA lattice, being classified as type A and type B substitutions. The first type is the substitution of CO_3^{2-} ions for OH^- group [129] and the second type involves the substitution of CO_3^{2-} ions for PO_4^{3-}ions [12]. The substitution type B will result in a decrease of the *a* axis and an increase of the *c* axis. The incorporation of CO_3^{2-} will increase the solubility of the apatite [120]. The amount of CO_3^{2-} incorporation into the structure is influenced by the presence of other ions in solutions, for example the presence of Na^+ allows a maximum incorporation, while the presence of Sr^{2+} diminish its$^-$ incorporation [120].

Silicate Substitutions

Gibson *et al* demonstrated that silicate (SiO_4^{4-}) ions can substitute for the PO_4^{3-} site in HA [119, 130]. Through Rietveld structural refinement of the X-ray diffraction it was demonstrated that the incorporation of 0.4, 0.8 and 1.5 wt. % silicate ions decreased the *a* axis and increased the *c* axis of the unit cell of hydroxyapatite [119, 131]. The ionic bond lengths of a P-O bond (0.157 nm) with tetrahedral coordination are comparable to a similarly

coordinated Si-O bond (0.166 nm) [132]. Preliminary results showed that the incorporation of silicate ions into the HA structure increases the solubility and enhances osteoblast-like cells activity [133]. And more recently Patel *et al* demonstrated that the incorporation of silicate groups enhances bone regeneration [25].

Silicon

Several theories have been developed regarding the effect of silicon in several metabolic processes.

Silicon is one of the most common elements on earth. It can be found in igneous rocks and sedimentary rocks, in different forms such as: quartz (SiO_2), potassium feldspar ($KAlSi_3O_8$) and plagioclase ($NaAlSi_3O_8$+$CaAl_2Si_2O_8$). In the hydrosphere most of the silicon is in the form of silicic acid ($Si(OH)_4$), with small amounts of monosilicate ion ($SiO(OH)_3^-$) in sea water. The concentration of silicon in sea water is approximately 0.1 mM and 0.22 mM in river water [134].

A large number of studies regarding the effect of silicon on metabolic pathways were made using a diatom, unicellular algae, due to its metabolic similarities with the mammalian systems. Dietrich Werner [135] showed that a *Cyclotella cryptica* (diatom), had sequential metabolic effects when subjected to $Si(OH)_4$ starvation. Several changes in the metabolism occurred such as: inhibition of synthesis of a protein net, inhibition of DNA synthesis, inhibition of chlorophyll synthesis and an increase in the production of fatty acids synthesis by more than 100 %. Leading to a reduction of apparent photosynthesis and chrysolaminaran utilisation later on.

Volcani [136] showed, when these diatoms were subjected to silicon starvation, the exponential growth stopped, the rate of carbon dioxide fixation, oxygen evolution and ^{32}P assimilation decreased, until reaching a steady state. The synthesis of nucleic acids, proteins, carbohydrates, chlorophylls and fucoxanthin was also stopped, but the production of lipids was not affected. Throughout the culture the synthesis of nucleoside triphosphate (NTP), cellular carbon, DNA and diadinoxanthin increased slowly. When the silicon source was reinstated, the most notorious changes were in the lipid production that decreased abruptly, increased activity of the photosynthetic carbon reduction cycle intermediates and tricarboxylic acid cycle intermediates, as well an increase in protein production. So, the silicate uptake in

diatoms requires active transport. It is involved on DNA synthesis, through the synthesis of two nuclear DNA polymerases and it is also involved in the formation of thymidylate kinase.

The work of Marshal Darley [137] supported the results reported by Volcani [136]. It was demonstrated that in the absence of silicon *C. fusiformis* does not have nuclear division, indicating that silicon is required for DNA replication and or/mitosis. Baxter *et al* and Finkelstein *et al* [138, 139] suggested that in animal cells some the DNA-binding proteins may be implicated in the regulation of gene expression.

Through the measurement of different proteins synthesized in the presence of silicon, several hypotheses arised; being the most important related to the effect of silicon on the regulation of gene expression in the diatom. Two mechanisms were proposed to explain the differences observed: 1- the synthesis of a nuclear polymerase involved in DNA replication may be stimulated by silicate or derivative or even by a product of the silicate metabolism, resulting in DNA replication. Stein *et al* [140] suggested that this control could be at a transcriptional level; 2- silicon or a derivative can act as a post-translational level as a constituent of proteins, as a covalently bonded silicon in glycosaminoglycans and polyuronides. If these proteins did not have enough silicon, they could be translated on ribosomes, but not acquire a tertiary or quaternary conformation.

In a more specific area, bone biology, two different groups presented very similar results, Schwarz and Carlisle [22, 23, 141]. Schwarz demonstrated that a deficient diet in silicon in rats retarded the growth, disturbed the development of bone structure, namely, changes in the skull size and bone architecture. According to the author it is possible that silicon plays a special role in situations where an organism tries to bind structures due to the stability of the Si-O-Si bond. One of the most important findings of Schwarz was an enzyme capable to remove silicic acid from a bond synthetic form, Silicase. This enzyme is a membrane-bound located at the mitochondria and microsomes in pancreas, stomach and kidney (lower concentration), it is quite stable and it can be heat at 100ºC for 10 min, without loosing activity. Schwarz also proposed a correlation between the effect of silicon and arthritis, bone diseases (osteomalacia and osteogenesis imperfecta), scleroderma, wound healing and atherosclerosis [141].

Carlisle demonstrated similar effects in chicks, leading to the conclusion that silicon may play an important role in mineralization [21]. The author also demonstrated that silicon plays an important role in bone growth and development, connective tissue metabolism, bone calcification processes, connective tissue formation as a structural component in aging of certain connective tissues [21]. It was demonstrated that chicks with a deficient diet in silicon

presented atrophied organs, retard skeletal development, less flexible legs, smaller skulls and flatter bones. Using electron microprobe Carlisle demonstrated that silicon is concentrated in the cytoplasm of osteoblasts in young bones and that there is a direct relation between the concentration of silicon and the degree of calcification. Further studies, showed that osteogenic cells have larger amounts of calcium, phosphorous, magnesium and silicon, being the later on the most abundant anion on these cells. The increase of calcium is followed by a decrease in silicon, especially when the concentration of calcium reaches the values observed in bone apatite. The maximum amount of silicon observed was with a Ca/P ratio of 0.7 and decreases dramatically when Ca/P ratio reaches 1.67. It has been suggested that one of the most important factors in calcification is the binding of calcium and these studies suggested that silicon plays an important role in the processes. The abnormalities observed in the bone skull are related with a deficiency in collagen of the connective tissue matrix. In the articular cartilage of the chicks fed with a deficient diet in silicon presented lower amount of cartilage, glycosaminoglycans and collagen. Therefore, Carlisle showed that the site of action of silicon in connective tissue metabolism is on the glycosaminoglycan-protein complexes of the ground substance. In higher animals it was founded that silicon is bounded to glycosaminoglycans and associated with polysaccharide and smaller protein moieties.

The mechanism proposed for the role of silicon in the architecture of connective tissue is related to its ability to act as a cross-link between polysaccharide chains and linking polysaccharide chains to proteins. Silicon can also be related with the aging of some tissues. A significant decrease in this ion in the human normal aorta and human skin was reported with time. In addition, a decrease on the concentration of silicon was observed on the arterial wall leading to atherosclerosis [21].

Loeper, Loeper and Charnot [142, 143] showed that the decrease of silicon is followed by an accumulation of lipid deposits. According to these authors silicon partially inhibits lipidic accumulation, maintains the normal calibre of the elastic fibres, conserves the integrity of mucopolysaccharides and increases the impermeability of the endothelium to lipids.

Voronkov [144] demonstrated that nucleic acids contain silicon. In DNA one atom of silicon corresponds to an average of 20-30 atoms of phosphorus, and in the RNA this ratio changes to 25-45 atoms. Therefore, according to Voronkov this result proves the key role of silicon on the mechanism of protein biosynthesis and the transmission of hereditary information and in the structure of nucleic acids. Keeting *et al* [145] showed that Zeolite A stimulate the proliferation and differentiation of osteoblast-like cells in culture. This material

releases silicic acid and aluminium salts, so is not possible to isolate the effect of the silicic acid.

More recently, Hildebrant *et al* [146] demonstrated that certain genes are activated by hydrated silicon and Reffit *et al* [147] showed that at a physiologic concentration (10 – 20 μM) silicon stimulates collagen type I synthesis, differentiation, alkaline phosphatase activity and osteocalcin synthesis in human osteoblast like cells.

All the studies clearly demonstrated the enormous advantage of the incorporation of silicon in the biomaterials lattice aimed at regenerating bone tissue.

References

1. Hench LL, Wilson J. Introduction. In: An introduction to bioceramics. Singapore: World Scientific, 1993.

2. Hench LL. Biomaterials: a forecast for the future. Biomaterials, 1998;19:1419-1423.

3. Williams DF. Definition in biomaterials. In: Proceeding of a consensus conference of the European society for biomaterials. Chester, England: Elsevier New York, 1987.

4. Keating JF, McQueen MM. Substitutes for autologous bone graft in orthopaedic trauma. Journal of Bone and Joint Surgery, 2001;83B:3-8.

5. Summers BN, Eisenstein S. Donor site pain from the ilium: A complication of lumbar spine fusion. Journal of Bone and Joint Surgery, 1989;71B:677-680.

6. Younger EM, Chapman MW. Morbidity at bone graft donor site. Journal of Orthopaedic Trauma, 1989; 3:192-195.

7. Klein C, Driessen A, De Groot K, Hooff A. Biodegradation behaviour of various calcium phosphate materials in bone tissue. Journal of Biomedical Materials Research, 1983;17:769-782.

8. Ikeda N, Kawanabe K, Nakamura T. Quantitative comparison of osteoconduction of porous, dense A-W glass-ceramic and hydroxyapatite granules (effects of granule and pore sizes). Biomaterials, 1999;20:1087-1095.

9. LeGeros RZ. Apatites in biological systems. Progress in Crystal Growth and Characterization of Materials, 1981;1-2:1-45.

10. LeGeros RZ. Dense hydroxyapatite. In: An Introduction to Bioceramics. Singapore: World Sientific, 1993.

11. LeGeros RZ. Effect of carbonate on the lattice parameters of apatite. Nature, 1965;205:403-404.

12. Nelson DGA, Featherstone JDB. Preparation analysis and characterization of carbonated apatites. Calcified Tissue International, 1982;34:569-581.

13. Yasukawa A, Ouchi S, Kandori K, Ishikawa T. Preparation and characterization of magnesium-calcium hydroxyapatites. Journal of Materials Chemistry, 1996;6:1401-1405.

14. Jha LJ, Best SM, Knowles JC, Rehman I, Santos JD, Bonfield W. Preparation and characterization of fluoride-substituted apatites. Journal of Materials Science: Materials in Medicine, 1997;8:185-191.

15. De Maeyer E, Verbeeck R. Possible substitution mechanisms for sodium and carbonate in calcium hydroxyapatite. Bulletin des Societes Chimiques Belges, 1993;102:601-609.

16. Jha L, Santos J, Knowles J. Characterisation of the apatite layer formation on P_2O^5-CaO, P_2O_5-CaO-Na_2O and P_2O_5-CaO-Na_2O-Al_2O_3 glass hydroxyapatite composites. Journal of Biomedical Materials Research, 1996;31:481-485.

17. Santos JD, Jha LJ, Monteiro FJ. *In vitro* calcium phosphate formation on SiO_2-Na_2O-CaO-P_2O_5 glass reinforced hydroxyapatite composite: A study by XPS analysis. Journal of Materials Science: Materials in Medicine, 1996;7:181-185.

18. Santos JD, Hastings GW, Knowles JC, inventors; Sintered Hydroxyapatite Compositions and Method for the Preparation Thereof. WorldWide (PCT), 1999.

19. Afonso A, Santos JD, Vasconcelos M, Branco R, Cavalheiro J. Granules of osteoapatite and glass reinforced hydroxyapatite implanted in rabbit tibiae. Journal of Materials Science: Materials in Medicine, 1996;7:507-510.

20. Lopes M, Santos JD, Monteiro FJ, Ohtsuki C, Osaka A, Kaneko S, *et al.* Push-out testing and histological evaluation of glass reinforced hydroxyapatite composites implanted in the tibiae of rabbits. Journal of Biomedical Materials Research, 2001;54:463-469.

21. Carlisle E. Essentiality and function of silicon. In: Biochemistry of silicon and related problems. In: Proceedings of the 40th Nobel Symposium; Lidingö, Sweden, 1977.

22. Carlisle E. Silicon: a possible factor in bone calcification. Science, 1970;167:179-280.

23. Schwarz K, Milne D. Growth-promoting effects of silicon in rats. Nature, 1972;239:333.

24. Jha LJ, Best S, J.D. S, Gibson IR, Bonfield W, inventors; Silicon-substituted apatites and process for the preparation thereof. Worldwide patent, PCT/GB97/02325 and US Patent Serial Nº 09/147773, 1999.

25. Patel N, Best S, Gibson IR, Hing K, Damien E, Bonfield W. A comparative study on the *in vivo* behaviour of hydroxyapatite and silicon substituted hydroxyapatite granules. Journal of Materials Science: Materials in Medicine, 2002;13:1199-1206.

26. Ross MH, Romrell LJ, Kaye GI. Histology a text and atlas. 3rd ed. New York, 1995.

27. Patel N, Brooks R, Clarke M, Lee P, Rushton N, Gibson IR, *et al*. *In vivo* assessment of hydroxyapatite and substituted apatites for bone grafting. Cambridge, 2003.

28. Tencer AF, Johnson KD. Factors affecting the strength of bone. In: Tencer AF, Johnson, KD and Martin Duntz Ltd, editor. Biomechanics in orthopedic trauma: bone fracture and fixation. London, 1994:18-34.

29. Aubin JE, Turksen K, Heersche JNM. Osteoblastic cell lineage. In: Noda M, Academic Press, editor. Cellular and molecular biology of bone. Tokyo and London, 1993:1-45.

30. Ogden JA. The scientific basis of orthopaedics, 1987.

31. Sevitt S. Bone repair and fracture healing in man. Edinburgh: Churchill; 1981.

32. Hayes WC. Biomechanics of cortical and trabecular bone: implications for assessment of fracture risk. In: Van C and Hayes, WC, editor. Basic orthopaedic biomechanics. New York: Raven Press; 1991:93-142.

33. Hunter G, Goldberg H. Nucleation of hydroxyapatite by bone sialoprotein. In: Proceedings of the National Academy of Sciences of the United States of America, 1993: 8562-8565.

34. Goldberg H, Hunter G. The inhibitory activity of osteopontin on hydroxyapatite formation *in vitro.* Annals of the New York Academy of Sciences, 1995;760:305-308.

35. Ramachandran GN. Structure of collagen at the molecular level. In: Ramachandran GN, editor. Treatise on collagen. New York: Academic Press, 1967:103-183.

36. Rossert J, De Crombrugghe B. Type I collagen: structure, synthesis and regulation. In: Bilezikian J, Rais Z. Rodan GA, editors. Principles of bone biology, Academic Press, 1996.

37. Prockop D, Kivirikko K, Tuderman L, Guzman N. Biosynthesis of collagen and its disorders 2. New England Journal of Medicine, 1979;301(2):77-85.

38. Prockop D, Kivirikko K. Heritable diseases of collagen. New England Journal of Medicine, 1984;311:376-386.

39. Vuorio E, DeCrombrugghe B. The family of collagen genes. Annual Review of Biochemistry, 1990;59:837-872.

40. Van Der Rest M, Garrone R. Collagen family of proteins. FASEB Journals, 1991;5(13):2814-2823.

41. Robinson R, Watson ML. Collagen-crystal relationships in bone as seen in the electron microscope. Anatomical Record, 1952;114:383-410.

42. Kielty C, Hopkinson I, Grant M. Collagen: the family: structure, assembly and organization in the extracelular matrix. In: Connective tissue and its heritable disorders, Wiley- Liss, 1993:103-147.

43. De Jong WF. Le substance minerale dans le os. Recueil des Travaux Chimiques, 1926;45:445.

44. Posner AS. Crystal chemistry of bone mineral. Physiological Reviews, 1969;49:760-792.

45. Driessens FCM. Formation and stability of calcium phosphate in relation to the phase composition of the mineral in calcified tissue. In: DeGroot, K, editor. Bioceramics of calcium phosphate. Boca Raton, Florida, CRC Press, 1983.

46. Sobel AE, Rockenmacher M, Kramer B. Composition of bone in relation to blood and diet. Journal of Biological Chemistry, 1945:159.

47. Neuman WF, Neuman MW. The chemical dynamics of bone mineral. Chicago: University of Chicago Press, 1958.

48. Daculsi G, LeGeros RZ, Mitre D. Crystal dissolution of biological and ceramic apatites. Calcified Tissue International, 1989;45:95-103.

49. Posner AS. The chemistry of bone mineral. Bulletin of the Hospital Joint Diseases, 1978;39:126-144.

50. Betts F, Posner AS. An X-ray radial distribution study of amorphous calcium phosphate. Materials Research Bulletin, 1974;9:353-360.

51. Harper R, Posner A. Measurement of noncrystalline calcium phosphate in bone mineral. Proceedings of the society for experimental biology and medicine, 1966; 122:136-142.

52. Glimcher MJ, Bonar LC, Grynpas MD, Landis WJ, Roufosse AH. Recent studies of bone mineral: Is the amorphous calcium phosphate theory valid? Journal of Crystal Growth, 1981;53:100-119.

53. Glimcher MJ. Recent studies of the mineral phase in bone and its possible linkage to the organic matrix by protein-bound phosphate bonds. Philosophical Transactions of the Royal Society of London, 1984;B304:479-508.

54. Ducy P, Schinke T, Karsenty G. The osteoblast: a sophisticated fibroblast under central surveillance. Science 2000, 289:1501-1504.

55. Aubin JE. Bone stem cells. Journal of Cellular Biochemistry Supplements, 1998;30-31:73-82.

56. Friedenstein AJ. Osteogenic stem cells in the bone marrow. In: Heersche J, Kanis J, editors. Bone and mineral research. Amsterdam: Science Publishers, 1990.

57. Teitelbaum S. Bone resorption by osteoclasts. Science, 2000;289(5484):1504-1508.

58. Rasmussen H, Bordier P. Bone cells-morphology and physiology. In: Williams and Wilkins Co, editor. The physiology and cellular basis of metabolic bone disease. Baltimore, 1974:9-69.

59. Owen M. The origin of bone cells in the postnatal organism. Arthritis and Rheumatism, 1980;23:1073-1080.

60. Baron R. General principles of bone biology. In: Favus MJ, editor. Primer on the metabolic bone diseases and disorders of mineral metabolism. 5th ed: Lippincott Williams, 2003:1-8.

61. Suda T, Takahashi N, Martin TJ. Modulation of osteoclast differentiation. Endocrine Reviews, 1992;13:66-88.

62. Suda T, Takahashi N, Martin TJ. Cells of bone: osteoclasts generation. In: Bilezikian JP, Raisz, LG, Rodan GA, editors. Principles of bone biology. Academic Press; 1996:97-102.

63. Lerner U. Osteoclast formation and resorption. Matrix Biology, 2000;19(2):107-120.

64. Boyle W, Simonet W, Lacey D. Osteoclast differentiation and activation. Nature, 2003;423:337-342.

65. Rodan GA, Heath JK, Yoon K, Node M, Rodan SB. Diversity of the osteoblastic phenotype. In: Evered D, Harnett S, editors. Cell and molecular biology of vertebrate hard tissues. Chicester, U.K: John Willey and Sons; 1988:78-91.

66. Pritchard JJ. The general histology of bone. In: Bourne G, editor. The biochemistry and physiology of bone. New York: Academic Press, 1972:1-20.

67. Scott BL, Pease DC. Electron microscopy of the epipyseal apparatus. Anatomical Record 1956;126:465-482.

68. Vaananen H, Horton M. The osteoclast clear zone is a specialized cell-extracellular matrix adhesion structure. Journal of Cell Science, 1995;108:2729-2732 Part 8.

69. Blair H, Kahn A, Crouch E. Isolated osteoclasts resorb the organic and inorganic components of bone. Journal of Cell Biology, 1986;102(4):1164-1172.

70. Silver I, Murrills R, Etherington D. Microelectrode studies on the acid microenviroment beneath adherent macrophages and osteoclasts. Experimental Cell Research, 1988;175(2):266-276.

71. Li Y. Atp6i-deficient mice exhibit severe osteopetrosis due to loss of osteoclast-mediated extracellular acidification. Nature Genetics, 1999;23(4):447-451.

72. Gowen M, Lazner F, Dodds R. Cathepsin K knockout develop osteopetrosis due to a deficit in matrix degradation but not demineralization. Journal of Bone and Mineral Research, 1999;14(10):1654-1663.

73. Schultz R. The language of fractures. In. Baltimore: Williams and Wilkins, 2nd, 1999:1-333.

74. Davies JE, Hosseini MM. Histodynamics of endosseous wound healing. In: Davies, JM editor. Bone Engineering. Toronto: em^2, 2000.

75. Dyson M. Dermal repair. In: Bannister L, Berry M, Collins P, editors. Gray´s anatomy. 38th ed. New York, NY: Churchill Livingstone, 1995:412-416.

76. Winet H, Bao J, Moffat R. A control model for tibial cortex neovascularization in the bone chamber. Journal of Bone Mineral Research, 1990;5:19-30.

77. Gorer PA, Loutit JF, Micklem HS. Proposed revision of transplantese. Nature, 1961;189:1024.

78. Arrington ED, Smith WJ, Chambers HG. Complications of iliac crest bone graft harvesting. Clinical Orthopaedics, 1996; 329:300-309.

79. Urist MR, O´Connor BT, Burwelli RG. Bone grafts, derivatives and substitutes. Oxford: Butterworth and Heinemann, 1994.

80. Sieler JG, Johnson J. Iliac crest autogenous bone grafting: donor site complications. Journal of the Southern Orthopaedic Association, 2000; 9:91-97.

81. Stevenson S. Biology of bone grafts. Orthopedic Clinics of North America, 1999;30:543-552.

82. Urist M. Bone formation by autoinduction. Science, 1965;150:893.

83. Prendergast PJ, Tayler, D. A Stress analysis of the proximo-medial femur after total hip athroplasty. Journal of Biomedical Engineering, 1990;12:379-382.

84. Black J. Systemic effects of biomaterials. Biomaterials, 1984;5:11-19.

85. Anderson JM. The cellular cascades of wound healing. In: Davies JE, editor. Bone Engineering. Toronto: Em^2; 1999.

86. Ganz T. Neutrophil receptors: in neutrophils and host defense. Annals of Internal Medicine, 1988;109:127-142.

87. Henson PM, Johnston RBJ. Tissue injury in inflammation: oxidants, proteinases, and cationic proteins. Journal of Clinical Investigation, 1987;79:669-674.

88. Malech HL, Galin JI. Currents concepts: immunology: neutrophils in human diseases. New England Journal of Medicine 1987; 317:687-694.

89. Heimke G. The aspects and modes of fixation of bone replacements. In: Heimke G, editor. Osseo-Integrated Implants,1990:2-34.

90. Hench L. Bioceramics: From concept to clinic. Journal of American Ceramics Society, 1991; 74:1487-1510.

91. De Groot K. Degradable ceramics. In: Williams D, editor. Biocompatibility of implant materials. Boca Raton, Florida: CRC Press, 1981.

92. Jarcho M. Calcium phosphate ceramics as hard tissue prosthetics. Clinical Orthopaedics and Related Research, 1981;157:259-278.

93. Neo M, Nakamura T, Yamamuro T, Ohtsuki C, Kokubo T. Transmission electron microscopic study of apatite formation on bioactive ceramics *in vivo*. In: Communications RH, editor. Bone-bonding biomaterials. Leiderdorp, Holland, 1992:111-120.

94. Niki M, Ito G, Matsuda T, Ogino M. Comparative push-out data of bioactive and non-bioactive materials of similar rugosity. In: Davies JE, editor. Bone-material interface. Toronto, Canada: University of Toronto Press, 1991:350-356.

95. Albee FH. Studies in bone growth. Triple calcium phosphate as a stimulus to osteogenesis. Annals of Surgery, 1920;71:32-36.

96. Monroe Z, Votawa W, Bass D, McMullen J. New calcium phosphate ceramic material for bone and tooth implants. Journal of Dental Research, 1971:860-862.

97. Levitt G, Crayton P, Monroe E, Condrate R. Forming methods for apatite prosthesis. Journal of Biomedical Materials Research, 1969;3:683-685.

98. Jarcho M, Bolen CH, Thomas MB, Bobick J, Kay JF, Doremus RH. Hydroxylapatite synthesis and characterization in dense polycrystalline form. Journal of Materials Science, 1976;11:2027-2035.

99. Jarcho M, Kay JF, Gumaer KI, Doremus RH, Drobeck HP. Tissue, cellular and subcellular events at a bone-ceramic hydroxylapatite interface. Journal of Bioengineering, 1976;1:79-92.

100. De Groot K. Ceramic of calcium phosphates. In: De Groot K, editor. Bioceramics of calcium phosphate. Boca Raton, Florida: CRC Press, 1983:100-114.

101. Aoki H, Kato K, Ogiso M, Tabata T. Sintered hydroxyapatite as a new dental implant material. Journal of Dental Outlook, 1977;49:567-575.

102. Yuan H, Bruijin JD, Li Y, Feng J, Yang Z, De Groot K, et al. Bone formation induced by calcium phosphate ceramics in soft tissue of dogs: a comparative study between porous TCP and TCP. Journal of Materials Science: Materials in Medicine, 2001;12:7-13.

103. Yamaguch K, Hirano T, Yoshida G, Iwasaki K. Degradation-resistant character of synthetic hydroxyapatite blocks filled in bone defects. Biomaterials, 1995;13:983-998.

104. Constantz BR, Ison IC, Fulmer MT, Poser RD, Smith ST, Van Wagoner M, *et al*. Skeletal repair by *in situ* formation of the mineral phase of bone. Science, 1995;267:1796-1798.

105. Lavernia C, Schoenung JM. Calcium phosphate ceramics as bone substitutes. Bulletin of the American Ceramic Society, 1991; 70:95-100.

106. Barralet J, Akao M, Aoki H. Dissolution of dense carbonate apatite subcutaneously implanted in wistar rats. Journal of Biomedical Materials Research, 2000;49:176-182.

107. Ducheyne P, Qiu Q. Bioactive ceramics: The effect of surface reactivity on bone formation and bone cell function. Biomaterials, 1999;20(2287-2203.).

108. Aoki H. Science and medical applications of hydroxyapatite. Tokyo, Japan: Takayama Press; 1991.

109. Raemdonck VW, Ducheyne P, De Meester P. Calcium phosphate ceramics. In: Metal and ceramic biomaterials, 1984:143-165.

110. Tampieri A, Celotti G, Szontagh F, Landi E. Sintering and characterization of HA and TCP bioceramics with control of their strength and phase purity. Journal of Materials Science: Materials in Medicine, 1997;8:29-37.

111. Beevers CA, McIntyre DB. The atomic structure of fluorapatite and its relation to that of tooth and bone mineral. Mineralogical Magazine, 1956;27:254-256.

112. Posner AS, Perloff A, Dionio AF. Refinement of the hydroxyapatite structure. Acta. Crystallographica, 1958;11:308-309.

113. Kay JF. Calcium phosphate coatings for dental implants. Dental Clinics of North America, 1992;36:1-18.

114. Bystrov V, Bystrova N, Paramonova E, Sapronova A, Filippov S. Modeling and computation of hydroxyapatite nanostructures and properties. Materials Science Forum, 2005; In press.

115. Ravaglioli A, Krajewski A. Bioceramics: materials properties applications. London: Chapman and Hall, 1992.

116. Bonfield W, Grynpass MD, Tully AE, Bowman J, Abram J. Hydroxyapatite reinforced polyethylene - a mechanically compatible implant material for bone-replacement. Biomaterials, 1981;2:185-186.

117. Ioku K, Yoshimura M, Somiya S. Microstructure and mechanical properties of hydroxyapatite ceramics with zirconia dispersion prepared by post-sintering. Biomaterials, 1990;11:57-61.

118. Santos J, Reis RL, Monteiro FJ, Knowles JC, Bonfield W. Liquid phase sintering of hydroxyapatite by phosphate and silicate glass additions: structure and properties of the composites. Journal of Materials Science: Materials in Medicine, 1995;6(6):348-352.

119. Gibson IR, Best SM, Bonfield W. Chemical characterization of silicon-substituted hydroxyapatite. Journal of Biomedical Materials Research, 1999; 44:422-428.

120. LeGeros RZ. Calcium phosphates in oral biology and medicine. Monographs in oral science. Karger, S., Basel, 1991.

121. LeGeros RZ, Tung M. Chemical stability of carbonate and fluoride on dissolution behaviour of synthetic apatites. Carries Research, 1983;17:19-29.

122. LeGeros RZ, Lijkowsa R, LeGeros JP. Formation and transformation of octacalcium phosphate, OCP: a preliminary report. Scanning Electron Microscopy, 1984;5:17771-1777.

123. LeGeros RZ, Orly I, Gregoire M, Daculsi G. Substrate surface dissolution and interfacial biological mineralization. In: Davies JE, editor. The Bone-biomaterial interface. Toronto: University of Toronto press, 1991:76-88.

124. LeGeros R, Kijkowska R, Tung M, LeGeros JP. Effect of strontium on some properties of apatites. In: Fearnhead RW, Suga S, editors. Enamel Symposium V. Amsterdan: Elsevier, 1990.

125. LeGeros RZ. Incorporation of magnesium in synthetic and in biological apatites. In: Fearnhead RW, Suga S, editors. Tooth enamel IV. Amesterdam: Elsevier Science Publishers, 1984:32-36.

126. LeGeros RZ, Singer L, Ophaug R, Quirolgico G. The effect of fluoride on the stability of synthetic and biological (bone mineral) apatites. In: Menczel J, Robin GC, Making, M, editor. Osteoporosis: New York Wiley, 1982.

127. LeGeros RZ, Daculsi G, Orly I, Abergas T, Torres W. Solution-mediated transformation of OCP to apatite. Scanning Microscopy, 1989;3:129-138.

128. Young R, Elliott J. Atomic scale bases for several properties of apatites. Archives of Oral Biology 1966;11(36):60-66.

129. Bonel G. Contribution a L'tuede de la carbonation des apatite: I - synthese et etude des proprietes physico-chemiques des apatites carbonatees du type A. Annales Chimica, 1972;7:65-88.

130. Kim SR, Lee JH, Kim YT, Riu DH, Jung SJ, Lee YJ, et al. Synthesis of Si, Mg substituted hydroxyapatites and their sintering behaviors. Biomaterials, 2003;24:1389-1398.

131. Porter AE, Patel N, Skepper JN, Best SM, Bonfield W. Effect of sintered silicate-substituted hydroxyapatite on remodelling processes at the bone-implant interface. Biomaterials, 2004;25(16):3303-3314.

132. Shannon RD, Prewitt CT. Effective ionic radii in oxides and fluorides. Acta Crystallographica, 1969;B25.

133. Gibson IR, Huang J, Best SM, Bonfield W. Enhanced *in vitro* cell activity and surface apatite layer formation on novel silicon-substituted hydroxyapatites. In: Ohgushi H, Hastings GW, Yoshikawa T, editor. Bioceramics 12, Nara, Japan: World Scientific Publishing Co. Pte. Ltd, 1999:191-194.

134. Ingri N. Aqueous silicic acid, silicates and silicate complexes. In: Biochemistry of silicon and related problems. In: Proceedings of the 40th Nobel Symposium, Lidingö, Sweden; 1977.

135. Werner D. Regulation of metabolism by silicate in diatoms. In: Biochemistry of silicon and related problems. In: Proceedings of the 40th Nobel Symposium, Lidingö, Sweden; 1977.

136. Volcani BE. Role of silicon in diatom metabolism and silicification. In: Biochemistry of silicon and related problems. In: Proceedings of the 40th Nobel Symposium, Lidingö, Sweden; 1977.

137. Darley W, Volcani B. Role of silicon in diatom metabolism. A silicon requirement for deoxyribonucleic acid synthesis in diatom *cylindrotheca-fusiformis* reimann and lewin. Experimental Cell Research, 1969;58(2-3):334.

138. Baxter J, Rousseau G, Benson M, Garcea RR, Ito J, Tomkins G. Role of DNA and Specific cytoplasmic receptors in glucocorticoid action. Proceedings of the National Academy of Sciences of the United States of America, 1972;69(7):1892.

139. Finkelstein D, Butow R. DNA-binding proteins in yeast - effect of growth phase and mitochondrial-function. Archives of Biochemistry and Biophysics, 1976;174(1):52-65.

140. Stein G. Nonhistone chromosomal-proteins and gene regulation. Science, 1974; 183(4127):817-824.

141. Schwarz K. Significance and functions of silicon in warm-blooded animals. In: Biochemistry of silicon and related problems. In: Proceedings of the 40th Nobel Symposium, Lidingö, Sweden; 1977.

142. Loeper J, Loeper J. Silice et artherosclerose. Presse Medical, 1958;66:883.

143. Charnot Y, Peres G. Contribution to study of endocrin regulation of silicic metabolism. Annales d Endocrinologie, 1971;31:397.

144. Voronkov MG, Skorobogatova VI, Vugmeíster EK, Makarskii VV. Silicon in nuclei acids. Doklady Biochemistry, 1975;222:29.

145. Keeting PE, Oursler MJ, Wiegand KE, Bonde SK, Spelsberg TC, Riggs LB. Zeolite A increases proliferation, differentiation, and transforming growth factor production in normal adult human osteoblast-like cells *in vitro*. Journal of Bone and Mineral Research, 1992;7(11):1281.

146. Hildebrand M, Higgins D, Busser K, Benjamin E. Silicon-responsive cDNA clones isolated from the marine diatom *Cylindrotheca fusiformis*. Gene, 1993;132(2):213-218.

147. Reffitt D, Ogston N, Jugdaohsingh R, Cheung H, Evans B, Thompson R, *et al*. Orthosilicic acid stimulates collagen type I synthesis and osteoblastic differentiation in human osteoblast-like cells *in vitro*. Bone, 2003;32:127.

Chapter 2

Physical-Chemical Characterisation

Preliminary studies carried out by Gibson *et al* showed that the incorporation of silicon into the HA lattice resulted in enhanced bioactivity. It was also demonstrated that the incorporation of this ion induced structural changes, such as distortion in the lattice of HA, *a* axis decreased and the *c* axis increased with the silicate content.

In this chapter we tried to further characterize the structural changes induced by the incorporation of silicon. We also characterize the changes occurred in the materials during *in vitro* dissolution. This work was done in collaboration with Dr. Alexandra Porter from the Department of Materials Science and Metallurgy, University of Cambridge who performed the transmission electron microscopy (TEM) analysis.

Hydroxyapatite (HA) and silicon-substituted hydroxyapatite (Si-HA) were characterised by several techniques, such as: X-ray photoelectron spectroscopy (XPS), electrophoretic mobility (zeta potential), Fourier transform infra-red spectroscopy (FTIR), transmission electron microscopy (TEM), environmental scanning electron microscopy (ESEM), energy dispersive X-ray (EDX).

The incorporation of silicon into the HA structure resulted in a decrease of the surface charge of the material towards more negative values and also an increase on the hydrophilicity of the material.

XPS and FTIR results clearly support the substitution mechanism proposed by Gibson *et al*. Vibrational wavelength at 888 cm^{-1} and 504 cm^{-1} indicate the presence of SiO_4^{4-} and the binding energy of silicon at 101 eV corresponds to (Si-O) bonding. The XPS and EDX results showed that silicon is preferential released from the Si-HA material to the medium. The FTIR spectra also demonstrated a decrease on the intensity of the OH^- band, being a direct result of the substitution of the phosphate groups by the silicate groups and the loss of hydroxyl groups due to a charge balance.

After incubation in SBF an apatite layer was formed on the surface of Si-HA earlier than on unmodified HA. The more electronegative Si-HA surface provides a preferential site for the nucleation of an amorphous calcium phosphate apatite layer than the HA surface. This could occur via the adsorption of Ca^{2+} ions onto the electronegative surface, resulting in an increase in surface charge and the attraction of phosphate groups.

An important finding of this study was the similarities between the dissolution mechanism *in vitro* and *in vivo*. In both cases, 1.5 wt% Si-HA was the most soluble, followed by 0.8 wt % Si-HA and HA.

Structural Analysis of Si-Substituted Hydroxyapatite: Zeta Potential and X-ray Photoelectron Spectroscopy (XPS)

C. M. Botelho[1], M.A. Lopes[1,2], I.R. Gibson[3], S.M. Best[4], J.D. Santos[1,2*]

[1]INEB – Instituto de Engenharia Biomédica, Rua do Campo Alegre, 823, 4150-180 Porto, Portugal

[2]Departamento de Engenharia de Metalúrgica e Materiais, Faculdade de Engenharia, Universidade do Porto, Rua Roberto Frias 4200-465 Porto, Portugal

[3]Department of Biomedical Sciences, Institute of Medical Sciences, University of Aberdeen, Foresterhill, Aberdeen, AB25 2ZD, UK

[4]Department of Materials Science and Metallurgy, University of Cambridge, Pembroke Street, Cambridge, CB2 3QZ, UK, and St John's College, Cambridge, CB2 1TP

Journal of Materials Science: Materials in Medicine 13:1123-1127 2002

Abstract

The aim of this study was to determine the effect of the incorporation of silicon on the surface charge of hydroxyapatite (HA) and to assess surface structural changes of HA and Si-HA induced by dissolution in a static and dynamic system. X-ray photoelectron spectroscopy (XPS) analysis showed that $SiO4^{-4}$ groups were substituted for $PO4^{-3}$ groups in the silicon-hydroxyapatite (Si-HA) lattice according to a previously proposed substitution mechanism without formation of other crystalline phases, such as tricalcium phosphate or calcium oxide. The substituted silicon induced a decrease in the net surface charge and the isoelectric point of HA as determined by zeta potential (ZP) measurements. At physiological pH=7.4 the surface charge of Si-HA was significantly lowered compared to unmodified HA, i.e. -50 ± 5 eV to -71 ± 5 eV, caused by the presence of silicate groups in HA lattice, which may account for a faster *in vitro* apatite formation using SBF testing. XPS results indicated that silicon seems to be preferentially leached out from Si-HA surface compared to other ionic species after dissolution studies in tris-buffer using a dynamic system.

Keywords**:** Silicon-Substituted Hydroxyapatite, Dissolution, Zeta Potential, XPS

Introduction

In the 1970´s several groups demonstrated that bone mineralization requires a minimum concentration of soluble silicon [1-4] and Voronkov suggested that gene activation by silicon may be due to the presence of Si-O bonds within the DNA and RNA and he concluded that silicon is an inherent component of nucleic acids where it substitutes P^{5+}[5]. Hench reported that the deterioration in the proliferation and function of osteoblasts due to osteopenia and osteoporosis are related with the loss of biologically available silicon [6] and according to Keeting *et al* bone cells in culture proliferate more rapidly in the presence of soluble silicon [7]. These studies clearly demonstrate the enormous advantage of the incorporation of silicon in the biomaterials lattice aimed at regenerating bone tissue.

Specifically related to the biomaterials field, glasses and glass-ceramics with SiO_2– based components have been developed and are now being used in several clinical applications [8]. When these materials are introduced in physiological solutions the reactions involving the silicate groups are very rapid, which enhances the bioactivity of materials [9] leading to the formation of an apatite layer on the surface. *In vivo* a similar layer is also observed at the bone/implant interface [8].

In order to take advantage of the positive biological effect of silicon a new apatite bioceramic has been developed, Si-substituted hydroxyapatite (Si-HA), using a chemical precipitation route [10, 11]. Previous studies have shown that the silicon substitution resulted in enhanced cell activity *in vitro* [12] and increased bone apposition/ingrowth *in vivo* [13] relative to stoichiometric hydroxyapatite.

It is well known that surface charge plays an important role in the cell adhesion process [14-16]. Cells adhere on both positively and negatively charged surfaces but the morphology of adhering cells may vary depending on the sign of the electrical charge [16, 17]. Numerous studies have demonstrated that the surface structure and composition of bioceramics influence their cytocompatibility and affect the sequence of steps that lead to bone bonding [18-23].

The aim of this study was to determine the effect of the incorporation of silicon on the surface charge of HA and to assess surface structural changes of HA and Si-HA induced by dissolution testing performed in a SOTAX-Flow through dissolution system. Surface charge was calculated by electrophoretic mobility and surface analysis by Fourier transformed infra-red spectroscopy (FTIR) and X-ray photoelectron spectroscopy (XPS).

Material and Methods

The preparation of the Si-HA was done using a precipitation chemical route and is fully described elsewhere [11, 12]. Sintered powders of the HA and Si-HA materials were prepared by compacting the as-precipitated powders and sintering them at 1300^{o}C and then grinding/milling the sintered specimens to form a fine powder. Powders with a specific granule size (between 20-53 μm) were selected for use in this study by sieving in a variety of sieve sizes.

To determine phase purity of the precipitated material used in this study X-ray diffraction (XRD) was performed using a Siemens D5000 X-ray diffractometer. Data were collected between 25º and 40 2 θ using a step size of 0.02^{o} and a count time of 2.5 seconds. Phase identification was carried out by comparing the peak positions of the diffraction patterns with ICDD (JCPDS) standards. The X-ray fluorescence confirmed the incorporation of 0.8 wt % Si and 1.2 wt % Si in the HA lattice using a Philips PW1606 spectrometer. Surface charge was measured in 10^{-4} M KNO_3 solution in a Zeta meter 3.0+ System at different values of pH ranging from 3 to 10, according to Smoluchowki`s equation:

$$ZP = \frac{4\pi \times \eta}{D} \times EM \qquad \text{(Eq.1)}$$

where η, D and EM are the viscosity, in poise, and the dielectric constant of the suspending liquid and electrophoretic mobility, respectively.

The dissolution of HA and Si-HA in a static system was assessed, whereby sintered samples were soaked in a simulated body fluid (SBF K-9). In addition to studying the dissolution in a static environment, this test would distinguish between the ability of an apatite layer to form on a HA and a Si-HA surface. Polished dense (98% of the theoretical density of HA) discs were placed into 20 ml of SBF K-9 solution and incubated at 37^{o}C and pH = 7.4 for periods of time between 0 and 28 days. After each time point, the Ca^{2+} and PO_4^{3-} ion concentration of the SBF solution was measured using inductively coupled plasma-emission spectrometry, ICP-ES (Department of Geology, Imperial College, London).

As an alternative to the static dissolution experiment a dynamic dissolution test was performed in a Flow Through Dissolution System (Sotax CE6, a fraction collector Sotax C-160) in a Tris-hydroxymethyl amino-methane buffer solution at 37ºC and pH = 7.4 using a flow rate of 5.0 ml/min.

The HA and Si-HA powders were analysed by XPS and FTIR before and after the dynamic dissolution test. In the XPS analyses Mg-Kα was used as the radiation source and spectra referred to adventitious carbon at 285.0 eV. A Gaussian-Lorentzian function was applied for fitting the spectra using the XPSPEAK Version 4.0 software. FTIR spectra were obtained using a System 2000 FT-IR/NIR FT-Raman with a resolution of 4 cm^{-1} and by averaging 100 scans.

Results

The X-ray diffraction patterns of the HA and 1.2 wt% Si-HA sintered powders are presented in Figure 1. The substitution of silicon into the HA lattice did not affect the phase composition, as no secondary phases, such as tricalcium phosphate or calcium oxide, were formed.

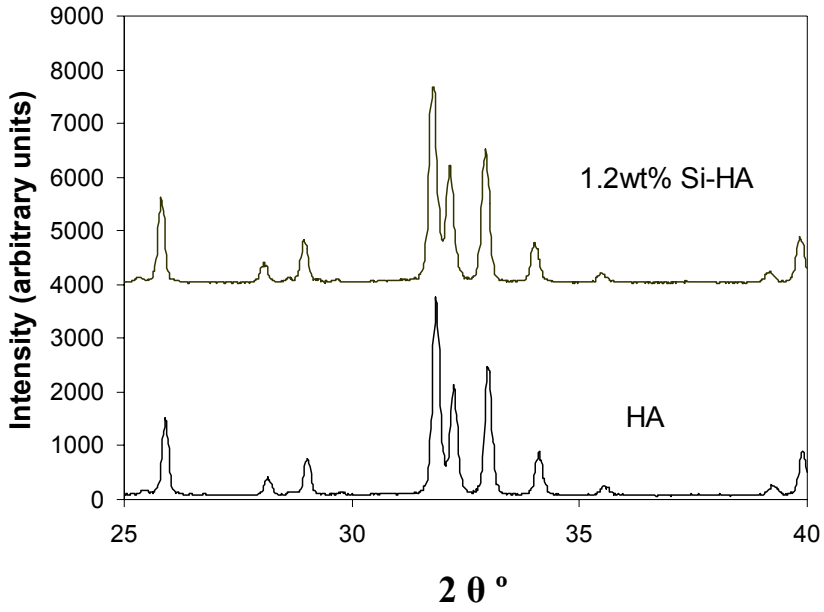

Figure 1- X-Ray diffraction patterns for HA and Si-HA.

Figure 2 shows the FTIR spectra of HA and Si-HA. In the spectrum of HA is possible to observe the peaks that correspond to PO_4^{3-} group, 1089, 1046, 958, 600 and 569 cm^{-1} and to the OH^- group, 3570 and 630 cm^{-1}, whose wavelengths are in accordance with literature values [25]. For the 1.2 wt % Si-HA, two additional peaks were detected at 888 and 504 cm^{-1} that can be assigned to the SiO_4^{4-} group [26]. It is also worth noting that the peak that

corresponds to the OH^- group at 630 cm^{-1} underwent a significant decrease in intensity with the introduction of silicon in to the HA lattice.

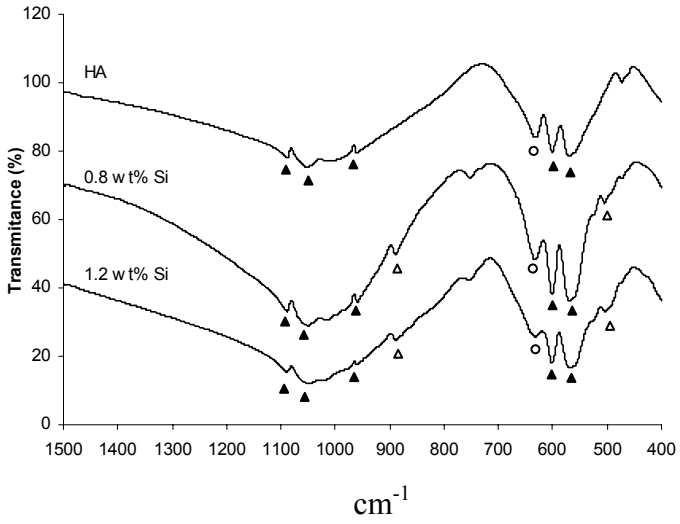

Figure 2 – FTIR spectra of HA, 0.8 wt % Si-HA and 1.2 wt % Si-HA.
▲ – PO_4^{-3}; △ - SiO_4^{-4}; ○- OH^-

The results in Figure 3 showed that the isoelectric point of HA was at a pH≈5.5 and with the substitution of 0.8 wt % of silicon in to the HA, a shift was observed towards a lower pH≈3.8. Another interesting observation was that at a physiological pH=7.4±0.1 the zeta potential of HA was –50 ± 5 eV, whereas the zeta potential for 0.8 wt % Si was -71 ± 5 eV. Therefore, a significant shift to more negative values as a result of silicon substitution was observed.

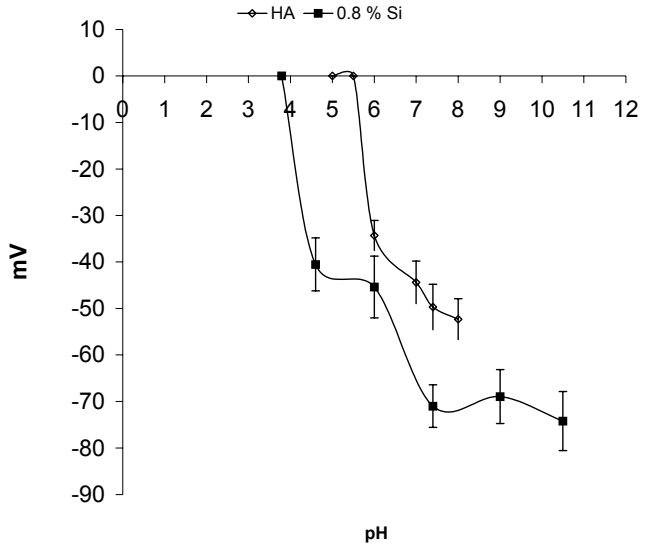

Figure 3 – Zeta potential values of HA and 0.8 wt % Si-HA.

Soaking HA and 1.2wt% Si-HA samples in a simulated body fluid for periods of up to 28 days showed two different results. Firstly, at the first time point (7 days) both the HA and the Si-HA behaved similarly, showing an increase in the calcium and phosphate ion content of the SBF solution, which corresponded to dissolution of these ions from the test specimens (Figure 4 and 5). It should be noted that the increase in the Ca^{2+} ion content (approximately 0.3mmol/l) was significantly greater than the increase in the PO_4^{3-} ion content (0.05mmol/l). Secondly, the Si-HA sample resulted in a rapid decrease in the ion concentration of the SBF after 7 days, whereas the same behaviour in the HA sample appeared to be delayed by several days. This decrease in the calcium and phosphate ion concentration corresponded to the precipitation of an apatite phase from the SBF solution on to the surface of the test specimens, as confirmed by SEM (data not shown). Although the HA sample initially resulted in the continued dissolution of calcium ions after 7 days, it is interesting to note that when the behaviour of both materials changed from dissolution to precipitation/apatite layer formation, the decrease in the calcium and phosphate ion contents was approximately 1mmol/l and 0.6mmol/l, respectively. The Ca/P molar ratio of this decrease corresponds to approximately 1.66, which correlates to a hydroxyapatite-like phase being formed from the solution.

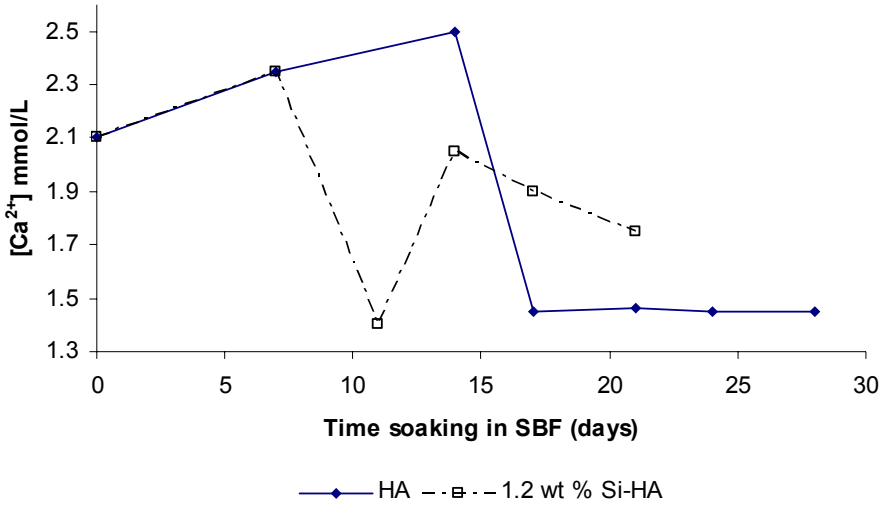

Figure 4 – $[Ca^{2+}]$ concentration in SBF

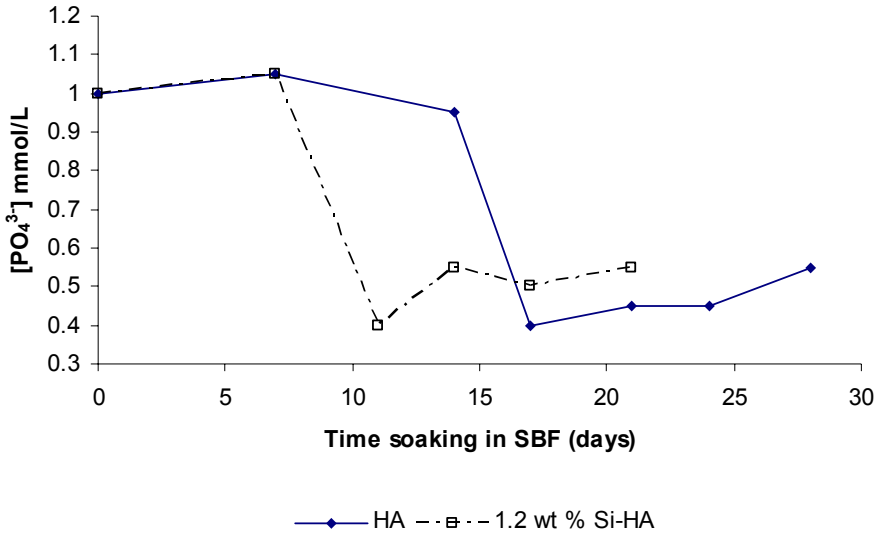

Figure 5 – $[PO_4^{3-}]$ concentration in SBF.

Comparing the FTIR spectra of HA before and after dissolution no significant change was detected. For Si-HA, however, a decrease in the peak intensities that correspond to the most important groups (SiO_4^{4-}, OH^- and PO_4^{3-}) was observed.

The FTIR results were complement with XPS analysis of the surface of samples before and after dynamic dissolution testing, and although only small changes in the atomic percentage of Ca^{2+}, P^{5+}, and O^{2-} could be quantified after dissolution (see Table 1), the Si^{5+} showed a decrease after dissolution, indicating preferential release. From the Figure 6, which shows the silicon peak detected in the Si-HA, the binding energy at 101 eV corresponds to (Si-O) bonding [27].

Table 1 – Relative atomic percentages of Ca, P, O and Si elements before (b) and after (a) dynamic dissolution testing.

	Ca	P	O	Si
HA – b	23.31	16.60	60.09	-
HA – a	23.03	17.58	59.39	-
1.2 wt % Si-HA - b	23.46	15.98	59.28	1.28
1.2 wt % Si-HA - a	22.71	15.85	60.42	1.02

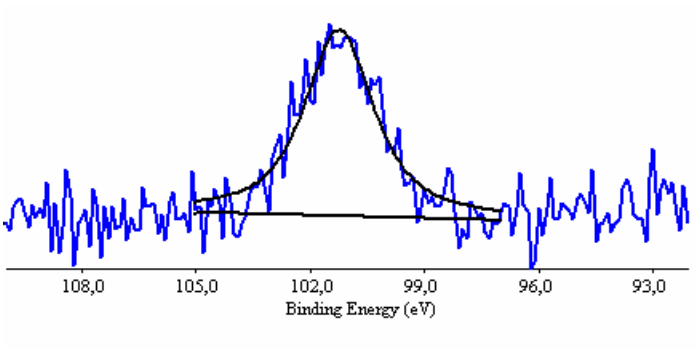

Figure 6 – XPS spectra of 1.2 wt % Si-HA.

Discussion and Conclusion

Analysis of the HA and Si-HA compositions produced for this study using XRD and FTIR confirmed that the proposed mechanism of silicon (or silicate) substituting for phosphorus (or phosphate), in accordance with the results reported previously [12]. The analysis by XPS, however, has been able to confirm conclusively that the silicon does exist as a tetrahedral silicate, SiO_4 group, rather than as a polymeric or as a SiO_2 form. This important finding supports the analogy between silicon, or silicate substitution with the well-characterised carbonate substitution of phosphate groups in hydroxyapatite.

The displacement observed in the zeta potential curves is attributed to the substitution of some PO_4^{-3} groups by SiO_4^{-4} groups that occurred in the Si-HA material, which can be explained by the mechanism of substitution showed in equation (2).

$$10Ca^{2+} + (6\text{-}x)PO_4^{3-} + xSiO_4^{4-} + (2\text{-}x)OH^- \rightarrow Ca_{10}(PO_4)_{6-x}(SiO_4)_x(OH)_{2-x} \quad \text{(Eq.2)}$$

In fact, it is known that PO_4^{-3} groups are preferentially located at HA surface [28] and therefore the substitution of these ions for SiO_4^{-4} groups should result in a decrease in surface charge, as indicated by zeta potential measurements. The decrease of intensity of the peak in the FTIR spectra that corresponds to the OH^- group on the Si-HA was expected since according to the mechanism of equation (2) the substitution of the phosphate group for the silicate group leads to some OH^- loss in order to maintain the charge balance.

FTIR and XPS results clearly support the substitution mechanism of equation 2 for Si-HA. Vibrational wavelength of 888 cm^{-1} and 504 cm^{-1} indicate the presence of SiO_4 and the binding energy of silicon at 101 eV corresponds to (Si-O) bonding [27].

To complement the above-mentioned interpretation, zeta potential results indicate the dislocation of zeta potential of Si-HA towards negative values compared to unmodified HA. Literature reveals that PO_4^{3-} seem to be preferentially located at surface of HA, which may somehow contribute to the lower Ca/P ≈ 1.4 observed under XPS analysis when compared to the stoichiometric value of Ca/P ≈ 1.67 since under this technique only around the first nanometers are analysed.

Soaking the HA and the 1.2wt% Si-HA samples in a simulated body fluid produced comparable trends, but differed in the time-scale of the events. In particular, the Si-HA changed from a dissolution behaviour (increased ion concentration in the SBF solution) to a surface precipitation behaviour (a decrease in ion concentration in the SBF solution) in less time than the HA sample. This result may be due to a greater solubility of the Si-HA material, leading to a faster super-saturation of the SBF solution and therefore a faster precipitation of an apatite layer from the super-saturated SBF. The data in Figure 4 and 5 does, however, suggest that the Ca^{2+} and PO_4^{3-} ion concentrations of the SBF solutions from the HA and Si-HA samples were comparable at 7 days, which is the measured time point before apatite layer formation occurred with the Si-HA. The surface properties of the HA and Si-HA ceramics may therefore have controlled the time-scale for the change from dissolution to apatite precipitation. The results in this study show that the surface charge/zeta potential of the two materials were significantly different at pH=7.4. The more electronegative Si-HA surface may provide a preferential site for the nucleation of an amorphous calcium phosphate apatite layer than the HA surface. This could occur via the adsorption of Ca^{2+} ions onto the electronegative surface, resulting in an increase in surface charge and the attraction of phosphate groups. The effect of the real-time formation of an apatite layer on the surface charge of Si-HA and HA will be studied in the future.

Due to low dissolution rate of the materials under study, a higher amount of silicon was incorporated in the material to be analysed (1.2 wt % Si) in the dissolution testing. No compositional modification was detected for HA before and after dissolution, as shown in Table 1. However, preferential ionic release of silicon was observed for Si-HA. Previous results showed that the silicon substitution caused a substantial increase in distortion index of HA and a decrease in the number OH^- groups [29]. It is possible that these lattice disturbances by silicon incorporation may lead to higher susceptibility of SiO_4^{4-} release from HA structure.

Acknowledgement

The authors wish to acknowledge the financial support of ref. SFRH/BD/6173 grant financed by FCT (Fundação para a Ciência e Tecnologia).

References

[1] E. M. CARLISLE, *Fed. Proc.,* **43** (1984) 680.

[2] E. M. CARLISLE, in: *Silicon Biochemistry,* (D. Evered and M. O'Connor, eds.), Wiley, New York 1986.

[3] K. SCHWARZ, in: *Biochemistry of Silicon and Related Problems.* (G. Bendz and I. Lindqvist, eds.), Plenum Press, New York (1978), 207-230.

[4] K. SCHWARZ, AND D.B. MILNE, *Nature* **239** (1972) 333.

[5] M.G.VORONKOV, V. I. SKOROBOGATOVA, E.K. VUGMEISTER, V. MAKARSKII, *Dok/ady Biochemistry* **222** (1975) 29.

[6] L.L. HENCH, in: Sol-Gel Silica Properties, Processing and technology Transfer, (1999), chapter 10 Biological Implications, 116-163.

[7] P.E. KEETING, M.J OURSLER, K.E. WEIGAND, S.K. BONDS, T.S. SPELSBERG, B.L. RIGGS, *J Bone Minera/ Res.* **7** (1992) 1281.

[8] L.L. HENCH, *J. Phys.* **43** (1982) 625.

[9] L.L. HENCH, *J. Am. Ceram. Soc*. **74** (1991) 1487.

[10] L.L. HENCH, J. WILSON; An Introduction to Bioceramics, World Scientific Publishing Co. Pte. Ltd., (1999).

[11] L.J. JHA, S. BEST, J.D. SANTOS, I.R. GIBSON, W. BONFIELD, Silicon-Substituted Apatites and Process for the Preparation Thereof, Worldwide patent, PCT/GB97/02325 and US Patent Serial Nº 09/147773, 1999.

[12] I.R. GIBSON, S.M. BEST, W. BONFIELD, *J. Biomed. Mat. Res*., **44** (1999) 422.

[13] I.R. GIBSON, J. HUANG, S.M. BEST, W. BONFIELD, pp. 191-194 in Bioceramics, Vol. 12, Proceedings of the 12th International Symposium on Ceramics in Medicine (Nara, Japan November 1999). Edited by H. Ohgushi, G.W. Hastings and T. Yoshikawa. World Scientific Publishing Co. Pte. Ltd., London, 1999.

[14] I.R. GIBSON, K.A. HING, P.A. REVELL, J.D. SANTOS, S.M. BEST, W. BONFIELD, *Key Engin. Mat.* **218-2** (2002) 203.

[15] N.G. MAROUDAS, *J. Theoret. Biol.* **49** (1975) 417.

[16] P.B. van WACHEM, A.H. HOGT, T. BEUELING et al., *Biomaterials* **8** (1987) 323.

[17] J.E. DAVIES, In: Ratner BD, editor, Surface characterization of biomaterials, Amsterdam, Elsevier, (1998), 219-34.

[18] R.M. SHELTON, A.C. RASMUSSEN, J.E. DAVIES, *Biomaterials* **9** (1988) 24.

[19] P. DUCHEYNE, J. BEIGHT, J. CUCKLER, B. EVANS, AND S. RADIN, *Biomaterials* **11** (1990) 531.

[20] H. OHGUSHI, V.M. GOLDBERG, AND A.I. CAPLAN, *J. Orthop. Res.* **7** (1989) 568.

[21] G. DACULSI, R.Z. LE GEROS, E. NERY, K. LYNCH, B. KEREBEL, *J. Biomed. Mater. Res.* **23** (1989) 883.

[22] K. HYAKUNA, T. YAMAMURO, Y.KOTOURA, Y. KAKUTANI, T. KITSUGI, H. TAKAGI, M. OKA, T. KOKUBO, *J. Biomed. Mater. Res.* **23** (1989) 1049.

[23] Y. KOTOURA, T. YAMAMURO, J. SHIKATA, Y. KAKUTANI, T. KITSUGI, K. HYAKUNA, H. TANAKA, *Orthop. Res. Sci*. **13** (1986) 633.

[24] T. FUJIU, M. OGINO, *J. Biomed. Mater. Res.* **18** (1984) 845.

[25] I. REHMAN, W. BONFIELD, *J. Mat. Sci.: Mater. in Med.* **8** (1997) 1.

[26] RICHARD A. NYQUIST, CURTIS L. PUTZIG, AND M. ANNE LEUGERS, *Infrared and Raman Spectral Atlas of Inorganic Compounds and Organic Salts,* **3** (1995).

[27] NIST – National Institute of Standards and Technology Database.

[28] W. VAN RAEMDONCK; P. DUCHEYNE, AND P DE MEESTER, *Metal and Ceramic Biomaterials, CRC Press, chp. 6* (1984) 143-146.

[29] I.R. GIBSON, L.J. JHA, J.D. SANTOS, S.M. BEST AND W.BONFILED, Bioceramics, Vol. 11, Proceedings of the 11th International Symposium on Ceramics in Medicine (New York, NY, USA, November 1998). Edited by R. Z. LeGeros and J. P. LeGeros, World Scientific Publishing Co. Pte. Ltd., USA, 1998.

Ultrastructural comparison of dissolution and apatite precipitation on hydroxyapatite and silicon-Substituted hydroxyapatite *in vitro* and *in vivo*

Alexandra E. Porter[1], Claudia M. Botelho[2,3], Maria A. Lopes[2,3], José D. Santos[2,3], Serena M. Best[1], and William Bonfield[1]

[1]Department of Materials Science and Metallurgy, University of Cambridge, Pembroke Street, Cambridge, CB2 3QZ, UK.

[2]INEB- Instituto de Engenharia Biomédica, Laboratorio de Biomaterials, Rua do Campo Alegre, 823, 4150-180 Porto, Portugal.

[3]FEUP- Faculdade de Engenharia da Universidade do Porto, DEMM, Rua Dr. Roberto Frias, 4200-465 Porto, Portugal.

Journal of Biomedical Materials Research 69a:670-679, 2004

Abstract

Recent histological studies have demonstrated that the substitution of silicate ions into hydroxyapatite (HA) significantly increases the rate of bone apposition to HA implant. The enhanced bioactivity of silicon-substituted HA (Si-HA) over pure HA has been attributed to the effect of silicate ions in accelerating dissolution. In the present study, high-resolution transmission electron microscopy (HR-TEM) was employed to compare dissolution of HA and Si-HA in an acellular simulated body fluid (SBF) to dissolution in an *in vivo* model.

HR-TEM observations confirmed a difference in morphology of apatite precipitates *in vivo* and in SBF: apatite deposits were plate like *in vivo* and nodular in SBF. Compositional mapping suggested that preferential dissolution of silicon from the implant promotes the nucleation of carbonate apatite around the implant. The i*n vivo* findings illustrated an absence of dissolution at the bone-HA or Si-HA interface, whereas dissolution was extensive from within the implant. The amount of dissolution in acellular SBF was similar to dissolution from within the implant, although the site at which dissolution nucleates was different: dissolution predominates at crystallite surfaces in SBF, whereas, grain

boundary dissolution predominates *in vivo*. These findings suggest that proteins in the *in vivo* milieu modify the processes of dissolution from the implant.

***Keywords*:** Dissolution, Silicon, Simulated Body Fluid, Ultrastructure, Precipitation.

Introduction

Hydroxyapatite (HA) possesses a hexagonal Bravais lattice and a $P6_3/m$ space group with cell dimensions of a = 9.1404 and c = 6.8747 Å, and is known to be bioactive [1, 2]. The substitution of silicate ions (SiO_4^{4-}) for phosphate ion tetrahedra (PO_4^{3-}) in the HA unit cell has been shown to have the potential to increase the rate and amount of bone apposition to HA bioceramic implants [2]. However, uncertainty remains about the mechanism by which silicate ion incorporation increases the *in vivo* bioactivity. In previous studies, defect structures in silicon-substituted HA (Si-HA) were observed and characterized using high-resolution transmission electron microscopy (HR-TEM) [1]. Phase pure, sintered granules of HA and Si-HA were implanted for 6 and 12 weeks in an ovine model. Samples containing the bone-implant interface were prepared for TEM via ultramicrotomy using an anhydrous sample preparation procedure. HR-TEM was used to compare the *in vivo* reactivity of sintered granules of HA and Si-HA at both 6 and 12 weeks [3].

Recent HR-TEM results revealed the presence of dislocations and grain boundaries in pure HA and Si-HA with a significant increase in density of triple junctions per unit area in Si-HA over pure HA [1]. Dissolution was found to be particularly prevalent at grain boundaries and triple junctions *in vivo* and followed the order 1.5 wt% Si-HA > 0.8 wt% Si-HA > pure HA [3]. These findings suggested that increased numbers of defects in Si-HA play a significant role in increasing the rates of dissolution of calcium, phosphate and silicate ions from Si-HA.

As an alternative approach to using *in vivo* studies for evaluating the bioactivity at the bone-biomaterial interface, *in vitro* immersions in simulated body fluid (SBF) or cell-containing media may be employed. The commonly proposed mechanism underlying the phenomenon of the bioactivity of HA involves the dissolution of calcium and phosphate ions from HA [4]. This process may occur through the surrounding environment (extracellular fluid) and may also be actively mediated by osteoclast cells [5]. Dissolution generates increased concentrations of calcium and inorganic phosphate in the spaces between the existing bone and the implant [4]. Precipitation of HA into this space will ensure

incorporation of the implant into the existing bone [6]. It is commonly believed that dissolution and reprecipitation of apatite crystallites promote incorporation of biological molecules [7].

The evaluation of bioactivity using *in vitro* immersion techniques have been criticized because they do not fully replicate the complicated series of dynamic reactions that occur at the bone-biomaterial interface *in vivo*. In particular, the biological response of CaP biomaterials implanted *in vivo* might be different from that evaluated with standard *in vitro* tests because of the interaction of calcium phosphate compounds with the complex array of constituents in the body, in particular macromolecules. Nevertheless, these systems aid evaluation of specific cellular and proteinaceous responses at the bone-implant interface [8-11]. *In vitro* studies also minimize the need for animal experiments and offer potential to study the dissolution-reprecipitation mechanism at very early time points.

A recent study demonstrated that many interfacial reactions are paralleled *in vivo* and *in vitro* [12]. A study by Fujibayashi *et al* comparing *in vivo* bone ingrowth and *in vitro* apatite formation on Na_2O-CaO-SiO_2 glasses illustrated that the depth of bone ingrowth among glass particles increased in proportion to their apatite forming ability *in vitro* [12]. The *in vitro* results of an investigation of the apatite forming ability of Si-HA with several compositions, corroborate our histological *in vivo* studies: the time required to form a surface apatite layer on Si-HA in SBF decreased with increasing silicate ion substitution [11]. Furthermore, silicate ion substitution stimulates osteoblast-like cell activity *in vitro* when compared to stoichiometric HA. Despite these similarities on the microstructural scale, questions remain as to whether mechanisms of apatite dissolution and precipitation at the ultrastructural level are similar in both *in vivo* and *in vitro* model systems.

The objective of the current study was to use HR-TEM to compare *in vitro* dissolution of ultrathin (<90 nm) sections of HA and Si-HA in acellular SBF at 6 hours, 1 and 3 days, with the results of a previous study investigating dissolution and bone remodelling around pure HA, and Si-HA (0.8 and 1.5 wt%) *in vivo* [13]. We proposed that the combination of *in vivo* and *in vitro* studies may lead to an improved understanding of surface reactions of bioactive ceramics in the body and their effects on bone formation and cell function. Only a few studies have investigated the ultrastructure of apatite deposits in SBF solutions [14]. The lack of information that describes ultrastructural characteristics arises from the difficulty of preparing samples for TEM observation. This study develop a simple, alternative methodology for preparing samples for *in vitro* TEM observation.

Material and Methods

Chemical Synthesis

Phase pure HA with a Ca/P molar ratio of 1.67 was prepared by a precipitation reaction between calcium hydroxide [$Ca(OH)_2$] and orthophosphoric acid, [H_3PO_4] solution according to the methods described elsewhere [15]. Two types of Si-HA (0.8 wt% and 1.5 wt%) were also prepared by acid-base neutralization reactions according to the methods of Gibson *et al* [16]. In addition to calcium hydroxide and orthophosphoric acid, silicon acetate [$Si(CH_3COOH)_4$] was incorporated into the reaction mixture as a source of silicate ions. The quantities of reactants were calculated by assuming that silicate ions would substitute for phosphate ions in the HA lattice. Therefore, the number of moles of H_3PO_4 in phase pure HA was the same as the number of moles of H_3PO_4 + $Si(CH_3COOH)_4$ for the Si-HA samples, with the number of moles of $Ca(OH)_2$ being kept constant. Precipitation reactions were carried out at room temperature and the pH was maintained at 10.5 by the addition of ammonium hydroxide solution. After complete mixing of the reactants, the suspensions were aged overnight. The resulting precipitates were filtered, washed and dried at 80 ^oC overnight.

Sample Preparation

HA and Si-HA were prepared both as powders to compare dissolution in SBF and as granules to compare dissolution *in vivo*.

Aged, filtered and dried precipitates of pure HA and 1.5 wt% Si-HA were ground into a fine powder. The powders were subsequently calcined at 1200 ^oC for 120 minutes using a ramp rate of 2.5 ^oC/minute. An X-ray fluorescence (XRF) analysis was performed from previous work [3] showed the Ca/P molar ratio of the pure HA to be 1.67, which is equivalent to stoichiometric HA. The Ca/(P+Si) molar ratios of 0.8 wt% Si-HA and 1.5 wt% Si-HA were 1.68. The X-ray diffraction (XRD) measurements for HA powders indicated that the sintered HA, 0.8 wt% and 1.5 wt% Si-HA were phase pure, with no additional phases present. The effect of the silicate ion substitution on the crystal structure of HA was determined by Rietveld structure refinement of the XRD data. Silicate ion substitution resulted in a decrease in the *a* axis and an increase in the *c* axis of the unit cell of HA and a slight decrease in the unit cell volume. These results suggest that the larger silicate ion (SiO_4^{4-}) substitutes for the phosphate (PO_4^{3-}) group in the HA lattice [1].

Embedding of the HA and Si-HA powders

Powders of HA and Si-HA were treated with three changes of 100% ethanol and three of propylene oxide over 1 hour, and then infiltrated with Spurr's resin (Agar Scientific, Essex, UK) over several days: Spurr's resin was prepared with 10 g epoxy monomer vinyl cyclohexene dioxide (ERL), 4.5 g diglycidyl ether of polypropylene glycol (DER-736), 26 g nonenyl succinic anhydride (NSA), and 0.7 g benzlydimethylamine (BDMA). The samples were agitated at room temperature in 1:1 solutions of propylene oxide and Spurr's resin for 2 days, 1:3 solutions of propylene oxide/Spurr's resin for 1 day, then 100% Spurr's for 2 weeks under vacuum. The Spurr's resin was changed every 24 hours. Samples were then cured in fresh Spurr's resin for 23 hours at 60 ^{o}C. Pre-casting a ~ 200 μm layer of Spurr's resin into the truncated beam capsules before adding the HA powders facilitated sectioning of the blocks.

Dispersion of powders in SBF and transmission electron microscopy preparation

Sections (90 nm) of HA, 0.8 wt% Si-HA and 1.5 wt% Si-HA powders were cut onto a water bath using a diamond knife a Leica Ultracut. Sections were collected on lacey carbon support gold TEM grids and most of these were dispersed in SBF solutions [9] at a pH of 7.4, at 37 ^{o}C for 6 hours, 1, 3 and 5 days. It was assumed that convection would be sufficient to stir the SBF solutions. The fluid was prepared by dissolving reagent-grade NaCl, KCl, $K_2HPO_4 \cdot 3H_2O$, $MgCl_2 \cdot H_2O$, $CaCl_2$, and $NaSO_4$ into distilled water and buffered to pH 7.4 with tris [hydroxymethyl]aminomethane, $[(CH_2OH_3)_3CNH_3)]$, and hydrochloric acid.

Transmission electron microscopy

TEM and selected area electron diffraction (SAED) were performed in a Philips CM30 operated at 300 kV. Diffraction contrast was employed for bright-field imaging.

Environmental scanning electron microscopy (ESEM)

ESEM was performed on the Phillips ESEM-FEG, XL30 in low vacuum mode, using an off axis gaseous secondary electron detector and a 10 kV operating voltage.

Results

TEM observations of sintered powders

The TEM of the pure HA, 0.8 and 1.5 wt% Si-HA powders in ethanol revealed smooth, discrete edges with no loss of mineral at the subgrain boundaries or triple junctions. An example of a representative crystallite of 0.8 wt% Si-HA is illustrated in Figure 1.

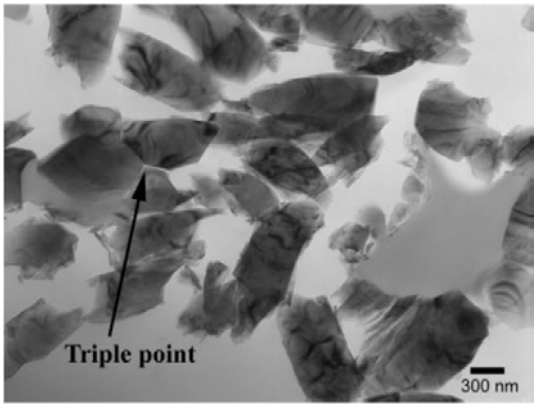

Figure 1 - ATEM micrograph of a sintered 0.8 wt% Si-HA powder, illustrating a triple-junction grain boundary.

Dispersion in Simulated Body Fluid

Pure HA

After 6 hours dispersion in SBF, the ultrastructure of the HA was preserved; there was no loss of mineral from the pure HA. After 1 day, in a few regions, apatite deposits had nucleated on the surface of the HA and in the surrounding region (Figure 2a). SAED confirmed these deposits to be crystalline. The apatite precipitates were composed of several almost nodular shaped crystals, which had agglomerated. In many regions the surfaces of the HA grains appeared mottled, suggesting dissolution had occurred (Figure 2b). This mottled morphology was present throughout the grains and was most prevalent at their surfaces. At 3 days, both dissolution and reprecipitation of apatite mineral were much more prevalent. In many regions, extensive dissolution of the HA occurred (Figure 2c) as indicated by the presence of voids and it was not related to beam damage [3]. In several regions there were needlelike crystallites that emanated from the surface of many of the HA crystallites (Figure 2c). These crystallites grew almost perpendicular to the surface of the HA crystallites (Figure 2c). The apatite deposits were associated with regions of the HA that exhibited mottled contrast (Figure 2d). In other regions there were nodular precipitates of apatite, which

nucleated on the surface of the HA (Figure 2e). Energy dispersive X-ray (EDX) analysis showed these precipitates had 55.26 wt % Ca, 41.69 wt.% P, 2.91 wt % Si in region 1; 53.94 wt % Ca, 45.96 wt % P, 0.78 wt % Si in region 2; and averages 54.60 wt % Ca, 43.83 wt % P, and 1.85 wt % Si. Indexing of the SAED patterns confirmed the precipitates to be apatite (Figure 2f).

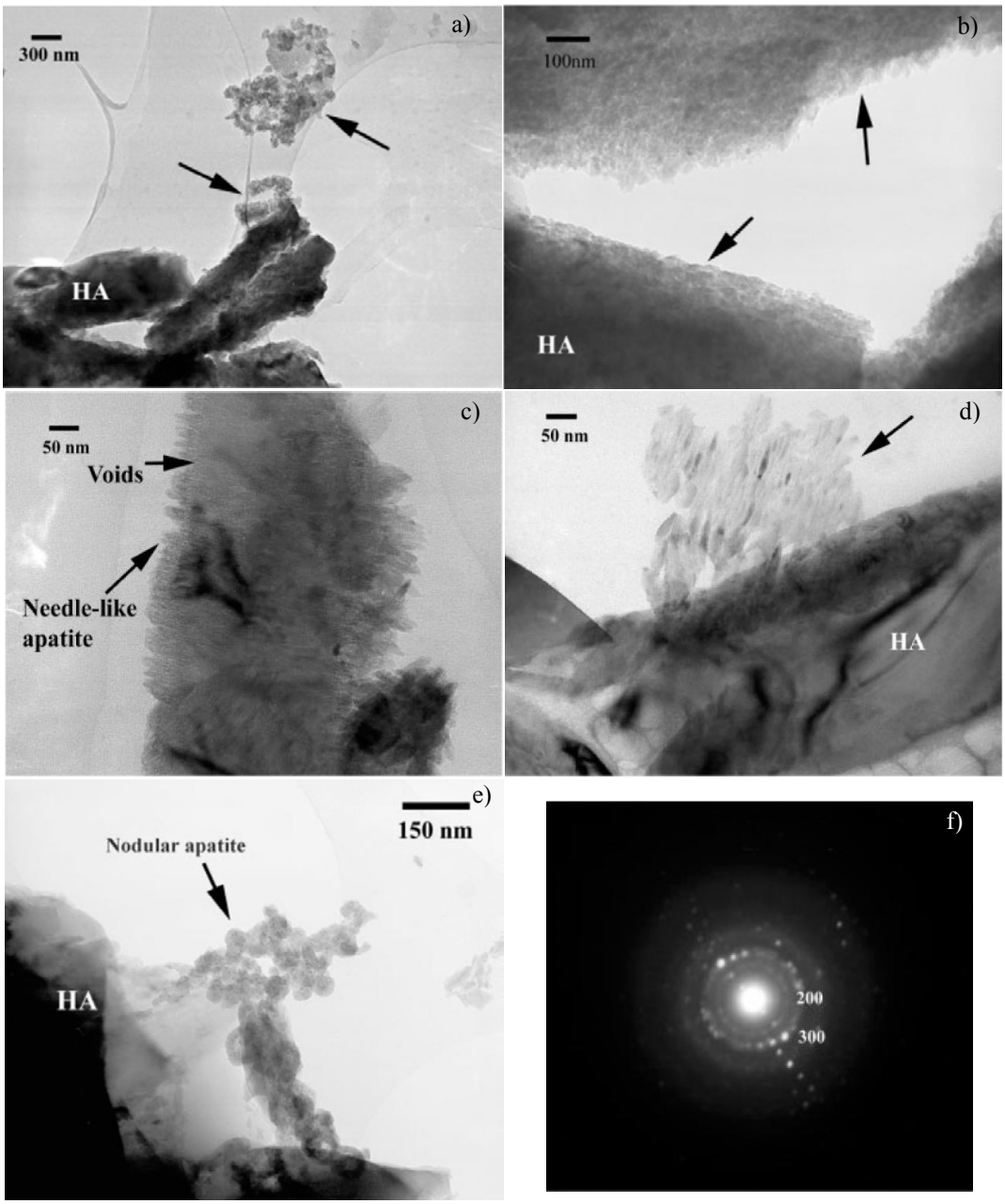

Figure 2 - TEM micrograph of grains of pure HA 1 day after dispersion in SBF, indicating (a) apatite deposits precipitated on the surface of HA and in the surrounding region (arrows) and (b) the mottled appearance of grains suggesting the occurrence of dissolution (arrows). Pure HA after 3-day dispersion in SBF, illustrating (c) needlelike crystallites emanating from

regions comprising of voids, which is related to dissolution; (d) needle-like apatite deposits precipitated on the surface of the implant; and (e) nodular precipitates of apatite, nucleated on the surface of the HA, with (f) the associated SAED pattern from the apatite deposits.

0.8 wt. % Si-HA

In general, the dissolution and reprecipitation of apatite appeared more extensive on the surface of the 0.8 wt% Si-HA grains after 6 hours dispersion in SBF solution. In a few regions the apatite deposits nucleated both on the surface of the 0.8 wt% Si-HA and in the surrounding regions (Figure 3a). Apatite deposits were also observed on the 0.8 wt% Si-HA grains at 1 day (Figure 3b). After 3 days, dissolution and reprecipitation of apatite appeared to be more extensive (Figure 3c), and many needlelike apatite deposits had nucleated in the vicinity of and on the surface of the grains (Figure 3c).

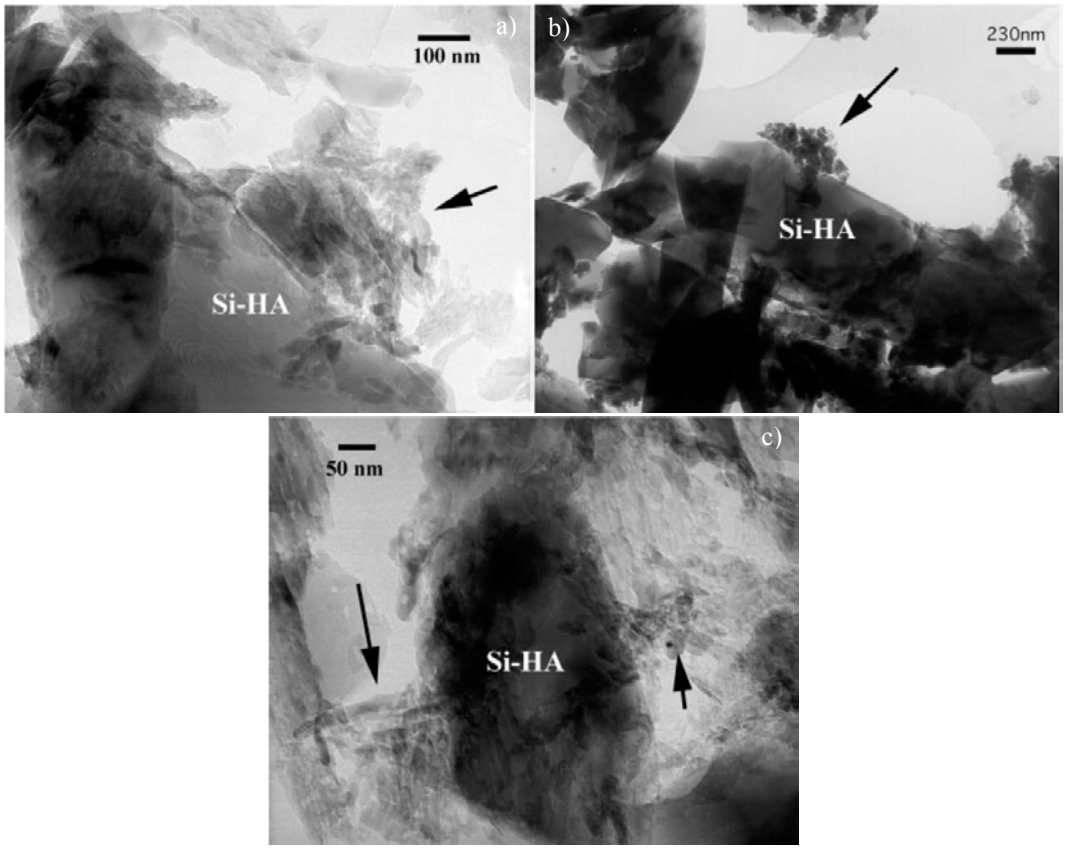

Figure 3 - TEM micrographs of 0.8 wt% Si-HA illustrating apatite deposits (a) 6 hours after dispersion in SBF; (b) 1 day after dispersion in SBF with apatite deposits nucleated on the surface of the 0.8 wt.% Si-HA (arrows), and (c) 3 days after dispersion in SBF, illustrating extensive dissolution and precipitation of apatite (arrows).

1.5 wt % Si-HA

At 6 hours, in several regions, clusters of apatite nucleated on the surface of the Si-HA and in the surrounding regions (Figure 4a). These apatite precipitates appeared to be nodular. A SAED analysis confirmed these deposits to be apatite. In other regions the Si-HA appeared to have undergone some dissolution (Figure 4b). After 1 day, dissolution and reprecipitation of the Si-HA were much more extensive than on the HA and 0.8 wt% Si-HA (Figure 4c). In several regions there were apatite deposits with needlelike morphology present and they appeared to emanate from the surfaces of grains. SAED confirmed that the precipitates were apatite. Dissolution from the surface of the Si-HA was even more extensive after 3 days in SBF (Figure 4d). Many grains appeared to have almost entirely dissolved. Furthermore, many of the grains of Si-HA were very unstable under the electron beam (Figure 4e). Indexing of the electron diffraction patterns from a dissolving grain confirmed that the dissolved regions corresponded to HA. Dissolution from the Si-HA predominated at the crystal surfaces. The apatite precipitates maintained the nodular morphology at 3 days. EDX revealed them to have 59.31wt.% Ca, 26.68 wt.% P and 3.92 wt.% Si in region 1; 47.76 wt% Ca, 49.28 wt% P, and 2.57 wt% Si in region 2; 49.18 wt% Ca, 47.99 wt.% P and 2.27 wt% Si in region 3; and averages of 52.08wt.% Ca, 41.32 wt.% P, and :2.92wt% Si.

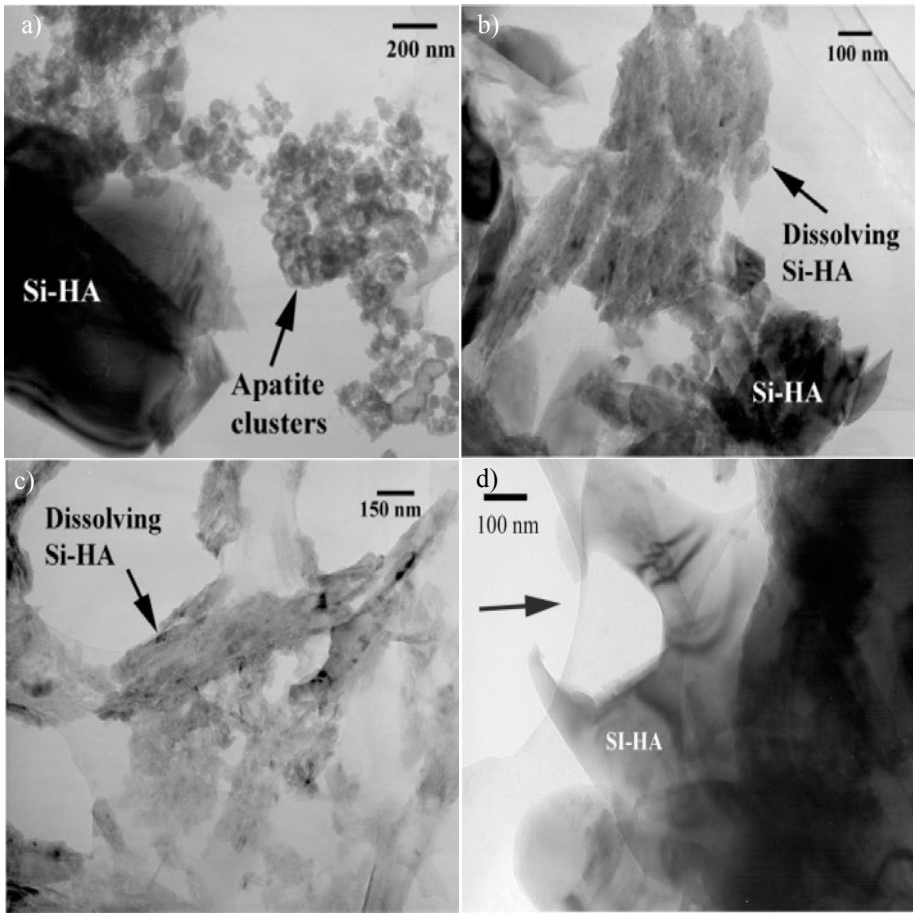

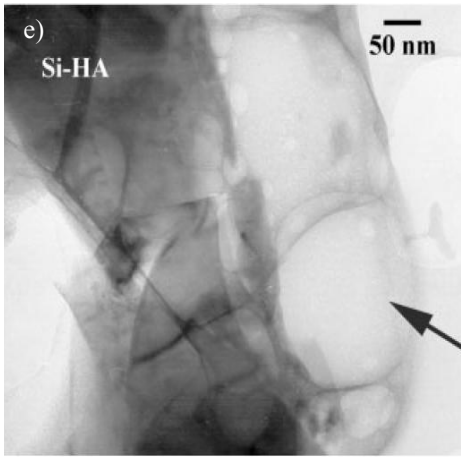

Figure 4 - TEM micrographs illustrating 1.5 wt.% Si-HA (a,b) after 6-h dispersion in SBF, showing (a) clusters of apatite nucleated on the surface of the Si-HA and in the surrounding regions, and (b) some dissolution extending throughout the grains; (c) after 1-day dispersion in SBF, illustrating apatite deposits with a needle-like morphology emanating from the surfaces of grains; (d) after 3-day dispersion in SBF, showing extensive dissolution of grains (arrow); and (e) after 3-day dispersion in SBF, indicating a grain that was particularly unstable under the electron beam (arrow).

Environmental Scanning Electron Microscopy (ESEM)

The ESEM of 1.5 wt% Si-HA after 5 days in SBF confirmed that dissolution had occurred in several regions (Figure 5a). EDX mapping revealed preferential dissolution of silicon from these dissolving regions (Figure 5b).

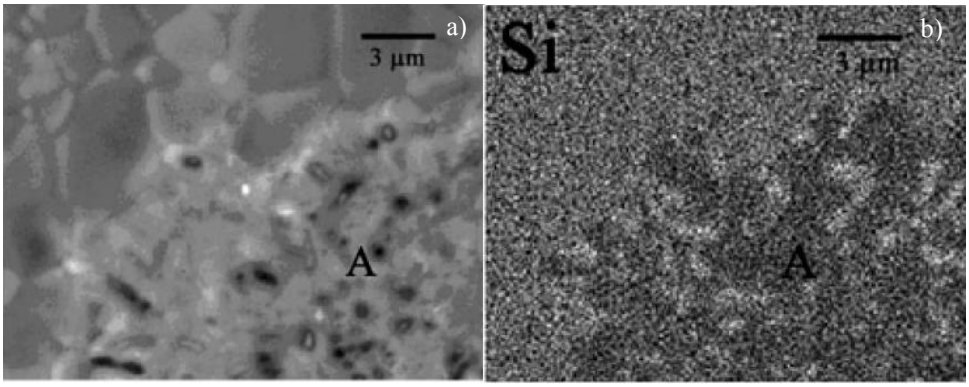

Figure 5 - ESEM of 1.5 wt.% Si-HA after 5 days in SBF (a) confirming that dissolution had occurred in several regions and (b) a corresponding EDX map revealing preferential dissolution of silicon from the dissolving regions (Region A).

In vivo study

The results of an *in vivo* study were described in a recent article [13]. Therefore, this paper only highlights the most important findings, which are relevant to this study. After 6 and 12 weeks *in vivo*, dissolution of the HA (Figure 6a) and 0.8 and 1.5 wt% Si-HA grains (Figure 6b) was not observed at the bone/implant interface of any of the ceramics, although extensive dissolution was observed within the implant (Figure 6c). After 12 weeks *in vivo*, needle-like crystallites emanated from the surface of many of the Si-HA crystallites within the implant, indicating that extensive dissolution had occurred (Figure 6c). A widespread mottled effect was observed on the surface of the 1.5 wt% Si-HA samples localized between the needle-like crystallites and the dissolving grains (Figure 6d). Dissolution within the implant predominated at the grain boundaries and triple junctions.

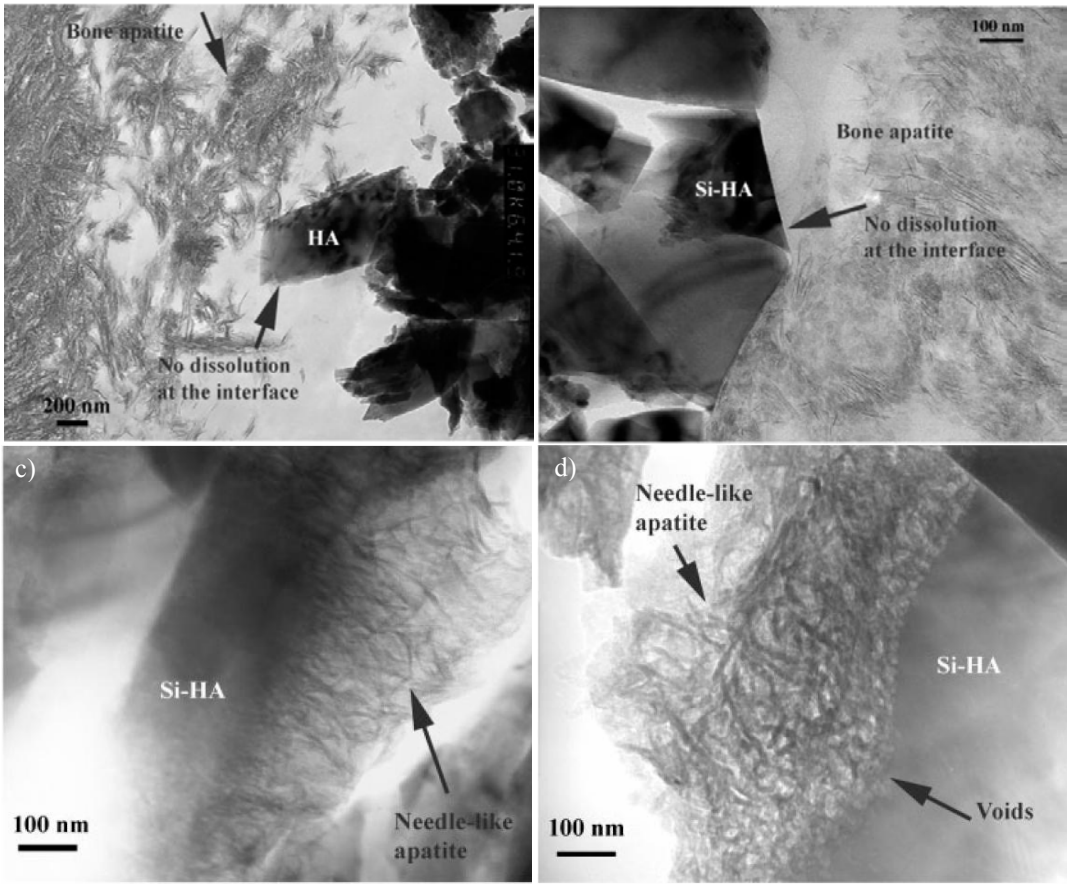

Figure 6 - TEM micrographs of the bone/implant interface after 12 weeks *in vivo,* demonstrating no dissolution of either (a) the HA or (b) the 0.8 wt.% Si-HA grains at the bone/implant interface and (c) needlelike crystallites emanating from the surface of many of the Si-HA crystallites within the implant, indicating that extensive dissolution had occurred. (d) An extensive mottled effect comprising of voids on the surface of the 1.5 wt.% Si-HA grains within the implant and localized between the needlelike crystallites and the dissolving grains.

Discussion

In vivo and *in vitro* studies have suggested that the formation of the apatite layer is an essential requirement in events leading to subsequent osteointegration of the implant [4]. The bioactivity of calcium phosphate and many other materials has been related to their propensity to nucleate carbonate apatite crystals [17]. Formation of a biologically equivalent apatite layer can be reproduced *in vitro* by immersion experiments using SBF. *In vitro* studies by Gibson *et al* demonstrated that the time required to form an apatite layer on Si-HA in SBF decreased with increasing silicate ion substitution [11]. These results corroborate *in vivo* histological findings by Patel *et al*, illustrating increased amounts of bone apposition to Si-HA implants compared to pure HA [2]. These findings demonstrate the value of SBF bioactivity tests to model the *in vivo* system. Nevertheless, uncertainty remains about whether the ultrastructural characteristics of *in vitro* dissolution-reprecipitation processes mimic those processes occurring *in vivo*.

The lack of information describing the ultrastructural characteristics of HA immersed in SBF results from the difficulty in preparing these samples for TEM observation. In the current study, a procedure was developed for preparing ultrathin samples for TEM by sectioning embedded powders using an ultramicrotome and immersing the sections in SBF. This methodology does not allow for direct comparison between the timing of events at the bone-HA and SBF-HA interface. Nevertheless, for the purpose of this study it was successful in providing a qualitative comparison of the changes in the ultrastructure of synthetic HA and apatite deposits *in vi*vo and *in vitro*.

A notable finding in this study was that the current *in vitro* results uphold *in vivo* findings of dissolution following the order 1.5 wt% Si-HA> 0.8 wt% Si-HA > pure HA after 6 and 12 weeks [3]. Dissolution of the 1.5 wt% Si-HA was extensive after 3 days in SBF, whereas dissolution was less extensive on the surface of the pure HA at 3 days. These results suggest that SBF is a valuable medium for modelling the amount of dissolution *in vivo.*

It was interesting finding in this study that the silicon content of apatite deposits surrounding the Si-HA was higher than that surrounding the pure HA after 3 days in SBF. The effect of silicic acid on calcium phosphate precipitation *in vitro* was investigated in order to test the possible involvement of silica in dental plaque as a promoter of calculus formation [18]. An *in vitro* study by Damen *et al* [19], illustrated that silica decreases the time for spontaneous precipitation of HA from supersaturated solutions with a wide range of Ca/P ratios *in vitr*o. Furthermore, the study demonstrated that silica was capable of stimulating

apatite precipitation in the presence of bacterial inhibitors to calcium phosphate precipitation [19]. The current results suggest that dissolution of silicate ions from the implant promotes the heterogeneous nucleation apatite.

In a previous study, Rietveld structural refinements clearly illustrated silicate ions were being substituted for phosphate ions in the HA lattice [1]. These HR-TEM observations confirmed that grain boundaries in pure HA and 0.4 wt% Si-HA did not contain second phases such as tricalcium phosphate or silicon-rich amorphous phases. In comparison, energy filtered TEM imaging of some triple junctions in 1.5 wt% Si-HA revealed the presence of a less crystalline phase at some the triple-junctions, extending along the grain boundaries. These combined XRD and HR-TEM observations suggested that silicon as silicate ions is generally distributed uniformly within the lattice of the HA but silicon may also be segregating as a silicon-rich secondary phase at some grain boundaries in Si-HA. A subsequent, *in vivo* dissolution study demonstrated that grain boundary dissolution was prominent in Si-HA but was not observed in phase pure HA. Instead, the presence of voids, within grains of pure HA containing dislocations at 12 weeks *in vivo* suggested that dislocations may be the major initiation sites for dissolution. These investigations of the dissolution of HA and Si-HA provided further evidence for the proposed difference in the grain boundary structure between pure HA and Si-HA. These findings suggested that the less crystalline phase is dissolving preferentially *in vivo*. If this phase were silicon rich, these results would imply preferential dissolution of silicon from the Si-HA. In an *in vitro* study using X-ray photoelectron spectroscopy (XPS), Botelho *et al* demonstrated a preferential release of silicate ions from Si-HA compared to HA [20]. The authors suggested that the incorporation of silicate ions into the HA lattice would distort and destabilize the structure, therefore making it energetically favourable for silicate ions to dissolve preferentially from the HA [20]. The current *in vitro* findings suggest that these two dissolution models are plausible. EDX mapping of the Si-HA after 5 days immersion in SBF demonstrated a preferential loss of silicon in dissolving regions of the ceramic. These results are particularly significant, because silicon has been shown to be a promoter of bone calcification [21]. If silicon is being rapidly released as a bolus from the implant, silicon may accelerate bone mineralization.

The current study also highlights the differences in apatite morphology observed *in vivo* and *in vitro*. In the *in vitro* model, apatite deposits were frequently nodular and agglomerated, whereas *in vivo* apatite deposits were plate- or needlelike. These results reflect the difference in the *in vivo* and *in vitro* environments and suggest that noncollagenous

proteins, such as phosphoproteins and albumin and also the collagen fibrils, act as the controllers of apatite nucleation, as well as growth and morphology [22].

The results of a recent HR-TEM study, which investigated dissolution from HA, 0.8wt% Si-HA and 1.5wt% Si-HA implants after 6 and 12 weeks *in vivo*, illuminated differences in the morphology of apatite deposits at the Si-HA/bone interface and within the pores of the implant [3]. Larger, needlelike crystallites were observed on the surface of the 1.5wt% Si-HA granules in the deeper regions of the implant when compared to the smaller plate like apatite crystallites at the bone/Si-HA interface. Furthermore, extensive dissolution was observed from the Si-HA within the implant, whereas no signs of dissolution were observed at the interface between the bone and the Si-HA. A study by Combes *et al* demonstrated that in the *in vitro* system proteins act not only as promoters but also as inhibitors to CaP precipitation, because the proteins slow down the ionic diffusion to the crystal surfaces [23]. This recent study hypothesized that these differences in ultrastructure were caused by proteins (e.g fibronectin) that adsorb onto the surface of the implant and form a surface layer, which may prevent degradation of the implant surface. Based on these findings, it was suggested that the biological environment of the HA within the implant was more analogous to that of an acellular *in vitro* medium. The current findings confirmed this hypothesis to be valid and demonstrated similarities in the morphology of dissolution features on HA and Si-HA within the implant *in vivo* and dispersed in SBF.

The current study clearly illustrates similarities in the amount of dissolution and the morphology of dissolution features *in vivo* and SBF models. Despite these similarities, the current HR-TEM observations reveal differences in the site at which nucleation initiates *in vivo* and *in vitro: in vitro* dissolution predominates throughout grains, whereas dissolution within the implant initiates predominantly at grain boundaries in the *in vivo* model. This difference may be the attributable to the interaction of proteins with the implant surface prior to dissolution and apatite formation *in vivo*. Future work will establish whether factors associated with non-collagenous proteins, such as protein size or concentration, are the controllers of the dissolution and apatite formation processes both *in vitro* and *in vivo* [24].

Conclusions

This study confirmed a difference in the morphology of apatite precipitates *in vivo* and in SBF: apatite deposits were plate like *in vivo* and nodular in SBF. The site at which dissolution nucleates was also different: dissolution predominates at crystal surface in SBF,

whereas grain boundaries dissolution predominates *in vivo.* Compositional mapping in this study suggested that silicon dissolves preferentially from the Si-HA and encourages nucleation of carbonate apatite around the implant. A previous study illustrated that no dissolution whatsoever occurred at the bone-HA or Si-HA interface *in vivo*. In comparison, dissolution within the implant was similar to dissolution observed in SBF. These results suggest that the proteins and cells prevent dissolution from the surface of the implant. In summary, the present study suggests that, despite being unable to accurately model the ultrastructure of dissolution and reprecipitation features found *in vivo*, SBF is a valuable medium for modelling the amount of dissolution and precipitation.

Acknowledgements

The authors acknowledge Nelesh Patel and Jeremy Skepper for their kind assistance with sample preparation; the HREM group at the University of Cambridge for use of their facilities and the financial support of EPSRC, Apatech Ltd and also Fundação para a Ciência e Tecnologia for the second author´s (C.M.B.) grant (ref. SFRH/BD/6173) and project funding (POCTI/CTM/49238/2002).

References

[1] - Porter AE, Best SM, Bonfield W. Ultrastructural Comparison of Hydroxyapatite and Silicon-Substituted Hydroxyapatite for Biomedical Applications. J of Biomed Mater Res 2003;68A:133-141.

[2] - Patel N, Gibson IR, Hing KA, Best SM, Revell PA and Bonfield W. A comparative study on the *in vivo* behaviour of hydroxyapatite and silicon substituted hydroxyapatite granules. J Mater Sci: Mate Med 2002;13:1199-1206.

[3] - Porter AE, Patel N, Skepper JNS, Best SM, Bonfield W. Comparison of *in vivo* dissolution processes in hydroxyapatite and silicon-hydroxyapatite bioceramics. Biomaterials 2003;24:4609-4620.

[4] - Weng J, Liu Q, Wolke JGC, Zhang X, de Groot K. Formation and characteristics of the apatite layer on plasma-sprayed hydroxyapatite coatings in simulated body fluid. Biomaterials 1995;18:1027-1035.

[5] - Doi Y, Shibutani T, Moriwake Y, Kajimoto T, Iwayama Y. Sintered carbonate apatites as bioresorbable bone substitutes. J Biomed Mater Res 1997;39:603-610.

[6] - Schepers E, Declercq M, Ducheyne P, Kempeneers R. Bioactive glass particulate material as a filler for bone lesions. J Oral Rehab 1991;18:439-52.

[7] - Ducheyne P, Qiu Q. Bioactive ceramics: The effect of surface reactivity on bone formation and bone cell function. Biomaterials 1999;20:2287-2303.

[8] - Ducheyne P, Radin S, King L. The effect of calcium-phosphate ceramic composition and structure on in vitro behaviour. I. Dissolution. J Biomed Mater Res 1993;27:25-34.

[9] - Kukubo T, Kushitani H, Sakka S. Solutions able to reproduce in vivo surface-structure changes in bioactive glass-ceramic A-W. J Biomed Mater Res 1990;24:721-34.

[10] - Radin SR, Ducheyne P. The effect of calcium phosphate ceramic composition and structure on in vitro behavior. II. Precipitation. J of Biomed Mater Res 1993:27:35-45.

[11] - Gibson IR, Hing KA, Best SM, Bonfield W. Enhanced in vitro cell activity and surface apatite layer formation on novel silicon-substituted hydroxyapatites. In : Ohgushi H, Hastings GW, and Yoshikawa T, editors. 12th International Symposium on Ceramics in Medicine, Nara, Japan, 1999. p. 191-94.

[12] - Fujibayashi S, Neo M, Kim H-M, Kokubo T and Nakamura T. A comparative study between *in vivo* bone ingrowth and *in vitro* apatite formation on Na_2-CaO-SiO_2 glasses. Biomaterials 2003;24:1349-1356.

[13] - Porter AE, Patel N, Skepper JN, Best SM and Bonfield W. Effect of sintered silicate-substituted hydroxyapatite on remodelling processes at the bone-implant interface. Biomaterials 2003;25:3303-3314.

[14] - Leng Y, Chen J, Qu S. TEM study of calcium phosphate precipitation on HA/TCP ceramics. Biomaterials 2003;24:2125-2131.

[15] - Akao M, Aoki H and Kato K. Mechanical properties of sintered hydroxyapatite for prosthetic applications. J Mater Sci 1981;28:809.

[16] – Gibson IR, Best SM, Bonfield W. Chemical characterization of silicon-substituted hydroxyapatite. J Biomed Mater Res 1999;44:422-428

[17] - Rey C. Calcium phosphates for medical applications. In: Amjad Z, editor. Calcium phosphates in biological and industrial systems. Bostono: Kluwer Academic Publishers, 1998. p. 217-51.

[18] - Tanizawa Y, Suzuki T. Effects of silica ions on the formation and transformation of calcium phosphates in neutral aqueous solutions. J Chem Soc Faraday Trans 1995;91(19)3499-3503.

[19] - Damen JJM and Ten Cate JM. Silica-induced precipitation of calcium phosphate in the presence of inhibitors of hydroxyapatite formation. J Dent Res 1992;71(3):453-457.

[20] - Botelho CM, Lopes MA, Gibson IR, Best SM, Santos JD. Structural analysis of si-substituted hydroxyapatite: zeta potential and X-ray photoelectron spectroscopy (XPS). J Mater Sci: Mater Med 2002;13:1123-1127.

[21] - Carlisle EM. Silicon. Nutr Rev 1975; 33:(9)257-260.

[22] - Termine JD, Eanes ED, Conn KM. Phosphoprotein modulation of apatite crystallization. Calcif Tissue Int 1980;31:247-51.

[23] - Combes C, Rey C. Adsorption of proteins and calcium phosphate materials bioactivity. Biomaterials 2002;23:2817-2823.

[24] - Horbett TA. Proteins at interfaces – an overview. ACS Symp Ser 1995;602-23.

Chapter 3

Si-HA and Human Serum Proteins Interaction

Protein adsorption is one of the first events that occur after implantation in a living system. This event takes place well before cells appear, consequently cells will respond to this layer. Thus, the protein layer is a key factor that can control the bioreaction to implants. The formation of an apatite layer is considered to be an important step to osteointegration. Therefore, in this chapter we study the effect of human serum proteins on the dissolution and apatite layer formation on hydroxyapatite (HA) and silicon-substituted hydroxyapatite (Si-HA). We also study the adsorption of specific proteins to the materials, such as: collagen type I (COL I), immunoglobulin G (IgG) and albumin (BSA).

HA, 0.8 wt % Si-HA and 1.5 wt % Si-HA were incubated in solutions containing human serum proteins for different periods of time. Therefore, it was possible to follow the effect of these proteins in different stages of the apatite formation. Additionally, another set of samples was incubated in solutions containing single proteins (COL I, IgG and BSA) and 10 % (v/v) of human serum proteins, in order to study the affinity of the proteins to the different substrates.

On the basis of the result presented in this chapter, it is proposed that the presence of a protein layer surface on HA and Si-HA acts as a dissolution barrier, preventing ions from diffusing directly from the surface of Si-HA to the solution. As dissolution constitutes the first step in physiological apatite formation, this proposed mechanism accounts for the retarded apatite layer formation observed in the HS-supplemented groups. Furthermore, the dissolution features observed on Si-HA surfaces and in particular on 1.5 wt % Si-HA after incubation in SBF free of human serum proteins suggest the importance of silicon dissolution in the formation of the apatite layer on Si-HA.

All incubated materials demonstrated a higher binding affinity to collagen. A slight increase in the affinity of collagen was observed with the increase of the silicon content. HA and Si-HA showed the same affinity to IgG, but in the case of the albumin a slight decrease was observed on the Si-HA. 0.8 wt % Si-HA showed to have a higher affinity for human serum proteins when compared to the other two materials.

Effect of human serum proteins on the surface of pure Hydroxyapatite and silicon-substituted Hydroxyapatite: AFM and ESEM studies

C.M. Botelho[1,2], D.J.Stokes[3], R. A. Brooks[4], S.M. Best[5], M. A. Lopes[1,2], J.D. Santos[1,2], N. Rushton[4], W. Bonfield[5]

[1]INEB- Instituto de Engenharia Biomédica, Laboratório de Biomateriais, Rua do Campo Alegre, 823, 4150-180 Porto, Portugal.

[2]Departamento de Engenharia Metalúrgica e de Materais, Faculdade de Engenharia, Universidade do Porto, Rua Dr. Roberto Frias, 4200-465 Porto, Portugal.

[3]Department of Physics; University of Cambridge, Cavendish Lab., Madingley Road, Cambridge, CB3 0HE, UK.

[4]Orthopaedic Research Unit, Box 180, Addenbrooke´s Hospital, Hills Road Cambridge, CB2 2QQ.

[5]Department of Materials Science and Metallurgy, University of Cambridge, CB2 3 QZ, UK.

Materials Science Forum, 455-456, 378-382, 2003.

Abstract

Human serum proteins adhere to calcium phosphate within seconds after implantation. This layer influences the biological behaviour of the biomaterials. Hydroxyapatite (HA) and 0.8 wt% of silicon substituted hydroxyapatite (Si-HA) were incubated in three different solutions; simulated body fluid, simulated body fluid with 0.1 % and 10 % in volume of human serum. The surface of Si-HA underwent significant surface changes more rapidly than the HA surface. After a period of 7 days incubation in SBF an apatite layer was observed by ESEM and AFM on the Si-HA surface, but not on the HA surface. At the HA surface calcium phosphate deposits were only observed after 28 days of incubation. The formation of an apatite layer on the surface of both materials seems to have been delayed with the addition of human serum proteins.

***Keywords*:** Proteins, Atomic Force Microscopy (AFM), Environmental Scanning Electron Microscopy (ESEM), Hydroxyapatite (HA), Silicon-Substituted Hydroxyapatite (Si-HA).

Introduction

Several studies have demonstrated the enormous advantage of the incorporation of silicon in the biomaterials lattice aimed at regenerating bone tissue [1-3]. Therefore to take advantage of the positive biological effect of silicon, Si-substituted hydroxyapatite (Si-HA) has been developed using a chemical precipitation route [4, 5].

The organic matrix has an important role in the ossification process by guiding mineral deposition and favouring mineralization [6]. Collagen provides an oriented matrix for mineral deposition, but it seems that noncollagenous matrix substances, which can bind to calcium phosphates, modify the calcium/phosphorous ratio and so will influence crystal formation and growth [7]. The role of these proteins is still poorly understood. Several factors can alter the behaviour of these proteins, such as the supersaturation ratio of the solution, the local concentration of co-precipitating ions, and the presence of others proteins and whether proteins are free in solution or immobilized [6].

This work is aimed at assessing the effect of human serum (HS) proteins on the dissolution and ability to form an apatite layer of HA and Si-HA. Tapping mode AFM and ESEM were the techniques used to examine the physical changes that occurred at the surface of the HA and Si-HA as result of immersion in different physiological solutions.

Material and Methods

The preparation Si-HA and HA has been fully described elsewhere [4, 5]. As-prepared dense discs were placed into three different solutions: Simulated Body Fluid (SBF), SBF with 0.1 % and 10 % in volume of Human Serum (HS) (HD Supplies, UK), incubated at 37 º C for a period of time between 0 and 28 days. The ratio of solution surface area per volume used was 0.1 cm^{-1}. The surface changes were observed using atomic force microscopy (AFM) and environmental ESEM. AFM imaging was performed with a help a Digital Instruments NanoScope III and ESEM signals were collected in low vacuum mode, with an off axis gaseous secondary electron detector**.**

Results

The materials were analysed by X-ray diffraction to assess their phase purity. The surface of the materials was observed by ESEM and AFM before incubating in the different solutions. No dissolution features or deposits were detected.

At day 1 no changes were detected on the HA surface after incubation in SBF and SBF with 0.1 % (v/v) HS, while some deposits were observed on the HA surface incubated with 10 % (v/v) HS. These deposits were seen on all samples incubated in SBF with 10 % (v/v) HS, and at all immersion time points (Figure 1 (a,b)). Until now, it was not possible to determine the chemical composition of these deposits due to their fragility and disintegration when exposed to the electron beam. When incubating Si-HA in SBF for 1 day, it was possible to observe some calcium phosphate deposits in the Si-HA grains, and also dissolution at the grain boundaries (Figure 2 (a,b)). This may be due to the preferential dissolution of silicon from the grain boundaries, as no significant change was detected in the calcium and phosphorous concentrations of the SBF. These results are in agreement with previously published work [8]. Another interesting result was observed on the Si-HA surface incubated in SBF with 10 % (v/v) HS (Figure 3). Due to the interaction between the surface and the solution, the deposits on the surface were aligned at the grain boundaries. These features were also observed at different time points.

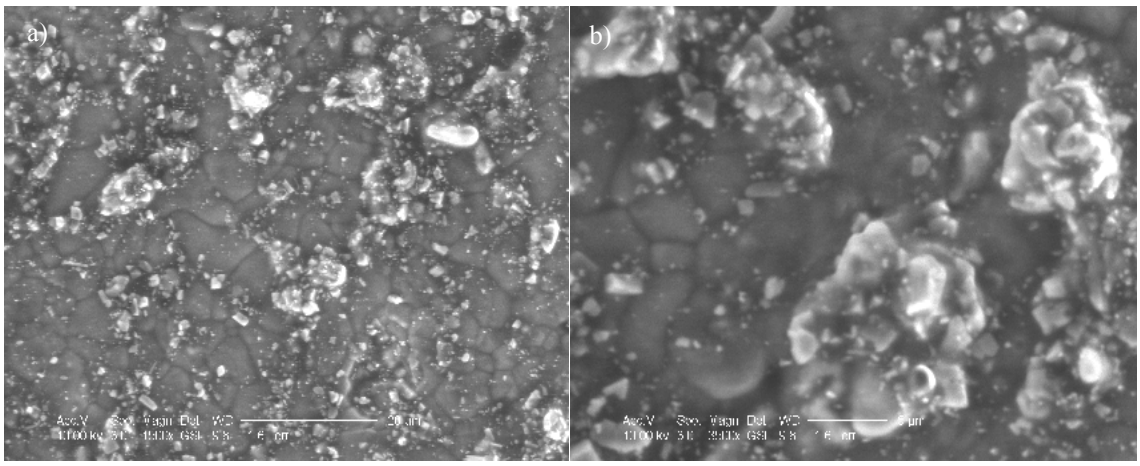

Figure 1 – Deposits on the HA surface after incubating in SBF with 10 % (v/v) HS for 1 day (a – scale bar 20 μm) and 3 days (b- scale bar 5 μm) observed by ESEM.

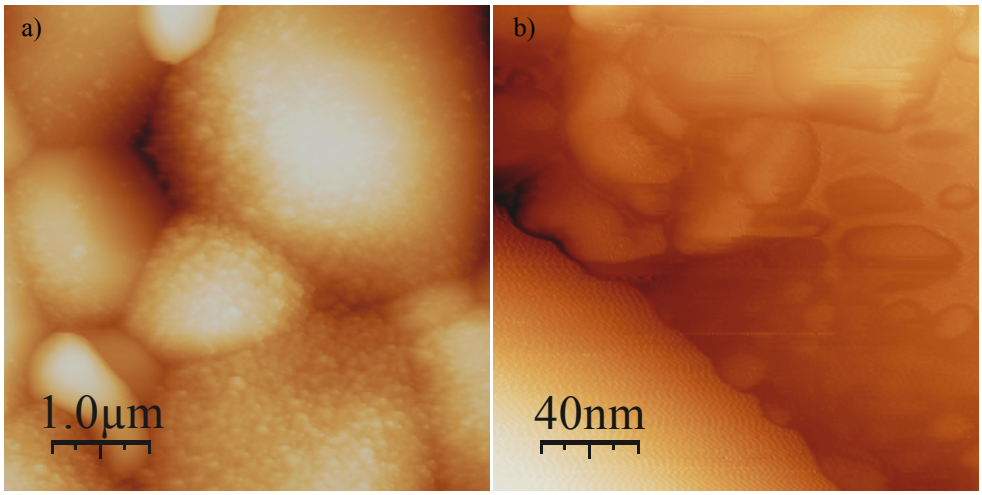

Figure 2 – Deposits at the Si-HA surface after 1 day in SBF (a – 5 x 5 µm) and clear dissolution features at the grain boundaries (b – 200 x 200 nm)

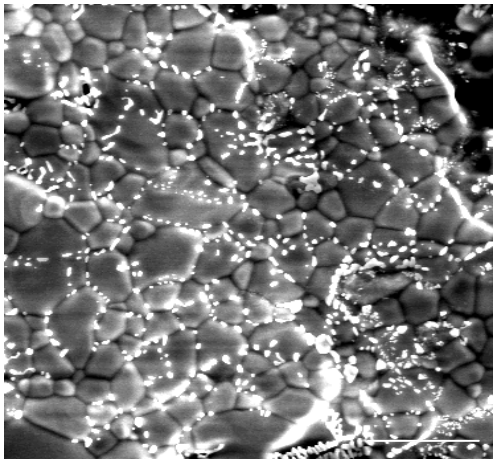

Figure 3 – Deposits at the Si-HA grain boundaries after 1 day in SBF with 10 % (v/v) HS (scale bar 10 µm).

When HA was incubated for a period of 7 days in SBF, most of the grains were intact with no dissolution features or significant deposits, although when incubated in SBF with 0.1 % (v/v) and 10 % (v/v) HS the surface was partially covered by an amorphous film (Figure 4 (a,b)). Significant changes were detected on the Si-HA surface for the same period of incubation. An apatite layer was observed on the samples incubated in SBF, although the surface was not completely covered. This can be seen in Figure 5 and 6, where in some areas of the sample it is still possible to observe the grains. On the surface of the samples incubated in SBF with 0.1 % (v/v) of HS for the same period of time, dissolution features were mainly observed. Over the same period of time, no calcium phosphate deposits appeared on the surface of the samples incubated with 10 % (v/v) of HS.

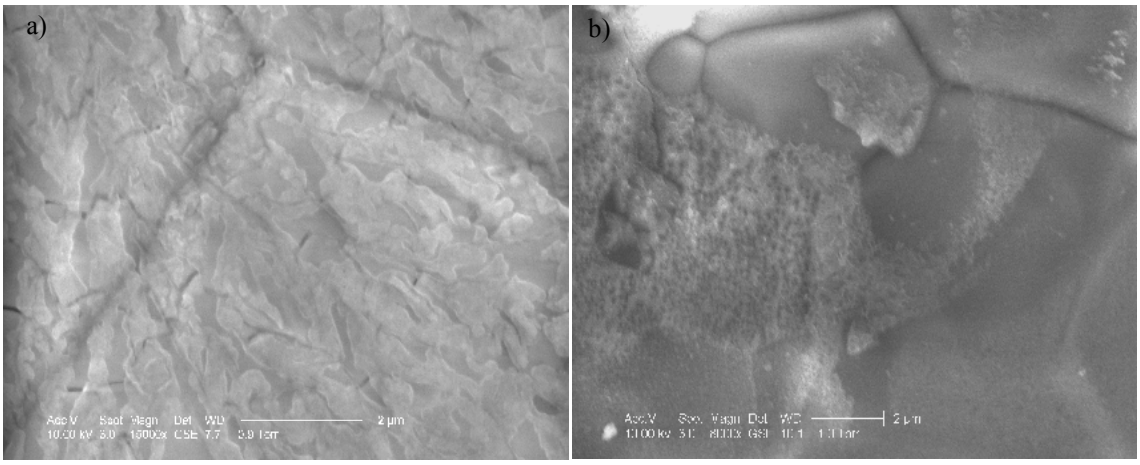

Figure 4 – An amorphous film on the HA surface after incubation in SBF with 0.1 % (v/v) HS (a – scale bar 2 μm) and in SBF with 10 % (v/v) HS (b- scale bar 2 μm) for a period of 7 days.

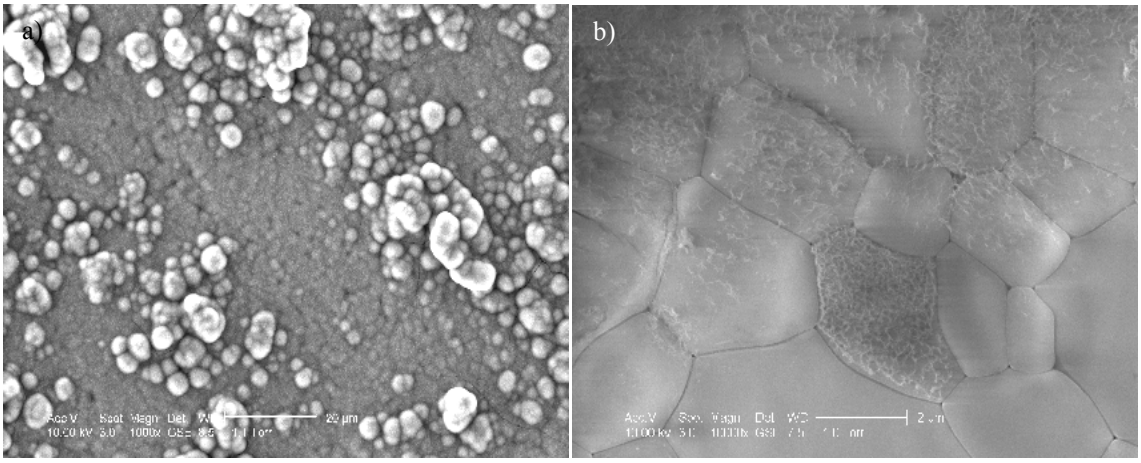

Figure 5 – Apatite layer partially covering the Si-HA surface, after 7 days of incubation in SBF (scale bar a – 20 μm, b – 2 μm).

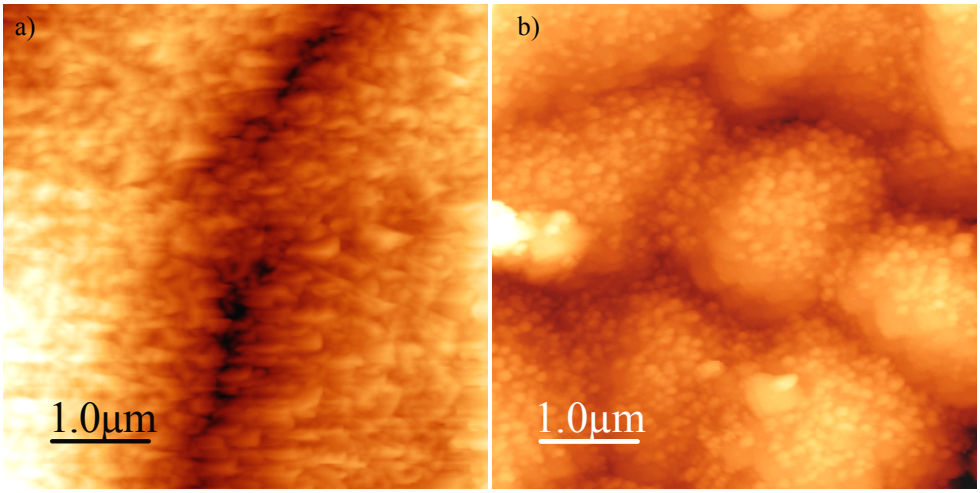

Figure 6 – An apatite layer partially covering the Si-HA surface after 7 days of incubation in SBF as observed by AFM (a,b) 5 x 5μm).

At day 10 a complete apatite layer had formed on the surface of the Si-HA incubated in SBF (Figure 7). This apatite layer appears to be more crystalline than the apatite layer observed after 7 days immersion, as shown by the shape of the crystals shown in Figure 8 (a,b). After 14 days of incubation in SBF it was not possible to observe an apatite layer. Only after 28 days of incubation in SBF, calcium phosphate deposits were observed on the surface of the HA substrate (Figure 9 (a)). These deposits were not detected in the samples incubated in SBF with 0.1 % (v/v) HS, although an amorphous film was observed to partially cover the surface (Figure 9 (b)).

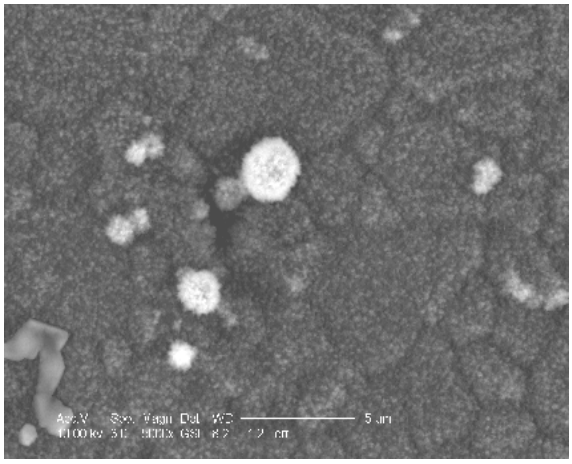

Figure 7 – A complete apatite layer on Si-HA afer incubation in SBF for a period of 10 days (scale bar 5 μm).

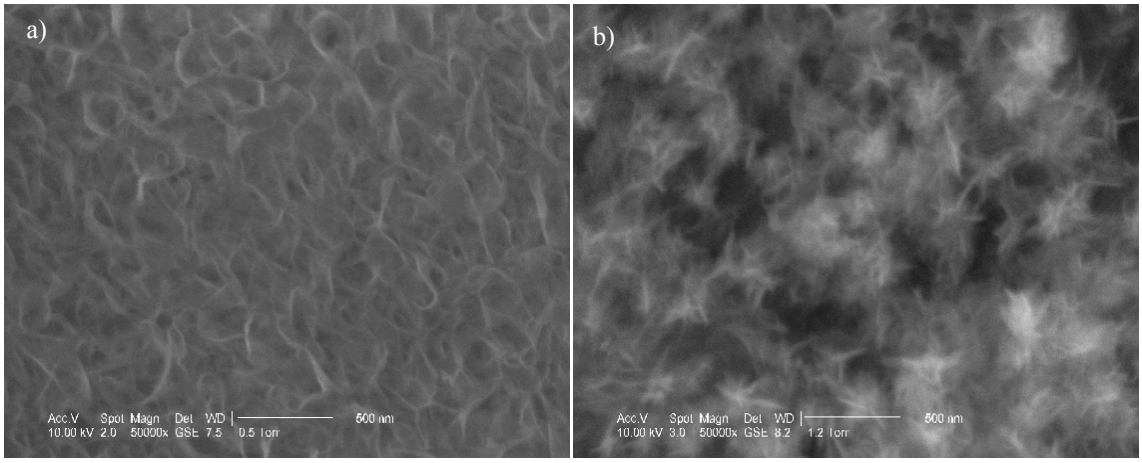

Figure 8 - Calcium phosphate crystals at Si-HA surface after incubation in SBF for a period of 7 days (a – scale bar 500 nm) and 10 days (b – scale bar 500nm).

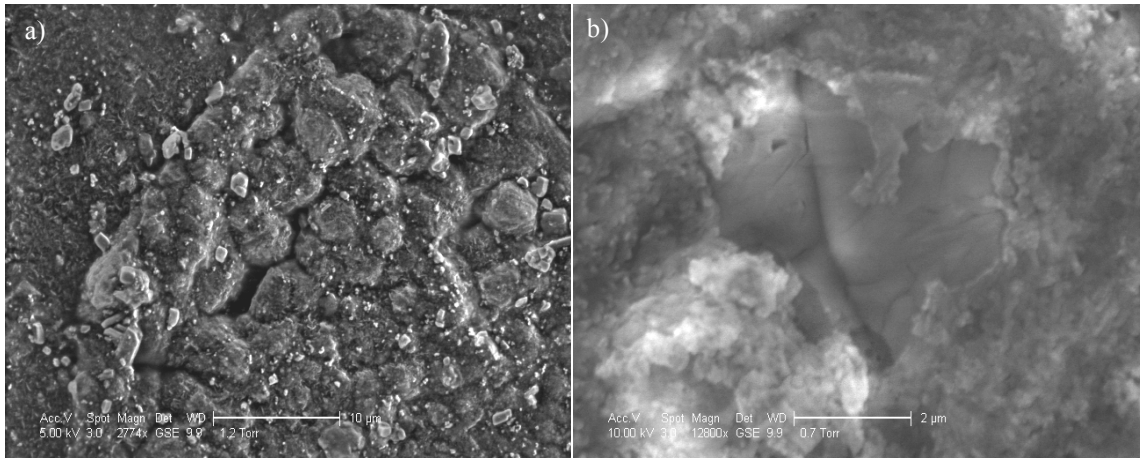

Figure 9 - (a) Calcium Phosphate deposits on the HA surface after 28 days of incubation in SBF (Scale bar 10 μm), and a thin film deposit on HA surface for the same period of time when incubated in SBF with 0.1% (v/v) HS (Scale bar 2μm)

Discussion and Conclusion

The composition of the protein layer formed on the surface of these calcium phosphates influences the biological response to the material after implantation [9]. The results indicate that when these proteins are present in higher concentrations (10 % (v/v) HS), the dissolution and consequent formation of the apatite layer is delayed. These results are in agreement with those reported in literature [10]. When the materials were incubated in SBF with 0.1 % (v/v) HS, the dissolution was higher than in the samples incubated in SBF with 10 % (v/v) HS. This may be due to the lower coverage of the surface of the samples incubated in the different solutions, and also due to the different conformations of these proteins. The samples incubated in SBF with 10 % (v/v) HS may be completely covered by a protein layer, protecting the surface from dissolution which is required for the formation of the apatite layer. A lower concentration of proteins may decrease the competition between proteins and change the conformation of these proteins, influencing the formation of the calcium phosphate deposits. It is known that the adsorption of some proteins has a maximum at low concentration of HS, such as fibrinogen or albumin [13]. When fibrinogen is deposited on a glass surface, it has a maximum adsorption with 1 % (v/v) HS, although albumin, under the same conditions has a maximum adsorption with 6 % (v/v) HS [13]. Using the technique of AFM and ESEM it was possible to verify that changes on the Si-HA surface begin at day 1,

with dissolution at the grain boundaries. This may be due to preferential dissolution of silicon, as no significant changes in the concentration of calcium or phosphorous were detected in the SBF solution. It has been already reported that when Si-HA is incubated in Tris buffer solution, there is a preferential dissolution of silicon [8]. The surface of Si-HA underwent significant changes more rapidly than the HA surface. The introduction of 0.8 wt% silicon in the HA lattice increases the bioactivity of the HA. These results are in agreement with the literature [14, 15]. Further studies are needed in order to fully understand the mechanisms by which the HS proteins influence the ability of these biomaterials to form an apatite layer.

Acknowledgements

The authors wish to acknowledge the financial support of ref. SFRH/BD/6173 grant, the project entitled "Revestimento de Hidroxiapatite modificada com silício para aplicações biomédicas" ref. POCTI/CTM/49238/2002 financed by FCT (Fundação para a Ciência e Tecnologia) and would also like to thank Dr. Nadia Stelmashenko from Department of Materials Science, University of Cambridge, UK, for her assistance in the AFM.

References

[1] L.L. HENCH, in: Sol-Gel Silica Properties, Processing and technology Transfer, (1999), chapter 10 Biological Implications, 116-163

[2] L.L. HENCH, *J. Phys.* **43** (1982) 625

[3] L.L. HENCH, *J. Am. Ceram. Soc*. **74** (1991) 1487

[4] L.J. JHA, S. BEST, J.D. SANTOS, I.R. GIBSON, W. BONFIELD, Silicon-Substituted Apatites and Process for the Preparation Thereof, Worldwide patent, PCT/GB97/02325 and US Patent Serial Nº 09/147773, 1999.

[5] I.R. GIBSON, S.M. BEST, W. BONFIELD, *J. Biomed. Mat. Res*., **44** (1999) 422

[6] D. COUCHOUREL, et all, *J. of Inorganic Biochemistry,* **73** (1999) 129

[7] A.L. BOSKEY, *Connect. Tissue Res*., **35** (1996) 357-363

[8] C. M. BOTELHO, *J. of Mater. Sci.: Mater. in Med.* **13** (2002) 1123

[9] R. J.GREEN, et al., *Biomaterials*, **20** (1999) 385

[10] S. RADIN, et al., *J. Biomed. Mater. Res*., **39** (1998) 234

[13] J. D. ANDRADE, et al., *Advances in Polymer Science*, (1986) 1

[14] I. R. GIBSON, et al., *in Proceedings of the 12th International Symposium on Ceramics in Medicine*, Nara, Japan, (1999), p. 191

[15] N. PATEL, et al., *J. of Mater. Sci.: Mater. in Med.* **13** (2002) 1199

Surface characterisation of silicon-substituted hydroxyapatite: A phase imaging atomic force microscopy study

Abstract

The adsorption of human serum proteins plays a key role on the biological response to a biomaterial *in vivo*, such as apatite layer formation and cell behaviour. Several factors may alter the adsorption of these proteins, namely the physical-chemical properties of the materials. We previously reported that the incorporation of silicon into the HA lattice induces a more negative surface charge, in this study it was shown that the incorporation of silicon increased the hydrophilicity of the HA material. In order to assess the effect of these proteins on the dissolution of the Si-HA material and apatite formation, several samples of Si-HA where incubated in serum-free SBF and in serum SBF. In serum-free SBF the incorporation of silicon (1.5 wt % Si) into the HA lattice decreased the time required for apatite formation when compared to phase pure hydroxyapatite. The images obtained by AFM and phase image AFM showed extensive dissolution on the samples incubated on serum-free SBF at early time points, on the other hand the samples incubated in serum SBF showed to be covered by protein layer. This result was confirmed by XPS analysis, which showed an increase in the nitrogen concentration on the surface of the samples. The ICP measurements confirmed that the protein layer slows down the ionic release to the surrounding solution. Consequently this delay will result in a delay on the formation of an apatite layer.

***Keywords*:** Proteins, Atomic Force Microscopy (AFM), Phase Atomic Force Microscopy (AFM), Silicon-Substituted Hydroxyapatite (Si-HA).

Introduction

Since 1970´s several studies demonstrated the positive effect of silicon on bone mineralization [1-3]. More recently, Patel *et al* showed the beneficial role of the incorporation of silicon into the hydroxyapatite (HA) lattice *in vivo* [4], the silicon-substituted hydroxyapatite material enhanced bone regeneration. Although, the mechanism behind the enhanced bioactivity of the silicon-substituted hydroxyapatite (Si-HA) is still poorly understood. Due to the complexity of the *in vivo* model, several *in vitro* studies have been

performed in order to clarify the mechanism behind the positive effect of silicon [5-11]. It has been shown that the incorporation of 0.8 wt % of silicon into the HA lattice decreases the time required for apatite formation in 64 % (28 days for phase pure HA to 10 days for 0.8 wt % Si-HA), when incubated in simulated body fluid (SBF) at physiologic conditions [6].

The ability of a biomaterial to form an apatite layer is considered to be an important characteristic for osseointegration [12]. Although, when a biomaterial is implanted there are several steps that will lead to the osseointegration, being the first event the adhesion of proteins to the surface, this step will take less than a second [13, 14], following the formation of a protein monolayer. Only after the adsorption of the protein layer cells reach the implanted site. Therefore, cells will mainly respond to this layer instead of the biomaterial surface itself [14]. The integrin receptors present in most cells recognize the adsorbed proteins, being this mechanism responsible for the bioreaction to an implant [15]. In the presence of a solid phase proteins in solution have the tendency to adsorb [16]. Proteins change their conformation to maximize the energy gain from adsorption, this adsorption will be irreversible if the conformational change required for desorption is energetically unfavourable [17]. Although, some proteins may be desorbed from the surface by other molecules in solution, as described by the "Vroman effect" [18]. This theory states that the more profuse and smaller proteins from blood plasma can be displaced by the fewer larger proteins that have higher affinities for the surface [18]. Several studies showed that determined proteins may induce (e.g. fibronectin) or inhibit (e.g. albumin) the nucleation of the calcium phosphate crystals [19], therefore a possible function of the specific crystal proteins could be to control the nucleation and growth of physiological apatite during the mineralization process [19]. In previous studies Botelho *et al* reported that the presence of human serum proteins in different concentrations delayed the formation of an apatite layer on 0.8 wt % Si-HA and HA [6].

The physicochemical properties of the material, such as surface chemistry, surface charge and surface energy, will influence protein adsorption and functionality, through changes in its orientation and conformation [16, 20, 21], and consequently cell behaviour [22-24]. It has been shown that HA and Si-HA have different physicochemical properties, namely surface charge [5], the incorporation of silicon on the HA lattice induce a more negative surface charge.

In order to better understand the biological behaviour of the Si-HA two additional physical-chemical properties were determined, surface wettability and interfacial tension. These properties can be determined through the measurement of contact angle, being the most common experimental technique the sessile drop [25]. In this method a droplet is placed very

slowly on the surface of the material, originating three-phase equilibrium. The contact angle formed by the drop and the interfacial tension of the solid-vapour, liquid-vapour and solid-liquid interface can be related through the Young´s [26] equation (Eq. 1):

$$\gamma_{LV}\cos\theta = \gamma_{SV} - \gamma_{SL} \qquad \text{(eq. 1)}$$

where γ_{LV} is the interfacial tension of a liquid in equilibrium with its vapour, γ_{SV} is the solid-vapor interfacial tension and γ_{SL} is the solid-liquid interfacial tension and θ represents the contact angle of a liquid drop on a solid surface. This equation has two unknowns variables, therefore another equation is requires. Several approaches have been proposed, for example the geometric mean method proposed initially by Scatchard and Hildebrand [27, 28] and later on adapted by Owens and Wendt´s [29], the harmonic mean proposed by Wu [30] and the van Oss, Good and Chaudhury method [31]. The Owens and Wendt´s method is the most used and it states that the interfacial tension between two phases in contact, particularly between a solid and a liquid can be described by the following equation (Eq.2),

$$\gamma_{SL} = \gamma_L + \gamma_S - 2\sqrt{\gamma_S^d.\gamma_L^d} - 2\sqrt{\gamma_S^p.\gamma_L^p} \qquad \text{(eq. 2)}$$

This method assumes that the dispersive (γ^d) and polar (γ^p) intermolecular forces operate across the interface and therefore the total surface tension is the sum of the two components (Eq. 3).

$$\gamma = \gamma^d + \gamma^p \qquad \text{(eq. 3)}$$

The combination of equation 1 and 2 leads to a forth equation that will allow the determination of γ_{SV} and γ_{LV},

$$\gamma_{LV}(\cos\theta + 1) = 2\sqrt{\gamma_{SV}^d\gamma_{LV}^d} + 2\sqrt{\gamma_{SV}^p\gamma_{LV}^p} \qquad \text{(eq. 4)}$$

Using these equations and experimental values of contact angles measured with a pair of testing liquids of known dispersive and polar surface tension components, γ_{SV} and γ_{SL} can be determined.

In order to determine if there is a relationship between the incorporation of silicon into the HA lattice and the time required for the formation of an apatite layer, 1.5 wt % Si-HA was incubated in SBF for a period up to 10 days, at 37 ºC.

To study the effect of human serum proteins (HS) on the surface dissolution and consequently apatite formation different compositions of Si-HA were incubated in SBF with HS (serum SBF). In this study several techniques were used: environmental scanning electron microscopy (ESEM), atomic force microscopy (AFM), phase imaging AFM, X-ray photoelectron spectroscopy (XPS) and inductively couple plasma spectroscopy (ICP).

Material and Methods

Materials Preparation

The preparation of Si-HA was performed through an aqueous precipitation chemical route between calcium hydroxide, orthophosphoric acid and silicon tetraacetate as a source of silicate ions and it can be described by the following equation.

$$10Ca^{2+} + (6-x)PO_4^{3-} + xSiO_4^{4-} + (2-x)OH^- \rightarrow Ca_{10}(PO_4)_{(6-x)}(SiO_4)_x(OH)_{(2-x)} \quad \text{(eq.5)}$$

Where, x is the number moles of silicon. A detailed protocol is fully described elsewhere [5, 9, 32].

X-ray diffraction (XRD) and X-ray fluorescence (XRF)

To determine the phase purity of the precipitated material used in this study X-ray diffraction (XRD) was performed using a Philips PW1710 X-ray diffractometer (PANalytical Inc., Almelo, The Netherlands) Data were collected between 25º and 40º 2 θ using a step size of 0.02º and a count time of 2.5 seconds. Phase identification was carried out by comparing the peak positions of the diffraction patterns with ICDD (JCPDS) standards. The X-ray fluorescence was used to confirm the incorporation of 0.8 wt % Si, 1.2 wt % Si and 1.5 wt % Si into the HA lattice using a Philips PW1606 spectrometer.

Contact Angle Measurements

The powder containing the intermediate level of silicon 1.2 wt % Si-HA and HA were uniaxially pressed and sintered at 1300 ºC for 2 hours, with a heating rate of 2.5 ºC/min and

cooled down at a rate of 10ºC/min. The samples were polished until a final Ra of (0.5 ± 0.1) μm. The contact angle was measured on the materials surface (HA and 1.2 wt % Si-HA) by the sessile drop method, at 25 ºC in a chamber saturated with a pool of liquid sample. Pictures of the drops were taken as a function of time, at regular intervals using a videocamera mounted on a microscope to record the drop image. The program used to analyse the profile of the drop was Axisymmetric Drop Shape Analysis-Profile (ADSA-P) and it was developed by Neumann and co-workers [33, 34]. The interfacial tension was assessed by the Owens-Wendt using as testing liquids deionised water and diiodomethane (>99%, Merk Schuchardt), doubly distilled under vacuum. The polar and dispersive components of the surface tension of the liquids at 25ºC were taken from the literature [35], the γ_{LV} of water and diiodomethane are 72 mJ/m^2 (γ^d = 21.3 mJ/m^2, γ^p = 50.7 mJ/m^2) and 50.3 mJ/m^2 (γ^d = 49.9 mJ/m^2, γ^p = 0.4 mJ/m^2), respectively.

Si-HA and human serum proteins interaction

Dense discs

The powders containing the lower and upper levels of silicon, 0.8 wt % Si and 1.5 wt % Si, respectively, were uniaxially pressed into dense discs. The samples were incubated in different solutions: SBF (serum free-SBF) and SBF with 10 % (v/v) of HS (serum-SBF) (HD Supplies, UK) at 37ºC for different periods of time to analyse the effect of protein on the surface dissolution. The ratio of surface area per volume used was 0.1 cm^{-1}. The surface of the materials was characterized before and after incubation by AFM and ESEM. AFM imaging was performed with a help a Digital Instruments NanoScope III. The topographic image on the AFM was obtained by tapping mode using the changes in the cantilever oscillation amplitude, but in the case of the phase image, the phase lag of the cantilever motion relative to the driving oscillator was also registered and used to generate images [17, 36-39]. ESEM signals were collected in low vacuum mode, with an off axis gaseous secondary electron detector**.**

In order to access the presence of proteins on the ceramic surface, the atomic percentage of nitrogen was analysed by XPS. The Si-HA samples were incubated in SBF, SBF with 10 % (v/v) HS and in an additional solution with 0.1 % (v/v) of HS for 5 days.

Powders

To determine the effect of human serum proteins on silicon release to the surrounding medium Si-HA powders were immersed in SBF, serum SBF (10 % (v/v) HS). The surface

area was measured by the Brunauer-Emmett-Teller method (BET) (Micromeretics TriStar 3000) and the ratio surface area per volume was increased 100 times (10 cm^2/mL), and the silicon concentration in solution measured by inductively couple plasma spectroscopy (ICP).

Statistical Analysis

All results were statistically evaluated by ANOVA and post-hoc testing with Bonferroni's correction on SPSS statistical software. Significance was set at the 5 % level ($p<0.05$).

Results

The XRD analysis did not detected secondary phases, such as tricalcium phosphate (TCP) or calcium oxide (CaO), indicating a phase pure material. The XRF results confirmed the presence of 0.8 wt % Si, 1.2 wt % Si and 1.5 wt % Si in the Si-HA material.

Contact angle measurements showed that Si-HA has an initial contact angle of (64.9 ± 6.1°, n=10) that is lower than HA (71.8 ± 4.1°, n=10), although the differences observed did not reach statistical significance. As the water droplet sat on the surface of both materials the contact angle undergone a small decreased, although after that period of time the contact angle tended toward a constant value (Figure 1). When using the diiodomethane as a testing liquid, contact angles reached a plateau in a few seconds, (42.8 ± 5.8 °, n = 6) for HA and (44.1 ± 3.3 n = 6), for Si-HA (Figure 1). According to the OWRK approach it was possible to determine the interfacial tension of the substrates; 42.9 mJ/m^2 (γ_{SV}^d = 35.1 mJ/m^2 and γ_{SV}^p = 7.82 mJ/m^2) for HA and 45.5 mJ/m^2 (γ_{SV}^d = 33.8 mJ/m^2 and γ_{SV}^p = 11.80 mJ/m^2), for Si-HA. The dispersive component of the interfacial tension is predominant in both materials, although the polar component gives a significant contribution. The non-dispersive component or polarity ($\frac{\gamma_{SV}^P}{\gamma_{SV}}$) can be used as a quantitative indicator of hydrophilicity, so the Si-HA material is more hydrophilic than HA, $\frac{\gamma_{SV}^P}{\gamma_{SV}}$ = 0.18 and $\frac{\gamma_{SV}^P}{\gamma_{SV}}$ = 0.25, for HA and Si-HA, respectively.

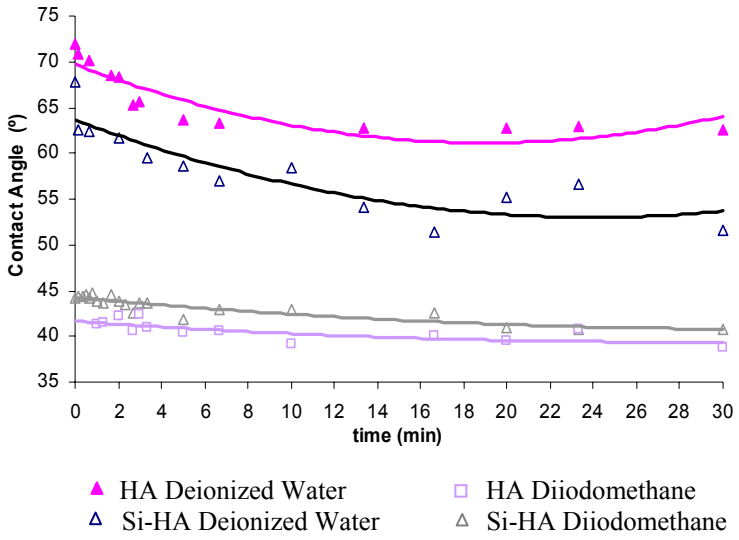

Figure 1 - Variation of the contact angle with time for 1.2 wt % Si-HA and HA.

The surface of the materials was analysed by ESEM, AFM and phase imaging AFM before incubation. Prior to incubation no specific features or deposits were observed, the grains and grain boundaries were clearly visible (Figure 2).

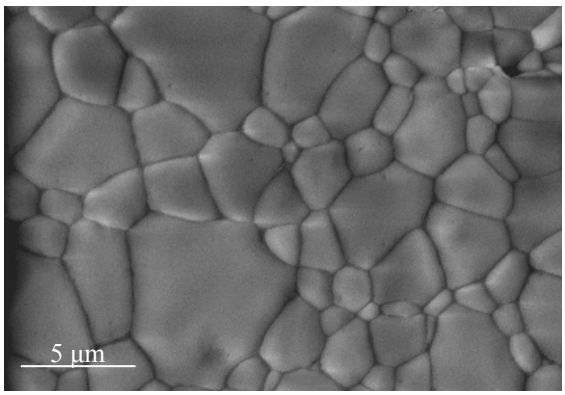

Figure 2 – Environmental Scanning Electron Microscopy image of 1.5 wt % Si-HA before incubation. Similar image was obtained for 0.8 wt % Si-HA (data not shown).

On the ESEM images it is possible to observe the formation of dissolution features (white arrow) on several grains, after incubation in serum free-SBF for a period of 1 day (Figure 3). These features grew in size and number with incubation time leading to the formation of calcium phosphate deposits in particular on the surface of 1.5 wt % Si-HA.

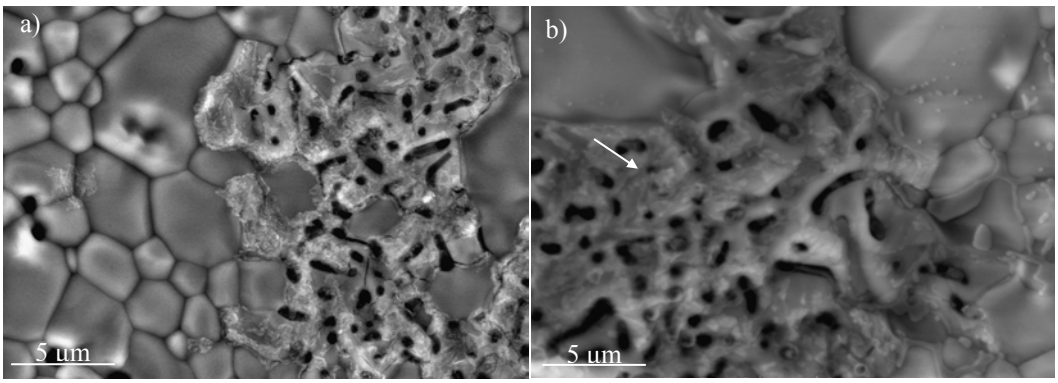

Figure 3 – Environmental scanning electron microscopy images of 1.5 wt % Si-HA after incubation in SBF for 1 day, showing extensive dissolution features (white arrow).

After 7 days a confluent apatite layer was observed at the surface of this material (Figure 4). Thin-film XRD (Th-XRD) corroborated this data (data not shown). The incorporation of higher concentration of silicon decrease the time required for the apatite formation in 30 % (from 10 days to 7 days) and when compared to HA in 75 % (from 28 days to 7 days).

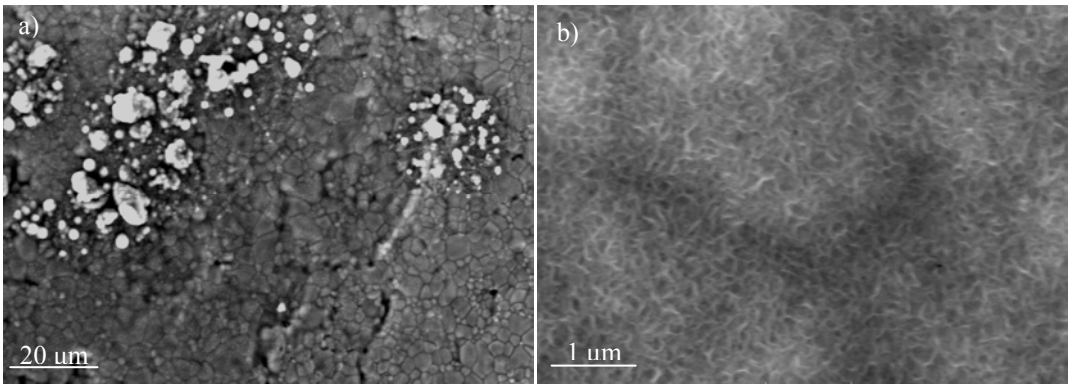

Figure 4 – Environmental scanning electron microscopy images of 1.5 wt % Si-HA after incubation in SBF for 7 days.

The differences on the behaviour of the samples incubated in serum free-SBF and SBF with proteins started at day one; they are more evident on the AFM images. On the phase image it is clear that the surface has different characteristics, due to significant differences on the contrast (Figure 5). As reported in a previous paper the dissolution on 0.8 wt % Si-HA starts as early as day 1 [6]. Similar results were observed for 1.5 wt % Si-HA where extensive dissolution was observed at day 1 (data not shown). At day 2, the samples showed clear signs of dissolution, as it can be seen at the topographical AFM images and phase image AFM

(Figure 5). Dissolution at the grain boundaries and on the surface of the grains was clear, it seems that a grain boundary is completely dissolved (white arrow) (Figure 5).

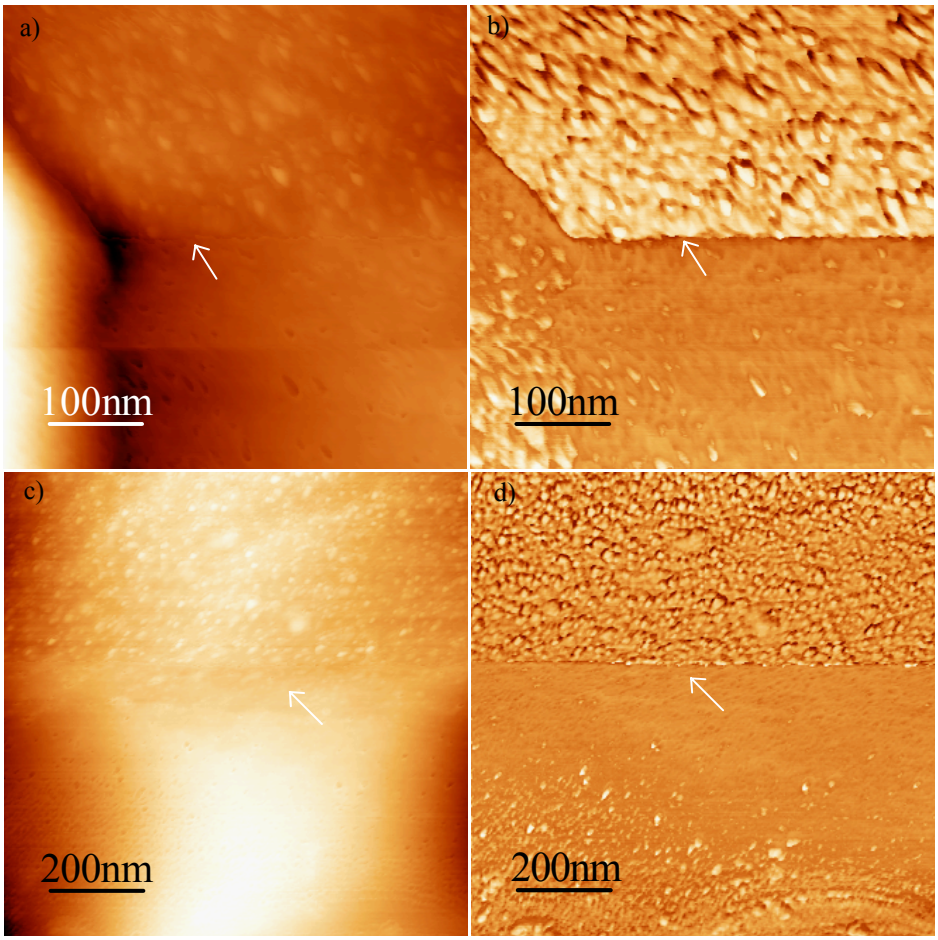

Figure 5 – Atomic force microscopy and phase maging of (a,b) 0.8 wt % Si-HA and (c,d) 1.5 wt % Si-HA after incubation in SBF for a period of two days. a,c – topographical images; c,d – phase image.

Different features were observed on the samples surface when incubated in serum-SBF. Through the ESEM imaging it was not possible to observe significant dissolution features on the surface of these samples. When these samples were analyzed by AFM and phase imaging AFM, the presence of a second layer was detected (Figure 6). The contrast observed on the surface shows that this layer has different characteristics from the underlying surface, which could indicate the presence of a protein layer on top of the samples. This layer may prevent the release of the ions into the surrounding medium and consequently delaying the formation of an apatite layer. At day 7 none of the substrates presented an apatite layer on their surface (data not shown).

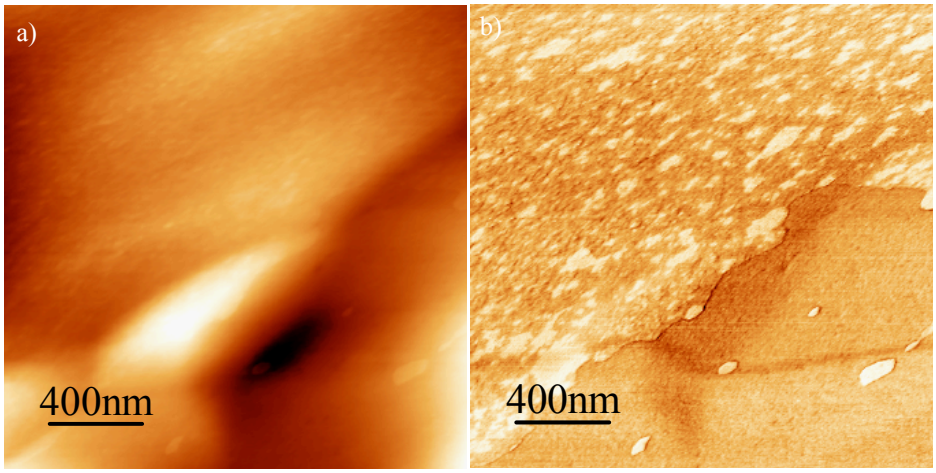

Figure 6 – Atomic force microscopy and Phase Imaging of 1.5 wt % Si-HA after incubation in serum- SBF for a period of one day. a – topographical image; b – phase image.

In order to verify if the layer on the surface of the samples incubated on serum-SBF is a protein layer XPS analysis were performed. Proteins are biological macromolecules, formed by specific co-polymerization of up to 20 different amino acids [40]. The amino acids have a central or α carbon, to which four groups are bounded, a hydrogen, an amino group, a carboxyl group and a side chain usually designated by R. Nitrogen from the amino group (NH_3^+) and carbon for the carboxyl group (COO^-) can be measured and used as an indicator of the presence of proteins. Although, in the case of the XPS technique there are some contaminations by carbon, so it is not possible to use this element to assess the presence of proteins. In this case a new solution was used SBF with a smaller concentration of human serum (HS) proteins (0.1% (v/v)). At the surface of both materials an increase in the atomic percentage of nitrogen was observed with the increase of proteins concentration, which indicates that this layer is indeed a protein layer (Table 1). The concentration of nitrogen detected on the surface of the samples incubated in serum free-SBF is related with the presence of tris-hydroxymethyl amino-methane buffer (TRIS) in the SBF solution that adsorbed on the surface of the sample. Therefore, higher concentrations of nitrogen can be attributed to the proteinaceous layer present on the surface of the sample incubates in serum SBF.

Table 1- Atomic percentages of nitrogen at the surface of Si-HA after incubation for a period of five days.

	0.8 wt % Si-HA	1.5 wt % Si-HA
Solutions	N (At %)	N (At %)
SBF	0.8	0.5
SBF + 0.1 % (v/v) HS	6.5	9.1
SBF + 10 % (v/v) HS	10.4	10.8

In order to study the effect of proteins on silicon dissolution a different experiment was performed. This experiment comprised the suspension of Si-HA powders, in serum free-SBF and serum SBF. The powders had similar surface areas, 0.242 m^2/g, 0.250 m^2/g, for 0.8 wt% Si-HA and 1.5 wt % Si-HA, respectively. The surface area per volume ratio used was 100 cm^2/mL and the ionic release was measured by ICP. Silicon was released from both substrates during the incubation period to the surrounding media. A higher content of silicon on the solution containing 1.5 wt % Si-HA was measured when compared to 0.8 wt % Si-HA (Figure 7a,b). The kinetics dissolution of the materials incubated in serum free-SBF and serum SBF was different. In the presence of proteins a slower rate was observed. This result confirms that the proteins layer on the surface of the material delays the diffusion of the ions from the surface of the ceramic material to the surrounding solution.

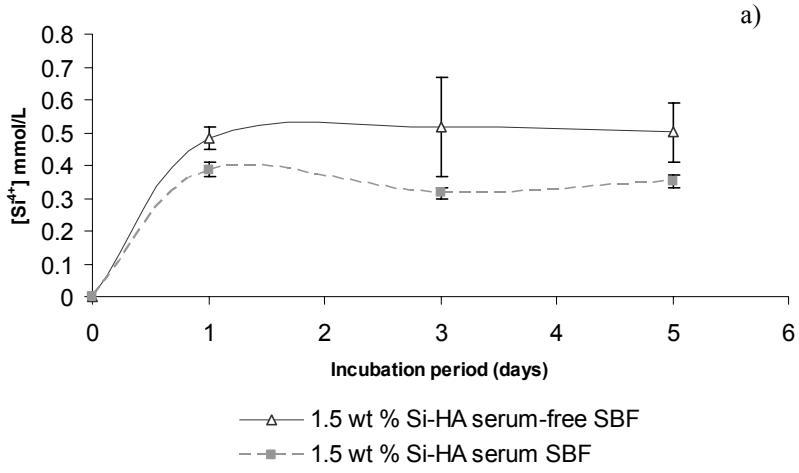

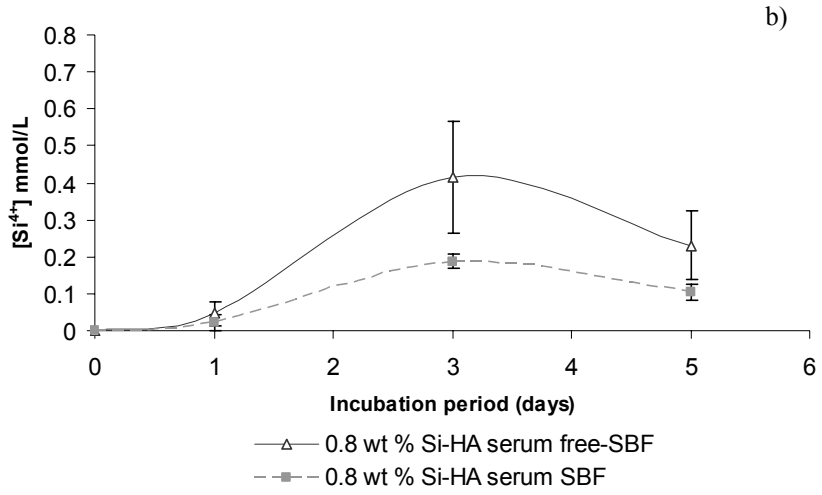

Figure 7 - Curves of silicon release from a) 1.5 wt % Si-HA and b) 0.8 wt % Si-HA, after incubation in serum free-SBF and serum SBF.

Discussion and Conclusion

In previous studies it was demonstrated that the incorporation of silicon into the HA lattice alters the surface charge of HA [5], leading to more negative values. Due to the importance of the surface properties on the interaction between biomaterials, physiological fluids, and the host tissue after implantation [41-43], it was important to further characterize the surface of Si-HA by determining its surface energy and wettability. Our results showed that the incorporation of silicon increased the hydrophilicity of HA, leading to a higher interfacial tension. Although these differences did not reach statistical significance, they corroborate the zeta-potential results due to the increase on the polar component on the Si-HA material, therefore the increase of the interfacial tension can be due to the presence of unsaturated Si-O bonds leading to the formation of Si-OH in the presence of an aqueous medium. Similar results are described in the literature for SiO_2- containing material and phase pure HA [44-46].

Another important property for osteointegration is the formation of an apatite layer. It has been reported that the incorporation of 0.8 wt % Si into the HA lattice decreased the time required for the formation of an apatite layer in 64% when incubated in SBF (28 days for HA and 10 days for 0.8 wt % Si-HA) [6]. A further increase on the concentration of silicon

resulted in an additional decrease on the time required for the formation of the apatite (75 % when compared to phase pure HA). These results support the mechanism proposed for the enhanced bioactivity of Si-HA on previous reports, where it was stated that this increased is due to a combination of its high dissolution rate of the Si-HA material and its physical-chemical properties. Its high solubility leads to a faster super-saturation of the serum free-SBF, and therefore a faster precipitation of an apatite layer and the more electronegative Si-HA surface can provide a preferential site for the nucleation of an amorphous calcium phosphate apatite layer than the HA surface, which can occur through the adsorption of Ca^{2+} ions on to the electronegative surface, resulting in an increase in surface charge and the attraction of phosphate groups [5].

The dissolution of Si-HA in the presence of serum-free SBF starts at early time points, on the AFM image the dissolution on the grain boundaries and grain are clear, therefore an apatite layer will form in a short period of time, as mentioned previously. Although, when a biomaterial is implanted in a living system, there are several proteins, enzymes and type of cells that will influence its behaviour [47], therefore, the dissolution-precipitation process is much more complex *in vivo*. In order to mimic the initial stages of the *in vivo* reactions the materials were incubated in serum-SBF to assess its effect on the dissolution and apatite formation. The dissolution kinetics of the materials incubated in serum SBF was slower when compared to the dissolution in serum free-SBF. At the same time point, no significant dissolution features were observed or apatite layer was visualized. The phase imaging AFM indicated the presence of a layer on top on these materials that could be a proteinaceous layer. The XPS analysis confirms this result, due to the increase on the concentration of nitrogen on the surface of the samples incubated in the presence of proteins.

Several mechanism have been proposed to explain the mechanism behind the effect of proteins on the apatite formation, namely that proteins can bind to the surface of the ceramic and control secondary nucleation, affecting the dissolution reprecipitation process in the ceramic [47], according to Kaufmann *et al* the protein layer will protect the surface and prevent early dissolution [48]. The ICP results demonstrated that in the presence of proteins a release of silicon into the surrounding medium was lower when compared to the samples incubated in serum free-SBF. Therefore, the results presented here are in agreement with Kaufman *et al*, indicating that the presence of the protein layer will indeed protect the surface of the material, delaying the diffusion of the atomic species to the surrounding medium, delaying the supersaturation of the solution and consequent apatite layer.

Acknowledgements

The authors wish to acknowledge to Dr. Julian Jones from the Imperial College, University of London, for his support on the ICP analysis and the FCT (Fundação para a Ciência e Tecnologia) for the financial support of ref. SFRH/BD/6173 of C. Botelho.

References

1. Carlisle E. Essentiality and function of silicon. In: Biochemistry of silicon and related problems. In: Proceedings of the 40th Nobel Symposium; Lidingö, Sweden; 1977.

2. Schwarz K, Milne D. Growth-promoting effects of silicon in rats. Nature. 1972;239:333.

3. Schwarz K. Significance and functions of silicon in warm-blooded animals. In: Biochemistry of silicon and related problems. In: Proceedings of the 40th Nobel Symposium; Lidingö, Sweden; 1977.

4. Patel N, Best S, Gibson IR, Hing K, Damien E, Bonfield W. A comparative study on the in vivo behavior of hydroxyapatite and silicon substituted hydroxyapatite granules. Journal of Materials Science: Materials in Medicine 2002;13:1199-1206.

5. Botelho C, Lopes M, Gibson I, Best S, Santos J. Structural analysis of Si-substituted hydroxyapatite: Zeta potential and x-ray photoelectron spectroscopy. Journal of Materials Science: Materials in Medicine 2002;13:1123-1127.

6. Botelho C, Stokes D, Brooks R, Best S, Lopes M, Santos JD. Effect of human serum proteins on the surface of pure HA and Si-substituted HA: AFM and ESEM Studies. Materials Science Forum 2003;455-456:378-382.

7. Botelho C, Brooks R, Lopes M, Santos JD, Best SM, Bonfield W. Biological and physical-chemical characterization of phase pure HA and Si-Substituted hydroxyapatite by different microscopy techniques. Key Engineering Materials 2004;254-2:845-848.

8. Botelho C, Brooks R, Kawai T, Ogata S, Ohtsuki C, Lopes M, et al. *In vitro* analysis of proteins adhesion to phase pure hydroxyapatite and silicon-substituted hydroxyapatite. Key Engineering Materials 2005;17:461-464.

9. Gibson IR, Best SM, Bonfield W. Chemical Characterization of Silicon-Substituted Hydroxyapatite. Journal of Biomedical Materials Research 1999; 44:422-428.

10. Gibson IR, Huang J, Best SM, Bonfield W. Enhanced In Vitro Cell Activity and Surface Apatite Layer Formation on Novel Silicon-Substituted Hydroxyapatites. In: Ohgushi H, Hastings, GW, Yoshikawa T., editor. Bioceramics 12; Nara, Japan: World Scientific Publishing Co. Pte. Ltd; 1999:191-194.

11. Gibson I, Best S, Bonfield W. Effect of silicon substitution on the sintering and microstructure of hydroxyapatite. Journal of the American Ceramic Society 2002;85(11):2771-2777.

12. Hench LL, Wilson J. Introduction. In: An Introduction to Bioceramics. Singapore: World Sientific; 1993.

13. Eskin SG, Horbett T, McIntire L, Mitchell R, Ratner B, Schoen F, et al. Some Background Concepts, Part II Biology, Biochemistry and Medicine. In: Biomaterials Sciences; 2004:237.

14. Lyman D, Metcalf L, Albo D, Richards K, Lamb J. The effect of chemical structure and surface properties of synthetic polymers on the coagulation of blood. In vivo adsorption of proteins on polymer surfaces. Transactions American Society for Artificial Internal Organs, 1974;20:474-478.

15. Horbett TA. The role of adsorbed proteins in tissue response to biomaterials" in Biomaterials Sciencs, Part II Biology, Biochemistry and Medicine. In: Biomaterials Sciences, Part II Biology, Biochemistry and Medicine; 2004:237-245.

16. Norde W, Lyklema J. BSA structural changes during homomolecular exchange between the adsorbed and the dissolved states. Journal of Biotechnology 2000;79:259-268.

17. Holland N, Marchant R. Individual plasma proteins detected on rough biomaterials by phase imaging afm. Journal of Biomedical Materials Research 2000;51:307-315.

18. Vroman L, Adams A. Why plasma proteins interact at the interfaces.Protein at the interfaces: Physicochemical and biochemical studies. In: Horbertt T, Brash J, editors. ACS Symp; 1986; Washington: ACS; 1986:154-164.

19. Daculsi G, Pilet P, Cottrel M, Guicheux G. Role of fibronectin during biological apatite crystal nucleation: ultrastructural characterization. Journal of Biomedical Materials Research 1999;2(47):228-233.

20. Rosengren A, Oscarsson S, Mazzocchi M, Krajewski A, Ravagliolo A. Protein adsorption onto two bioactive glass-ceramics. Biomaterials 2003;24:147-155.

21. MacDonald D, Deo N, Markovic B, Stranick M, Somasundaran P. Adsorption and dissolution behaviour of human plasma fibronectin on thermally and chemically modified titanium dioxide particles. Biomaterials 2002;23:1269-1279.

22. Lapin M, Warocquier-Clérout R, Legris C, Degrange M, Luizard M. Correlation between roughness and wettability, cell adhesion and cell migration. Journal of Biomedical Materials Research 1997;36:99-108.

23. Williams DF, Bagnall R. Adsorption of proteins on polymers and its role in the response of soft tissue. In: Williams D, editor. Fundamental aspects of biocompatibility. Raton, Florida: CRC Press; 1998. p. 113-127.

24. Groth T, Altankov G, Kostadinova A, Krasteva N, Albrecht W, Paul D. Altered vitronectin receptor (α_v integrin) function in fibroblasts adhering on hydrophobic glass. Journal of Biomedical Materials Research 1999;44:341-351.

25. Adão M, Saramago B, Fernandes A. Estimation of the surface properties of styrene-acrylonitrile random copolymers from contact angle measurements. Journal of Colloid and Interface Science 1999;217:94-106.

26. Young T. Miscellaneous works. London:Murray; 1835.

27. Hildebrand J. Journal of American Chemistry Society 1929;57(66).

28. Scatchard G. Equilibrium in non-electrolyte mixtures. Chemical Reviews 1949;44(1):7-35.

29. Owens D, Wendt R. Estimation of the surface free energy of polymers. Journal of Applied Polymer Science 1969;13:1741.

30. Wu S. Polymer Interface and Adhesion. New York: Deker; 1982.

31. van Oss C, Chaudhury M, Good R. Interfacial Lifshitz-Van der Waals and polar interactions in macroscopic systems. Chemical Reviews 1988;88(6):927-941.

32. Jha LJ, Best S, J.D. S, Gibson IR, Bonfield W, inventors; Silicon-Substituted Apatites and Process for the Preparation Thereof. Worldwide patent, PCT/GB97/02325 and US Patent Serial Nº 09/147773, 1999.

33. Bale M, Wohlfahrt L, Mosher D, Tomasini B, Sutton R. Identification of vitronectin as a major plasma protein adsorbed on polymer surfaces of different copolymer composition. Blood 1989;74:2698-2706.

34. Underwood P, Steele J, Dalton B. Effects of polystyrene surface chemistry on the biological activity of solid phase fibronectin and vitronectin, analysed with monoclonal antibodies. Journal of Cell Biology 1993;104:793-803.

35. Serro A, Fernandes A, Saramago B. Dynamic Interfacial behaviour of bovine serum albumin solutions on titanium surfaces. Colloids and surfaces. A: Physicochemical and Engineering Aspects 1997;125:209-219.

36. Cacciafesta P, Hallam K, Watkinson A, Allen G, Miles M, Jandt K. Visualization of human plasma fibrinogen adsorbed on titanium implant surfaces with different roughness. Surface Science 2001;491:405-420.

37. Jandt K. Developments and perspectives of scanning probe microscopy (SPM) on organic materials systems. Materials Science and Engineering 1998;R21:221-295.

38. Putman C, van der Werf K, de Grooth B, van Hulst H, Greve J. Tapping mode atomic force microscopy in liquid. Applied Physics Letters 1994;63:2454-2456.

39. Cleveland J, Anazykowski B, Schimd A, Elings V. Energy dissipation in tapping-mode atomic force microscopy. Applied. Physics Letters 1998;72:2613-2615.

40. Andrade J, Hlady V. Protein Adsorption and Materials Biocompatibility: A tutorial review and suggested hypotheses. Advances in Polymer Science 1986;1-58.

41. Aoki H. Science and Medical Applications of Hydroxyapatite. Tokyo, Japan: Takayama Press; 1991.

42. Davies J. The importance and measurment of surface charge species in cell behaviour interface. In: Ratner BD, editor. Surface characterization of biomaterials. New York: Elsevier; 1988:219-234.

43. Hench LL, Ethridge E. Biomaterials: an interfacial approach; 1982.

44. Lopes M, Monteiro FJ, Santos JD, Serro A, Saramago B. Hydrophobicity, surface tension and zeta potential measurements of glass reinforced hydroxyapatote composites. Journal of Biomedical Materials Research 1999;45:370-375.

45. Ferraz M, Monteiro FJ, Serro A, Saramago B, Gibson IR, Santos JD. Effect of chemical composition on hydrophobicity and zeta potential of plasma sprayed HA/CaO-P_2O_5 glass coatings. Biomaterials 2001;22:3105-3112.

46. Amaral M, Lopes M, Santos J, Silva R. Wettability and surface charge of Si_3N_4-bioglass composites in contact with simulated physiological liquids. Biomaterials 2002;23:4123-4129.

47. Rohanizadeh R, Padrines M, Bouler J, Couchourel D, Fortun Y, Daculsi G. Apatite precipitation after incubation of biphasic calcium-phosphate ceramic in various solutions: Influence of seed species and proteins. Journal of Biomedical Materials Research 1998;20:2287-2303.

48. Kaufmann E, Ducheyne P, Radin S, Bonnel D, Composto R. Initial events at the bioactive glass surface in contact with a protein, containing solutions. Journal of Biomedical Materials Research 2000;52(825-830).

In vitro analysis of protein adhesion to phase pure hydroxyapatite and silicon substituted hydroxyapatite.

C.M. Botelho[1,2], R. A. Brooks[3], T. Kawai[4], S. Ogata[4], C. Ohtsuki[4] S.M. Best[5], M. A. Lopes[1,2], J.D. Santos[1,2], N. Rushton[3], W. Bonfield[5]

[1]INEB- Instituto de Engenharia Biomédica, Laboratório de Biomateriais, Rua do Campo Alegre, 823, 4150-180 Porto, Portugal

[2]FEUP- Faculdade de Engenharia da Universidade do Porto, DEMM, Rua Dr. Roberto Frias, 4200-465 Porto, Portugal

[3]Orthopaedic Research Unit, Box 180, Addenbrookes Hospital, Hills Road Cambridge, CB2 2QQ, U.K.

[4]NAIST- Nara Institute of Science and Technology, Nara, 630-0192 Japan

[5]Department of Materials Science and Metallurgy, University of Cambridge, CB2 3 QZ, U.K.

Key Engineering Materials Vols. 284-286, (2005) 461-464

Abstract

The adhesion of bovine collagen type I, bovine serum albumin, bovine IgG, 1 % and 10 % (v/v) human serum to hydroxyapatite (HA), silicon-substituted hydroxyapatite (Si-HA) and tissue culture plastic were studied. The materials were incubated at 37 ºC for 30 minutes, after which the protein solution was removed and analysed. The adsorbed protein was evaluated by electrophoresis and immunoassay after extraction from the materials. The degree of adhesion was higher for collagen, followed by IgG and albumin on all materials. However there was no significant difference in the amount of collagen adsorbed onto the surface of each material and this was also the finding with albumin and IgG. These results suggest that the increased bioactivity seen with Si-HA is not only due to the degree of protein adhesion, but may possibly be due to changes in the conformation of the bound proteins.

Keywords: Silicon-Substituted Hydroxyapatite, Human Serum Proteins, Bovine Collagen type I, Bovine Serum Albumin, Immunoglobulin G (IgG).

Introduction

In vivo studies have demonstrated that silicate ions incorporated into crystal lattice significantly enhance the bioactivity of hydroxyapatite bone grafts [1-3]. In particular, high-resolution transmission electron microscopy studies have shown notable differences in apatite deposits at the surface of HA and Si-HA implants. Organised collagen fibrils were observed at the Si-HA/bone interface after 6 weeks *in vivo*. In contrast, organised collagen fibrils were only observed after 12 weeks around HA implants. These findings suggest that the bone apposing Si-HA implants was at a more developed stage [4], and corroborate *in vitro* findings of enhanced osteoblast-like cell attachment on Si-HA ceramics [2, 3]. In an attempt to understand the mechanism of this enhanced bioactivity, several *in vitro* studies were performed. Plasma protein adsorption is one of the first events that occur after implantation [5]. We hypothesised that one of the reasons for the increased bioactivity could be altered or preferential protein adhesion.

To assess the adhesion of human serum proteins two different protein concentrations were used 1 % (v/v) and 10 % (v/v). To study preferential adhesion three proteins belonging to different groups were used; bovine serum albumin (BSA) a globular protein with an isoelectric point of approximately of 4.7 [6], immunoglobulin G (IgG) also a globular protein that can be characterised by its multi-domains showing strong structure-function relations for the different domains [7] with an isoelectric point of approximately 6.8 [6], and bovine collagen type I a glycoprotein with a triple-helical structure of collagen fibrils and an isoelectric point of approximately 8-9 [8].

Materials and Methods

The preparation of phase pure HA and Si-HA is fully described elsewhere [9, 10]. The powders were uniaxially pressed into discs and sintered at 1300 ºC for 2 hours. Human AB serum was diluted in a phosphate buffer saline solution (PBS), to obtain a concentration of 1 % (v/v) and 10 % (v/v). Albumin, IgG and collagen were diluted in PBS to obtain a concentration of 0.250 mg/mL. The dense discs were incubated in the protein solution (pH = 7) for 30 min at 37 ºC, after which the solution was removed. The protein concentration before and after incubation was measured by two methods, biocinchoninic acid (BCA from Pierce) and NanoOrange from Sigma. Two further experiments were performed to assess the adhesion of collagen to the HA and Si-HA surface. Samples were incubated with 0.250 mg/ml

of bovine collagen type I. After rinsing the materials the adherent protein was removed by incubating the samples for 1 hour at 37º C with an SDS-buffer. The final solution was run on a 10% SDS-PAGE gel. The gel was stained with silver stain DAIICHI (Daiichi pure chemicals, Japan). The second experiment involved incubating the samples in two different solutions: 10 µg/ml of bovine collagen type I and 10 µg/ml of bovine collagen, type I with 10 µg/ml of IgG (R&D Systems), for 30 minutes at 37 ºC, after which the protein solution was again removed. The adherent collagen was measured by ELISA, using goat anti-collagen type I as the first antibody and HRP-conjugated Avidin was used to detect the first antibody. The colour was developed using a TMB Peroxidase EIA substrate kit and the absorbance measured at 450 nm.

Results

No significant difference between the adhesion of the proteins to the HA and Si-HA was observed. However the degree of adhesion was greater for collagen, followed by IgG and albumin (Figure 1a). The adhesion behaviour of the 1 % (v/v) and 10 % (v/v) of human serum is similar on the ceramic materials (Figure 1b).

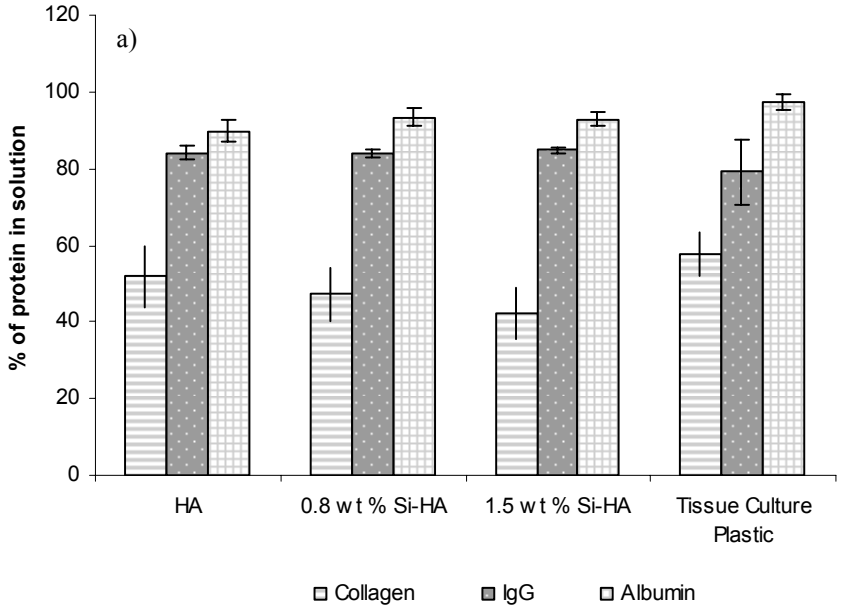

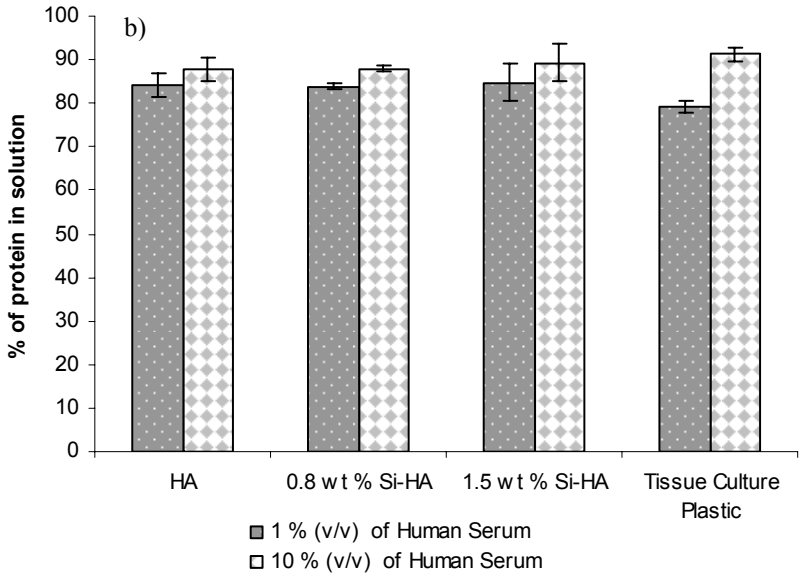

Figure 1 - Percentage of protein remain in solution for the different materials, measured by the BCA method (mean ± standard error of the mean; n=3.)

To determine the total binding capacity, the mass of adherent protein was normalized by the surface area. As can be seen in figure 2, all materials demonstrated a higher binding affinity to collagen. A slight increase in the affinity of collagen was observed with the increase of the silicon content. No difference was observed in the adhesion of IgG, but in the case of the albumin a slight decrease was observed on the Si-HA compared to HA. For human serum proteins, again a slight decrease in adhesion was observed onto 1.5 wt % Si-HA. However, none of these differences were significant.

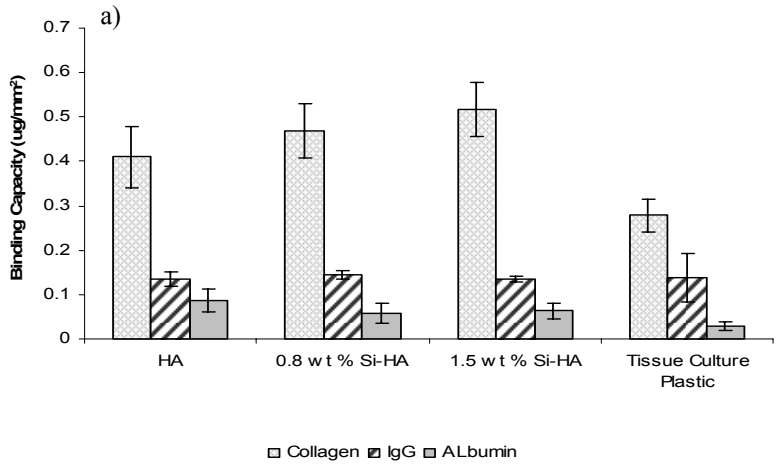

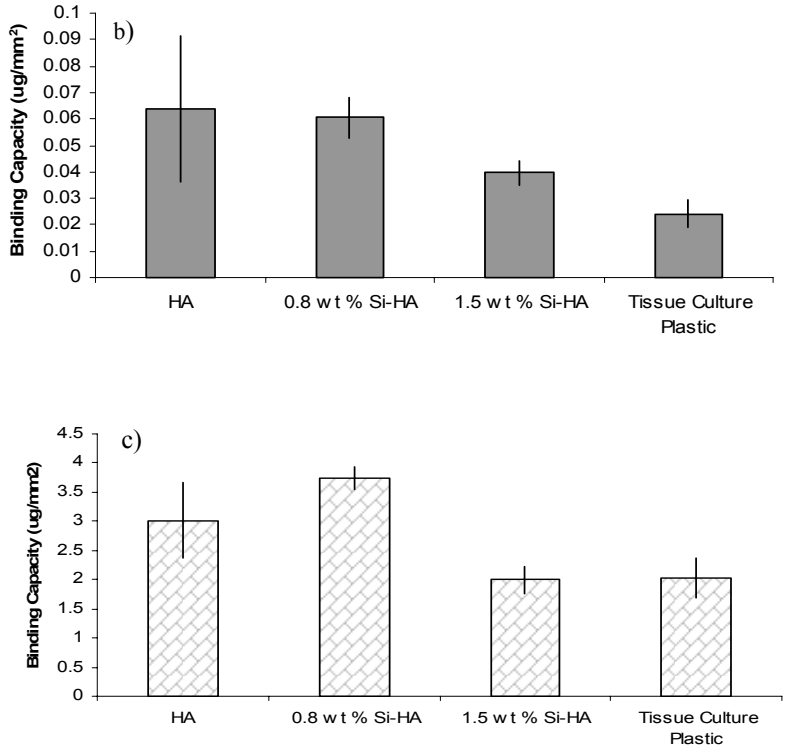

Figure 2 - Total binding capacity (µg of adherent protein/surface area (mm^2), a – collagen type I, IgG and albumin, b – 1 % (v/v) of HS and c – 10 % (v/v) HS (mean ± standard error of the mean; n=3.)

Similar results were observed when the samples were analyzed using the NanoOrange kit (data not shown).

Due to the slight increase of collagen binding to the Si-HA material two experiments were carried out to investigate this further, as it can be seen in figure 3A.

It appears to be a higher concentration of collagen adhering to 1.5 wt % Si-HA, although upon repeating this result was not consistent, as seen in figure 3B. A similar result was observed with the ELISA method (data not shown).

A

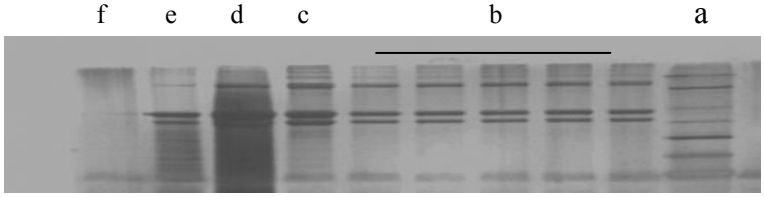

B

c b a

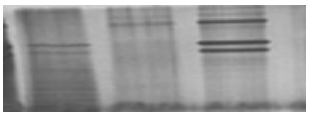

Figure 3 - Two SDS-PAGE gels with different samples prepared in the same way: (A) -a – molecular weight markers, b – Collagen standard, c- Collagen removed from Tissue culture plastic d - Collagen removed from 1.5 wt % Si-HA, e – Collagen removed from 0.8 wt % Si-HA and f - Collagen removed from HA; B - a – Collagen standard, b- Collagen removed from 1.5 wt % Si-HA, c - Collagen removed from HA.

Discussion

The pattern of adsorbed proteins observed in the study could be explained by the electrostatic interactions between the proteins and the substrates used. The three proteins studied have different structures and different isoelectric points, therefore the overall net charge of these proteins will be different at pH 7. Collagen would have an overall positive charge, IgG a slight negative charge and albumin a more negative charge. As reported in previous studies, the surface charge of HA and Si-HA is negative [11], therefore the electrostatic interactions between the materials and the protein is greater if the protein has an overall positive charge, and could be one of the reasons for the higher affinity of collagen to the different substrates, followed by IgG and albumin as was observed. Muller *et al* also reported a higher adhesion of albumin and IgG to a positively charged surface, although IgG presented a lower adhesion due to its lower negativity. In that study a basic protein, lysozyme, demonstrated higher adhesion to a negatively charged substrate [12]. The adhesion of proteins from the different concentrations of human serum was not conclusive and further studies are required. In an attempt to quantify the adhesion of collagen to Si-HA and HA, two further methods were used, SDS-PAGE and ELISA. No consistent differences in the adsorption of collagen to the HA and Si-HA surface were observed. We had hypothesized that the increase in bioactivity of Si-HA could be due to a higher adhesion of proteins. These results suggest that the increase bioactivity seen with Si-HA is not only due to the degree of protein adhesion. Although the composition of the protein layer formed *in vivo* is still poorly understood, it has been reported that the protein pattern on calcium phosphates surfaces *in vivo* is different from the one obtained *in vitro*. This pattern also changes with implantation time, in part due to

cellular proteolytic activity and secretion of proteins by cells [13]. An alternative theory for the increased bioactivity of Si-HA is related to changes in the conformation of proteins, as it is known that the activity and specificity of a protein is related to its conformation. In addition Reffit *et al* demonstrated a positive effect of soluble silicon in human cells [15]. In previous studies we have demonstrated that there is a preferential release of silicon into the incubation solution [11], therefore the enhanced bioactivity may also be due to a direct effect of silicon on the cells**.**

Conclusions

These results suggest that the increased bioactivity seen with Si-HA is not only due to the degree of protein adhesion. It may be due to changes in the conformation of proteins or a direct effect of silicon on the cells. Further studies will be performed to pursue these hypotheses**.**

Acknowledgements

The authors wish to acknowledge the financial support of ref. SFRH/BD/6173 grant for C. M. Botelho and the project entitled “Revestimento de Hidroxiapatite modificada com silício para aplicações biomédicas” ref. POCTI/CTM/49238/2002, financed by FCT (Fundação para a Ciência e Tecnologia).

References

[1] Patel *et al*, J. of Mat. Sci.: Mat. in Med., Vol. 13 (2002) p. 1199.

[2] I.R. Gibson *et al*, in Bioceramics, Vol. 12, (1999), p. 191.

[3] C.M. Botelho *et al*, in Key Engineering Materials, Vol. 254-256, (2003), p. 841-844.

[4] Porter *et al*, in Biomaterials, Vol. 5, (2004), p. 3303-3314.

[5] Takami *et al*, in J. Biomed Mater. Res., Vol. 40, (1998), p. 24-30.

[6] Kandori *et al*, in J. Colloid and Interface Science, Vol 273, (2004), p. 406-413.

[7] Vermeer *et al*, Biochimica et Biophysica Acta Vol 1526 (2001), p 61-69.

[8] Kikuchi *et al*, Biomaterials, Vol 22, (2001), p. 1705-1711.

[9] L.J. Jha, *et al*, Worldwide patent, PCT/GB97/02325 and US Patent Serial Nº 09/147773, (1999).

[10] I.R. Gibson *et al*, J. Biomed. Mat. Res., Vol. 44, (1999), p.422.

[11] C. M. Botelho *et al*, J. Mater. Sci:Mater. Med**,** Vol**.** 13 (2002), p. 1123-1127.

[12] Muller *et al*, Macromol. Rapid Commun. Vol. 20, (1999), p. 607-611.

[13] Veerman *et al*, in Biomaterials, Vol. 8, (1987), p. 442-448.

[14] Haynes *et al*, in Colloids and Surfaces B: Biointerfaces, Vol. 2 , (1994) 517-566.

[15] D. M. Reffit *et al*, Bone, Vol. 32, (2003) p.127.

Chapter 4

In Vitro Biological Characterisation

In vivo studies carried out by Nelesh Patel *et al* using a lapine and ovine model demonstrated the positive effect of silicon-substituted hydroxyapatite (Si-HA) on bone regeneration. The two main types of cells involved in bone regeneration are the osteoblasts and osteoclasts. Due to the complexity of the *in vivo* system it was not possible to determine the mechanism behind the enhanced bone regeneration. So, we performed several *in vitro* tests using human osteoblasts and osteoclasts.

Human osteoblasts were seeded on dense HA and two compositions of Si-HA (0.8 wt % Si-HA and 1.5 wt % Si-HA). The effect of the incorporation of silicon on the HA lattice on osteoblasts was assessed by the measurement of different osteoblastic markers such as: collagen type I (COL I), alkaline phosphatase (ALP), osteocalcin (OC) and protein expression, at different time points.

The cells seeded on the three substrates adhered, proliferate and expressed different osteoblastic markers. The incorporation of 0.8 wt % of silicon into the HA lattice induced higher proliferation of human osteoblast and protein expression. Although, in the presence of a higher concentration of silicon (1.5 wt %) the cells responded with an increase on the ALP expression, indicating that the cells were differentiating faster.

Osteoclasts precursors were seeded at the surface of the 3 materials. Several osteoclasts markers such as, actin rings, several nuclei, TRAP and vitronectin receptors were measured. The increase on the concentration of calcium and phosphorous in the medium culture was used as an indicator of activity and resorption.

HA and Si-HA allowed the differentiation of osteoclasts precursors (peripheral mononuclear blood cells and monocytes CD 14+) to mature osteoclasts. All the cells expressed osteoclasts markers. Significant differences on the concentration of the calcium and phosphorous on the medium from the Si-HA samples seeded with osteoclasts were detected, indicating the osteoclasts are active and resorbing, especially on 1.5 wt % Si-HA.

Biological and physical characterisation of phase pure HA and Si-substituted hydroxyapatite by different microscopy techniques

C.M. Botelho[1,2], R. A. Brooks[3], S.M. Best[4], M. A. Lopes[1,2], J.D. Santos[1,2], N. Rushton[3], W. Bonfield[4]

[1]INEB- Instituto de Engenharia Biomédica, Laboratório de Biomateriais, Rua do Campo Alegre, 823, 4150-180 Porto, Portugal.

[2]FEUP- Faculdade de Engenharia da Universidade do Porto, DEMM, Rua Dr. Roberto Frias, 4200-465 Porto, Portugal, jdsantos@fe.up.pt.

[3]Orthopaedic Research Unit, Box 180, Addenbrookes Hospital, Hills Road Cambridge, CB2 2QQ.

[4]Department of Materials Science and Metallurgy, University of Cambridge, CB2 3 QZ, UK.

Key Engineering Materials, 254-256, 2004, 845-848

Abstract

Two different microscopy techniques were used to investigate the response of human osteoblast cells to hydroxyapatite (HA) and silicon substituted hydroxyapatite (Si-HA), namely, fluorescence and confocal microscopy. The changes in the surface of HA and Si-HA, after incubation for different periods of time in simulated body fluid, were assessed using atomic force microscopy and environmental electron scanning microscopy. Cell proliferation was higher on Si-HA compared to HA. In addition more focal points of adhesion were seen on Si-HA than on HA. Using atomic force microscopy and environmental scanning electron microscopy it was possible to observe changes in the surface of both materials, namely dissolution features and the formation of an apatite layer. These findings support the results of a previous study, which showed that Si-HA had a higher dissolution with the preferential release of silicon into the medium and this fact may account for the changes observed in the cell behaviour.

***Keywords*:** Silicon-Substituted Hydroxyapatite, Human Osteoblast Cells, Confocal Microscopy, Fluorescence Microscopy, Atomic Force Microscopy and Environmental Electron Scanning Microscopy.

Introduction

In the 1970´s several groups demonstrated that bone mineralization requires a minimum concentration of soluble silicon [1-4]. Hench reported that the deterioration in the proliferation and function of osteoblasts due to osteopenia and osteoporosis is related to the loss of biologically available silicon [5] and Keeting *et al* reported that, bone cells in culture proliferate more rapidly in the presence of soluble silicon [6]. A recent study by Reffit *et al* demonstrated that physiological concentrations of soluble silicon stimulate collagen type I synthesis in human osteoblast-like cells and promote osteoblastic differentiation [7]. These studies clearly demonstrate the possible advantage of incorporation of silicon into the lattice of biomaterials intended for applications in bone tissue regeneration. Therefore to take advantage of the positive biological effect of silicon, Si-substituted hydroxyapatite (Si-HA) has been developed using a chemical precipitation route [8, 9]. Patel *et al* demonstrated that the *in vivo* bioactivity of hydroxyapatite is significantly enhanced with the addition of silicate ions into the lattice of hydroxyapatite [10]. Gibson *et al* [11] also demonstrated that Si-HA increases the metabolic activity of human osteosarcoma cells. The aim of this work was to assess the effect of Si-HA on human osteoblast (HOB) cells and to correlate these findings with the rate of dissolution of the Si-HA. The techniques used to analyse the effect of silicon on dissolution of the material and on the cells were: confocal laser scanning microscopy (CM), fluorescence microscopy (FM), environmental scanning electron microscopy (ESEM) and tapping mode atomic force microscopy (AFM).

Materials and Methods

The preparation of phase pure HA and Si-HA is fully described elsewhere [8, 9]. The powders were uniaxially pressed to discs and sintered at 1300 ºC for 2 hours. The HOB cells were grown in McCoy's 5A modified medium, supplemented with 10 % (v/v) foetal calf serum, 30 $\mu g ml^{-1}$ vitamin C, and 1 % (v/v) L-Glutamine at 37 ºC. Cells of passage number 5 were seeded onto two different materials, HA and 0.8 wt% Si-HA at a density of 10 000

cells/cm^2. After 3 and 7 days of culture, the cells were fixed in 4 % formaldehyde/phosphate buffer saline solution, pH 7.4 at room temperature for 15 min.

The staining procedure is described elsewhere [12]. After staining the samples were mounted with Vectashield fluorescent mountant and viewed using both FM and CM. At each time point the lactate dehydrogenase (LDH) release was determined, using an enzyme assay kit (Promega, UK). LDH is a cytosolic enzyme present within all mammalian cells [13]. If the cell membrane is damaged there is a leakage of LDH into the medium, through this method is possible to have an accurate measure of cell membrane integrity and cell viability [14]. To determine the changes on the surface of HA and Si-HA, samples of both materials were incubated in simulated body fluid (SBF), at 37 ºC, for different periods of time. Changes were assessed by AFM and ESEM. AFM imaging was performed using a Digital Instruments NanoScope III and ESEM signals were collected in low vacuum mode, using an off axis gaseous secondary electron detector**,** the beam intensity used was 10 kV.

Results

The number of cells on the 0.8 wt% Si-HA was significantly higher than on phase pure HA, which could indicate that the silicon enhances the proliferation of HOB cells (Figure 1a), and there was no significant variation in the LDH release with time. When the LDH was expressed per cell, this parameter was significantly lower on Si-HA than on HA, and this could indicate that there are more viable cells on the surface of Si-HA than on the HA surface (Figure 1b).

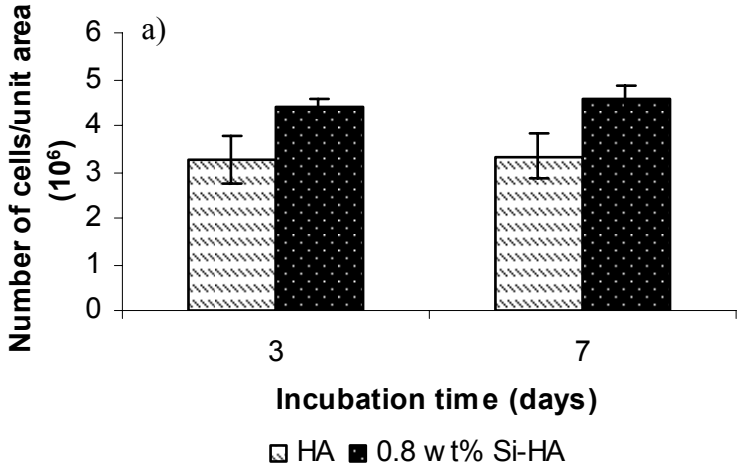

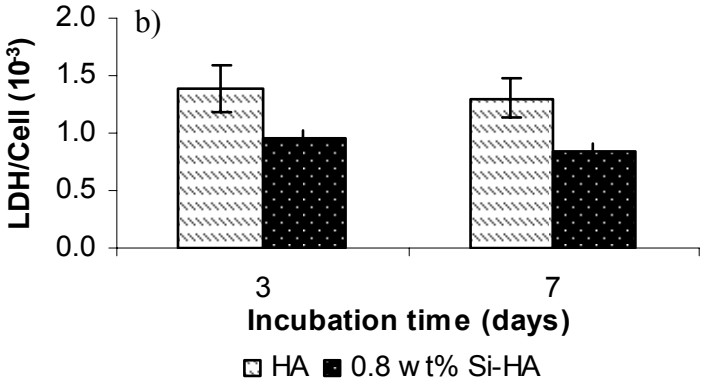

Figure 1 – Variation of the number of cells (a) and LDH/Cell release (b) on phase pure HA and Si-HA with time, (mean ± standard deviation, n=3).

Using FM it was possible to view the distribution and number of cells on the HA and Si-HA. The number of HOB cell on the Si-HA surface appeared to be higher and more closely packed than on HA, (Figure 2 a,b and Figure 3 a,b).

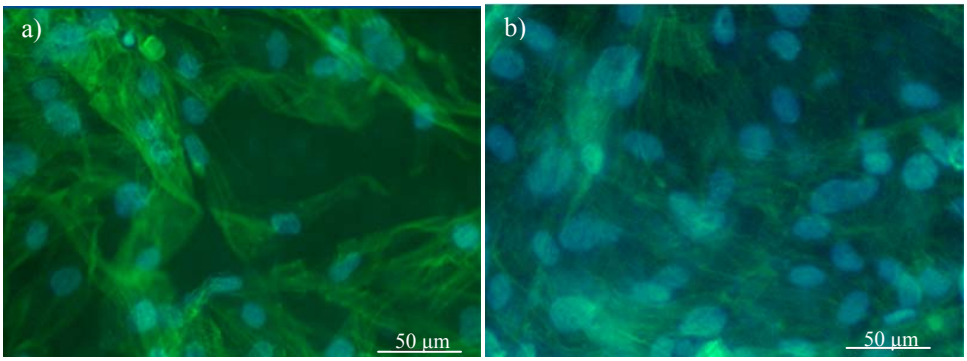

Figure 2 – FM images of HOB onto HA (a) and Si-HA (b) after 3 days of incubation.

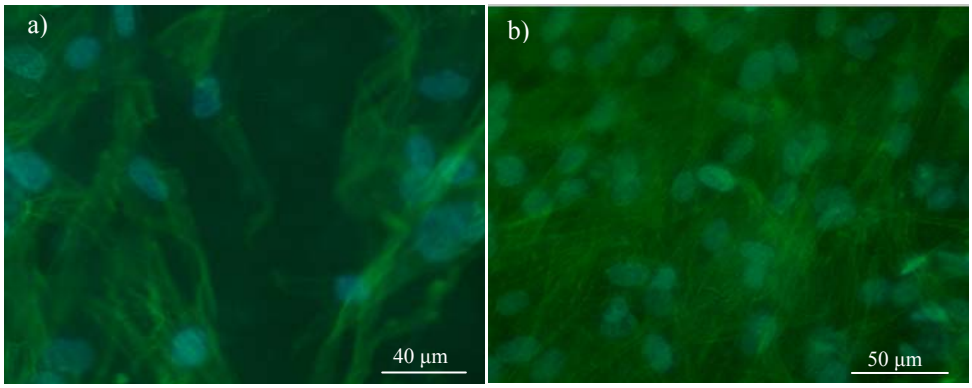

Figure 3 – FM images of HOB onto HA (a) and Si-HA (b) after 7 days of incubation.

The cell cytoskeleton and vinculin in focal adhesion complexes were visualized using confocal microscopy to image the cells on the different materials. At day 3, cells were spread

on the substrates as shown in Figure 4 a,b. Although at day 7 the cells seemed to be less spread on both materials (Figure 5 a,b). There appeared to be more focal points of adhesion on the Si-HA than on the HA.

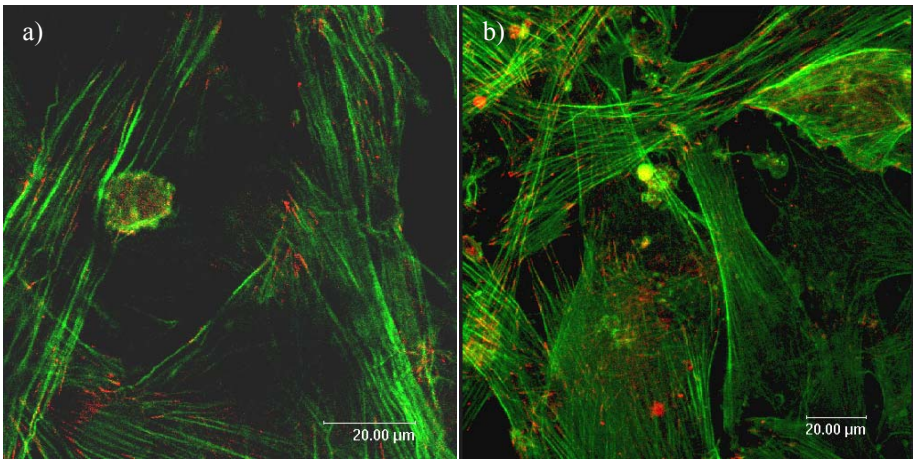

Figure 4 – CM image of HOB on HA (a) and Si-HA (b) after a period of 3 days of incubation.

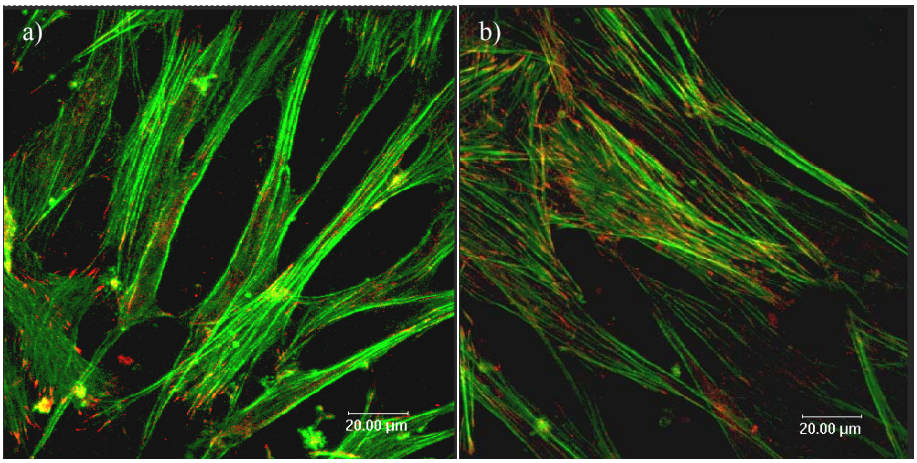

Figure 5 – CM image of HOB on HA (a) and Si-HA (b) after a period of 7 days of incubation.

Both AFM and ESEM revealed that the dissolution of the Si-HA started earlier than the dissolution of HA. After 7 days of incubation the Si-HA surface was partially covered by an apatite layer (Figure 6 b), indicating, that there had been extensive dissolution of Si-HA at earlier time points [15], while for HA significant changes were only detected after 14 days of incubation (results not shown). AFM was used to observe small features in the surface of both materials. At day 1, dissolution features were visible at the surface of Si-HA, but not on the HA surface (Figure 7 a,b) and it was not possible to observe significant dissolution features on the HA surface after 7 days (data not shown).

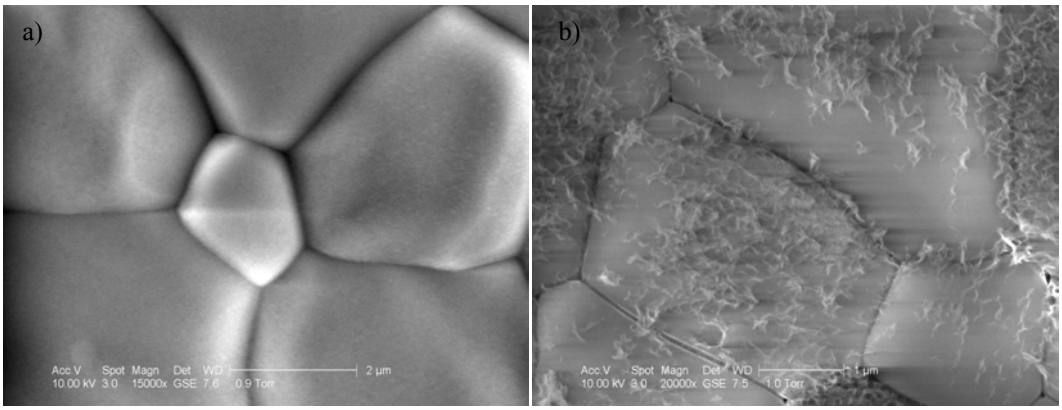

Figure 6 – ESEM image of HA (a) and Si-HA (b) after incubation in SBF for 7 days.

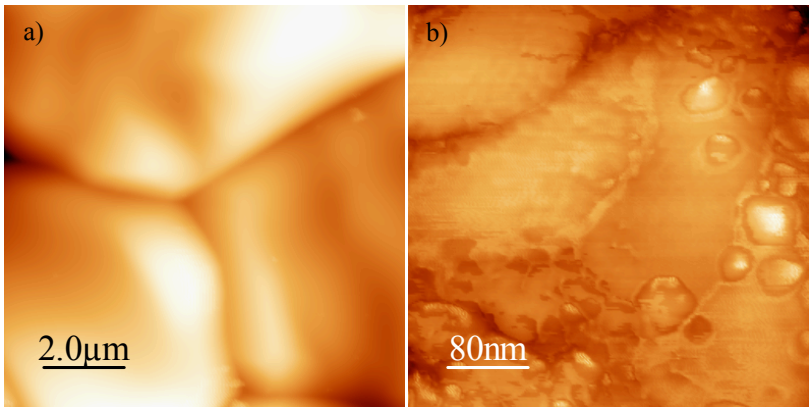

Figure 7 – AFM image of HA (a) and Si-HA (b) after incubation in SBF for 1 day

Discussion

These results show an increase in proliferation and an increase in the number of viable HOB grown on Si-HA compared to HA. These results complement those of Gibson *et al* [11], who showed that Si-HA increase the activity of osteoblast-like cells. The adhesion of cells to a substrate involves extracellular matrix proteins, cell membrane proteins and cytoskeleton proteins which interact together to induce signal transduction, promoting the action of transcription factors and consequently regulating gene expression [16]. The external face of focal contacts present specific proteins such as integrins, these molecules bind to specific ligands. Bone cells can adhere to the substrate through $\alpha_2\beta_1$ integrin that binds to collagen [16]. According to the literature, there is a preferential dissolution of silicon in the Si-HA and we have shown early dissolution of this material, so there will be soluble silicon in the medium available to cells [17]. Reffit *et al* [7] showed that soluble silicon increases the production of collagen, and this could be an explanation for the increased number of focal

points of adhesion, observed on the HOB cell cultured on the Si-HA allowing the cells to attach and spread more extensively.

Conclusions

Si-HA increases the proliferation of human osteoblast cells, resulting in more viable cells on the surface compared to HA. The increase in the number of focal points of adhesion may be due to the release of silicon to the medium stimulating the production of collagen by HOB cells. However the mechanism by which the silicon increases the collagen production and increases the proliferation is not still fully understood and more studies are required.

Acknowledgements

The authors wish to acknowledge the financial support of ref. SFRH/BD/6173 grant for C. M. Botelho financed by FCT (Fundação para a Ciência e Tecnologia).

References

[1] E. M. Carlisle, Fed. Proc., Vol. 43, (1984), p. 680.

[2] E. M. Carlisle, in: *Silicon Biochemistry,* (D. Evered & M. O'Connor, eds.), Wiley, N. York 1986.

[3] K. Schwarz, in: *Biochemistry of Silicon and Related Problems*, N. York, (1978), p .207.

[4] K. Schwarz, and D.B. Milne, Nature, Vol. 239, (1972), p. 333.

[5] L.L. Hench, in: *Sol-Gel Silica Properties, Processing and technology Transfer*, (1999), chapter 10 Biological Implications, p .116-163.

[6] P.E. Keeting, *et a*l, J. Bone Mineral Res. Vol. 7, (1992), p. 1281.

[7] D. M. Reffit *et al*, Bone, Vol. 32, (2003) p.127.

[8] L.J. Jha, *et al*, Worldwide patent, PCT/GB97/02325 and US Patent Serial Nº 09/147773, (1999).

[9] I.R. Gibson *et al*, J. Biomed. Mat. Res., Vol. 44, (1999), p.422.

[10] Patel *et al*, J. of Mat. Sci.: Mat. in Med., Vol. 13 (2002) p. 1199.

[11] I.R. Gibson *et al*, in Bioceramics, Vol. 12, (1999), p. 191.

[12] M. J. Dalby *et al*, Biomaterials, Vol. 24 (2003), p. 927.

[13] M. Allen *et al*, Clinical Materials, Vol. 16 (1994), p. 189.

[14] T. Rae *et al*, J. Biomed. Mater. Res, Vol. 11, (1977), p. 839.

[15] C.M. Botelho *et al*, Advanced Materials Fórum, in Press.

[16] K. Anselme, Biomaterials, Vol. 21 (2000), p. 667.

[17] C. M. Botelho *et al*, J. Mater. Sci:Mater. Med**,** Vol**.** 13 (2002), p. 1123.

Human osteoblast response to silicon-substituted hydroxyapatite

C. M. Botelho[1,2], R.A Brooks[3], S. M. Best[4], M. A. Lopes[1,2], J. D. Santos[1,2], N. Rushton[3], W. Bonfield[4]

[1]INEB- Instituto de Engenharia Biomédica, Laboratorio de Biomateriais, Rua do Campo Alegre, 823, 4150-180 Porto, Portugal.

[2]FEUP- Faculdade de Engenharia da Universidade do Porto, DEMM, Rua Dr. Roberto Frias, 4200-465 Porto, Portugal.

[3]Orthopaedic Research Unit, Box 180, Addenbrooke's Hospital, Hills Road Cambridge, CB2 3QZ, UK.

[4]Department of Materials Science and Metallurgy, University of Cambridge, Pembroke Street, Cambridge, CB2 3QZ, UK.

Journal of Biomedical Materials Research, submitted

Abstract

Human osteoblasts were cultured on hydroxyapatite (HA) and 0.8 wt % and 1.5 wt % silicon substituted hydroxyapatite (Si-HA) discs. The influence of these substrates on cell behaviour *in vitro* was assessed by measuring total protein in the cell lysate and the production of several phenotypic markers: collagen type I (COL I), alkaline phosphatase (ALP), osteocalcin (OC) and the formation of bone mineral. After 7 days β-glycerophosphate and physiological levels of hydrocortisone were added to the culture medium to stimulate cell differentiation and mineral production. There was a significantly higher production of ALP on 1.5 wt % Si-HA at day 7 following which, the addition of hydrocortisone promoted the differentiation of cells on the other two substrates. Hydrocortisone addition also decreased the production of OC. During the period when hydrocortisone was present no significant difference in behaviour was seen between cells on Si-HA and HA however, following removal of hydrocortisone, cells responded to 0.8 wt % Si-HA with a significant increase in protein production. Using fluorescence microscopy nodular structures labelled with tetracycline were observed on the surface of all substrates after 21 days. These structures were

deposited on areas of high cell density but were not related to the presence or level of silicon in the substrate. These results indicate that human osteoblasts are affected by the presence of silicon in the HA substrate and that the timing of these effects may be dependent upon the level of silicon substitution.

Keywords: Silicon, Human Osteoblasts, Hydrocortisone, β-glycerophosphate and Nodular Mineral Formation

Introduction

Calcium phosphates when implanted *in vivo* create a functional interface with the host tissue [1-4] and this has led to an increased interest in the materials for clinical use. This behaviour results from several physicochemical reactions at the interface, namely protein and cell adhesion, that will ultimately result in the deposition of a calcified matrix. One of the most common materials used as a bone graft is hydroxyapatite (HA). Although, it has been demonstrated that HA has the ability to form an apatite layer and promote mineralization in both *in vitro* [5] and *in vivo* environments [6], the process is relatively slow, hence the material may be ineffective in the treatment of complex orthopaedic conditions, for example in fracture repair non-union or in proximity to a spinal fusion. In an attempt to increase the bioactivity of HA, silicon ions were incorporated into the HA lattice [7, 8].

Silicon biochemistry and its involvement in several metabolic pathways it has been study for several years. It has been reported that in 1878 Louis Pasteur said "*Effects of silicic acid are destined to play a great and major role in therapy*" [9]. Several reports mentioned the positive effect of silicon in several situations, such as DNA synthesis, protein synthesis, atherosclerosis and bone formation and development [9-17]. In 1972, Carlisle, Schwarz and Milne *et al* reported for the first time that a silicon deficiency diet in chicks and rats, led to abnormally shaped bones and defective cartilaginous tissue, but that these effects could be corrected by the incorporation of silicon in their diet [9, 15-17]. These and further studies indicated that silicon might play an important role in connective tissue metabolism especially in bone and cartilage [18-20]. Others studies showed that silicon can have an effect on gene activity [21-23]. Baxter *et al* and Finkelstein *et al* suggested that in animal cells some DNA-binding proteins might be implicated in the regulation of gene expression [10, 12]. Voronkov demonstrated that nucleic acids contain silicon atoms. In DNA one atom of silicon corresponds to an average of 20-30 atoms of phosphorous, and in the RNA this ratio changes

to 25-45 atoms. Indicating that silicon has a key role in the structure of nucleic acids, in the mechanism of protein biosynthesis, and in the transmission of hereditary information [22]. Keeting *et al* showed that Zeolite A, a particulate material containing silicon, stimulates the proliferation and differentiation of osteoblast-like cells in culture [24]. A recent study by Reffit *et al* demonstrated that physiological concentrations (10 – 20 μM) of soluble silicon stimulate collagen type I synthesis in human osteoblast-like cells and promote osteoblast differentiation [19]. *In vivo*, Patel *et al* have demonstrated that the bioactivity of HA is significantly enhanced by the addition of silicate ions into the lattice. [6]. *In vitro* studies by Gibson *et al* [25] demonstrated that silicon-substituted hydroxyapatite (Si-HA) increased the metabolic activity of human osteosarcoma cells and Botelho *et al* [26] demonstrated an increase in the adhesion of human osteoblasts when cultured on Si-HA. It has been demonstrated that an increase in silicon content in the HA lattice results in enhanced bioactivity, resulting in a more rapid apatite formation [27].

The aim of this work was to study the effect of silicon-substituted hydroxyapatite on the differentiation of human osteoblasts (HOBS) and on their ability to induce mineralization. Therefore, HOBS were cultured on discs of phase pure HA, 0.8 wt % and 1.5 wt % Si-HA. Cell proliferation and differentiation markers were followed with time.

Materials and Methods

Materials preparation

HA, 0.8 wt % and 1.5 wt % of Si-HA were prepared according to the method described by Gibson *et al* [8]. Using an aqueous precipitation chemical reaction, between calcium hydroxide and orthophosphoric acid solutions. Silicon tetraacetate was incorporated into the reaction mixture as a source of silicate ions. The HA and Si-HA powders were uniaxially die pressed and sintered at 1300 ºC for 2 hours.

Cell culture

Human osteoblast cells (HOBS) were isolated from trabecular bone from patients undergoing hip joint replacement surgery (PromoCell GmbH). HOBS were grown in McCoy´s medium supplemented with 10 % (v/v) of foetal calf serum (FCS), 1 % (v/v) L-glutamine-penicillin-streptomycin (200 mM glutamine, 10,000 units/ml penicillin and 10 mg/ml streptomycin) and 30 μg/ml of vitamin C (growth medium). All cell culture reagents

were obtained from Invitrogen, Paisley, UK and all other chemicals from Sigma, Poole, UK except where indicated. Cells were seeded (8000 cells/cm^2) onto HA and Si-HA discs and cultured in growth medium. The medium was changed every two days. From day 7, 7.5 mM of β-glycerophosphate and 200 nM hydrocortisone were added at each medium change until day 25, from this day until the end of the culture only growth medium was added.

Tetracycline and labelling of cell nuclei

Nine μg/ml of tetracycline was added to the medium, 24 hours prior the termination of the culture, to visualize mineral nodule formation.

At each time point, cells were fixed in 4 % formaldehyde/phosphate buffer saline solution, pH 7.4 at room temperature for 15 min and stained with 4`,6 – diamidino-2-phenylindole (DAPI) to visualize cell nuclei.

Measurement of total protein

At day 1, 3, 7, 10, 14, 21 and 27 the samples were analysed for total protein, using the bicinchoninic acid method (BCA, Merck, Poole UK).

Measurement of collagen type I (COL I) and osteocalcin (OC)

Culture medium was harvested at each medium change on days 1, 5, 7, 10, 12, 14, 18, 21, 25 and 27 days. Quantification of collagen type I synthesis was performed on each sample by measuring the amount of carboxy-terminal propetide of type I collagen (CICP) released into the culture medium by an immunoassay (Metra™ CICP EIA kit, Quidel, Dorking, U.K.). Osteocalcin in the medium was also measured by an enzyme immunoassay (Metra™ Osteocalcin EIA kit, Quidel) at the same time points.

Cellular alkaline phosphatase (ALP)

Alkaline phosphatase was measured at day 1, 3 7, 10, 14, 21 and 27. The medium was removed, the samples were rinsed with phosphate buffer saline solution (PBS) and attached cells lysed by adding 500μl PBS and 500μl 1% (v/v) Triton X-100/PBS, followed by two freeze-thaw cycles of 10 min each at -70°C and 37°C. The ALP activity was assessed colourimetrically by monitoring the release of *p*-nitrophenol phosphate from *p*-nitrophenol phosphate as described by Sabokar *et al* [28]. The ratio of ALP/COL1 was used as a measure of differentiation.

Statistical analysis

All results were statistically evaluated by ANOVA and post-hoc testing with Bonferroni's correction on SPSS statistical software. Significance was set at the 5 % level ($p<0.05$).

Results

Total protein

The measurement of total protein can be related to cell number, until the culture reaches confluence. After 7 days, at the seeding concentration used in this study, the cells were approaching confluence. Using confocal laser scanning microscopy it was possible to visualize the cells fully spread (Figure1). We have therefore used total protein to correct for cell number at early time points. At day 1 and day 3 the level of protein was below the sensitivity of the analytical method used. The HOBS seeded on all materials expressed a significantly higher concentration of proteins at day 27 compared to day 7 ($p<0.006$). Comparing the three materials at day 7 the cells seeded on 0.8 wt % Si-HA expressed higher concentration of protein, but this did not reach statistical significance. At day 27 the protein concentration was significantly higher on 0.8 wt % Si-HA in comparison with the other two materials ($p<0.001$ for HA and $p<0.013$ for 1.5 wt % Si-HA) (Figure 2).

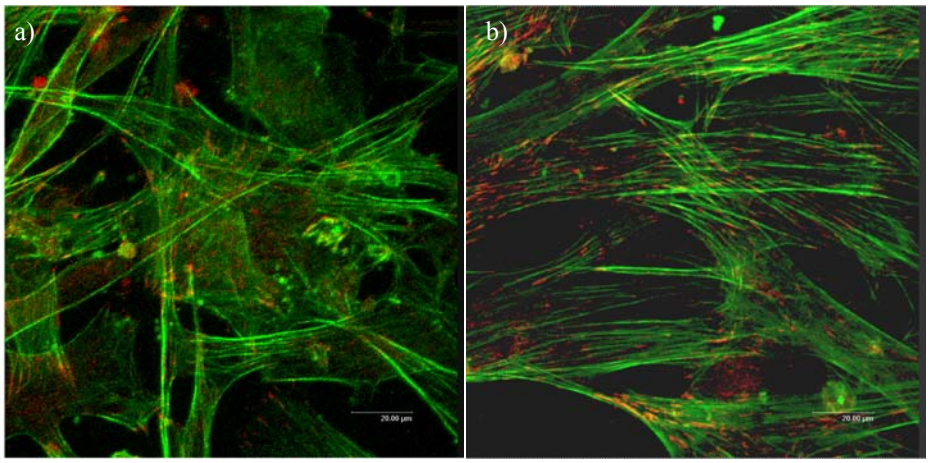

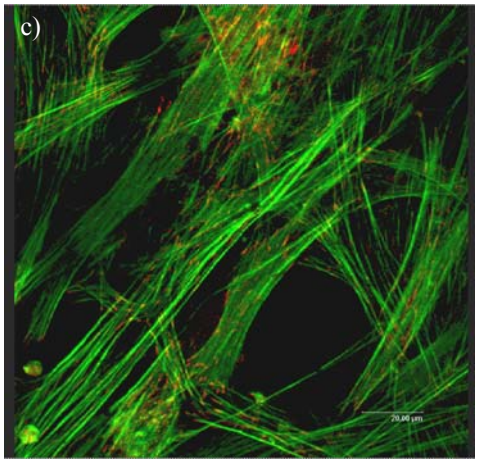

Figure 1 a-c) – Confocal laser scanning microscopy of human osteoblasts seeded on HA (a), 0.8 wt % Si-HA (b) and 1.5 wt % Si-HA (c) for a period of 7 days.

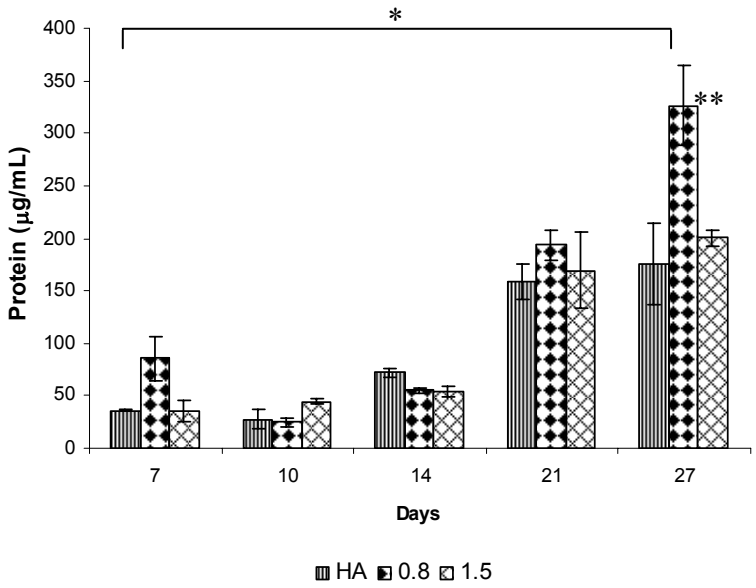

Figure 2 – Total protein (µg/mL) measured at different time points. (* statistical difference between time points, ** between materials; $p<0.05$; n=3).

Collagen type I production (COL I)

The release of C-terminal collagen propetide (CICP) provides a stoichiometric representation of the production of collagen; therefore these results can be expressed as COL I production.

An overall increase in the concentration of COL I release into the medium, with time was detected (Pearson correlation coefficient $R = 0.876$, $p<0.001$ for HA; $R = 0.925$, $p<0.001$ for 0.8 wt % Si-HA and $R = 0.785$, $p<0.007$ for 1.5 wt % Si-HA). In particular there was an

increase in collagen at later time points that could be related to the lack of hydrocortisone in the medium (Figure 3a). A higher production of COL I was observed at day 1 for Si-HA materials when comparing the values of COL I production per total protein (due the low sensitivity of the BCA method at day 1 the value of total protein used was the lower limit of the method), but these differences were not significant. The levels expressed by the cells at day 14 are significantly lower than those measured at day1 ($p<0.002$ for HA; $p<0.000$ for 0.8 wt % Si-HA and $p<0.000$ for 1.5 wt % Si-HA) (Figure 3b).

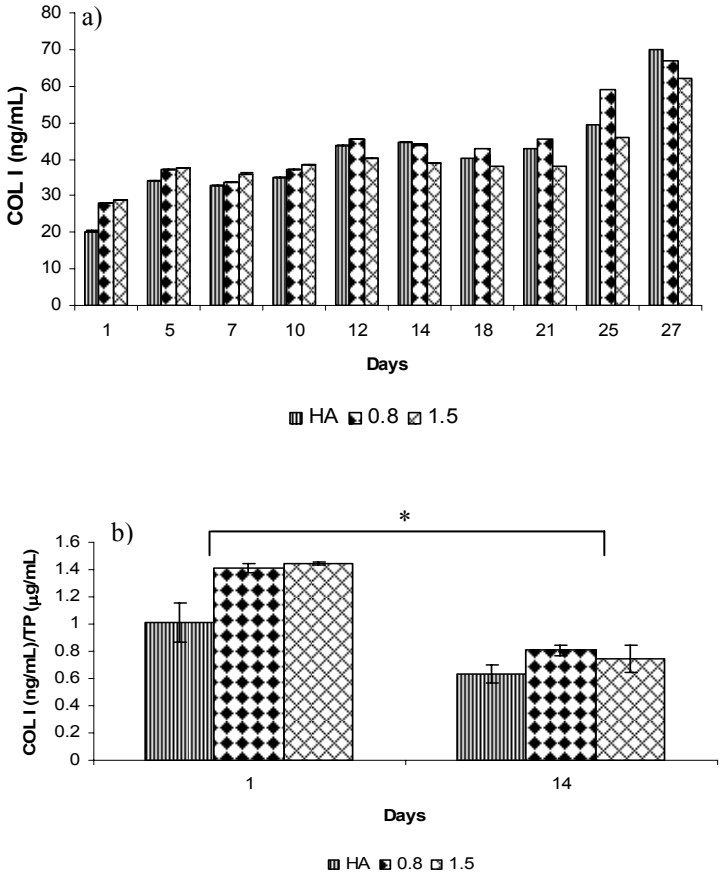

Figure 3 – a) COL I release to the medium at different time points (n=2); b) expression of COL I per total protein in two time points of the culture (* statistical difference between time points, n=3).

Alkaline phosphatase release (ALP) and ALP/COL I

The level of ALP at day 1 and 3 were below the detection limit of the analytical method used. The level of ALP expressed by the HOBS seeded on the different materials for day 21 and 27 was significantly higher than the levels at day 7 ($p<0.002$ for all materials), with the exception of 1.5 wt % Si-HA (Figure 4a). The level of ALP expressed by the cells

seeded on 1.5 wt % Si-HA was similar throughout the culture period and higher at day 7 than on the other two substrates.

The ALP/COL I ratio can be used as a measurement of differentiation. A significant increase in the ALP/COL I (Figure 4b) ratio was observed between days 7 and 21, for HA and 0.8 wt % Si-HA ($p<0.001$), but not for 1.5wt % Si-HA. When comparing the three materials at day 7 the ratio ALP/COL I on 1.5 wt % Si-HA was significantly higher ($p<0.001$), indicating greater differentiation. Once the HOBS were no longer under the influence of hydrocortisone, a decrease on the ALP/COL I was observed, that can be due to the increase in COL I expression (Figure3a).

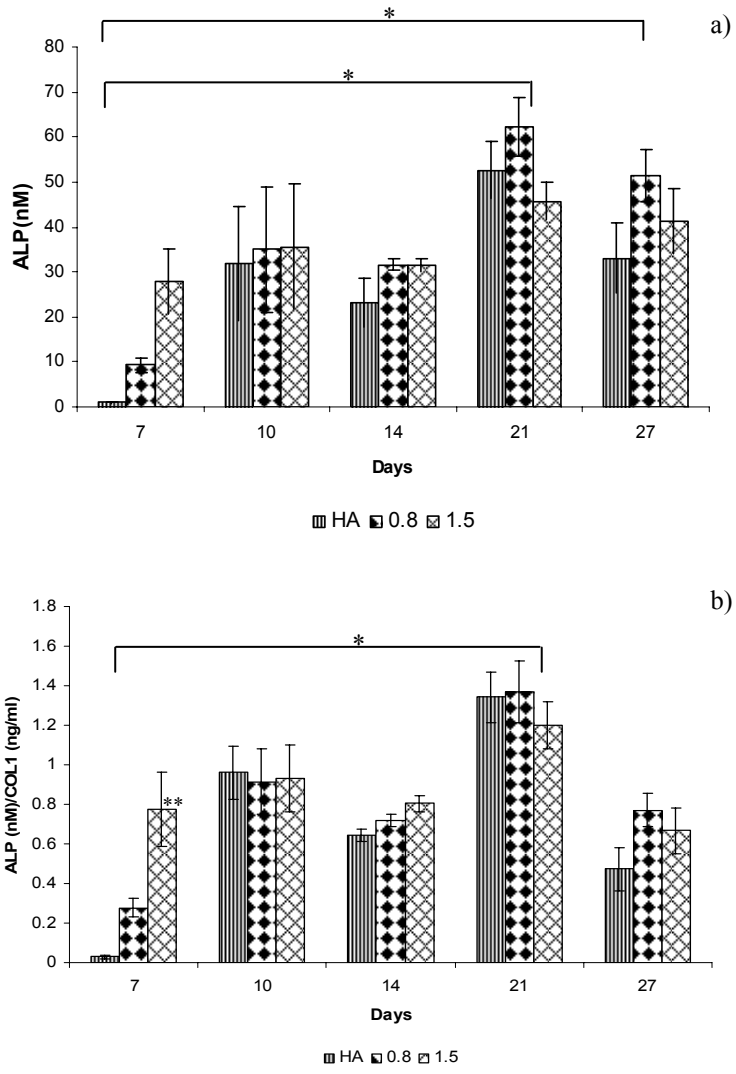

Figure 4 –Production of ALP a) with time; and b) variation of the ratio ALP/COL I with time. (* statistical difference between time points; $p<0.05$; ** between materials; $p<0.05$, n=3).

Osteocalcin release (OC)

The level of OC in culture medium before adding it to the cells was 10.3 ng/ml. At the earlier time points no release of OC into the medium was detected. At day 7 a significant increase was observed ($p<0.001$), which indicates the beginning of a post-proliferative stage. After the introduction of hydrocortisone to the medium the values of OC decreased below the baseline value. Due to the onset of mineralization at day 21 the addition of hydrocortisone and β-glycerophosphate was stopped at day 25, there was no need for further stimulation of the culture to mineralize. The lack of hydrocortisone in the medium induced a significant increase in the OC levels by day 27, except for 1.5 wt % Si-HA (Figure 5). With the exception of day 7, higher levels of OC release were observed on cells seeded on 0.8 wt % Si-HA. The levels expressed by the HOBS on 1.5 wt % Si-HA were constant throughout the culture.

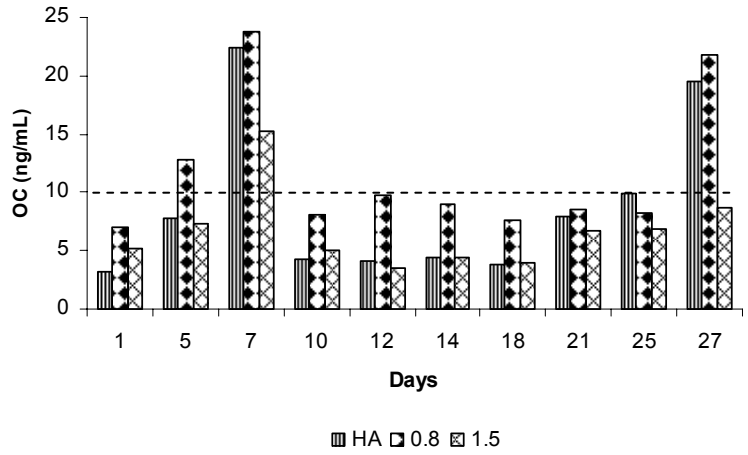

Figure 5 – OC release to the medium at different time points. (* statistical difference between time points; $p<0.05$; except for 1.5 wt % Si-HA⁃⁃⁃⁃⁃ baseline; n=2).

Mineral nodular formation

At days 7 and 14 no mineral deposits were visualized on the surface of any of the materials. At day 21 the first deposits were observed on all materials. These deposits coincided with the areas of high cell density. At day 27 a larger number of deposits were observed (Figure 6). No difference in the pattern or timing of mineralization was seen between the materials.

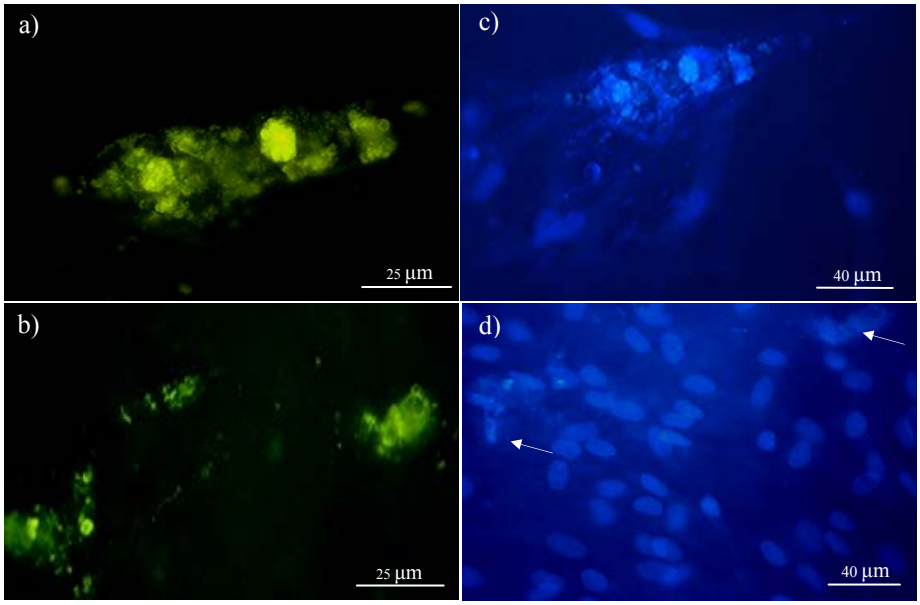

Figure 6 - a) Mineral deposits labelled with tetracycline on the surface of 0.8 % wt Si-HA and (b) 1.5 wt % Si-HA after 28 days; c) cell nuclei stained with DAPI and the mineral deposits (arrow) on the surface of 0.8 wt % Si-HA and (d) on 1.5 wt % Si-HA. Similar deposits were observed on HA.

Discussion

In this paper we have demonstrated that HA and Si-HA substrates support HOBS proliferation and differentiation for up to 27 days. In all cultures the HOBS expressed the phenotype markers, COL I, ALP and OC. These markers can be used to identify the different stages of osteoblast differentiation [29]. Although the mechanism behind this process is not fully understood, it is known to be a multistep process [30]. All the steps are characterized by changes in gene and protein expression. It is known that endogenous systemic glucocorticoids are involved in bone formation and remodelling [31, 32], so to mimic the physiologic conditions, hydrocortisone (200nM) was added to the growth medium. β-glycerophosphate (7.5 mM) was used to stimulate the production of mineral.

The Si-HA substrates showed a higher cell number (0.8 wt %) and ALP production (1.5 wt %) when compared to HA. The higher ALP/COL I ratio at day 7 on 1.5 wt % Si-HA indicate that the HOBS were differentiating faster. Although, silicon is present in both Si-HA substrates an earlier release from 1.5 wt % Si-HA could be the stimulus to more advanced differentiation. The higher cell numbers on 0.8 wt % Si-HA, although statistically not significant, is in agreement with previous studies where we demonstrated higher adhesion on

0.8 wt % Si-HA than on HA and 1.6 wt % Si-HA [26], and also with the results reported by Gibson *et al*, who showed a higher metabolic activity of osteosarcoma cells when seeded on 0.8 wt % Si-HA when compared with HA [25].

The high levels of ALP and OC, before the addition of hydrocortisone are in accordance with the behaviour of HOBS from older donors in culture [33]. The cells used in this study were from donors between 55 and 65 years of age. These cultures are more differentiated than those from young donors at an equivalent passage [33]. Only post-proliferative HOBS produce OC, therefore an increase in OC at day 7 could be related to this stage [33, 34]. The production of OC was affected by the presence of hydrocortisone, a decrease on the OC expression was observed as soon as hydrocortisone was added to the medium (day 7) and increased at day 27 when the addition was stopped. It is well established that the presence of glucocorticoids influence osteoblast behaviour [35, 36]. These molecules induce differentiation of HOBS, but also inhibit some functions of differentiated osteoblasts. They induce the mature cells to mineralize and produce multilayered bone nodules [36, 37]. Glucocorticoids not only affect cell proliferation, but can also suppress type I collagen gene expression by decreasing the rates of transcription and destabilizing $\alpha 1$ collagen messenger ribonucleic acid (mRNA); they also decrease the expression of OC [35, 36] Osteocalcin and osteopontin are generally considered inhibitors of matrix mineralization [38]. In this experiment the OC production could not be used as a marker for mineralization, due to the inhibitory effect of hydrocortisone. After 21 days, it was possible to observe mineral deposits on the surface of the 3 materials. These deposits coincided with areas of high cell density, indicating that was a cell mediated process. The tetracycline label allowed visualization of mineralization, being the major advantage of this label over common calcium stains such as Alizarin Red and Von Kossa, its ability to distinguish physiological mineral from dystrophic mineral [39]. Mineral nodule formation increased with time but was similar in extent on all three substrates.

The results presented in this study do not allow the exact mechanism behind the response to silicon substituted HA materials to be described. However, they help in the formulation of further hypotheses. Several studies have demonstrated the positive effect of silicon in bone formation [6, 15-19] and more recently Reffit *et al* demonstrated a positive effect of soluble silicon on COL I synthesis, ALP and OC production and also an increase on the levels of mRNA of ALP and OC, after 3 days [19]. In previous studies we showed that there is a preferential release of silicon at early time points to the surrounding media, that can stimulate the human osteoblasts to proliferate and differentiate faster than on HA [40]. And

also it was demonstrated that the Si-HA has different surface properties, namely a more negative surface charge that can influence the adhesion of proteins. Therefore, the higher cellular adhesion and consequent proliferation on 0.8 wt % Si-HA and 1.5 wt % Si-HA, maybe due to the synergetic effect of silicon and its physical-chemical properties.

The human osteoblasts did not respond in the same way to both materials. The higher dissolution of silicon from 1.5 wt % Si-HA stimulates cells seeded on this substrate at early time points leading to earlier differentiation than on the other two materials at day 7, as it can be seen by the high expression of ALP. Other studies showed that a stable collagenous matrix is important for the progression of osteoblastic differentiation and is a prerequisite for an increase in ALP expression [41-45]. Although, 0.8 wt% Si-HA has the ability to adsorb higher concentration of total human serum proteins, 1.5 wt% Si-HA has higher binding affinity to COL I [46]. Therefore, the high expression of ALP by the HOBS seeded on the 1.5 wt% Si-HA may be due to a synergetic effect of silicon release and the presence of a stable collagenous matrix. The effects of silicon release from Si-HA on human osteoblasts over prolonged periods of time have not been previously demonstrated and our results show that in the presence of hydrocortisone the differences between the materials in ALP, COL I and OC production are diminished. However, at later time points there is the onset of mineralization and with the removal of hydrocortisone, the cells on 0.8 wt % Si-HA appear to respond by increasing protein production. We suggest here that there is continuing release of silicon from the Si-HA substrate at the later time points, whilst the percentage of silicon release from 1.5 wt % is higher than on 0.8 wt% and it was expected that this would result in a higher production of proteins however, this was not seen. Reffit *et al* demonstrated a similar pattern; at higher silicon concentrations the positive effect of silicon is diminished. This dose-dependant effect on bone cells has also been reported with other trace elements [47]. Gibson *et al* also found a similar result, the osteosarcoma cells seeded on 0.8 wt % Si-HA showed a higher metabolic activity than the cells seeded on 1.6 wt % Si-HA [25]. Therefore, there is an optimum concentration of silicon for the stimulation of osteoblasts proliferation and differentiation.

Conclusions

The effects of silicon release from Si-HA on human osteoblasts over a long period of time have not been previously demonstrated. Our results show that the presence of hydrocortisone diminished the positive effect of silicon with the removal of hydrocortisone,

the cells on 0.8 wt % Si-HA appear to respond by increasing protein production. The formation of bone mineral was observed on all materials after 21 days. The cells seeded on the three substrates expressed osteoblast markers and significant differences were detected at early time points on the Si-HA material. The level of osteoblasts markers on 1.5 wt % Si-HA was constant with time. In general the level of osteoblast markers expressed by 0.8 wt % Si-HA was higher than on 1.5 wt % Si-HA. Further studies are required to fully understand the mechanism by which Si-HA improves osteoconductivity.

Acknowledgments

The authors would like to acknowledge to FCT (Fundação para a Ciência e Tecnologia) for CM Botelho's grant (ref. SFRH/BD/6173) and the project entitled "Silicon-substituted hydroxyapatite coatings for biomedical applications", ref POCTI/CTM /49238/2002.

References

1. Hench L, Splinter R, Allen W, Greenlee T. Bonding mechanism at the interface of ceramic prosthetic materials. Journal of Biomedical Materials Research 1972;2:117-141.

2. Ducheyne P, Hench L, Kagan A, Martens M, Burssens A, Mulier J. The effect of hydroxyapatite impregnation on skeletal bonding of porous coated implants. Journal of Biomedical Materials Research 1980;14:225-237.

3. Jarcho M. Calcium phosphates ceramics as hard tissue prosthetics. Clinical Orthopaedics 1981;157:259-278.

4. Nakamura T, Yamamuro T, Higashi S, Kokubo T, Ito S. A new glass-ceramic for bone replacement: evaluation of its bonding to bone tissue. Journal of Biomedical Materials Research 1985;19:685-698.

5. Ducheyne P, Bianci P, Radin S, Schepers E. Bioactive materials: mechanism and bioengineering considerations. In: Ducheyne P, Kokubo T, van Blitterswijik C, editors. Bone-bioactive biomaterials. Leiderdorp, The Netherlands: Reed Healthcare Communications; 1993:1-12.

6. Patel N, Best S, Gibson IR, Hing K, Damien E, Bonfield W. A comparative study on the *in vivo* behaviour of hydroxyapatite and silicon substituted hydroxyapatite granules,. Journal of Materials Science: Materials in Medicine 2002;13:1199-1206.

7. Jha LJ, Best S, J.D. S, Gibson IR, Bonfield W, inventors; Silicon-Substituted Apatites and Process for the Preparation Thereof. Worldwide patent, PCT/GB97/02325 and US Patent Serial Nº 09/147773, 1999.

8. Gibson IR, Best SM, Bonfield W. Chemical Characterization of Silicon-Substituted Hydroxyapatite. Journal of Biomedical Materials Research 1999; 44:422-428.

9. Schwarz K. Significance and functions of silicon in warm-blooded animals. In: Biochemistry of silicon and related problems. In: Proceedings of the 40th Nobel Symposium; Lidingö, Sweden; 1977.

10. Baxter J, Rousseau G, Benson M, Garcea RR, Ito J, Tomkins G. Role of DNA and Specific cytoplasmic receptors in glucocorticoid action. Proceedings of the National Academy of Sciences of the United States of America 1972;69(7):1892.

11. Darley W, Volcani B. Role of silicon in diatom metabolism. A silicon requirement for deoxyribonucleic acid synthesis in diatom *cylindrotheca-fusiformis* reimann and lewin. Experimental cell research 1969;58(2-3):334.

12. Finkelstein D, Butow R. DNA-binding proteins in Yeats - effect of growth phase and mitochondrial-function. Archives of biochemistry and biophysics 1976;174(1):52-65.

13. Volcani BE. Role of silicon in diatom metabolism and silicification. In: Biochemistry of silicon and related problems. In: Proceedings of the 40th Nobel Symposium; Lidingö, Sweden; 1977.

14. Werner D. Regulation of Metabolism by silicate in diatoms. In: Biochemistry of silicon and related problems. In: Proceedings of the 40th Nobel Symposium; Lidingö, Sweden; 1977.

15. Carlisle E. Essentiality and function of silicon. In: Biochemistry of silicon and related problems. In: Proceedings of the 40th Nobel Symposium; Lidingö, Sweden; 1977.

16. Carlisle E. Silicon Biochemistry. New York: Wiley; 1986.

17. Schwarz K, Milne D. Growth-promoting effects of silicon in rats. Nature. 1972;239:333.

18. Seaborn C, Nielsen F. Dietary silicon affects acid and alkaline phosphatase and ^{45}calcium uptake in bone of rats. Journal of Trace Elements in Experimental Medicine 1994;7(1):11-18.

19. Reffitt D, Ogston N, Jugdaohsingh R, Cheung H, Evans B, Thompson R, et al. Orthosilicic acid stimulates collagen type I synthesis and osteoblastic differentiation in human osteoblast-like cells *in vitro*. Bone 2003;32:127.

20. Shi S, Kirk M, Kahan A. The role of type I collagen in the regulation of the osteoblast phenotype. Journal of Bone Mineral Research 1996;11:1139-1145.

21. Hildebrand M, Higgins D, Busser K, Benjamin E. Silicon-responsive cDNA clones isolated from the marine diatom *Cylindrotheca fusiformis*. Gene 1993;132(2):213-218.

22. Voronkov MG, Skorobogatova VI, Vugmeíster EK, Makarskii VV. Silicon in nuclei acids. Doklady Biochemistry 1975;222:29.

23. Hench L, Orcel G. Physical-chemical and Biochemical Factors in Silica Sol-Gel. Journal of Non-Crystalline Solids 1986;82:1-10.

24. Keeting P, Oursler M, Wiegand K, Bonde S, Spelsberg T, Riggs L. Zeolite A increases proliferation, differentiation, and transforming growth factor production in normal adult human osteoblast-like cells *in vitro*. Journal of Bone and Mineral Research 1992;7(11):1281.

25. Gibson IR, Huang J, Best SM, Bonfield W. Enhanced *in vitro* cell activity and surface apatite layer formation on novel silicon-substituted hydroxyapatites. In: Ohgushi H, Hastings, GW, Yoshikawa, T, editor. Bioceramics 12; Nara, Japan: World Scientific Publishing Co. Pte. Ltd; 1999:191-194.

26. Botelho C, Brooks R, Lopes M, Santos JD, Best SM, Bonfield W. Biological and physical-chemical characterization of phase pure HA and Si-Substituted hydroxyapatite by different microscopy techniques. Key Engineering Materials 2004;254-2:845-848.

27. Botelho C, Stokes D, Brooks R, Best S, Lopes M, Santos JD. Effect of human serum proteins on the surface of pure HA and Si-substituted HA: AFM and ESEM Studies. Materials Science Forum 2003;455-456:378-382.

28. Sakobar A, Millet P, Myer B, Rushton N. A rapid, quantitative assay for measuring alkaline phosphatase activity in osteoblastic cells *in vitro*. Bone Mineral 1994;27:57-67.

29. Lian J, Stein G, Aubin J. Bone formation: Maturation and functional activities of osteoblast lineage cells. In: Favus M, editor. Primer on the metabolic bone diseases and disorders of mineral metabolism. Philadelphia: Lippincott Williams and Wiilkins; 2003:13-28.

30. Boskey A. Biomineralization: Conflicts, challenges and opportunities. Journal of Cell Biochemistry Supplements 1998;30/31:83-91.

31. Jaiswal N, Haynesworth S, Caplan A, Bruder S. Osteogenic differentiation of purified culture-expanded human mesenchymal stem cells *in vitro.* Journal of Cell Biochemistry 1997;64:295-312.

32. Baylink D. Glucocorticoid-induced osteoporosis. New England Journal of Medicine 1983;309(5):306-308.

33. Ireland D, Bord S, Beavan S, Compston J. Hydrocortisone increases the rate of differentiation of culture human osteoblasts. Journal of Cell Biochemistry 2004;91:594-601.

34. Lian J, Stein G, Stein J, Wijnen A. Osteocalcin gene promoter: Unlocking the secrets for regulation of osteoblasts growth and differentiation. Journal of Cell Biochemistry Supplements 1998;30/31:62-72.

35. Canalis E. Mechanisms of glucocorticoid action in bone: Implications to glucocorticoid-induced osteoporosis. Journal of Clinical Endocrinology and Metabolism 1995;10:3441-3447.

36. Delany A, Gabbitas B, Canalis E. Cortisol down-regulattes osteoblast α 1 (I) procollagen mRNA by transcriptional and post-transcriptional mechanisms. Journal of Cell Biochemistry 1995;57:488-494.

37. Bellows C, Aubin J, Heersche J. Physiological concentrations of glucocorticoids stimulate formation of bone nodules from isolated rat calvaria cells *in vitro*. Endocrinology 1987(121):1985-1992.

38. Cheng S, Zhang S, Mohan S, Lecanda F, Fausto A, Hunt A, et al. Regulation of insulin-like growth factors I and II and their binding proteins in human bone marrow stromal cells by dexamethasone. Journal of Cellular Biochemistry 1998;71(3):449-458.

39. Boskey A, Paschalis E. Matrix proteins and biomineralization. In: Davie J, editor. Bone Engineering. Toronto: em^2; 1999: 44-62.

40. Botelho CM, Lopes MA, Gibson IR, Best SM, Santos JD. Structural analysis of Si-substituted hydroxyapatite: Zeta potential and X-ray photoelectron spectroscopy (XPS). Journal of Materials Science: Materials in Medicine 2002:1123-1127.

41. Shiga M, Kapila Y, Zhang Q, Hayami T, Kapila S. Ascorbic acid induces collagenase-1 in human periondontal ligament cells but not in MC3T3-E1 osteoblast-like cells: Potential association between collagenase expression and changes in alkaline phosphatase phenotype. Journal of Bone Mineral Research 2003;18(1):67-77.

42. Franceschi R, Iyer B, Cui Y. Effects of ascorbic acid on collagen matrix formation and osteoblast differentiation of murine MC3T3-E1 cells. Journal of Bone Mineral Research 1994;9:843-854.

43. Franceschi R, Iyer B. Relationship between collagen synthesis and expression of the osteoblast phenotype in MC3T3-E1 cells. Journal of Bone Mineral Research 1992;7:235-246.

44. Aronow M, Gerstenfeld L, Owen T, Tassinari M, Stein G, Lian J. Factors that promote progressive development of the osteoblast phenotype in cultured fetal rat calvaria cells. Journal of Cell Physiology 1990;143:213-221.

45. Chien H, Lin W, Cho M. Interkukin-1β-induced release of matrix proteins into culture media causes inhibition of mineralization of nodules formed by periodontal ligament cells *in vitro*. Calcified Tissue International 1999;64:402-413.

46. Botelho C, Brooks R, Kawai T, Ogata S, Ohtsuki C, Lopes M, et al. *In vitro* analysis of proteins adhesion to phase pure hydroxyapatite and silicon-substituted hydroxyapatite. Key Engineering Materials 2005;17:461-464.

47. Kaji T, Katwatani R, Takata M, Hoshino T, Miyahara T, Kozaka H, et al. The effects of cadmium, copper or zinc on formation of embryonic chick bone in tissue culture. Toxicology 1988;50(3):303-316.

Differentiation of mononuclear precursors into osteoclasts on the surface of Si-substituted hydroxyapatite

C.M. Botelho[1,2], R. A. Brooks[3], G. Spence[3], I. Mcfarlane[4], M. A. Lopes[1,2], S.M. Best[5], J.D. Santos[1,2], N. Rushton[3],W. Bonfield[5]

[1]INEB - Instituto de Engenharia Biomédica, Laboratório de Biomateriais, Rua do Campo Alegre, 823, 4150-180 Porto, Portugal

[2]FEUP- Faculdade de Engenharia da Universidade do Porto, DEMM, Rua Dr. Roberto Frias, 4200-465 Porto, Portugal.

[3]Orthopaedic Research Unit, Box 180, Addenbrookes Hospital, Hills Road Cambridge, CB2 2QQ, U.K.

[4] Clinical Biochemistry, Addenbrookes Hospital, Hills Road Cambridge, CB2 2QQ, U.K.

[5]Department of Materials Science and Metallurgy, University of Cambridge, CB2 3QZ, U.K.

Journal of Biomedical Materials Research, submitted

Abstract

In healthy bone, resorption and synthesis are in perfect coordination. In previous studies we demonstrated that the incorporation of silicon into the hydroxyapatite lattice enhances the proliferation and differentiation of human osteoblasts. Therefore, the aim of this study was to demonstrate the effect of silicon-substituted hydroxyapatite (0.8 wt % Si-HA and 1.5 wt% Si-HA) on the differentiation of mononuclear cells into osteoclasts, using two different starting cultures, peripheral blood mononuclear cells (PBMC) and monocytes expressing the CD 14 antigen (CD14+). Through this study, it was possible to demonstrate that Si-HA allows the differentiation of mononuclear cells into mature osteoclasts, independently of the starting culture, PBMC or CD14+. Most of the cells on the surface of the materials expressed osteoclastic markers: actin rings, several nuclei and positive for tartrate-resistant acid phosphatase (TRAP) and vitronectin receptor. In the presence of osteoclasts a higher release of calcium and phosphate to the medium from the 1.5 wt % Si-HA substrate was detected when compared to the HA substrate, therefore these results indicate higher osteoclastic resorptive activity on the 1.5 wt % Si-HA surface.

Silicon-substituted hydroxyapatite can be resorbed by cellular mechanisms and have a stimulatory effect on osteoclasts, although the underlying mechanism is still poorly understood.

Keywords: Osteoclasts, CD 14 +, Peripheral Blood Mononuclear Cells, Silicon-Substituted Hydroxyapatite.

Introduction

The ideal bone graft for many applications would be a material that can both be resorbed and induce bone formation, hence being completely replaced by new bone. Bone is a dynamic organ due to its constant remodelling. This process can be divided in two main steps; resorption, where the "old" bone is resorbed by the osteoclasts and synthesis, where the osteoblast lays down new layers of bone [1].

In healthy bone, resorption and synthesis are in perfect coordination. Disruption to the balance between resorption and formation can lead to osteoporosis that is characterized by the loss of bone mass [2] and osteopetrosis resulting from a failure of osteoclasts to resorb bone [3]. The osteoclast is the only cell capable of resorbing mature bone. It is a tissue-specific macrophage polykaryon created by the differentiation and fusion of monocyte/macrophage precursors cells [4]. The resorption takes place under the ruffled border, where protons and proteases are secreted, leading to the formation of resorption lacunae [4].

In the last decade there has been a breakthrough in the understanding of osteoclastogenesis, due to the discovery of the receptor activator of nuclear factor kβligand (RANKL) in 1998. It was identified as an osteoblast-produced ligand, which promotes osteoclast differentiation [4, 5]. RANK is a type I transmembrane receptor of the TNF receptor superfamily that was identified in a dendritic cell cDNA library [6]. Several studies showed that it is possible to generate osteoclasts *in vitro* from peripheral mononuclear blood cells (PBMC) using RANKL and macrophage colony stimulating factor (MCSF), a polypeptide growth factor [7, 8]. Quinn *et al* suggested that osteoclasts are derived from monocytes that expressed the macrophage-associated antigen CD 14 (CD14+). These results were supported by Massey *et al*, who showed that CD 14 + cells from PBMC showed enhanced osteoclastic bone resorption in co-cultures with UMR 106 rat osteoblast-like cells [9]. The use of co-culture is related to the ability of osteoblast/stromal cells to produce the two haematopoietic factors needed for osteoclastogenesis, RANKL and MCSF [4].

The use of soluble RANKL and MCSF allows the formation of mature osteoclasts *in vitro* directly from osteoclast precursors, eliminating the need of a co-culture system (PBMC and UMRS 106 rat osteoblast like cells). The major advantage of this method is that only one cell type is used and the final osteoclast culture is free of osteosarcoma cells [5]. RANKL and MCSF induce gene expression for tartrate-resistant acid phosphatase (TRAP), cathepsin K (CATK), calcitonin receptor and $\alpha_v ß_3$-integrin (vitronectin receptor) which are characteristic of mature osteoclasts [4]. Therefore, *in vitro* osteoclasts can be identified by TRAP staining (a characteristic shared with macrophages), multinuclearity, formation of an actin ring structure, a polar cell body during resorption and by the presence of $a_v ß_3$ integrin [5, 10]. This integrin belongs to the superfamily of adhesion proteins, named as "vitronectin receptor" because it binds to the plasma protein vitronectin [10]. In osteoclasts, $a_v ß_3$ is the predominant integrin quantitatively and functionally, and it can mediate the recognition of several RGD bone matrix proteins [10].

The biomaterials are designed to fulfil a purpose, in the case of bone regeneration; they should stimulate the proliferation and differentiation of osteoblast cells, leading to the formation of "new bone". And they also should be resorbed by cellular mechanism to keep the normal balance between bone formation and resorption. It has been shown that is possible to assess the resorbability of biomaterial by cellular mechanisms *in vitro* [1, 11, 12]. Schiling *et al* reported that PMMA can not be resorbed by osteoclasts as no resorption pits were visualized, although these features were present on the surface of calcium phosphate materials indicating the its resorbability by osteoclasts [1]. Doi *et al* reported that the incorporation of carbonate ions increased the osteoclast resorption *in vitro* [11]. Patel *et al* reported similar results *in vivo*, in this case the incorporation of carbonate ions to the HA lattice increased the number of multinucleated phagocytic cells resembling osteoclast, in close proximity or directly on the surface of carbonate hydroxyapatite, indicating that this material was resorbed by cellular mechanisms under physiologic conditions [13].

In previous studies we demonstrated that the incorporation of silicon into the HA lattice increases osteoblast proliferation and differentiation [14] and Gibson *et al* reported that the presence of this ion increases the metabolic activity of osteoblast-like cells *in vitro* [15]. Patel *et al* showed an increase in bone apposition/ingrowth related to the concentration of silicon incorporated into the HA lattice, although no osteoclast like cells were observed on the surface or proximity of this material [13]. Therefore, the aim of this study was to assess the effect of silicon incorporation into hydroxyapatite (HA), on the differentiation of mononuclear cells into mature osteoclasts, using two different precursor populations; PBMC

and monocytes expressing the CD 14 antigen and to determine if this material can be resorbed by osteoclasts.

Material and Methods

Hydroxyapatite (HA) and silicon-substituted hydroxyapatite (Si-HA) were prepared by a chemical precipitation route; the protocol is fully described elsewhere [16-18]. Sintered powders of the HA and Si-HA materials were prepared by compacting the as-precipitated powders and sintering at 1300ºC. The samples were sterilized by heat, 180 º C for a period of 2 hours.

Two different osteoclasts precursors were used; peripheral blood mononuclear cells (PBMC) and CD 14 positive monocytes (CD14+), as described below.

Peripheral blood mononuclear cells

The peripheral blood mononuclear cells were isolated from a buffy coat obtained from the blood of healthy donors. Buffy coat cells were diluted in phosphate buffer solution (PBS) and transferred to tubes containing Histopaque-1077® (Sigma-Aldrich, Poole, UK), that allows the separation of erythrocytes, neutrophils, platelets and PBMC by density and the protocol is fully described elsewhere [19]. The end product is a mix culture of monocytes, platelets and lymphocytes.

The cells were suspended in α – MEM medium with 10 % (v/v) human AB serum, 1 % (v/v) Glutamine and 30 µg/mL vitamin C (attachment medium). They were seeded at a concentration of 2 x 10^6 cells/mL and allowed to attach for 2 hours, at 37 ºC in a 5 % CO_2 atmosphere. After this period the non-adherent cells were washed off and 250 µL of attachment medium containing 25 ng/mL of MCSF and 30 ng/mL of RANKL was added. Experimental samples will be referred to as HA OC; 0.8 wt % Si-HA OC and 1.5 wt % Si-HA OC. After 2 hours of attachment a set of samples (n=3, for each material) was stained with toluidine blue to visualize the nucleus. The cells were visualized using a light microscope.

The medium was changed every three days for a period of 21 days and analyzed for calcium (Ca^{2+}) and phosphate (PO_4^{3-}) using a colorimetric assays, calcium flex® reagent cartridge and phosphorous® reagent cartridge from Dade Behring, respectively.

Two different controls were used: a) the samples without cells were incubated only in attachment medium (referred to as HA, 0.8 wt % Si-HA and 1.5 wt % Si-HA) and, b) the

samples were incubated with 2 x 10^6 cells/mL of PBMC, but only in attachment medium, without cytokines (designated as HA PBMC; 0.8 wt % Si-HA PBMC and 1.5 wt % Si-HA PBMC).

Following 21 days of culture the medium was removed and the samples washed with phosphate buffer saline solution (PBS), after which the cells were fixed for 5 minutes in 4 % paraformaldehyde and stained for TRAP [20]. The substrate was naphtol AS-BI phosphate (Sigma-Aldrich, Poole, UK). Tartrate resistance was assessed in the presence of 0.05 M sodium tartrate.

CD 14+

The first step to obtain a pure culture of CD14 + is the same as described above, but with the addition of a magnetic separation step. After centrifugation with histopaque the cells were labelled with magnetic microbeads® presenting anti-CD 14 antibodies and placed in a magnetic column (Miltenyi Biotec Ltd., Bisley, UK), where the CD14+ cells were retained by the column. Following removal from the magnetic source the column was washed with a Macs Buffer® (Miltenyi Biotec) and the CD14+ cells were collected. The cells were seeded at 2 x 10^6 cells/mL and incubated for a period of 2 hours in attachment medium at 37 º C in a 5 % CO_2 atmosphere. After this period the non-adherent cells were washed off and 250 µL of attachment medium containing 25 ng/mL of MCSF and 30 ng/mL of RANKL was added for a period of 21 days, (the experimental samples will be referred to as HA OC; 0.8 wt % Si-HA OC and 1.5 wt % Si-HA OC). Two different controls were used a) the cells were seeded at 2 x 10^6 cells/mL with attachment medium but no added cytokines (referred to as HA NC; 0.8 wt % Si-HA NC and 1.5 wt % Si-HA NC), b) the cells were also seeded at 2 x 10^6 cells/mL with attachment medium plus 25 ng/mL of MCSF (samples designated as HA MCSF; 0.8 wt % Si-HA MCSF and 1.5 wt % Si-HA MCSF).

The medium was changed every seven days for a period of 21 days and analyzed for calcium (Ca^{2+}) and phosphate (PO_4^{3-}) using a colorimetric assay.

After 21 days, the cells were fixed in 4 % paraformaldehyde/phosphate buffered saline solution, pH 7.4 at room temperature for 15 min. Using imunocytochemistry the cells were stained with Phalloidin FITC (1µg/mL), which binds to F-actin. The "vitronectin receptor" was identified using a primary mouse antibody against $a_v ß_3$, and a secondary antibody conjugated to TRITC to demonstrate vitronectin receptors (681µg/mL). The nuclei were stained using 4`,6 – diamidino-2-phenylindole – DAPI (20µg/mL). The fluorescent stains

were visualised using fluorescence microscopy (FM) and confocal laser scanning microscopy (CLSM).

Statistical analysis

All results were statistically evaluated by ANOVA and post-hoc testing with Bonferroni's correction on SPSS statistical software. Significance was set at the 5 % level. ($p<0.05$).

Results

Peripheral blood mononuclear cells

After 2 hours of incubation mononuclear cells attached at the surface of all materials. The cells attached to the surface of Si-HA seemed to form clusters (Figure 1).

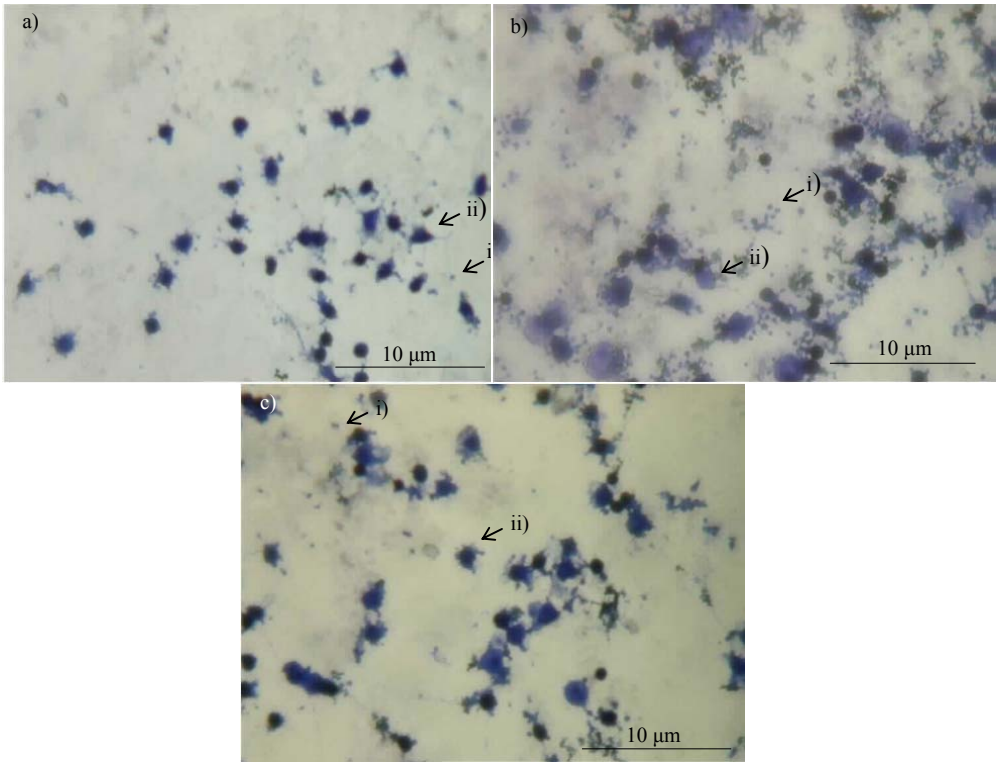

Figure 1- Distribution of the adherent PBMC on the HA (a), 0.8 wt% Si-HA (b) and 1.5 wt% Si-HA (c) after 2 hours of incubation. i) platelets and ii) the nucleus of mononuclear cells were stained with toluidine blue.

On the HA surface the cells were sparser than on Si-HA (Figure 2). Although, the difference of adherent cells between the materials did not reach statistical significance. These results support previous ones where a similar trend was observed regarding the adhesion of human osteoblasts, the 0.8 wt % Si-HA promoted greater adhesion and proliferation of human osteoblasts compared to HA [14]. Further research showed that 0.8 wt % Si-HA not only shows higher osteoblast adhesion when compared to HA but also when compared to 1.5 wt % Si-HA (data not shown).

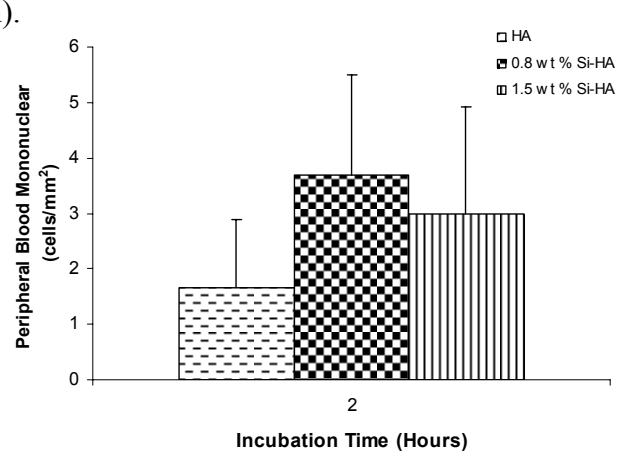

Figure 2 – Number of adherent PBMC per mm^2 after 2 hours of incubation.

After a period of 21 days the culture was terminated. The cells on the surface of the three materials showed typical features of osteoclasts, they were multinucleated (white arrow) and TRAP positive (Figure 3).

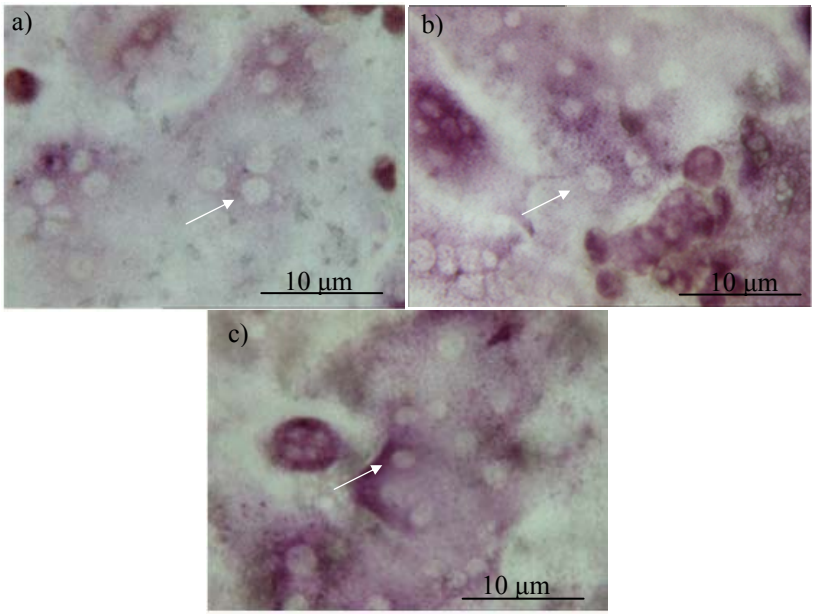

Figure 3 - Multinucleated, TRAP positive cells on the surface of a) HA; b) 0.8 wt % Si-HA and b) 1.5 wt % Si-HA after 21 days of incubation; white arrow – nuclei.

To evaluate the resorption ability of the osteoclasts the calcium and phosphate release to the medium was measured in the three experimental conditions.

The calcium release from HA to the medium was similar in all the three experimental conditions (Figure 4a); HA in attachment medium, HA PBMC and HA OC. Although, a slight increase in the phosphate concentrations was observed from the samples containing osteoclasts at day 19 (Figure 4b), it was not statistical significant and furthermore, the trend of phosphate release between the controls and the experimental samples is exactly the same. Therefore, it is not possible to conclude that the slight increase in phosphate release is due to osteoclast activity.

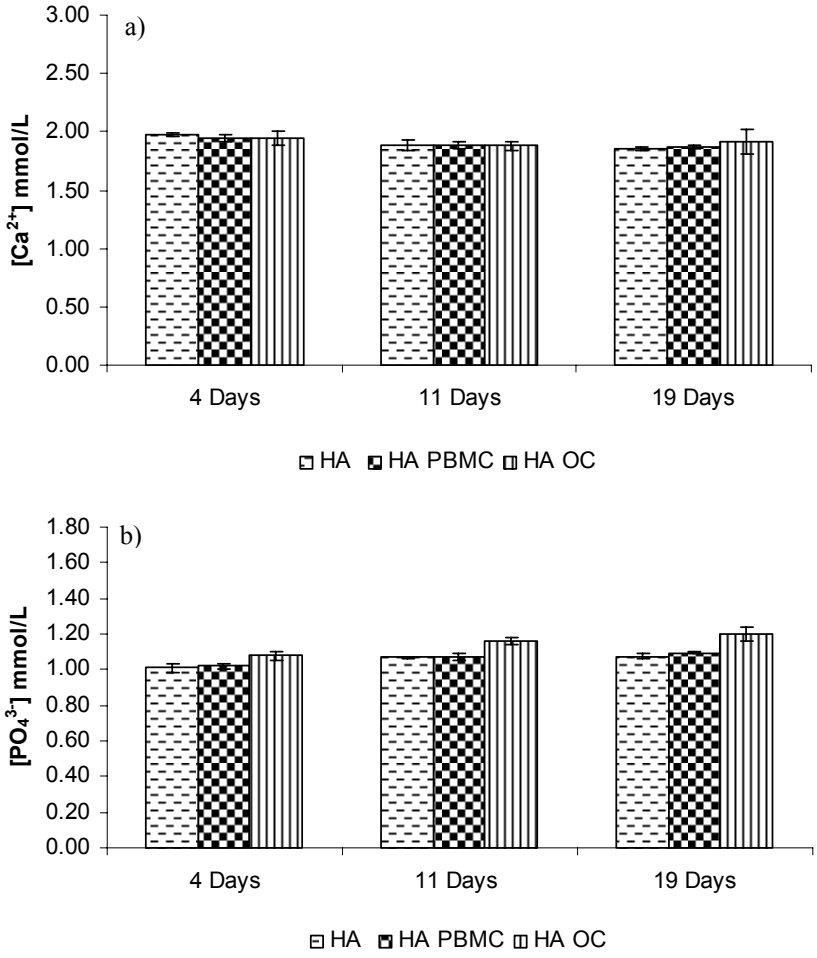

Figure 4 – Calcium (a) and phosphate (b) concentration in the medium at different points concentration, for the HA controls and the HA with osteoclasts (n=3).

The behaviour of the osteoclasts on the 0.8 wt % Si-HA surface differs from HA, in this case at day 19 a slight increase on the calcium content in the medium with osteoclasts was detected, although it did not reach a statistical significance (Figure 5a). While the increase in phosphate at day 19 reached statistical significance when compared to the values

observed with the controls 0.8 wt % Si-HA – 1.10 mmol/L, $p<0.007$; 0.8 wt % Si-HA PBMC – 1.11 mmol/L, $p<0.045$ and 0.8 wt % Si-HAOC – 1.42 mmol/L (Figure 5b). This, could indicate, that the osteoclasts observed on the surface of 0.8 wt % Si-HA are active and resorbing.

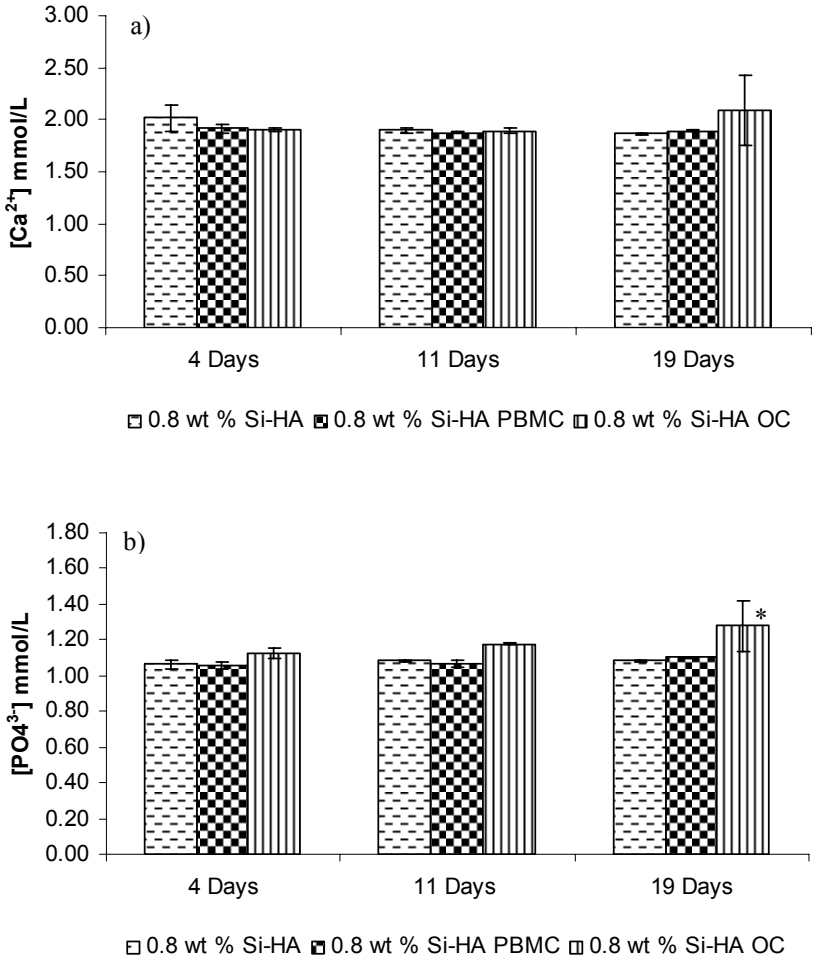

Figure 5 – Calcium (a) and phosphate concentration (b) in the medium at different points concentration, for the 0.8 wt % Si-HA controls and the 0.8 wt % Si-HA sample with osteoclasts. (* - statistical different $p<0.05$, n=3)

The calcium concentration in the medium from the experimental sample 1.5 wt % Si-HA OC, at day 19, was significantly higher when compared to the control samples (Figure 6a), 1.5 wt % Si-HA – 1.88 mmol/L $p<0.002$; 1.5 wt % Si-HA PBMC – 1.89 mmol/L $p<0.003$ and 1.5 wt % Si-HAOC – 2.39 mmol/L. A similar result was observed for the phosphate (Figure 6b), 1.5 wt % Si-HA – 1.10 mmol/L $p<0.001$; 1.5 wt % Si-HA PBMC – 1.11 mmol/L $p<0.001$ and 1.5 wt % Si-HAOC – 1.42 mmol/L. Once again this result could indicate that the osteoclasts are active and resorbing.

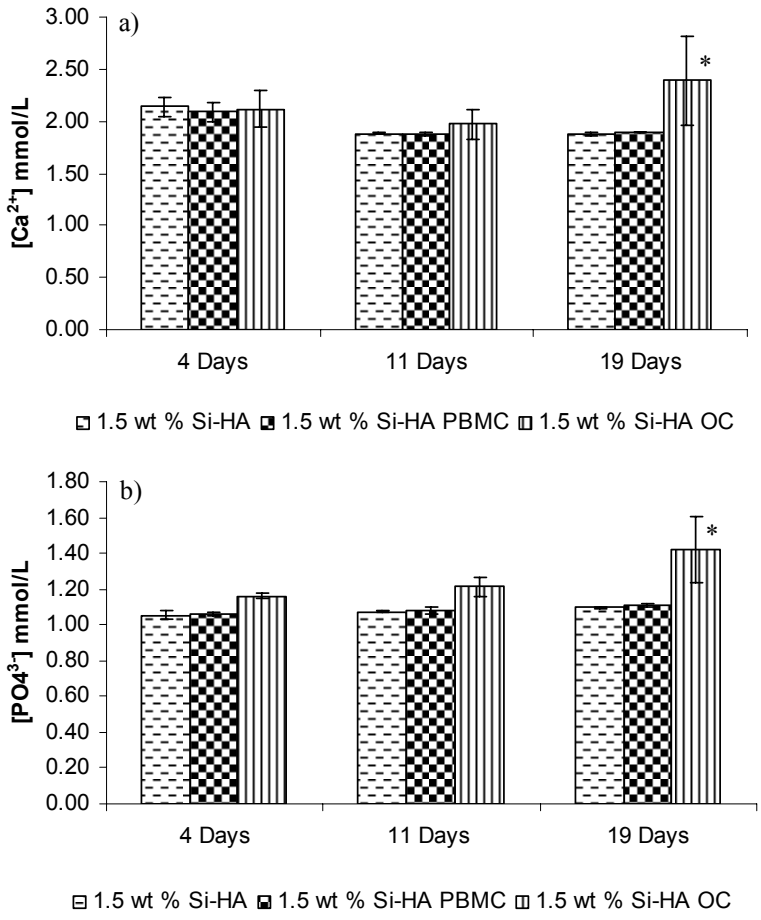

Figure 6 – Calcium (a) and phosphate (b) concentration in the medium at different points concentration, for the 1.5 wt % Si-HA controls and the 1.5 wt % Si-HA sample with osteoclasts. (* - statistical difference $p<0.05$, $n = 3$)

When comparing the samples with osteoclasts from the three materials at day 19, an increase in calcium and phosphate concentration in the medium with the increase of the silicon content. A statistical difference between HA and 1.5 wt % Si-HA (calcium $p<0.007$; phosphate $p<0.001$) was detected. Although, no statistical significant difference was observed between 0.8 wt % Si-HA and HA or between the two compositions of Si-HA.

CD14+

A similar analysis protocol was followed with the CD 14 + cultures, although in this case the osteoclast markers, actin rings and vitronectin receptor were assessed in addition to TRAP staining and measurement of the calcium and phosphate release.

After 21 days, most of the cells present at the surface of the 3 materials were TRAP positive and multinucleated. The localization of actin distribution using FITC – labelled phalloidin demonstrated the characteristic actin ring on the surface of HA and Si-HA. Very few cells differentiated on the controls surface (NC or MCSF) or formed actin rings, as it can be seen in the images of fluorescence microscopy (Figure 7). One the other hand, most of the cells on the surface of the experimental samples presented actin rings, although some of them had discontinuities. They were positive for vitronectin (Figure 8) and several nuclei were observed inside the actin ring (Figure 8d).

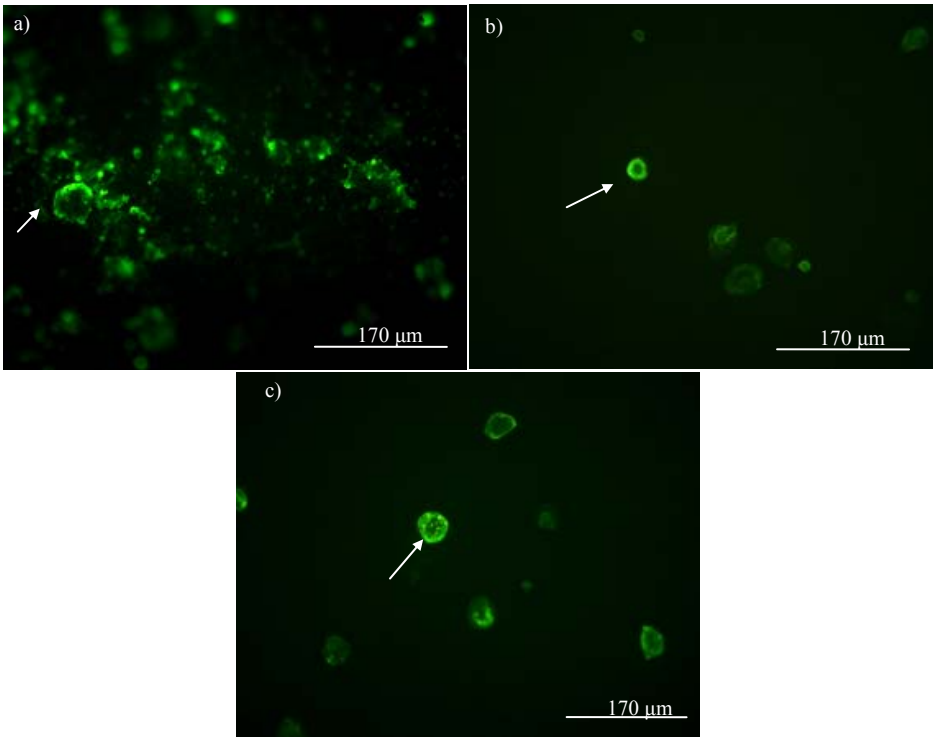

Figure 7 – Fluorescence microscopy showing few cells with actin rings (white arrow). a – HA MCSF; b – 0.8 wt % Si-HA MCSF; c – 1.5 wt % Si-HA MCSF, after 21 days of incubation

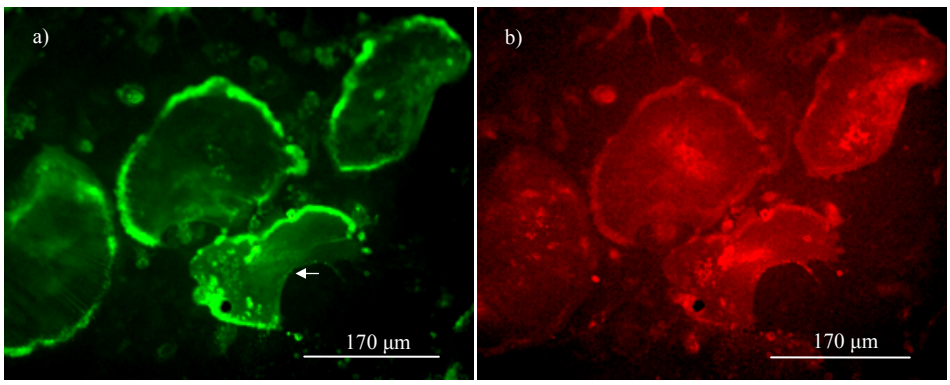

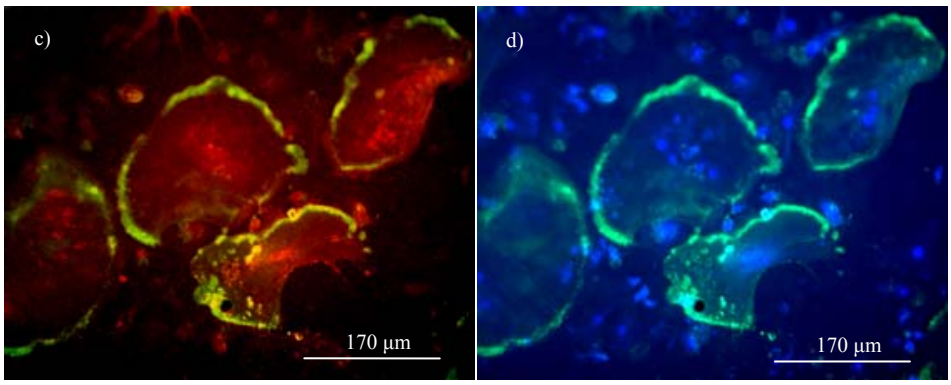

Figure 8 – Fluorescence microscopy image of the actin rings and vitronectin of multinucleated cells (osteoclasts), on the HA surface, after 21 days. a – actin ring; b – vitronectin; c- co-localization of the vitronectin receptor and actin ring; d – nuclei, discontinuities (white arrow)

Similar results were obtained for Si-HA; the cells were multinucleated, presented actin rings, most of them complete and they also presented podosomes rich in vitronectin. The cells showed to be positive for vitronectin and were multinucleated. On both compositions a large number of osteoclasts were present (Figure 9).

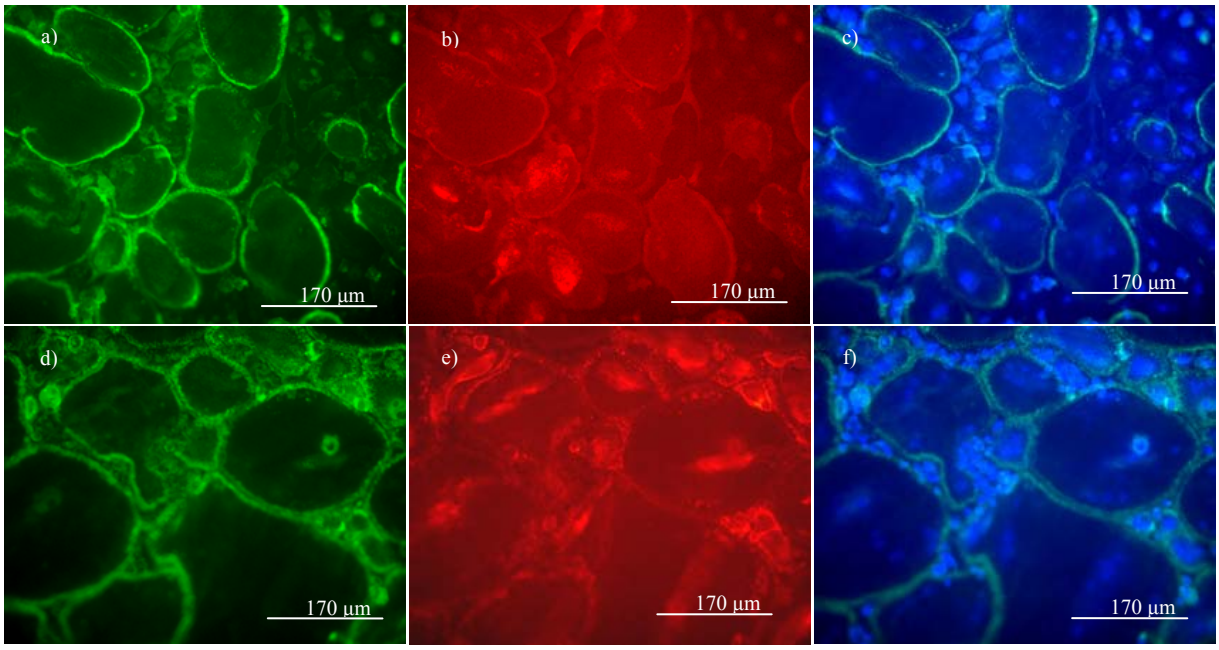

Figure 9 – A detail of the osteoclast on the surface of 0.8 wt % Si-HA (a,b,c) and 1.5 wt % Si-HA (d,e,f) after 21 days. a,d – actin rings; b,e – vitronectin; c,f – nuclei.

As mentioned before osteoclasts are actively migrating cells, and they can form microfilaments called podosomes, which are rich in vitronectin receptor $\alpha_v\beta_3$. The accumulation of these structures precedes the resorption phase. Podosomes were visible in

more detail by CLSM (Figure10). This fact could indicate that the osteoclasts are entering the resorption phase. It can be seen in the CLSM images that some cells on the surface on Si-HA formed podosomes (Figure 10 c,d white arrows). The localization of the microfilaments showing the actin ring is very important, because they reflect the osteoclast phases, migration and resorption.

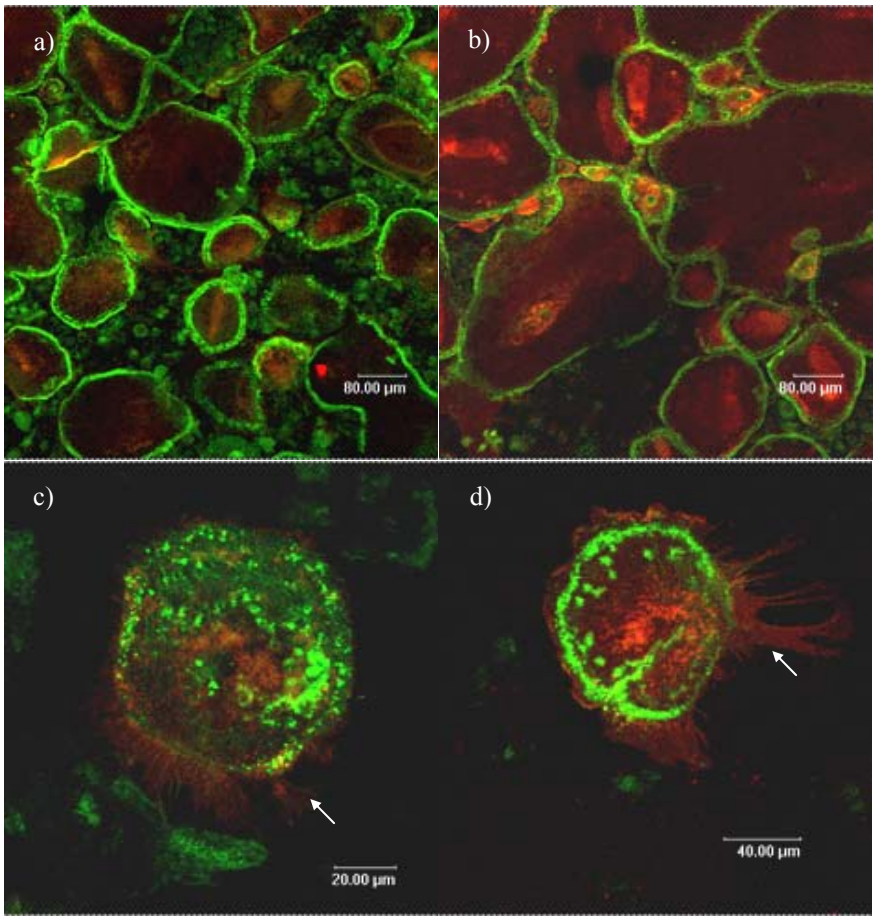

Figure 10 – Confocal laser microscopy images of the actin rings and vitronectin receptors of multinucleated cells – osteoclasts, on the 0.8 wt % Si-HA(a,c) and 1.5 wt % Si-HA (b,d) surfaces, after 21 days. a,b – actin rings; c,d – vitronectin (white arrow indicate podosomes)

The results obtained regarding the calcium and phosphate release were similar to these described previously for the PMBCs. The calcium and phosphate concentrations were analysed at every medium change until the final day of culture.

In this case earlier phosphate release into the medium of HA OC was observed, as soon as day 8 (Figure 11a). At day 21 a slight increase in the phosphate into the medium containing osteoclasts. A similar trend was observed for calcium, HA NC – 1.88 mmol/L; HA MCSF – 1.88 mmol/L and HA OC – 1.97 mmol/L (Figure 11b). Even though, none of these results reached a statistically significant difference.

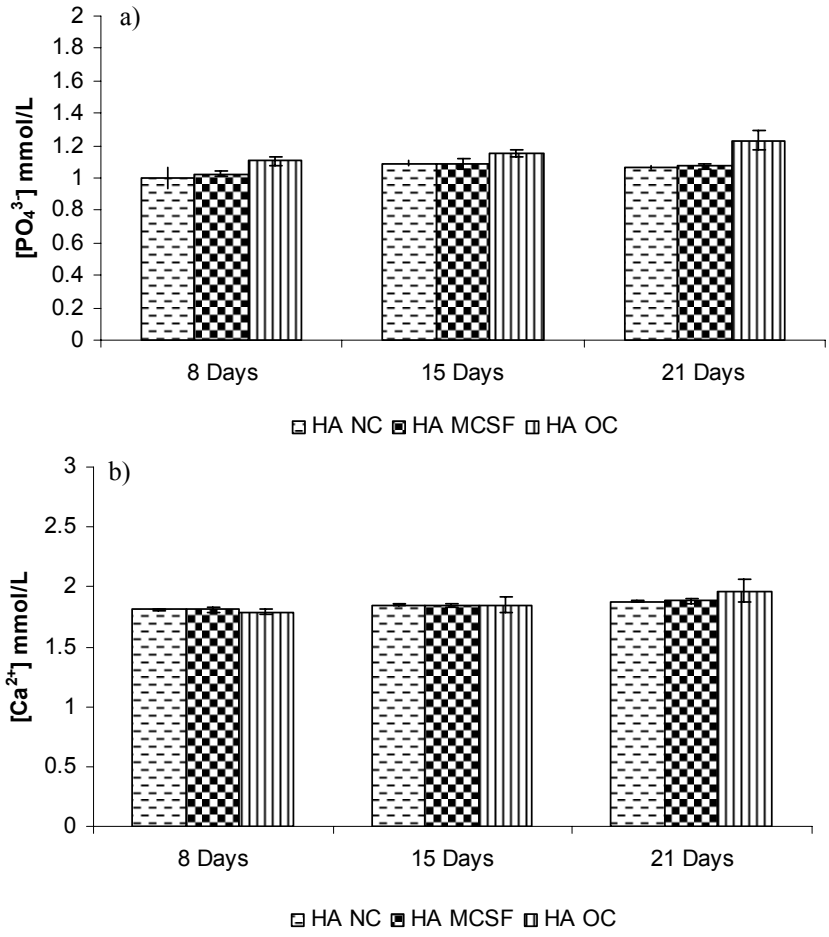

Figure 11 – Phosphate (a) and calcium (b) concentration in the medium at different points concentration, for the HA controls and the HA sample with osteoclasts (n = 3).

A higher concentration of phosphate was observed at day 8, 15 and 21 from the samples containing 0.8 wt % Si-HA OC, but when compared to the controls these were not statistically significant (Figure 12a). Once again, a higher release of calcium was observed by the end of the culture period (Figure 12b), but it was not statistically significant.

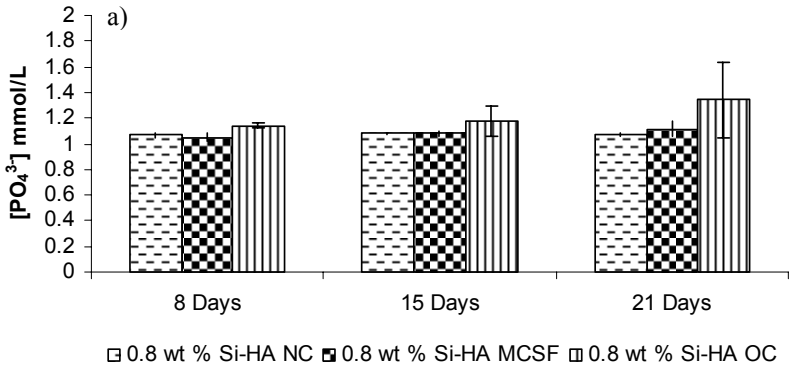

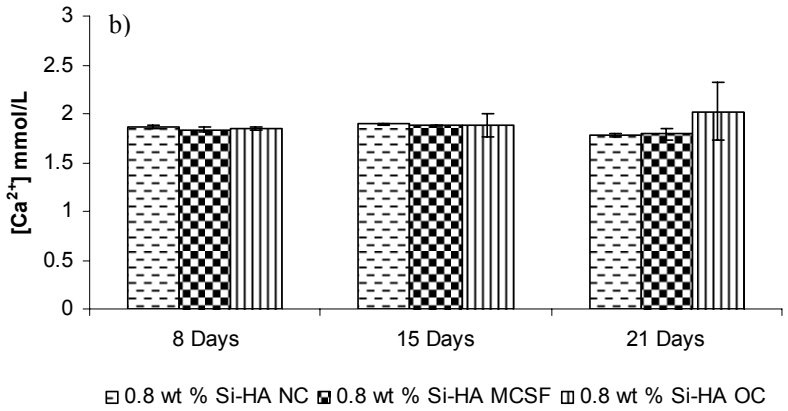

Figure 12 – Phosphate (a) and calcium (b) concentration in the medium at different points concentration, for the 0.8 wt % Si-HA controls and the 0.8 wt % Si-HA sample with osteoclasts

In the case of 1.5 wt % Si-HA the release of phosphate was significantly higher at day 15, when compared with the controls (Figure 13a); 1.5 wt % Si-HA NC - 1.07 mmol/L, $p<0.014$; 1.5 wt % Si-HA MCSF – 1.06 mmol/L $p<0.011$ and 1.5 wt % Si-HA OC – 1.27 mmol/L. While, the increase observed at the same time point for calcium it did not reach statistical significance (Figure 13b). At day 21 the calcium and phosphate content in the 1.5 wt % Si-HAOC medium was significantly higher than the controls (calcium – 1.5 wt % Si-HA NC – 1.77 mmol/L, $p<0.001$; 1.5 wt % Si-HA MCSF – 1.86 mmol/L, $p<0.001$; and 1.5 wt % Si-HA OC – 2.58 mmol/L; phosphate – 1.5 wt % Si-HA NC – 1.06 mmol/L, $p<0.001$; 1.5 wt % Si-HA MCSF – 1.17 mmol/L, $p<0.001$; 1.5 wt % Si-HA OC – 1.57 mmol/L). These results indicate that the osteoclasts are active and resorbing.

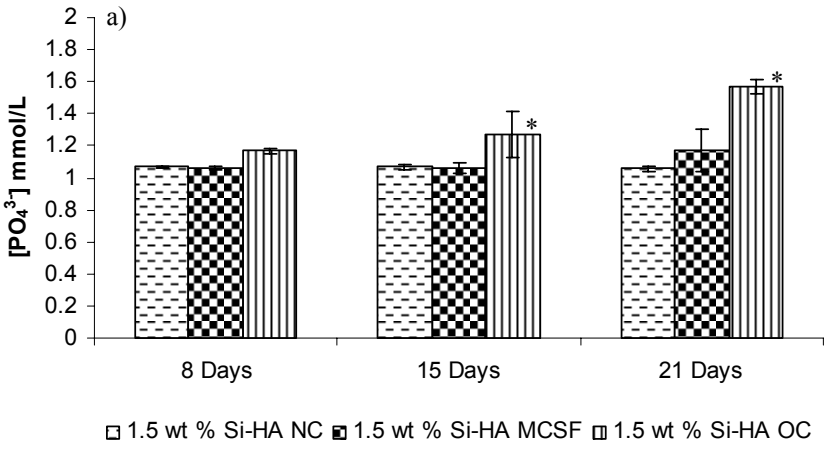

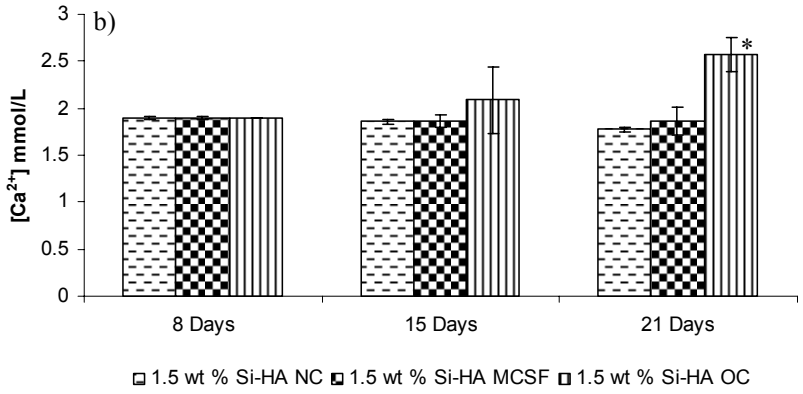

Figure 13 – Phosphate (a) and calcium (b) concentration in the medium at different points concentration, for the 1.5 wt % Si-HA controls and the 1.5 wt % Si-HA sample with osteoclasts. (* - statistical difference $p < 0.05$, $n = 3$)

Once again the calcium and phosphorous concentration of the experimental samples increased with the increase in silicon content. When comparing the three materials, the calcium and phosphate content in the medium of 1.5 wt % Si-HA OC at day 21 was significantly higher than for HA OC and 0.8 wt % Si-HA OC (calcium - HA OC $p<0.001$; 0.8 wt % Si-HA OC $p<0.001$; phosphate - HA OC $p<0.001$; 0.8 wt % Si-HA OC $p<0.015$). No significant difference was detected when the results from HA and 0.8 wt % Si-HA were compared.

Discussion

Through this study, it was possible to demonstrate that HA and Si-HA allows the differentiation of PBMC and CD 14 + selected mononuclear cells into mature osteoclasts. Most of the cells on the surface of the materials expressed osteoclastic markers: actin rings, multinuclearity, expressed TRAP and presented vitronectin receptors. Although, some of these markers are expressed by other cell types such as macrophages, according to Monchau *et al* the formation of an actin ring is the best *in vitro* method to confirm the osteoclastic phenotype [21]. In the fluorescence images it was possible to see the podosomes. It is through this structure that osteoclasts adhere to the surface, which originates in an intramembranous integrin ($\alpha_v\beta_3$). These molecules act as an intermediate between the extracellular matrix proteins and the intracellular cytoskeletal actin microfilaments. These microfilaments bind to

integrins through complex focal adhesion contacts containing several proteins in a ring shape at the periphery of the cell [22, 23]. In the fluorescence images it was possible to observe this structure, the actin ring, in the experimental samples. It is under this actin ring that the osteoclast makes a tight contact with the surface, followed by the secretion of protons and proteases, that will dissolve the bone crystals or the ceramic samples, as in this *in vitro* study [22, 23]. The resorption products are endocytosed from the ruffled border and then transcytosed and released at the functional secretory domain in the top of the osteoclast basal membrane [24, 25]. Some of the actin rings presented discontinuity, which could be due to the change in the osteoclast phase, resorption to migration or a decrease in the cellular activity [21]. When the osteoclast is changing from the non-resorbing to the resorbing stage a large reorganization takes place, in the first stage of the resorption cycle actin and vinculin are distributed throughout the podosomes. In the next stages these structures coalesce to a specific area of the osteoclast and the actin and vinculin stains dissociate. These changes are important because they reflect the cells interaction with the extracellular environment [26].

To ensure that the calcium and phosphate measured in the medium was related to the osteoclastic activity and not related to either acellular degradation or non-osteoclast cell activity several controls were performed. Each ceramic was simultaneously exposed to culture medium alone (without cells) and with cells but no cytokines (first experiment) and on the second experiment a different control was added; the samples were incubated with cells plus MCSF, to verify that resorption occurs only in the presence of osteoclasts. In this second control only MCSF was added and no RANKL, to avoid the differentiation of osteoclasts precursors into mature osteoclasts. Several studies have demonstrated the importance of RANKL for the differentiation and activation of osteoclasts precursors. It has been demonstrated that RANKL is fundamental for osteoclastogenesis and that this phenomenon can be affect by several factors, namely MCSF, interkukin-1, transforming growth factor-β, tumour necrosis factor-α, interlukin-6, vitamin D_3 and parathyroid hormone. Although, all these cytokines are very important, they cannot induce the differentiation of osteoclasts precursors alone [27-31]. The ability of TNF-α to induce osteoclastogenesis is still controversial, it has been shown that TNF-α, can induce osteoclastogenesis, but by the stimulation of osteoblast/stromal cells to produce RANKL [32] or if this cytokine acts directly on osteoclasts precursors at least a small amount of RANKL must be present [32]. RANKL has the ability to induce osteoclastogenesis in the presence of MCSF [28]. RANKL acts on osteoclasts precursors through a membrane receptor, RANK (receptor activator of NF-κβ) activating osteoclastogenesis, although if binds to the decoy receptor osteoprotegerin

(OPG) osteoclastogenesis will be inhibit [28]. It has been established that MCSF is involved in the proliferation and survival of osteoclast progenitors and osteoclasts, but it does not stimulate their resorbing activity [7, 33].

The analyses of the culture medium from the experimental samples showed significant differences. 1.5 wt % Si-HA had higher concentrations of calcium and phosphate in the medium from the samples containing osteoclasts when compared between the three materials and the controls, with the exception of 1.5 wt % Si-HA and 0.8 wt % Si-HA using PBMC as a starting culture, which indicates that the osteoclasts were active and resorbing on 1.5 wt % Si-HA. Similar increases in the calcium and phosphate in the medium was reported by Zhang *et al*, when he seeded mature osteoclasts on the surface of bioglass [34]. In the case of 0.8 wt % Si-HA a higher increase in phosphate was observed in both cultures. No significant difference was observed between HA and 0.8 wt % Si-HA. The difference between the results obtained in the two starting cultures, PBMC and CD14+, could be due to the presence of a mixed population of cells in the case of PBMC, only a small fraction of which are CD14+.

From these results it seems that HA is likely to be less resorbable *in vitro*, although other studies have shown evidences of resorption on HA [35, 36]. Several factors can influence the osteoclastic resorption, such as: sintering temperature, porosity, grain size and experimental conditions [11, 36].

It seems that there is an increased resorption from the Si-HA materials compared to HA. Similar results were obtained by Langstaff *et al* where it was demonstrated that a silicon-stabilized calcium phosphate coating and bulk ceramic showed evidence of osteoclast resorption, while no evidence of cellular resorption was observed on the HA samples [12]. Although Patel *et al* did not reported the presence of osteoclast-like cells *in vivo* [13], we were able to demonstrate that Si-HA material can be resorbed by cellular mechanisms and that silicon has a positive effect on osteoclast activity, although the mechanism behind this is still unknown and further studies are required.

The primary objective for synthetic bone substitute research is the development of an implantable material which combines initial rapid healing with the subsequent capability to be progressively resorbed by osteoclasts during normal continuous tissue remodelling [12]. So, Si-HA seems to be a good candidate.

Conclusions

HA and Si-HA allow the differentiation of osteoclast precursors into mature osteoclasts. A higher release of calcium and phosphate into the medium from the 1.5 wt % Si-HA OC indicates higher osteoclast activity. Therefore, Si-HA can be resorbed by osteoclasts.

Silicon can have a stimulatory effect on osteoclasts, although the underlaying mechanism is still poorly understood.

Acknowledgments

The authors would like to acknowledge to Fundação para a Ciência e Tecnologia (FCT) for CM Botelho's grant (ref. SFRH/BD/6173) and the project entitled "Coatings with silicon-substituted hydroxyapatite coatings for biomedical", ref POCTI/CTM/49238/2002.

References

1. Schilling A, Linhart W, Filke S, Gebauer M, Schinke T, Rueger J*, et al.* Resorbability of bone substitute biomaterials by human osteoclasts. Biomaterials 2004;25(18):3963-3972.

2. Miller P, Baram D, Bilezkian J, Greenspan S, Lindsay R, Riggs B*, et al.* Practical clinical application of biochemical markers of bone turnover - Consensus of an Expert Panel. Journal of Clinical Densitometry 1999;2(3):323-342.

3. Flanagan A, Massey H, Wilson C, Vellodi A, Horton MA, Steward C. Macrophage colony-stimulating factor and receptor activator NF-kappa B ligand fail to rescue osteoclast-poor human malignant infantile osteopetrosis *in vitro*. Bone 2002;30(1):85-90.

4. Boyle W, Simonet W, Lacey DL. Osteoclast differentiation and activation. Nature 2003;423(6937):337-342.

5. Susa M, Luong-Nguyon NH, Cappellen D, Zamurovic N, Gamse R. Human primay osteoclasts *in vitro* generation and applications as a pharmacological and clinical assay. Journal of Translational Medicine 2004;2:6.

6. Anderson D, Maraskovsky E, Bilingsley W, Dougal W, Tometsko M, Roux E*, et al.* A homologue of the TNF receptor and its ligand enhance T-cell growth and dendritic-cell function. Nature 1997;390(6656):175-179.

7. Matsuzaki K, Udagawa N, Takahashi N, Yamaguchi K, Yasuda H, Shima N*, et al.* Osteoclast differentiation factor (ODF) induces osteoclast-like cell formation in human

peripheral blood mononuclear cell cultures. Biochemical and Biophysical Research Communications 1998;246(1):199-204.

8. Quinn J, Elliot J, Gillespie M, Martin T. A combination of osteoclast differentiation factor and macrophage-colony stimulating factor is sufficient for both human and mouse osteoclast formation in vitro. Endocrinology 1998;139(10):4424-4427.

9. Massey H, Flanagan A. Human osteoclasts derive from CD14-positive monocytes. British Journal of Haematology 1999;106(1):167-170.

10. Horton M. The $\alpha_v\beta_3$ integrin "vitronectin receptor". The International Journal of Biochemistry & Cell Biology 1997;29(5):721-725.

11. Doi Y, Shibutani T, Moriwaki Y, Kajimoto T, Iwayama Y. Sintered carbonate apatites as bioresorbable bone substitutes. Journal of Biomedical Materials Research. 1998;39:603-610.

12. Langstaff S, Sayer M, Smith T, Pugh S. Resorbable bioceramics based on stabilized calcium phosphates. Part II: evaluation of biological response. Biomaterials 2001;22(2):135-150.

13. Patel N, Gibson IR, Hing KA, Damien E, Revell PA, Best SM*, et al.* A comparative study on the *in vivo* behaviour of hydroxyapatite and silicon-substituted hydroxyapatite granules. Journal of Materials Science: Materials in Medicine 2002;13:1199-1206.

14. Botelho CM, Brooks RA, Best SM, Lopes MA, Santos JD, Rushton N*, et al.* Biological and physical-chemical characterization of phase pure hydroxyapatite and silicon-substituted hydroxyapatite by different microscopy techniques. Key Engineering Materials 2004;254-256:845-849.

15. Gibson IR, Hung J, Best SM, Bonfield W. Enhanced *in vitro* cell activity and surface apatite layer formation on novel silicon-substituted hydroxyapatites. In: Ohgushi H, Hastings GW, Yoshikawa T, editors. Bioceramics 12; Nara, Japan: World Scientific Publishing Co. Pte. Ltd; 1999. p. 191-194.

16. Jha LJ, Best SM, Santos JD, Gibson IR, Bonfield W, Jha LJ, Best SM, Santos JD, Gibson IR, Bonfield WJha LJ, Best SM, Santos JD, Gibson IR, Bonfield W; Silicon-substituted apatites and process for the preparation thereof. Worldwide patent PCT/GB97/02325. 1999.

17. Gibson I, Best SM, Bonfield W. Chemical characterization of silicon-substituted hydroxyapatite. Journal of Biomedical Materials Research. Part B, Applied Biomaterials 1999;44(4):422-428.

18. Botelho CM, Lopes MA, Gibson IR, Best SM, Santos JD. Structural analysis of Si-substituted hydroxyapatite: zeta potential and X-ray photoelectron spectroscopy (XPS). Journal of Materials Science: Materials in Medicine 2002:1123-1127.

19. Winchester RJ, Ross G. Methods for enumerating lymphocyte populations. In: Rose NR, Friedman H, editors. Manual of clinical immunology. Washington DC: American society for microbiology; 1976. p. 64-76.

20. Burstone MS. Histochemical demonstration of acid phosphatases with naphthol AS-phosphate. Journal of National Cancer Institute 1958;21:423-539.

21. Monchau F, Lefevre A, Descamps M, Belquin-myrdyez A, Laffargue P, Hildebrand HF. *In vitro* studies of human and rat osteoclast activity on hydroxyapatite, beta-tricalcium phosphate, calcium carbonate. Biomolecular engineering 2002;19(2-6):143-152.

22. Chambers TJ. The regulation of osteoclastic development and function. Ciba Foundation Symposium 1988;136:92-107.

23. LakkaKorpi P, Tuukkanen J, Hentunen J, Jarvelin K, Vaananen K. Organization of osteoclast microfilaments during the attachment to bone surface *in vitro*. Journal of Bone and Mineral Research 1989;4(6):817-825.

24. Nesbitt S, Horton MA. Trafficking of matrix collagens through bone-resorbing osteoclasts. Science 1997;276(5310):266-269.

25. Salo J, Lehenkari P. Removal of osteoclast bone resorption products by transcytosis. Science 1997;276(5310):270-273.

26. Vaananen K, Horton MA. The osteoclast clear zone is a specialized cell extracellular matrix adhesion structure. Journal of Cell Science 1995;108:2729-2732.

27. Kong YY, Feige U, Sarosi I, Bolon B, Tafuri A, Morony S*, et al.* OPGL is a key regulator of osteoclastogenesis, lymphocyte development and lymph-node organogenesis. Nature 1999;402:304-309.

28. Wittrant Y, Thepleyre S, Couillaud S, Dunstan C, Heymann D, Rédini F. Relevance of an *in vitro* osteoclastogenesis system to study receptor activator of NF-kappa B ligand and osteoprotegerin biological activities. Experimental cell research 2004;293(2):292-301.

29. Heymann D. gp130 cytokine family and bone cells. Cytokine 2000;12(10):1455-1468.

30. Heymann D, Gouin F, Passuti N, Daculsi G. Cytokines, growth factors and osteoclasts. Cytokine 1998;10(3):155-168.

31. Burgess T, Qian Y, Kaufman S, Ring B, Van G, Capparelli C*, et al.* The ligand for osteoprotegerin (OPGL) directly activates mature osteoclasts. The Journal of Cell Biology 1999;145(3):527-538.

32. Teitelbaum S. Bone resorption by osteoclasts. Science 2000;289(5484):1504-1508.

33. Udagawa N, Takahashi N, Jimi E, Matsuzaki K, Tsurukai T, Itoh K*, et al.* Osteoblasts/stromal cells stimulate osteoclast activation through expression of osteoclast differentiation factor/RANKL but not macrophage colony-stimulating factor. Bone 1999;25(5):517-523.

34. Zhang YM, Cai YR, Monchau F, Lefevre A, Zhao YM, Hildebrand HF. Biodegradation of synthetic bioglass with different crystallinity *in vitro*. In: 7th World Biomaterials Congress; 2004; Sydney; 2004. p. 1904.

35. Gomi K, Lowenberg B, Shapiro G, Davies JE. Resorption of sintered synthetic hydroxyapatite by osteoclasts *in vitro*. Biomaterials 1993;2:91-96.

36. De Bruijin JD, Bovel YP, Davies JE, Van Blitterswijik CA. Osteoclastic resorption of calcium phosphate is potentiated in postosteogenic culture conditions. Journal of Biomedical Materials Research. 1994;28:105-112.

Chapter 5

General Discussion and Main Conclusion

Discussion and Main Conclusion

In this thesis we proposed to assess the effect of silicon incorporation into the hydroxyapatite (HA) lattice, focusing mainly on the biological response to the material *in vitro.*

Previous studies showed that the incorporation of silicon into the HA lattice induced few structural changes, namely on the lattice parameters, a decrease in the *a* axis and an increase on the *c* axis and also an increase on the distortion index of the phosphate (PO_4^{3-}) group, indicating that the PO_4^{3-} group is replaced by the silicate (SiO_4^{4-}) group. The presence of silicon into the structure of HA did not induce the formation of secondary phases, or influence the crystallinity of the material [1]. It was also shown that the silicon-substituted hydroxyapatite (Si-HA) has an enhanced bioactivity *in vitro* [2] an *in vivo* [3-5].

Looking at the previous studies the main question was: how does silicon affects the biological response to HA? The complexity of the *in vivo* system makes it difficult to determine the mechanism behind the enhanced bioactivity. Therefore, the study reported in this thesis focused on different *in vitro* tests, principally on the interaction of silicon-substituted hydroxyapatite (Si-HA) with proteins and human bone cells.

The formation of an apatite layer is considered to be an important factor for osseointegration, being related to the materials dissolution kinetics and its physical-chemical properties. So, in this work we started by characterising the Si-HA on a physical-chemical point of view. Our results showed that the Si-HA material has a higher electrophoretic mobility than HA, resulting in a more negative zeta potential. The Fourier transformed infra-red analysis (FTIR) and X-ray photoelectron spectroscopy (XPS) clearly support the substitution mechanism proposed by Gibson *et al* [1], according to the author the SiO_4^{4-} group substitutes for the PO_4^{3-} group and due to a charge balance some hydroxyl (OH^-) groups are lost. The binding energy at 101 eV (Si-O bonding) confirms conclusively that silicon exists as a tetrahedral silicate (SiO_4^{4-}), rather than as a polymeric or as a SiO_2 form. This finding supports the analogy between silicon or silicate substitution and the well-characterized carbonate (CO_3^{2-}) substitution of PO_4^{3-} groups in HA. The decrease of the peak at 631 cm^{-1} on the FTIR spectra confirms the loss of the OH^- group due to the charge balance. The bands at 888 cm^{-1} and 504 cm^{-1}, also confirmed the presence of a SiO_4^{4-} group. The incorporation of silicon increased the hydrophilicity of the material and consequently its interfacial tension, through an increase on its polar component. Although, the difference on the hydrophilicity

between the HA and Si-HA did not reach statistical significance, they corroborate the zeta potential results. Therefore, the increased hydrophilicity may be due to the presence of unsaturated Si-O bonds leading to the formation of Si-OH bonds in the presence of an aqueous medium.

The Si-HA material has a higher dissolution rate when compared to HA. When incubated in SBF, the incorporation of silicon into the HA lattice decreased the time required for the formation of an apatite layer in 64% and 75%, for 0.8 wt% Si-HA and 1.5 wt% Si-HA, respectively. Similar results were reported by Gibson *et al* [1] and Thian *et al* [6]. Following the analysis of our results we proposed that the formation of an apatite layer on the surface of Si-HA is a combination of two factors, dissolution and surface charge. The greater solubility of Si-HA causes a faster super-saturation of the SBF solution followed by a faster precipitation of an apatite layer from super-saturated SBF. In addition, the surface properties of the HA and Si-HA ceramics may control the time scale for the change from dissolution to apatite precipitation. The more electronegative Si-HA surface provides a preferential site for nucleation of an amorphous calcium phosphate apatite layer than the HA surface. This can occur via the adsorption of calcium (Ca^{2+}) ions onto the electronegative surface, resulting in an increase on the surface charge and the attraction of PO_4^{3-} groups.

Using atomic force microscopy (AFM) and AFM phase imaging it was possible to observe that there is a preferential dissolution at the grain boundaries of the Si-HA material. Energy dispersive X-ray (EDX) and XPS analysis showed that silicon is preferentially dissolved from the material surface to the surrounding media. Gibson *et al* [1] reported that silicon substitution caused a substantial increase on the distortion index of the PO_4^{3-} group and a decrease on the number OH^- groups. It is possible that these disturbances and the vacancies at the OH^- site may lead to higher susceptibility for SiO_4^{4-} to be released from the structure. Porter *et al* demonstrated that the incorporation of silicon into the HA lattice increased the number of grain boundaries and triple junctions. The Si-HA sample containing higher concentration of silicon (1.5wt%) has a less crystalline phase on the triple junctions [7]. Therefore, we proposed that silicon is preferentially located at the grain boundaries.

As mentioned previously the formation of an apatite layer is considered to be an important step for osseointegration and in the *in vivo* environment there is the presence of several biological molecules such as proteins. So, we studied the effect of human serum proteins on the formation of the apatite layer. Our results showed that the presence of proteins delayed the formation of an apatite layer in all substrates. Through, the AFM phase imaging it was possible to see a layer with different characteristics from the ceramic material on the

surface of the samples incubated with human serum proteins. The XPS analysis confirmed that this layer was a protein film due to the increase on nitrogen content. We hypothesised that the protein layer prevents the diffusion of ions from the surface of the material to the surrounding medium. This hypothesis was confirmed by inductively couple plasma spectroscopy (ICP), since we demonstrated that in the presence of human serum proteins a lower concentration of silicon was released to the medium from 0.8 wt% Si-HA and 1.5 wt% Si-HA.

It has been reported in the literature that cells respond mainly to the proteinaceous layer on the surface of the material rather than to the biomaterial itself [8]. So, the adhesion of total human serum proteins and individual proteins to Si-HA was studied. 0.8 wt% Si-HA has a higher binding capacity for total human serum proteins when compared to HA and 1.5 wt% Si-HA. IgG, albumin and collagen type I have different binding affinities to the materials. Collagen type I has higher binding affinity to Si-HA and its affinity increased with the increase of the silicon content. IgG has lower affinity to the materials, followed by albumin. The pattern of adsorbed proteins observed in this study can be explained by electrostatic interactions between the proteins and the substrates. The three proteins studied have different structures and different isoelectric points, therefore the overall net charge is different at pH 7, collagen type I has an overall positive charge, IgG has a slight negative charge and albumin has an even more negative charge. As mentioned previously the surface charge of Si-HA is more electronegative than HA, so the electrostatic interaction between the Si-HA and a protein is greater if a protein has an overall positive charge as in the case of collagen type I, followed by a lower binding affinity of IgG and albumin. In the case of the adhesion of a complex mixture of proteins there are other factors that can influence the adhesion such as, spatial charge distribution and the "Vroman effect".

Subsequently to the adhesion of proteins cells will reach the surface of the material. The osteoblasts are the cells responsible matrix deposition. Therefore, several experiments were carried out to assess the effect of Si-HA on the proliferation and differentiation of osteoblasts.

Human osteoblasts (HOBS) were seeded on the surface of the HA and Si-HA material. A higher number of cells was observed on the surface of 0.8 wt% Si-HA when compared to HA and 1.5 wt% Si-HA. It is known that the adhesion of cells onto a substrate involves extracellular matrix proteins, cell membrane proteins and cytoskeleton proteins, which interact together to induce signal transduction, promoting the action of transcription factors and consequently regulating gene expression [9]. Although, the difference on the number of

adherent cells did not reached statistical significance, the trend observed is similar to that observed regarding the adsorption of human serum proteins, where 0.8 wt% Si-HA showed to have higher binding capacity, when compared to the other materials. So, the higher adhesion of total proteins may account for the increase number of HOBS adhering to the 0.8 wt% Si-HA.

The HOBS seeded on Si-HA for a period of 27 days expressed the osteoblast phenotype markers, collagen type I (COL I), alkaline phosphatase (ALP) and osteocalcin (OC). The cells were well spread and confluent in all materials. The HOBS seeded on 0.8 wt% Si-HA expressed higher levels of proteins when compared to HA and 1.5 wt% Si-HA. The ALP/COL I ratio at day 7 expressed by the cells seeded on 1.5 wt% Si-HA indicated that the HOBS seeded on this material were at a higher stage of differentiation. Throughout, the culture period the osteoblastic markers expressed by the cells seeded on the samples with the higher concentration of silicon (1.5 wt%) was constant, while the cells seeded on 0.8 wt% Si-HA expressed higher concentration of proteins at different time periods of the culture. Although, there is release of silicon from both materials the higher release of silicon at earlier time points may stimulate differentiation of HOBS, as it has been demonstrated by Reffitt *et al* [10] that silicon increases the expression of osteoblast markers like COL I, ALP and OC. Reffit *et al* [10] also reported that if the concentration of silicon is too high the positive effect of silicon maybe diminished. It has also been reported that a stable collagenous matrix is important for the progression of osteoblastic differentiation and is a prerequisite for an increase in the ALP expression [11-15] and we previously demonstrated that 1.5 wt% Si-HA has a higher binding capacity to collagen. After 21 days it was possible to observe mineral deposits on the surface of the materials, these deposits coincide with areas of high cell density indicating a cell mediated process.

The ideal bone graft would be a material that can be resorbed and induce bone formation, hence being completely replaced by new bone. Bone is a dynamic organ due to its constant remodelling, being the osteoblasts responsible for producing the matrix and osteoclasts for resorbing it. It was shown that the Si-HA stimulates osteoblast proliferation and differentiation; therefore it was now important to assess the effect of this material onto osteoclast differentiation and activity. Peripheral blood mononuclear cells (PBMC) and CD 14 positive monocytes (CD 14+) were seeded onto the surface of HA and Si-HA. The adhesion of PBMC showed a similar trend to the adhesion of human osteoblasts and total protein, namely more cells adhered to 0.8 wt% Si-HA. Both materials were capable of supporting the differentiation of PBMC and CD 14+ into mature osteoclasts. Most of the cells

on the surface of the materials expressed osteoclastic markers, such as: actin rings, several nuclei, expressed TRAP and presented vitronectin receptors [16, 17]. The osteoclasts present on the surface of the materials had podosomes. It is through this structure that osteoclasts adhere to the surface, which originates in an intramembranous integrin ($\alpha_v\beta_3$) [18, 19]. Some of the actin rings presented discontinuities, which could be due to a change in osteoclast behaviour, resorption to migration or a decrease in the cellular activity [20]. The analyses of the culture medium from the osteoclasts seeded on 1.5 wt% Si-HA, on which osteoclast development had been stimulated, showed a higher concentration of calcium and phosphate, when compared between the three materials and the controls, which indicates that the osteoclasts were active and resorbing.

An increased resorption activity on Si-HA was observed when compared to HA. Therefore, it seems that silicon has a positive effect on osteoclast activity, but the cellular mechanism as several uncertainties.

The results presented here show the role of Si-HA on several physical, chemical and biological processes. These studies indicate that the enhanced bioactivity of the Si-HA is a combination of acellular and cellular mechanisms. The more negative surface and higher dissolution rate decreases the time required for the formation of an apatite layer, which is considered to be an important factor for osseointegration. And also the enhanced proliferation and differentiation of bone cells (human osteoblast and osteoclast) induced by the presence of Si-HA can lead to faster bone regeneration.

References

1. Gibson IR, Best SM, Bonfield W. Chemical characterization of silicon-substituted hydroxyapatite. Journal of Biomedical Materials Research 1999; 44:422-428.

2. Gibson IR, Huang J, Best SM, Bonfield W. Enhanced *in vitro* cell activity and surface apatite layer formation on novel silicon-substituted hydroxyapatites. In: Ohgushi H, Hastings GW, Yoshikawa T, editor. Bioceramics 12; Nara, Japan: World Scientific Publishing Co. Pte. Ltd; 1999:191-194.

3. Patel N, Best S, Gibson IR, Hing K, Damien E, Bonfield W. A comparative study on the in vivo behavior of hydroxyapatite and silicon substituted hydroxyapatite granules,. Journal of Materials Science: Materials in Medicine 2002;13:1199-1206.

4. Patel N, Brooks R, Clarke M, Lee P, Rushton N, Gibson I, et al. *In vivo* assessment of hydroxyapatite and silicate-substituted hydroxyapatite granules using an ovine defect model. Journal of Materials Science: Materials in Medicine 2005;16:429-440.

5. Patel N. *In vivo* assessment of hydroxyapatite and substituted apatites for bone grafting. Cambridge; 2003.

6. Thian E, Huang J, Best SM, Barber Z, Bonfield W. Fast apatite-forming ability of magnetron co-sputtered silicon-containing hydroxyapatite (Si-HA) thin films. Key Engineering Materials 2005;284-286:445-448.

7. Porter A, Best S, Bonfield W. Ultrastructral comparison of hydroxyapatite and silicon substituted hydroxyapatite for biomedical applications. Journal of Biomedical Materials Research 2004;68A:133-141.

8. Lyman D, Metcalf L, Albo D, Richards K, Lamb J. The effect of chemical structure and surface properties of synthetic polymers on the coagulation of blood. III *In vivo* adsorption of proteins on polymer surfaces. Transaction American Society for Artificial Internal Organs 1974;20:474-478.

9. Anselme K. Osteoblast adhesion on biomaterials. Biomaterials 2000;21:667-681.

10. Reffitt D, Ogston N, Jugdaohsingh R, Cheung H, Evans B, Thompson R, et al. Orthosilicic acid stimulates collagen type I synthesis and osteoblastic differentiation in human osteoblast-like cells in vitro. Bone 2003;32:127.

11. Shiga M, Kapila Y, Zhang Q, Hayami T, Kapila S. Ascorbic acid induces collagenase-1 in human periondontal ligament cells but not in MC3T3-E1 osteoblast-like cells: Potential association between collagenase expression and changes in alkaline phosphatase phenotype. Journal of Bone Mineral Research 2003;18(1):67-77.

12. Franceschi R, Iyer B, Cui Y. Effects of ascorbic acid on collagen matrix formation ans osteoblast differentiation of murine MC3T3-E1 cells. Journal of Bone Mineral Research 1994;9:843-854.

13. Franceschi R, Iyer B. Relationship between collagen synthesis and expression of the osteoblast phenotype in MC3T3-E1 cells. Journal of Bone Mineral Research 1992;7:235-246.

14. Aronow M, Gerstenfeld L, Owen T, Tassinari M, Stein G, Lian J. Factors that promote progressive development of the osteoblast phenotype in cultured fetal rat calvaria cells. Journal of Cell Physiology 1990;143:213-221.

15. Chien H, Lin W, Cho M. Interkukin-1β-induced release of matrix portiens into culture media causes inhibition of mineralization of nodules formed by periodontal ligament cells *in vitro*. Calcified Tissue International 1999;64:402-413.

16. Susa M, Luong-Nguyon NH, Cappellen D, Zamurovic N, Gamse R. Human primay osteoclasts *in vitro* generation and applications as a pharmacological and clinical assay. Journal of Translational Medicine 2004;2:6.

17. Horton M. The $\alpha_v\beta3$ integrin "vitronectin receptor". The International Journal of Biochemistry and Cell Biology 1997;29(5):721-725.

18. Chambers TJ. The regulation of osteoclastic development and function. Ciba Foundation Symposium 1988;136:92-107.

19. LakkaKorpi P, Tuukkanen J, Hentunen J, Jarvelin K, Vaananen K. Organization of osteoclast microfilaments during the attachment to bone surface *in vitro*. Journal of Bone and Mineral Research 1989;4(6):817-825.

20. Monchau F, Lefevre A, Descamps M, Belquin-myrdyez A, Laffargue P, Hildebrand HF. *In vitro* studies of human and rat osteoclast activity on hydroxyapatite, β-tricalcium phosphate, calcium carbonate. Biomolecular Engineering 2002;19(2-6):143-152.